Landslide Susceptibility Analysis and Developing Remedial Measures for Gore - Masha - Tepi Road Project.

By: - Mohammed Fetu

A Thesis Submitted to the Department of Civil Engineering, College of Civil Engineering and Architecture

Presented in Partial Fulfillment of The Requirement for The Degree of Masters in Civil Engineering (Geotechnical Engineering)

Office of Graduate Studies

Adama Science and Technology University

May, 2025

Adama, Ethiopia

Landslide Susceptibility Analysis and Developing Remedial Measures for

Gore - Masha - Tepi

Road Project.

By: - **Mohammed Fetu**

Advisor;

Dr Siraj Mulugeta

A Thesis Submitted to the Department of Civil Engineering, College of Civil Engineering and Architecture

Presented in Partial Fulfillment of The Requirement for The Degree of Masters in Civil Engineering (Geotechnical Engineering)

Office of Graduate Studies

Adama Science and Technology University

May,2025

Adama, Ethiopia

DECLARATION

I hereby declare that this Master Thesis entitled, "Landslide Susceptibility Analysis and Developing Remedial Measures for Gore-Masha-Tepi Road Project," is my original work. That is, it has not been submitted for the award of any academic degree, diploma or certificate in any other university. All sources of materials that are used for this thesis have been duly acknowledged through citation.

Mohammed Fetu	________________	*31/05/2025*
Student Name	*Signature*	*Date*

RECOMMENDATION OF ADVISOR

I, the advisor(s) of this thesis, hereby certify that I have read the revised version of the thesis entitled "Landslide Susceptibility Analysis and Developing Remedial Measures for Gore-Masha-Tepi Road Project prepared under my guidance by Mohammed Fetu. submitted in partial fulfillment of the requirements for the degree of Mater's of Science in Geotechnical Engineering. Therefore, I recommend the submission of revised version of the thesis to the department following the applicable procedures.

Siraj Mulugeta (PhD)	_______________	*31/05/2025*
Advisor Name	*Signature*	*Date*

APPROVAL PAGE

I, the advisors of the thesis entitled "Landslide Susceptibility Analysis and Developing Remedial Measures for Gore-Masha-Tepi Road Project, and developed" by Mohammed Fetu. hereby certify that the recommendation and suggestions made by the board of examiners are appropriately incorporated into the final version of the thesis.

Siraj Mulugeta (PhD)	_______________	*31/05/2025*
Advisor Name	*Signature*	*Date*

APPROVAL OF BOARD OF REVIEWERS

We, the undersigned, members of the Board of Examiners of the thesis by Mohammed Fetu have read and evaluated the thesis entitled "Landslide Susceptibility Analysis and Developing Remedial Measures for Gore-Masha-Tepi Road Project" and examined the candidate during open defense. This is, therefore, to certify that the thesis is accepted for partial fulfillment of the requirement of the degree of Master of Science in Geotechnical

Chairperson	*Signature*	*Date*
Reviewer1	*Signature*	*Date*
Reviewer2	*Signature*	*Date*

Finally, approval and acceptance of the thesis proposal are contingent upon submission of its final copy to the Office of Postgraduate Studies (OPGS) through the Department Graduate Council (DGC) and School Graduate Committee (SGC).

Department Head	*Signature*	*Date*
School Dean	*Signature*	*Date*
Office of Postgraduate Studies, Dean	*Signature*	*Date*

TABLE OF CONTENTS

LIST OF Figures

LIST OF TABLES

ABBREVIATIONS

AC ………………. Asphalt Concrete

AHP………………Analytic Hierarchy Process

ERA………………Ethiopian Roads Administration

FR………………. Frequency Ratio

GIS………………Geographical Information System

LHEF……………Landslide Hazard Evaluation Factor

LSM………………Landslide Susceptibility Map

FEM………………Finite Element Method

LEM………………Limit Equilibrium Method

SPT………………Standard Penetration Test

N…………………. SPT-blow number

UU………………Unconsolidated Un Drained

CU………………Consolidated Un Drained

CD………………Consolidated Drained

FS………………. Factor of Safety

YES……………. Vertical Electrical Sound

SSEP……………Slope Susceptibility Evaluation Parameters

ASL……………. Above Mean Sea Level

UTM……………Universal Transverse Mercator

SSEP……………Slope Susceptibility Evaluation Parameters

Msf…………. Global Factor of Safety

g……………Gravitational acceleration

γb……………Bulk unit weight

c'…………. Cohesion in terms of effective stress

c'lab. ………Cohesion obtained from laboratory

c'ans. ………Cohesion considered as the answer

ϕ'……………Angle of internal friction in terms of effective stress

ϕlab. ………Angle of internal friction obtained from laboratory

ϕans. ………Angle of internal friction considered as the answer

E'……………Effective modulus of elasticity

Ψ……………Dilatancy Angle

v'……………Effective Poisson's ratio

GWT………. Ground water table

ABSTRACT

The Gore-Masha-Tepi Road, which is the subject of this paper, is located in the southwestern part of the country It starts from town and generally runs north-south for a length of 141 km to reach the other end of the project, Tepi town. positioned in the southwest highlands where landslides are common.

This study evaluated the characteristics, failure mechanism, and extent of the landslides in the active landslide zones along the Gore-Masha-Tepi Road Geological, geomorphological, hydrological, and human aspects were all included in the methodical analysis a susceptibility map was created to pinpoint high-risk areas using field surveys, Geographic Information Systems (GIS), and data from remote sensing. Following their division into sub-characteristics using Analytical Hierarchy Process (AHP), the following important factors are taken into consideration and weighted: Lithology, Elevation, Rainfall, Slope, Slope aspect, land use/cover, Drainage patterns (distance to stream, distance to road), and curvature. The landslide susceptibility map is then created by overlaying the layers of causative factors using the weighted overlay technique in the ArcGIS environment.

The study further details the systematic assessment and formulation of remedial solutions for one critical landslide-affected cut slopes (Km 45+350–45+440,80+610-81+600 and 82+610-83+400). Following comprehensive geological analysis and geotechnical characterization of unstable slope materials through field and laboratory testing, numerical modeling via 2D PLAXIS finite element software was conducted to evaluate slope behavior. Using the knowledge gained from these evaluations, specific mitigation plans that balanced long-term stability and technical feasibility were suggested for every site.

The measures seek to improve road safety, reduce the risk of landslides. A crucial framework for designing robust road developments in landslide-prone locations is provided by this analysis to decision-makers.

Key words: *Landslide Susceptibility Map, ArcGIS, Analytic Hierarchy Process Failed cut slope, Factor of Safety, PLAXIS 2D,*

CHAPTER ONE

INTRODUCTION

1.1. Back Ground Study

In the past, Ethiopia has seen destructive landslides that have destroyed homes, severely damaged infrastructure, disrupted economic progress, impacted the environment, and claimed lives. Landslides are the movement of different types of soil, rock or debris. These movements happen down or along the slope (Serdarevic & Babic, 2019). These phenomena typically happen in regions with rugged terrain, such as mountains and escarpments. The beginning and intensification of the landslide are caused by a variety of reasons. Deforestation, active riverbank erosion that creates gullies, heavy and protracted rainfall, the existence of recent unconsolidated soil deposits in certain locations, human activities like building infrastructure and expanding cities, and so forth are some of the contributing reasons.

Landslides can be categorized as falls, topples, slides, flows, spreads, or any combination of these, and they can happen gradually or abruptly, depending on the physical properties of the sliding materials and their mode of motion. Ethiopia is a country in the Horn of Africa that is made up of flat plains, moderate slopes, escarpments, highlands, plateaus, and divided valleys. Locations that are primarily mountainous and escarpment terrain provide an ideal setting for the frequent occurrence of landslides. Such locations are the mountainous areas of Ethiopia dominantly located in the north-northwest (N-NW), central and south• southwest(S-SW) highlands, and rift margins, which frequently receive high intensity of rainfall for long duration of the year (Mewa, G; Megistu, F, 2022). As cited by (Azeze, 2019) the mountainous topography of Ethiopia is mainly characterized by a steep slope, deep gorge, frequent fault escarpment, highly weathered rocks, unconsolidated colluvium deposits, residual soil deposits, combined with intensive and extended rainfall which are favorable for the occurrence of slope movements and landslide hazards in most parts of the country (Tsege, 2017).

Numerous road development projects in the nation have frequently had landslides, which result in both financial and human losses. In Ethiopia's most untamed areas, road infrastructure projects involving deep excavation and high fill sections have a lengthy history of landslide disasters. Landslide accidents are particularly common in road development projects that involve deep excavation and high fill portions in Ethiopia's most rocky regions.

The road network's susceptibility to landslides has not yet been examined, and the Gore - Masha - Tepi Design and Build Road Project Segment is one of the corridors that were regularly impacted by landslide incidents. The current gravel road has failed at various points, numerous drainage infrastructures has been damaged, and homes and farmlands have been destroyed as a result of the landslide on the road segment that runs from Gore - Masha - Tepi town. It is crucial to carry out an integrated method of landslide assessment, evaluation of potential failure reasons, and susceptibility analysis/mapping in order to pinpoint the underlying causes of the current landslides and prevent any further occurrences.

Landslide susceptibility mapping has been carried out using a variety of methods by scholars and practitioners worldwide. It is crucial to perform landslide susceptibility analysis during the route selection and detail engineering design phase in order to identify landslide-prone areas using available landslide data, especially for road construction projects, in order to reduce the risk of failure due to landslide incidence. Various professionals in several geological and engineering streams have used a variety of methods and approaches for this aim, which are primarily classified as qualitative, quantitative, or semi-quantitative approaches.

Qualitative approach is widely used method which mainly characterized by its descriptive expression based on the subjective opinion of the professional conducting the analysis. The widely used qualitative methods for landslide susceptibility are Heuristic, Landslide Inventory, Landslide Hazard Evaluation Factor (LHEF) and Slope Stability Evaluation Parameter (SSEP) (Anbalagan, Azeze, & Fell, 2019)

However, the quantitative approach unlike the qualitative one it mainly depends on the statistical scheme and the involvement of the professional judgement is not significant the most popular quantitative approaches used for the landslide susceptibility analysis are statistical and deterministic approaches.

In statistical method the result of landslide inventory is compared with the physical terrain factors influencing landslides (Casagli, 2004). Even though such methods are theoretically simple, they have limitations due to the high level of complexity in identifying the slope-failure processes, methodically collecting and representing all contributing factors related to land slide and applying geomorphological predictive model of failure over large areas (Guzzetti F. , 1999) In addition, there are also various local indicators(creeps, crevices and trenches)that are essential in the forecasting of a landslide event but are not included in the analyses (Casagli, 2004).This approach is not equipped to come up with the factor of safety, which can be used as quantitative information about the slope stability (Dou J. , 2015). Engineers, on the other hand, have employed a deterministic approach to evaluate the area's landslide susceptibility using slope stability analysis in order to calculate a safety factor. When the area being studied is small and easily accessible to gather the necessary data, this method might be used.

The semi-quantitative approach is the fusion of both the qualitative and quantitative approaches which currently used by the various researchers for the preparation of landslide susceptibility map (Panchal , S; Shrivastave, A.K, 2022). The semi-quantitative approach widely employed by the engineers and practitioners mainly on the area of road sector due to its powerful capability to weight the contribution factors with less landslide inventory data (Fell, 2008).

1.2. Statement of the Problem

Due to landslides and associated failures, a considerable number of road projects over the past 50 years have encountered difficult issues both during construction and during operation. Considering the risks involved, the amount of time and effort spent on landslide research and vulnerability mapping before construction starts is insufficient. Before beginning any permanent engineering, work or building activities, thorough landslide evaluations are necessary due to the possibility of landslides on the road networks. A significant step toward comprehending the types and mechanisms of failure and creating a landslide susceptibility map is determining the elements that cause and worsen landslides. Road construction engineers and governmental road asset administration organizations can utilize the results of the landslide susceptibility analysis as input for project planning, route selection, engineering design preparation, construction work execution, road asset management, maintenance, and rehabilitation activities. Sufficient knowledge of the causative causes is also necessary in order to provide appropriate remedial actions for the active landslides.

Throughout its Asphalt Road service history, the Gore - Masha - Tepi Design and Build Road Project segment, which is distinguished by its rugged and steep landscape, has experienced frequent landslides and slope instabilities. The geography of the region, the state of surface drainage, the production of heavy residual soil, the presence of subsurface water, and the length of the rainy season are the main causes of slope instabilities, which occur at different scales and have distinct modes of failure.

Therefore, a road segment with several active landslide sites requires a thorough investigation to assess the kind and mode of failures, pinpoint the causes, and perform a landslide susceptibility analysis by considering the various factors that contribute to the occurrence of the landslide in order to identify areas that are vulnerable to it. Locations that have been identified as landslide-prone will receive the most attention, and a unique design and construction strategy will be used for them. Lastly, in order to stabilize the areas that have already been impacted by landslides, mitigation and corrective actions will be suggested.

The road section with several active landslide sites requires a thorough investigation to assess the kind and mode of failures, pinpoint the causes, and perform a landslide susceptibility analysis by considering the various factors that contribute to the occurrence of the landslide in order to identify areas that are vulnerable to it. Locations that have been identified as landslide-prone will receive the most attention, and a unique design and construction strategy will be used for them. Lastly, to stabilize the area, remedial measures will be suggested for areas that have already been impacted by landslides.

1.3. Research Questions

The purpose of the research is to respond to the following questions:

- What are the main causes and triggers of landslides along the portion of the study road?
- What landslide characteristics are present along the portion of the study road?
- Which landslide types and failure processes best describe the road segments that failed?
- How should the road section's landslide susceptibility analysis/map be created?
- What are the initial steps being taken to address the landslide along the road segments?

1.4. Research Objective

1.4.1. General Objective

This thesis work's primary goal is to conduct a thorough landslide assessment, susceptibility analysis, and mapping, as well as to offer initial remedial strategies for landslides along the Gore-Masha -Tepi Road Project.

1.4.2. Specific objectives

- To carry out an evaluation and inventory of landslides along the study road segment;
- To use the Analytic Hierarchy Process (AHP) method to create a landslide susceptibility map (LSM) of the road corridor
- To use PLAXIS Software to assess the slope's condition before and after treated.
- To propose a first-level corrective action for the landslide-affected road segments.

1.5. Scope of the Research

In addition to addressing the stated goals, the thesis proposes a remedial approach at the preliminary level. Using field data collecting and satellite image analysis, landslide inventory and mapping the study employed fieldwork, and software analysis are carried out slope condition before and after treated. along the road segment. The role of various conditioning and triggering elements, as well as the spatial distribution of landslides, are all methodically investigated. When doing the landslide assessment and susceptibility analysis, the results of the site survey and detailed desk study that were carried out to describe the mode of failure, material type, hydrological condition, extent, and severity of the landslide were used. Preliminary corrective actions are suggested in accordance with the identified cause factors for the landslide. The Gore-Masha-Tepi Road Project landslide portion is the only area where the study's conclusions and suggested corrective actions can be used.

1.6. Significance of the Research

These days, it is clear that landslides have grown to be a significant problem and the one that practicing engineers are most worried about during the road project's project assessment, route selection, engineering design, and construction phases. It will be easier to prevent or lessen the chance of failure due to a landslide if the intended routes' landslide susceptibility is known before permanent construction work begins. In a similar vein, it is crucial to assess the underlying reasons and offer workable corrective methods for road segments that have already been impacted by landslides.

The problem can be greatly addressed by combining a systematic multi-criteria decision-making approach with a powerful tool in the ArcGIS environment to assess the current landslide, analyze the susceptibility, identify the causative factors, and provide a workable remedial measure using all available geotechnical, geological, hydrological, climate, and environmental data. The results of this study can be applied to other road projects that are dealing with landslides; they are not just restricted to the project under consideration.

1.7. Structure of The Thesis

There are five major chapters in the thesis. The first chapter comprises the general introduction to landslide, statement of the problem, research objective, scope of the research, and significance of the research, Chapter Two presents the literature review of the general slope stability concepts, general cause's remedial measures for slope instability landslide susceptibility mapping using analytic hierarch process (AHP) and Slope stability analysis using PLAXIS2D software. Chapter Three is dedicated to a brief description of the road project with due emphasis on project location, topography, Geomorphology, climatic conditions, geology, topography and drainage condition of the study area. Furthermore, Chapter Four landslide inventory detailed investigation of the selected failed section, landslide contributing factors, model validation of landslide susceptibility analysis and analysis of failed cut slopes/landslide's locations remedial solutions for the slide locations and the conclusions and recommendations of this thesis report are discussed in Chapter Five.

CHAPTER TWO

LITERATURE REVIEW

2.1. General

Landslides, as described by (Varnes, 1984) (Wachal D. , Hudak P.F, 2000) (Varnes, 1984; Wachal D., Hudak P.F, 2000) and (Highland, L. & Bobrowsky, P., 2008) refer to the downward movement of rock and loose earth material near the surface, influenced by gravity, often occurring without a distinct sliding motion. These events are particularly frequent in tropical regions, where significant rainfall—both in quantity and intensity—contributes to their increasing occurrence (Nugroho, 2012).

Since the latter half of the 20th century, the number of destructive landslides has grown considerably across the globe, along with a surge in related research. However, studies on landslides within East Africa remain limited, despite the region experiencing widespread occurrences of slope failures. Factors such as steep terrain, substantial annual rainfall, expanding population pressure, deforestation, earthquakes, and extreme weather conditions render many East African areas highly prone to landslides. Additionally, these events impose substantial economic, social, and geomorphological impacts (Kissi, 2012).

Landslides have been recorded in multiple East African nations, including Uganda, Kenya, Tanzania, Rwanda, the Democratic Republic of Congo, and Ethiopia. Although various elements contribute to landslide susceptibility, certain common conditions are present across many affected regions. These factors fall into three categories: preconditions, preparatory factors, and triggering factors. Preconditions are static conditions that enhance the effectiveness of other factors, with steep slopes, deeply weathered clay-rich soils, and high annual rainfall being critical contributors in East Africa. Preparatory factors make the terrain vulnerable to movement without directly initiating landslides. Key examples include human activities such as deforestation, land-use modifications, construction, and excavation. Lastly, triggering factors are immediate causes that set landslides in motion, with earthquakes and extreme rainfall being the most significant drivers (Kissi, 2012).

As outlined by (Anbalagan R. , 1992) and (Reghuvanshi, 2014), landslide causative factors are classified into two primary categories: intrinsic or inherent factors and external or dynamic factors. By analyzing these influencing elements along with past landslide occurrences, it is possible to divide terrain into homogenous domains and rank them according to actual or potential landslide susceptibility (Reghuvanshi, 2014) (Varnes, 1984) (Wachal D. , Hudak P.F, 2000).

Given the severe consequences landslides impose on transportation systems, infrastructure, public works, private property, and both human and animal life (Dai,F & Lee,C.F, 2002) (Woldeargay, 2013), research on this natural hazard has gained global attention (Varnes, 1984).

2.2. Factors Influencing Landslides

2.2.1. Intrinsic Factors

As noted by (Anbalagan R. , 1992) and (Reghuvanshi, 2014), intrinsic parameters refer to the fundamental or fixed factors that influence whether a slope remains stable or becomes prone to instability. These include aspects such as the slope's shape and structure, the composition of its materials, the presence of fractures or structural discontinuities, patterns of land use and vegetation cover, as well as groundwater conditions.

2.2.2. Slope Geometry

Intrinsic parameters, such as slope morphometry and relative relief, play a crucial role in determining slope stability (Reghuvanshi, 2014). According to (Hoek.E & Bray,J.W, 1981), slope morphometry reflects the steepness of a slope, which directly impacts its susceptibility to instability. They state that as the slope becomes steeper, the probability of instability increases. (Varnes, 1984) further explained that while landslides can occur on any slope, the risk significantly rises with increasing slope steepness.

Relative relief, which represents the difference between the highest and lowest elevations within a section, also influences slope stability. The higher the relative relief, the greater the likelihood of instability (Bekele, 2010) (Reghuvanshi, 2014).

2.2.3. Slope Material

According to (Varnes, 1984), slope materials can consist of rock, soil, or a combination of both. Their shear strength, permeability, and susceptibility to physical and chemical weathering are influenced by factors such as composition, fabric, texture, and other intrinsic properties. The characteristics of slope material, including grain size, shape, sorting, and the quantity and type of cement, are essential in determining its overall stability. Unconsolidated materials tend to be more prone to instability than consolidated ones due to their lower cohesion and friction and higher infiltration rates (Varnes, 1984).

The interaction between slope material and morphometry plays a crucial role in defining the type of landslide that may occur. In regions with steep slopes and hard bedrock, such as basalt, welded ignimbrite, limestone, and sandstone, rockfalls, toppling failures, and rockslides or avalanches are common (Varnes, 1978) (Temesgen, 1999) When slope material consists of deeply weathered volcanic rocks, particularly pyroclastic deposits, rapid landslides involving eluvial-colluvial layers—such as debris slides and avalanches, debris flows, earth flows, and mudflows—are more frequent.

In areas where the slope material includes alluvial and colluvial deposits located at the base of steep slopes, or thick weathered layers on volcanic bedrock, rotational slides are prevalent, often transitioning into earth flows or mudflows. Additionally, rapid translational slides may occur in slopes where a hard-competent layer overlays a soft clay-rich bed dipping downward. On the other hand, slow translational movements are more likely to develop in terrain dominated by thick alluvial and colluvial deposits (Varnes, 1978) (David,M. Cruden & David J.varnes, 1996).

2.2.4. Structural Discontinuities

As noted by (Bell, 2007), a discontinuity refers to a structural weakness within a rock mass where the material is not continuous. Both primary and secondary discontinuities—including bedding, joints, foliation, cleavage, folds, and faults—act as weak zones within a slope. Their presence significantly affects slope stability, particularly when their inclination promotes downward movement.

The strength of joints and other geological surfaces is generally lower than that of the surrounding intact rock, making them the most fragile elements of slope geology. Consequently, understanding their characteristics—such as orientation, spacing, continuity, roughness, separation, and the composition of filling material—is essential in evaluating their influence on slope angle, direction, and overall stability. Additionally, fault zones contribute to an increased likelihood of landslides by forming steep slopes and generating weak, sheared zones (Wachal D. , Hudak P.F, 2000).

2.2.5. Land Use and Land Cover

Land use and land cover play a crucial role in determining slope stability. Vegetation enhances slope stability by increasing shear strength and influencing climatic interactions with the natural mass. By shielding the ground from direct exposure to sunlight, wind, and rainfall, it mitigates soil erosion.

Additionally, vegetation cover regulates water infiltration into the slope, though its effectiveness varies depending on factors such as soil depth, slope gradient, and vegetation type. Plant roots further contribute to stability by binding soil particles, strengthening the mass. Areas with dense vegetation tend to exhibit lower susceptibility to slope instability compared to regions dominated by sparse vegetation, agricultural activities, or urban expansion. Conversely, locations with minimal vegetation cover are more exposed to erosion and weathering, as ground cover plays a significant role in maintaining stability (Varnes, 1978) (Temesgen, 1999) (Turrini, A., & Visintainer, P, 1998) (Wachal D. , Hudak P.F, 2000) (Bekele, 2010) (Reghuvanshi, 2014) (Woldearegay K. , 2013).

2.2.6. Groundwater

Groundwater saturation within a slope weakens the shear strength of the material and generates pore water pressure, which plays a crucial role in slope stability (Waltham, 2009) (Highland, L. & Bobrowsky, P., 2008) As noted by (Waltham, 2009), when groundwater permeates jointed rock formations and soil masses, it reduces the overall shear strength of the slope material by increasing joint water and pore water pressure, making the slope more susceptible to instability.

2.3. External factor

As outlined by (Varnes, 1984), (Dai, F. C., & Lee, C. F., 2001), and (Reghuvanshi, 2014), external causative factors are dynamic and temporary influences introduced by new events. These factors include natural occurrences such as rainfall, volcanic activity, and seismic vibrations, as well as human-induced activities that can contribute to slope instability.

2.3.1. Rainfall

the impact of climatic factors, particularly rainfall, on landslides has been observed by (Ayalew, 1999). Climate plays a significant role in mass wasting events, as intense precipitation can generate hydrostatic pressure and facilitate slope movements. (Ngecu, W. M., & Mathu, E. M, 1999) documented that the landslides affecting Kenya between 1997 and 1998 were primarily caused by prolonged heavy rainfall, which led to excessive soil saturation. Rainfall is recognized as a key trigger for landslides, as increased water infiltration weakens soil strength.

Despite the widespread occurrence of landslides, research on the issue in Ethiopia—particularly in the southern regions—remains limited. There is a notable gap in data regarding rainfall thresholds, patterns of occurrence, and characteristics necessary for GIS-based landslide monitoring (Charlotte, 2010). Exceptionally intense rainfall on May 9, 2016, linked to the El Niño weather phenomenon, resulted in significant landslides in Ethiopia. Rainfall-induced flow-like landslides are common in mountainous landscapes across the globe (Version, 2000), posing serious natural hazards and causing extensive damage (Brenner, 2003).

Numerous statistical analyses have been conducted to establish rainfall threshold values and their correlation with landslide occurrences (Caine, 1980) (Glade, 2000) (Wieczorek, 2000) (Mikos, M., Cetina, M., & Brilly, M., 2004) (Shakoor, A., & Smithmyer, A. J, 2005). Water significantly affects soil cohesion, strength, and viscosity, making it a crucial factor in slope stability. (Crozier, 1986) argues that low-pressure systems, particularly tropical cyclones, are major contributors to landslide-triggering rainstorms due to their intensity. This observation aligns with (Temple, 1972) who found that tropical cyclones were responsible for exceptionally heavy rainfall in 1970, causing thousands of landslides in Tanzania’s Mgeta Valley.

When rainwater infiltrates the ground, pore water pressure rises, weakening the cohesion of soil particles. In extreme cases, the overburden of soil and water can become buoyant on the underlying pore water, eventually bursting from voids and initiating slope failure. Additionally, pore water pressure may surge when groundwater levels rise following intense rainfall, further compromising slope stability.

2.3.2. Seismicity

Earthquakes are a significant factor contributing to landslides in various regions across the globe. According to (Highland, L. & Bobrowsky, P., 2008), strong seismic ground motion serves as a key triggering mechanism for large-scale landslides, as ground shaking accelerates water infiltration and weakens slope stability. The shaking reduces the shear resistance of slope materials while simultaneously increasing excess pore water pressure, further exacerbating instability and increasing the likelihood of slope failure (Highland, L. & Bobrowsky, P., 2008).

2.3.2. Man-made Factors

Human activities significantly affect slope stability, often leading to instability either directly or indirectly. Changes in drainage patterns, slope destabilization, vegetation removal, excessive excavation at the base, loading of the upper slope, and irrigation are among the key factors that contribute to slope failure. These disturbances weaken the structural integrity of the slope, increasing the risk of landslides ((Highland, L. & Bobrowsky, P., 2008).

2.4. Classification of Landslides

Landslides have been classified in various ways, with one of the most widely accepted systems being the classification proposed by (Varnes, 1978). This system categorizes landslides based on two key aspects: the type of material involved and the nature of movement.

Regarding material composition, five distinct types are identified. Rock refers to a solid or firm mass that remained intact and in its original position before the onset of movement. Soil consists of a collection of solid particles, typically composed of minerals and weathered rock, either transported or formed in place. The pores within the soil may contain gases or liquids that are considered part of the soil structure. Earth describes material in which at least 80% of particles are smaller than 2mm, marking the upper limit for sand-sized particles. Mud consists predominantly of finer particles, with at least 80% measuring less than 0.06mm, which is the upper boundary for silt-sized material. Debris is characterized by a mix of coarse and fine particles, where 20% to 80% exceed 2mm in size, while the remaining portion consists of smaller particles.

In addition to material type, landslides are also classified by the manner in which they move. The five types of movement are described sequentially, reflecting variations in slope displacement dynamics and the mechanisms that govern their occurrence.

Table 2.1: Landslide classification version of mass movements

Mode of Movement		**Slope Material Type**		
			Residual/Transported Soil	
			Predominantly Coarse	**Predominantly Fine**
Fall		Rock Fall	Debris Fall	Earth Fall Topples
Topples		Rock Topples	Debris Topples	Earth Topples
Slide	Rotational	Rock Slide	Debris Slide	Earth Slide
	Translational			
Lateral Spread		Rock Spread	Debris Spread	Earth Spread
Flows		Rock Flows	Debris Flows	Earth Flows
Complex		A combination of two or more principal types of movements		

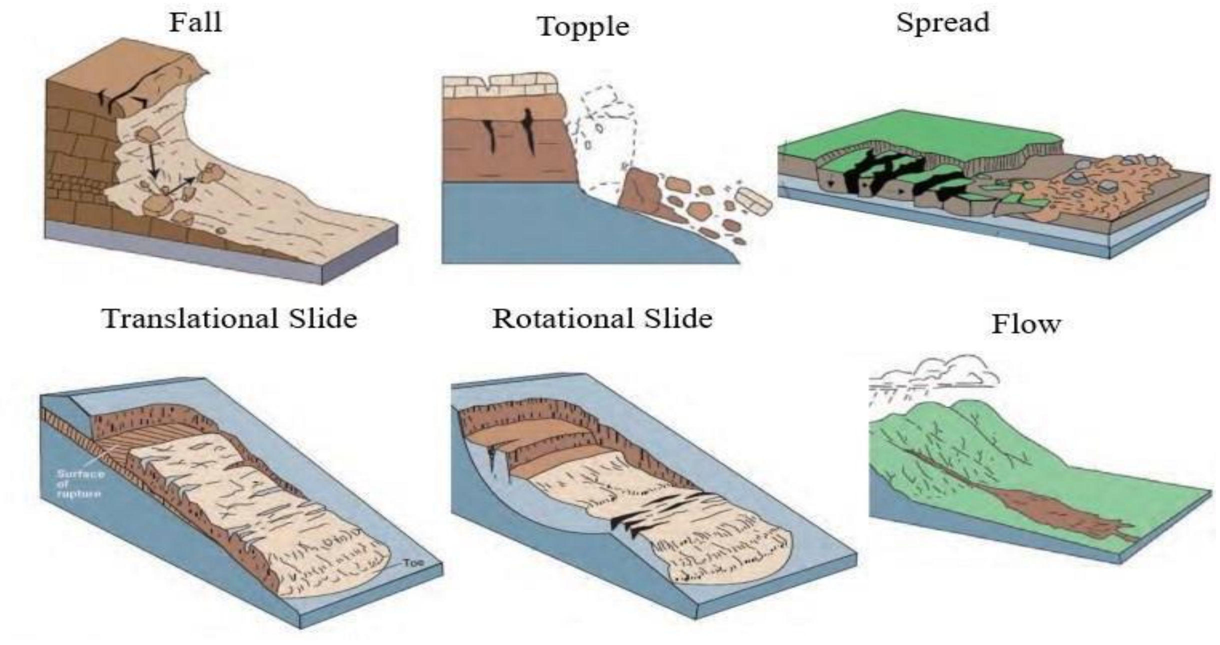

Figure 2.1:Typesofmassmovement ***(Cruden, 1996)***, ***(Varnes, 1978)***

2.5. Analysis of Landslide Susceptibility

Landslide susceptibility, as described by (Brabb, 1985), refers to the likelihood of a landslide occurring in a given area, considering both intrinsic and extrinsic factors. It provides insight into locations most prone to landslides. Similarly, landslide susceptibility maps serve as valuable tools for determining suitable areas for infrastructure projects, urban expansion, agriculture, industrial development, and settlements. These maps also help identify high-risk areas that require avoidance, protection, or rehabilitation before implementing development plans that might disrupt the area's natural stability (Fell, 2008) (Petchko, 2014).

A thorough landslide susceptibility study requires an inventory of the existing conditions along the area's borders and an in-depth analysis of all variables contributing to landslide occurrence (Arbanas & Arbanas., 2015); (Highland, L. & Bobrowsky, P., 2008). In road design and construction, susceptibility mapping plays a crucial role in pinpointing areas suitable for building roads and recognizing potentially hazardous zones that must be assessed before permanent engineering works commence.

Various techniques have been developed through multiple studies to evaluate and map landslide vulnerability. These methods fall into three main categories: semi-quantitative approaches, qualitative assessments (expert evaluation methods), and quantitative techniques based on statistical analysis (Tyagi, A Tiwari,R & James, N, 2022). There are fundamental assumptions that must be considered when conducting landslide susceptibility analysis and mapping to ensure accuracy and reliability.

I. The combined significance of the area's historical history and current state is extremely high when creating the landslide susceptibility map. Future landslides are more likely to occur in environments that are same to those that caused landslides in the past in terms of lithology, climate, geology, hydrology, and geomorphology. These circumstances are the primary causes of recent and current landslide incidents, and since they are violent and erratic, external triggering factors must to be taken in to account. (Guzzetti F. , 1999) (kanungo, D.P., Arora, M.K., sarkar, s. & Gupta, R.P., 2009)
II. Landslide occurs under the unique geomorphological and geological features can be determined, categorized and mapped both through site investigation and image interpretation (Fell, 2008; Guzzetti F. , 1999).
III. The majority of landslide events occur in the past and are marked by obvious geomorphological features that may be mapped and categorized using remote sensing or field surveys. . (Guzzetti F. , 1999; Serdavic, A; Babic, F, 2019; Varnes, 1978).
IV. Physical rules that can be described using statistical, empirical, or analytical methods influence the landslide process. A prediction model of the area's susceptibility to landslides can be created by identifying and analyzing factors that contribute to the occurrence of landslides with varying degrees of effect. (Guzzetti f. , 2005) (Guzzetti F. , 1999)
V. Mechanical the occurrence of landslide across the study area can be anecdote from the expert evaluations, analyzed from contributing factors condition or drawn from the modelling. Hence, an area can be categorized in to specific

susceptibility zone based on probabilities (Casagli, 2004) (Guzzetti f. , 2005) (Guzzetti F. , 1999)

2.5.1. Qualitative (Expert Evaluation) Method.

The data employed in the qualitative (Expert Evaluation) method are descriptive and non-numeric, and a sizable amount of subjectivity is incorporated into the creation of the area's landslip susceptibility study. This method mainly includes heuristic, landslide inventory mapping, landslide hazard evaluation factor (LHEF) and slope stability evaluation parameters. (SSEP)

I. Heuristic method

The landslide susceptibility map is created using the heuristic approach, which relies on the professional judgment of the person conducting the susceptibility study. ***(Fell, 2008)***. However, the primary drawback of this approach is its subjectivity when evaluating the relevant components. The expert's ability to illustrate the geotechnical, geological, geomorphological, and environmental processes in the region directly affects how reliable this method is. ***(Guzzetti F. , 1999)***.

II. Landslide inventory method

The most straightforward and straightforward qualitative technique for mapping landslide susceptibility is the landslide inventory approach, sometimes referred to as the distribution analysis method. With this approach, the susceptibility map was generated straight from the landslide inventory data that was gathered. ***(Casagli, 2004)***. Field surveys, historical event records, satellite imagery, and aerial photos can all provide information about landslides. This method's main drawback is that the susceptibility analysis does not include locations outside of existing landslides where no active landslides were detected during the study period. Additionally, this approach is unable to provide data on the variations in landslide distribution over time.

III. Slope Susceptibility Evaluation Parameters (SSEP)

The Slope Susceptibility Evaluation Parameter (SSEP) approach mainly use both intrinsic causative and extrinsic triggering factors in order to generate the landslide susceptibility map.

IV. Landslide Hazard Evaluation Factor

Unlike the SSEP approach, Landslide Hazard Evaluation Factor (LHEF) is exclusively relay on major intrinsic contributing factors such as geomorphology, ground water, hydrological and drainage condition of the area, land use/cover and lithology of the area ***(Anbalagan, Azeze, & Fell, 2019)***. The landslide susceptibility map excludes elements that trigger landslides, such as rainfall and the seismicity of the region being studied.

2.5.2. Quantitative (Statistical) Method

Numerical assessments (probabilities) of the likelihood of landslides in any danger zone are produced by quantitative approaches. ***(Guzzetti F. , 1999)***. The statistically based approaches evaluate the relationship between the current occurrence of landslides and the intrinsic and extrinsic elements that contribute to them. These methods, aided by knowledge of geographic information systems (GIS), have been applied to create maps of landslide vulnerability. This strategy primarily depends on the correlation between each element and the current distribution of landslides ***(Fell, 2008)***. Following that, a statistical correlation was found between potential contributing causes and the landslide inventory's mapped existing landslides. The method's limitations include from insufficient resolution of certain data sets, erroneous landslide inventory data, and mapping errors, as it heavily relies on the availability of high-quality data. ***(Fell, 2008)***. The primary benefit of the quantitative approach over the expert evaluation method is that the latter relies less on expert observation and more on mathematical models and expressions. Because of this characteristic, the quantitative approach yields more dependable results than the qualitative one. One kind of quantitative approach is the statistical method, which assesses the spatial distribution of slope stability by examining the relationship between the contributing elements and previous or current landslides. One of the problems with the statistical approach is the inability to locate high-quality and precise landslide factor data, which makes it laborious and logistically challenging to get over a wide area. Bivariate and multivariate methods are the two main groups into which statistical methods are further separated. The usage of strong GIS tools is quite helpful in this investigation.

2.5.3. Semi-Quantitative Method

The popular technique that developed from the qualitative approach is the semi-quantitative method. The semi-quantitative approach uses the ranking and weighting of the parameters that contribute to landslide occurrence in order to improve the qualitative method's high reliance on expert evaluation and its subjectivity. The highly effective semi-quantitative technique for landslide susceptibility assessments is Multi Criteria Decision assessments (MCDA).There are several well-known and commonly used techniques that employ a multi-criteria decision-making approach, including fuzzy logic, ordered weighted average, weighted linear combination, and analytical hierarchy process (AHP) In order to choose and rank the landslide contributing elements in the most reasonable manner, the Analytical Hierarchy Process (AHP) is a multi-criteria, multi-objective decision making technique

2.6. Methods of Slope Stability Analysis

For a long time, one of the main responsibilities in the discipline of geotechnical engineering was to analyze slope stability. The slope stability analysis's issues are statistically unpredictable and difficult to handle. this challenge, several analytical techniques are developed over time. Therefore, the Limit Equilibrium method and the Finite Element Method are the two well-known methodologies in this area.

2.6.1. Limit Equilibrium Method (LEM)

It is a traditional slope stability analysis technique that has been applied extensively to landslide issues for many years. This approach primarily relies on slice approaches, where a failure surface is assumed and the sliding mass and failure surface are divided into fewer slices. Although there are three possible orientations for cutting these slices—vertical, horizontal, and inclined—the majority of investigators prefer the vertical cut. It involves computing the factor of safety from the force and/or moment equilibrium equations, considering a single factor of safety across the entire failure mass, and using assumptions to lessen the issue of indeterminacy. In geotechnical engineering challenges, LEM has its own set of advantages as well as disadvantages.

Advantages;

- Because of its relative simplicity, geotechnical engineers have had extensive experience using it to calculate the factor of safety over the years.
- Its capacity to assess stability's sensitivity to different input parameters

Disadvantages;

- Taking in to account presumptions on the shape or location of the failure surface, the slice's side pressures, and their direction could result in needless mistakes or misunderstandings.
- It is oversimplified to assume that the FS is constant across the whole slip surface, particularly if there are various soil types along the failure surface.

Changes in stress or deformation are not taken into consideration when there is no stress-strain equilibrium in the soil. Depending on how reliable the input data is, this approach can be further separated into two categories. These are

- Deterministic slope stability analysis: this approach calculates the FS using a predetermined set of material properties and conditions. The slope is deemed unstable or prone to collapse if the factor of FS is less than unity. One of the limitations of a deterministic analysis is that it ignores the input parameters' variability (Duncan, 1996).

Probabilistic slope stability analysis: this technique measures the likelihood that a slope would fail by taking in to account variations in the input parameters. The material's variability can be taken into consideration (Duncan, 1996).

2.6.2. Finite Element Method (FEM)

This method uses the constitutive laws that are appropriate for the materials in the slope to divide the slope into a finite number of regions or elements. These elements are connected at their nodes and at the established bounds of the continuum. In slope stability analysis, the Finite Element approach has become more popular due to the widespread availability of personal computers. As mentioned below, this approach is more universal and avoids a number of LEM's limitations.

- used when there is an increasing complexity in the soil profile, configuration, and depositions.
- Since it doesn't make any assumptions about the location or form of the crucial slip surface beforehand, it is more accurate than the limit equilibrium technique.
- This technique eliminates the assumption used in LEM to convert a static-indeterminate problem into a statically determinate one by calculating the stability factor of the slope using the stress-strain behavior of the soil as determined by a finite element stress analysis.
- During construction, it can be used to compute pore pressure, tensions, displacements, and other properties of the earth mass. Additionally, it is employed to monitor progressive failure and compute seepage failure. (Duncan, 1996)
- There is no assumption for slice side forces because the finite element method does not use the slice technique.

Despite being more suitable, this analytical approach is very dependent on the caliber of the input data and the specifics of the model configuration. Accordingly, FEM of slope stability study is carried out more for scholarly than for practical reasons. This is also because there is a wealth of well-documented data regarding the sensitivity of the groundwater table, slope configuration, employed soil material qualities, mesh size, various element types, and element nodes in the numerical simulation. (Lu, C.-Y., & Chih-Wei, L, 2011) In order to quantify field variables (such as displacement, stress, and strains) that are sensed at the nodes and guarantee continuities along the grid lines through appropriate interpolation relations, FEM has traditionally employed the displacement type of formulation.

The following should be taken in to account when applying FEM to any geotechnical issues:

- The process of choosing a suitable constitutive model that can meet the challenges
- Taking in to account the existence of several finite element types (such as triangular, quadrilateral, or isoperimetric).
- Ascertain that the data from field and laboratory tests needed to characterize the soil properties and, consequently, the soil model, are available.
- choosing appropriate software package kinds (PLAXIS, ABAQUS).
- establishing a suitable geometric model (2D or 3D) based on the real state of the issue at hand
- Taking the subject geotechnical structure's drainage state (drained and undrained) into consideration

FEM is utilized in this thesis to calculate the factor of safety and conduct a stability analysis of the topic failed slopes in order to achieve comprehensive comprehension and practical applicability.

2.7. Landslide Prevention and Remedial Measures

A component of the landslide study is landslide assessment and susceptibility analysis, which involves a thorough investigation of the designated area in order to lower the likelihood of landslide incidence. There must be workable repair and mitigation measures in place to prevent or lessen damage when the area has already been impacted by a landslide or faces an impending possible collapse ***(Highland, L. & Bobrowsky, P., 2008)***

Few attempts are made to identify the possible causes and prevent slope instability issues, despite the fact that there are numerous slope instability issues across the country. Even the few landslides that have been reported thus far have been identified either because they are located near important commercial routes, particularly those that extend infrastructure (roads, railroads, dams), or because the local population is impacted and requires vital government support. Otherwise, the problem of landslides and ground failures caused by them continues to be far more prevalent than is actually recognized. Over time, the extent of landslide disturbance has grown, impacting agricultural lands, infrastructure, and the land's natural equilibrium. (Asmelash, 2012)

When it comes to preventing landslides caused by road construction activities, the simplest solution is to avoid road construction on hilly terrain with rough terrain and sections with the scar of old or active landslides; however, this is not always practical. The engineering design process and route selection primarily rely on landslide susceptibility analysis, mappings, and the characterization of the affected areas to reduce the occurrence of additional failure by landslide.

Additionally, these regions are marked by significant levels of weathering, erosion, and slope instabilities because of their steep slopes, severe faulting, and fracturing. (Asmelash, 2012) Despite the lack of well-documented evidence on the timing and mechanism of various landslide sizes in the investigated area, some local knowledge indicated that they are either caused by earthquakes or by excessive rains. Additionally, these regions are marked by significant levels of weathering, erosion, and slope instabilities because of their steep slopes, severe faulting, and fracturing. Many of the ideal conditions for landslides in Ethiopia's highlands and rift margins have been compiled by some experts and are primarily related to their regional features. These include (Woldearegay K. , 2005) (Ayele, 2009) (Asmelash, 2012)

- The crystalline basement has metamorphic banding that ranges in width from a few millimeters to ten centimeters, and prior research suggests the presence of different migmatite structures and folding.

- The area is covered by a variety of lithologies representing Cenozoic bimodal volcanic rocks, volcanoclastic sedimentary deposits and Precambrian crystalline rocks (the basement).
- Deep gorges are a result of the drainage systems that severely fragment the region as they follow faults and lineaments.
- Inappropriate slope cuts made when building the roads that link the densely populated towns that surround these areas
- A number of springs and features that serve as drainage structures between highlands and lowlands are emerging, either in response to geological structures (fracture springs) or the hydraulic variations of the different lithological stratifications (contact springs). Slope instability is further exacerbated by the significant variation in their discharge between the dry and wet seasons.

In cases where landslides already affect. serving structures or where their existence cannot be avoided, physical controls can be used. Monitoring and warning systems could be useful for preventing and early mitigating landslides, even though there isn't much experience with the Ethiopian environment. Water is essential to landslides, as has been shown on numerous occasions in the past. For some landslide sites, controlling the surface and subsurface water may be the only practical remediation strategy. Among the corrective actions associated with water control techniques are

- Redirecting surface water away from landslide-prone or landslide-affected areas;
- Drain the ground water away from the landslide to lessen the chance of the ground water table rising;
- As a corrective solution, an impermeable membrane can be placed across the landslide-prone area to prevent saturation;
- Steer clear of irrigation projects close to landslide-prone areas if at all possible.

Similarly, offering physical support could be suggested as a corrective action to limit and halt the sliding mass's movement. Structures known as retaining walls are designed to sustain a soil mass over time without experiencing significant distortion. They are also employed when extending the side or back slope of a fill or an excavation with a level inclination is not feasible due to right-of-way restrictions. Retaining walls are also utilized to prevent surface water scour and river erosion of the slope toe. These walls are utilized as a corrective solution for the current collapse, not as a preventative strategy against landslides. Previous Studies

2.8. Previous Landslide Studies

There was a restriction on expanding the practice toward landslide assessment and susceptibility analysis for road networks, despite the fact that numerous scholars have worked tirelessly to identify the nature, kind, cause, and consequence of the landslide in various parts of the country. There was a lack of thorough and systematic landslide assessment and susceptibility study on the majority of landslide-prone routes during the project planning, route selection, and design stages. As a result of this strategy, several landslides occur either during the road's operation time or after construction has begun, resulting in fatalities and serious damage to the road asset. In general, a large number of studies on landslides that occurred in different parts of the nation were carried out by different scholars. The majority of research, however, is done from a geological standpoint, and there was a lack of application of the study results to the development of creative engineering corrective actions.

(Melese, T., Belay, T., & Andemo, A., 2022) Dejen district, which has seen numerous landslide incidents, was the site of an extensive study on landslide vulnerability. Using the most popular, generally recognized ensemble models the analytical hierarchal process (AHP), frequency ratio (FR), and Shannon entropy (SE) this study sought to determine which areas were vulnerable to landslides and assess how well they performed. A landslide inventory map was created after 87 landslides were identified in this investigation. Using the spatial database, twelve landslide triggering variables were created. Based on the data, the high and very high percentage of landslide susceptibility classes encompass roughly 54% of the research region for general land use planning and management, the results showed that the AHP model, with a success rate of 86.5% and predictive rate of 85.8%, outperforms the SE model (success rate = 85.6%, and predictive rate = 85.3%) and the FR model (success rate = 82.5% and predictive rate = 81.8%).

(Vařilová, Z., Kropáček, J., Šťastný, M., & Vilímek, V, 2014) Conducted landslide hazard assessment of Dessie town. The rapidly expanding regional hub of Dessie and its infrastructure are at risk from landslides. Using both remote sensing and field observations from 2013, four representative recent landslides have been chosen and thoroughly examined. Both natural and man-made factors have contributed to the reactivation and new landslide episodes that have been reported. Precipitation data from the Dessie weather station were analyzed because the primary external triggering mechanism is seasonal rainfall. It was also discussed to what extent human activity contributes to slope instability. Adequate measures were proposed when the identified endangered zones and real risk in the researched localities were determined.

(Suryanarayana, T., Gezahegn, D., Assefa, E., Seid, A., & Belachew, E. B., 2021) In northern Ethiopia, a thorough investigation of landslide processes was conducted in the city of Dessie and the surrounding area. Prior to conducting a semi-quantitative field study of the geological, geotechnical, geomorphological, hydrogeological, and anthropogenic factors that influence the units' susceptibility to landslide activity, the area was first zoning into a discrete number of smaller units with comparable sliding susceptibilities. The final landslide susceptibility map was created by applying traditional overlay techniques to pre-existing maps that depicted the many impacting components. A landslide-hazard map that displayed the actual distribution of landslide episodes that have previously happened was used to verify the method's validity. Ultimately, 22 distinct active landslide sites and four general landslide susceptibility zones were found. Complex earth and debris slide and flows in silty clay soils linked with alluvial and colluvial deposits topping highly worn basalts were the most significant forms of landslides. In regions with steep slopes, intact basaltic rocks experienced rock fall and toppling. During the rainy season, surface water and groundwater have been the primary causes of large-scale landslides.

(Irshad, T. Harikrishnan, Bose, M. Kurniati, T., 2024) The decision-making process for landslide susceptibility zonation mapping is wholly dependent on how land cover and land use vary from one location to another. The quality of the metrics utilized to assess the frequency and severity of the landslides was correlated with the study's accuracy and precision. The Geological Survey of India (GSI) and Landsat-8 satellite imagery provided secondary data for this investigation. Using the semi-quantitative Analytical Hierarchy Process (AHP) Technique, the landslide conditioning factor was determined. Thirteen parameters were examined in this study. Landslides in a low or high influence grade are caused by each parameter. Every parameter was given a specific weight according to how much of an impact it had on the likelihood of landslides. The main cause of landslides in the Wayanad district is rainfall. With the use of landslide inventory points, the final landslide susceptibility zonation map was verified using the proper mathematical treatment to ensure its accuracy.

(Wendim S. , 2023) This study focuses on the Gedo-Dilb Asphalt Road and its corridor in northern Ethiopia as one of the regions impacted by these hazards. This study's goals were to assess the traits and contributing elements of landslides, identify the crucial slope sections' stability, create a road corridor susceptibility map for development planning, and suggest mitigation strategies. The study's findings indicate that there are 103 active landslides in the region, spanning 8.44 km². Rock falls are frequent on steep slopes, and the debris/earth slides, which are made possible by gully erosion, range in depth from 0.8 to 12 meters. It was discovered that 9.5 km of the 16 km asphalt road segment was impacted by a number of interconnected risks, such as landslides, siltation of the road hydraulic structures, and erosion/scouring. Landslide susceptibility maps were created using the Analytical Hierarchy Process (AHP) approach, and the model's validity was assessed using the area under the curve (AUC). 75% of the landslides that were inventoried fell into the high and very high susceptibility zones, according to the AUC value of 0.82, which indicates a very good prediction of landslide susceptibility. According to this study, landslides in the region are linked to a number of interconnected factors that call for integrated solutions, such as drainage-based water management (surface and subsurface water), gully rehabilitation and stabilization, and bio-engineering solutions for slope stabilization.

(Lemenew, 2024) The Jimma-Chida route in Ethiopia's southern highlands in the basins of the Gibe and Gojeb rivers, which is vulnerable to landslides, particularly following intense rains, is the study's primary emphasis. The researchers weighted important criteria to create a landslide susceptibility map using the Analytical Hierarchy Process (AHP) and GIS. like lithology, elevation, rainfall, slope, slope aspect, land use/cover, distance to streams, distance to roads, and curvature. They discovered that rainfall, distance to roads, and distance to streams are the main factors influencing the occurrence of landslides. Smaller regions are classified as low and high risk, whereas the majority of the area (62.87%) is classified as moderate risk on the susceptibility map. As initial mitigation strategies, the study suggests drainage systems, retaining walls, slope reinforcement, and slope contouring.

2.9. Gaps of the Research

Despite the growing body of research on landslide susceptibility mapping and mitigation, several gaps remain, particularly in the context of the Gore-Masha-Tepi Road region. First, although landslide susceptibility mapping using Geographic Information Systems (GIS) and Analytical Hierarchy Process (AHP) is widely applied, the subjectivity involved in assigning weights to factors such as lithology, elevation, rainfall, slope, and land use/cover remains a critical issue. This subjectivity can lead to inconsistencies in susceptibility classification. This study addresses this gap by employing a systematic approach to weight assignment, utilizing field surveys, remote sensing data, and GIS analysis to achieve a more objective and reliable susceptibility map.

Second, while remote sensing and GIS are frequently used for susceptibility analysis, there is limited research integrating these methods with detailed geotechnical and geomorphological assessments specific to Ethiopia’s southwestern highlands, where the Gore-Masha-Tepi Road is located. The unique geological, geomorphological, and hydrological characteristics of this region necessitate localized studies. This research bridges this gap by incorporating field observations and laboratory testing to assess the characteristics, failure mechanisms, and extent of landslides in active zones along the road.

Third, although numerical modeling tools like PLAXIS2D are extensively used worldwide for slope stability analysis, their application in Ethiopia is minimal. Most existing studies rely on qualitative assessments, lacking detailed numerical simulations that can provide insights into slope behavior under different conditions. This study fills this gap by using PLAXIS2D finite element software to model slope behavior, allowing for a more accurate evaluation of slope stability and the identification of critical failure mechanisms.

Additionally, many studies provide susceptibility maps without translating their findings into actionable mitigation strategies. This is a significant limitation, as it leaves decision-makers without practical guidance for reducing landslide risks. This study overcomes this by proposing specific remedial measures for one critical landslide-affected cut slopes (Km45+350–45+440, km80+700-81+600 and km82+610-83+400). These solutions are based on a detailed understanding of slope characteristics and failure mechanisms, balancing long-term stability with technical feasibility.

CHAPTER THREE

Research Methodology

A major natural hazard that affects infrastructure is landslides, especially in steep or mountainous regions. For the purpose of creating efficient preventive and corrective actions in road projects, landslide susceptibility assessment is essential. The materials, techniques, and procedures used in a landslide susceptibility analysis and the suggested corrective actions for road projects are described in this publication.

3.1. Description of the Study Area

3.1.1. Location of the Road Section

Geographically Gore - Masha - Tepi Design and Build Road Project is located connecting three National Regional States namely Oromia, Southern Western Ethiopia, and Gambella, two zonal administrations Ilu Ababora and Sheka zones and five Woreda Administrations named Ale and Didu found in Oromia National Regional State, Ilu Aba bora Zone and Masha, Anderacha and Yeki found in Southern Western Ethiopia in Sheka Zone.

This route starts at Gore town round about and follow the existing roadroute alignment traversing the control points Gordomo town (at km 24.0 to 27.5), Baro river bridge, Chawaka village, Masha town (at km 53.2 to 58.3), Gongeri river bridge Yina village, Genchi River bridge, Gecha town, Yoki Chichi village, Irmichi, Kobitu and Tepi town (at km 138.2 to 140.66). The dominant land use along the road c orridor apart from the above settlement include cropland, plantation and natural forest in the roadside that will be affected due to widening of the existing road. The existing route alignment option around Masha and Getcha traverse close to protected forest, and close to buffer zone of Sheka Forest Biosphere. The route traverses in flat, rolling, mountainous and escarpment terrain for about 3%, 73%, 18% and 5% of the total length respectively. The total length of the road is 140.66 km in the south part of the country.

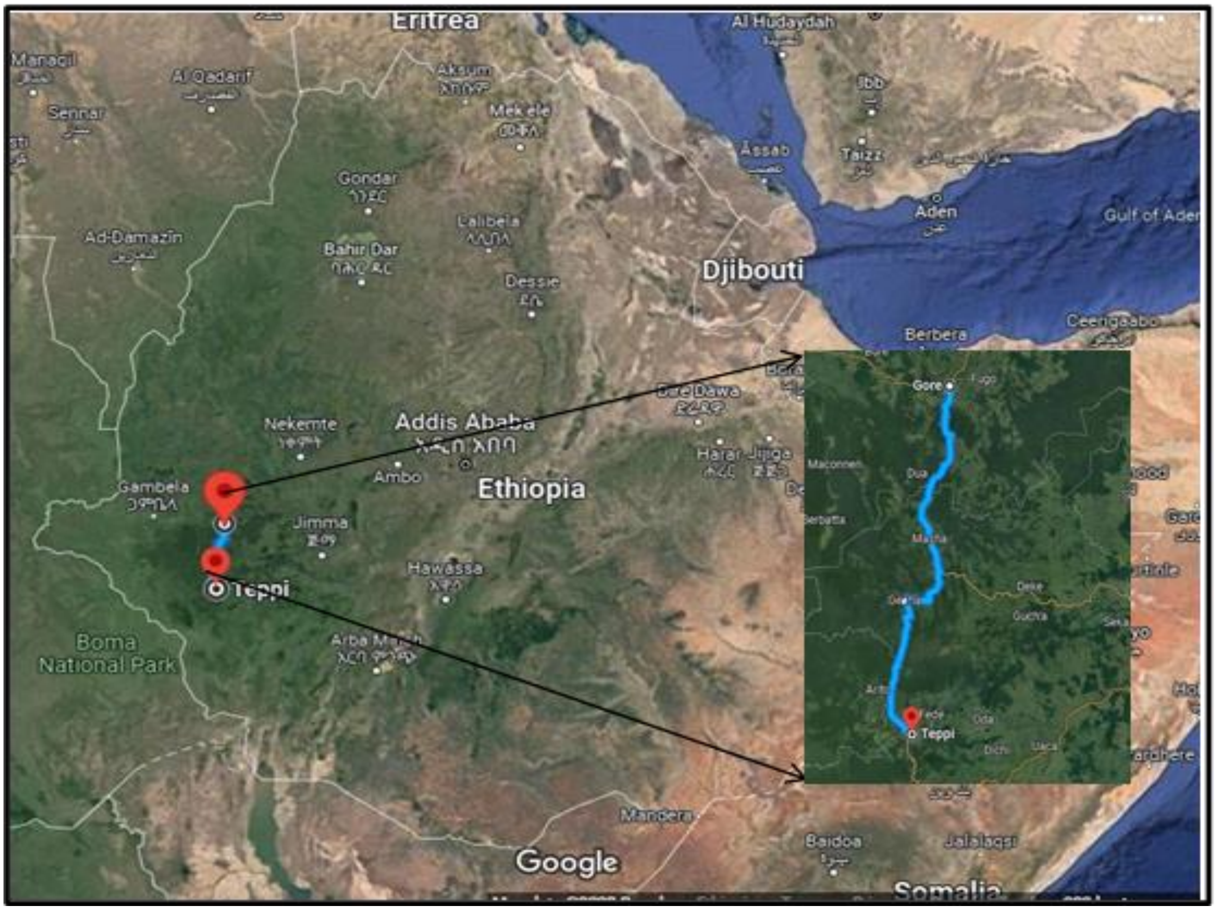

Figure 3.1: LocationMapof the Project

3.1.2. Topography (Physiography)

The project road starts in Gore town (Start of the project) at an elevation of 2046 m a.s.l. and the altitude rises from 2035 m to 2223 m when we go to Masha town at Km 53 and become 1,200 at the end of the project (Tepi town).

The project road starts in Gore town at an elevation of 2,035 m a.s.l. and gradually descends to an elevation of 1,800 m to the reach of Baro River, km 35 where it further descends to the river crossing 1,670 m. After crossing Baro River (the biggest river along the route) the alignment ground starts to ascend reaching to an elevation of 2,200 m (with a relief of 530 m) within a distance of about 10.5 km, Baro River crossing to km 50. Then the alignment ground gently rises to an elevation of 2,300 m before it starts falling to the Gongeri River crossing, km 66.9 and elevation 2,100m. From Gongeri River it ascends reaching a high of 2,540 m (km 78.5 the highest point) passing Yina Town/village. The alignment route then falls to an elevation of 1,890 m (Gonji River, km 86.8) where it starts to ascend to an altitude of 2,030 m then back to 1,800 m at Saki stream crossing. From this point, the route once again follows a rising ground to km117 where it finally starts to descend to lowest elevation resting at 1,200 m in Tepi town, the project end. The original ground profile for the project is shown in the figure 2-1 below. The original ground profile for the project is shown in the figure below.

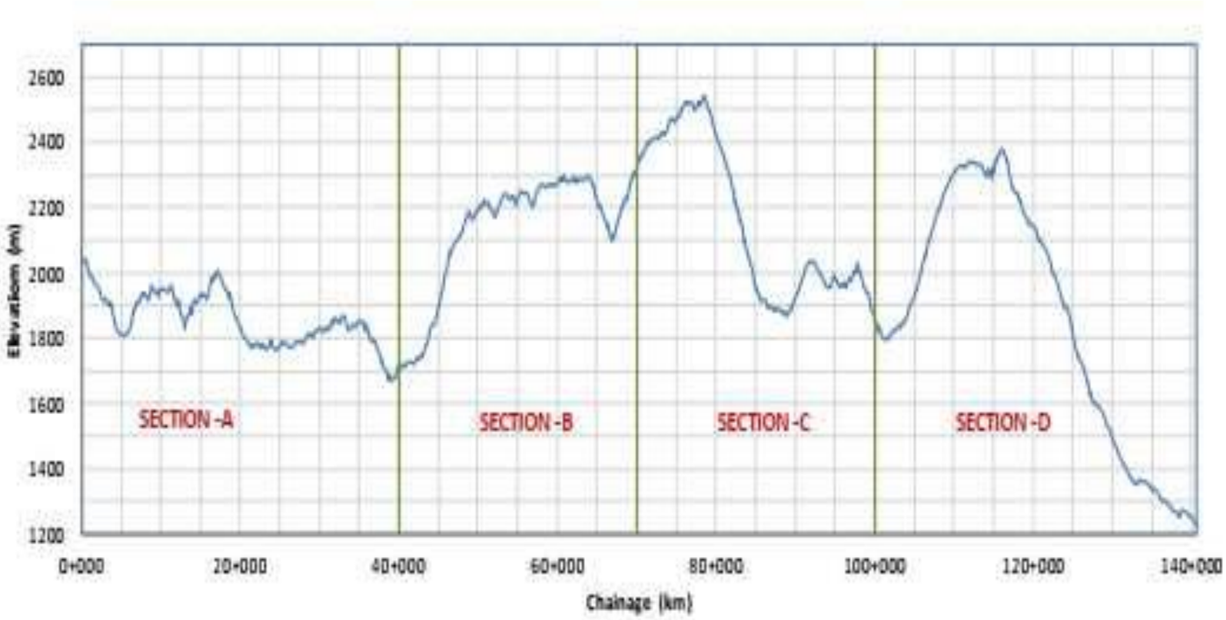

Figure 3.2 : Longitudinal profile of the existing road alignment

3.1.3. Geomorphology

The route alignment passes through the southwestern Ethiopian plateau in a general southerly direction starting from Gore veering to east and west influenced by abrupt This is depicted by morphometric elements (elevation and slope parameter) shown in Figure 4-1.

The land surface of the project corridor is marked by high relief (> 1,700 m) with a minimum altitude of 1,012 m ASL (around Tepi) and maximum 2,735 m ALS (km70 - km80), and mean value of 1,903 m at the standard deviation of 371.6m. The slope gradient is in the range of 0 to 44°, the mean value of 6.5° at the standard deviation of 5.1. More than 70% of the broad corridor of the project area is characterized by slope gradient below 1.5 -

6.5°, rolling. When the alignment strip is regarded it often traverses ground with slopes gradients in the range of 1.5 - 12°, rolling to mountainous. Land surface with higher slope gradient (ridges and escarpments) above 17° forms a small portion of the area and occurs along fault scarps.

The topography of the project site is dominantly rolling topography (5-25 degrees) while the remaining section consists of mountainous section with short occasional flat portions from site reconnaissance and Digital Elevation Model (DEM). The project road corridor is mostly sparsely populated and less farmed areas.

3.1.4. Climate

Climatic conditions in Ethiopia are largely governed by altitudinal variations that are controlling rainfall distributions to some degree and the temperature variation to a very large extent. The meteorological data for twenty years (from 1993 to 2012) for the three towns (Gore, Masha and Tepi) is collected from National Meteorological Agency of Ethiopia. The average monthly rainfall and temperature are presented in the figures below

Table3.1 Summary of Mean Monthly Rainfall (mm) Masha Town

Year	Jan.	Feb.	Mar.	Apr.	May	Jun.	Jul.	Aug.	Sep.	Oct.	Nov.	Dec.	Annual
2010	508	546	758	614	523	544	538	550	530	555	543	531	6739
2011	699	682	763	-	-	766	781	69	731	453	752	-	5694
2012	745	749	782	759	758	768	776	720	690	713	670	746	8876
2013	686	551	609	551	708	666	653	659	656	705	742	-	7185
2014	577	706	782	756	751	746	794	772	688	743	709	762	8785
2015	677	682	777	752	745	709	710	651	720	-	-	-	6422
2016	723	693	728	720	735	702	678	637	643	690	675	690	8312

2017	396	555	535	511	480	507	509	503	565	563			5122
2018	571	572	529	553	586	550	522	509	551	539	576	502	6560
2019	528	599	502	451	396	488	513	538	517	500	473	442	5948
2020	551	505	598	580	493	516	515	594	572	583	513	521	6541
Average	605	622	669	625	617	633	635	564	624	604	628	599	6926

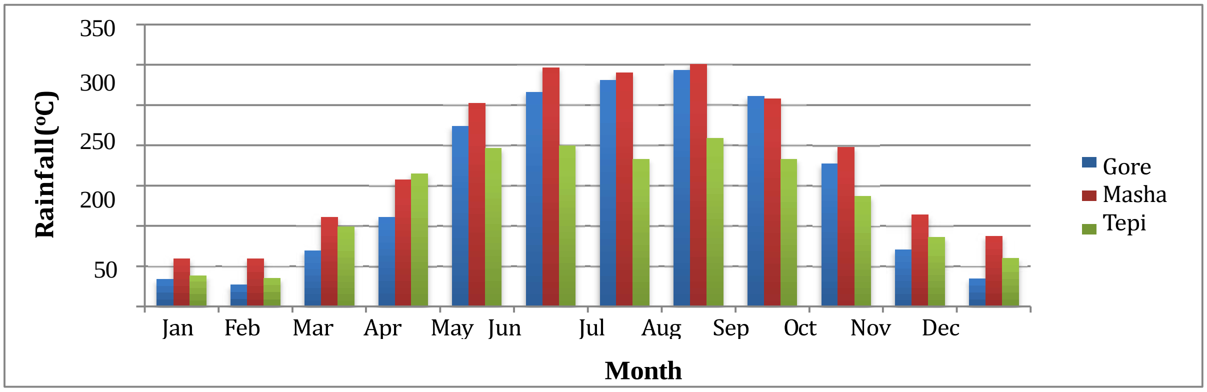

Figure 3.3: Mean Monthly Rainfall of Gore, Masha and Tepi

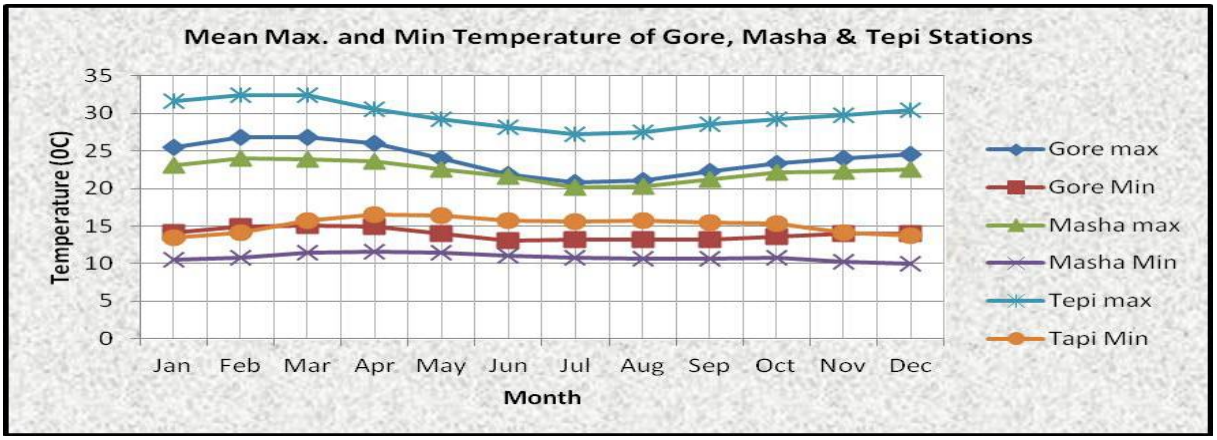

Figure 3.4: Average monthly minimum & maximum temperature of Gore, Masha &Tepi

From the meteorological data, Gore, Masha and Tepi get annual average rainfall of 1847, 2182; 1590 mm respectively indicating the area gets the highest rainfall amount in Ethiopia. The project area gets rainfall in all months of the year with relatively dry seasons with annual rainfall below 150 mm extends from November to March. The maximum average annual temperatures recorded for Gore, Masha and Tepi respectively are 23.9, 22.3 and 29.8^{0}C respectively. Generally, Masha gets highest amount of rainfall and small recorded average temperature as compared to Gore and Tepi.

3.1.5. Drainage and Landforms

owing to the high altitude and high rainfall the area exhibits dense drainage network that belongs mainly to the perennial Baro River The slope of drainage ranges from 0° to 28° and the mean value of 2.9°c. the stream network is characterized by a combination of dendritic, parallel and rectangular pattern that is related to bedrock type and geologic structures. An annular pattern in the southern part of the project route from Gecha to Tepi marks the occurrence of a volcanic shield in the area. The area is characterized by variable landforms comprising plateau plain, elevated hills (volcanic centers), high ridges, scarps of moderate height and valleys. Relatively elevated ridgelines show a linear and arcuate pattern and are associated with tectonic lineaments.

3.1.6. Regional Geology

In order to understand the geological features of the project area, a detailed site investigate on and desktop study of the geology of the project area was carried out. The project area is entirely located within the geological maps of Gore with Scale1:250,000 and Omovalley with scale 1:500,000 were used as reference during the study. The regional geology of the project area shows four types of geological formations. This are is covered by Cenozoic bimodal volcanic rocks, volcanoclastic sedimentary deposits and Precambrian crystalline rocks (the basement).

The basement represents the ancient metamorphic complex formed during the East African Orogeny in Neoproterozoic geologic time (900 Ma-500 Ma). The Cenozoic sequences are formed by igneous, tectonic and concomitant fluvio-lacustrine processes associated with the geodynamic development of a continental Rift extending to Kenya in the south. The tectonic activity started in middle Eocene ca. 49 Ma and has continued episodically to recent times. The distribution of the lithologic units is shown in Table3-1 and their general description is shown in Table below along with their roadbed geology. The characteristic feature of each lithostratigraphic unit is

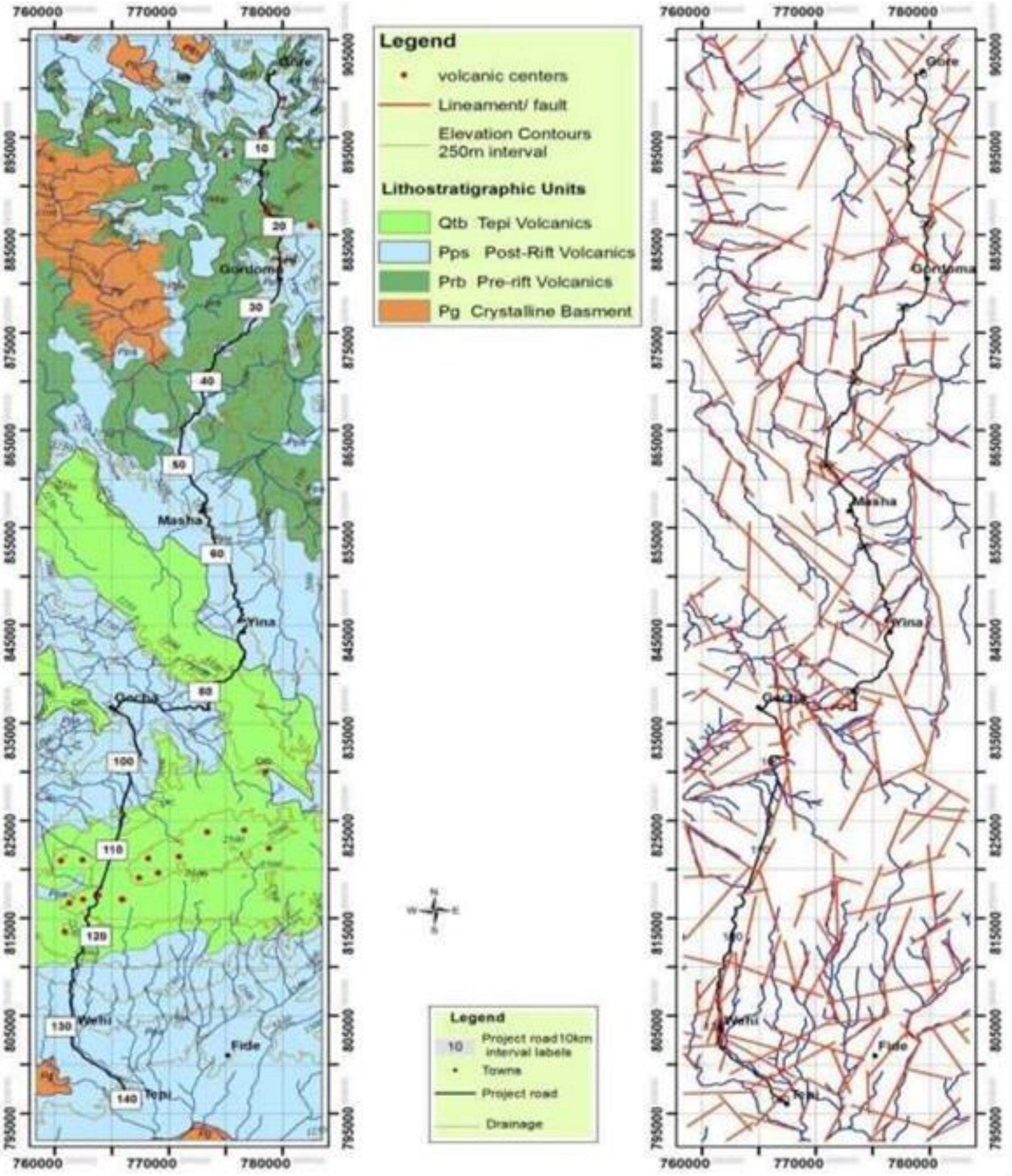

__Figure 3.5:__ Geological setting of the Project Area

Table 3.2: The distribution of the lithologic units

Geologic age			Formation	Lithology (symbol)	Description	Road geology, from-to (km)
Phanerozoic	Cenozoic	Quaternary	Superficial deposit	Qsd	Dark grey silty-clay and/or red-brown gravely sand silt (ferricrete)	Not mapped
			Tepi Volcanics	Qtb	Basalt and scoriaceous agglomerate	km 73~81, and km 107~123
		Oligocene Eocene	Post-Rift Volcanics	Pps	Trachy-basalt, rhyolite and pyroclastic rocks with minor trachyte and phonolite plugs	km 0~10, km 12~16, km 22~32, km 36~37, km 40~73, km 80~107, and km 123~141
			Pre-Rift Volcanics	Prb	Flood Basalts	km 10~12, km 16~22, km 32~36, and km 37~40
Precambrian			Granulite	Pg	Grey-light and greyish brown, banded pyroxene granulite and quartzofeldspathic gneiss	km 23.88~23.94

3.1.7. Regional Tectonic and Seismic Setting

The seismic hazard map of Ethiopia as provided in EBCS 8, 1995 is based on a 100-year return period or approximately 50% of being exceeded in 50 years. According to the map (Figure 4-15a), each seismic zone 1 to 4 is assigned a constant bedrock acceleration ratio, αo of 0.03, 0.05, 0.07 or 0.1, whereas Zone 0 is considered seismic free. The project site belongs to Zone 0 implying Seismic Free Zone.

A revised seismic hazard map for Ethiopia is prepared by Asrat Worku, Department of Civil Engineering Addis Ababa Institute of Technology, Addis Ababa University, based on Global Seismic Hazard Assessment Program (GSHAP), Journal of EEA, Vol. 28, 2011, Fig 2.2. It is prepared based on a return period of 475 years following the GSHAP standard as opposed to 100 years in the EBCS 8, 1995. Accordingly, five distinct seismic regions are identified with different ranges of PGA values as shown in the legend of Figure 4-15 b) below. Note that the ratio of the PGA to the gravitational acceleration, g, corresponds to αo, the bedrock acceleration ratio. When this is considered, the project area falls under PGA of<0.03 g. In conclusion, the geotechnical design will consider the project area seismic free. Seismic Hazard Map of Ethiopia as per EBC-8:1995

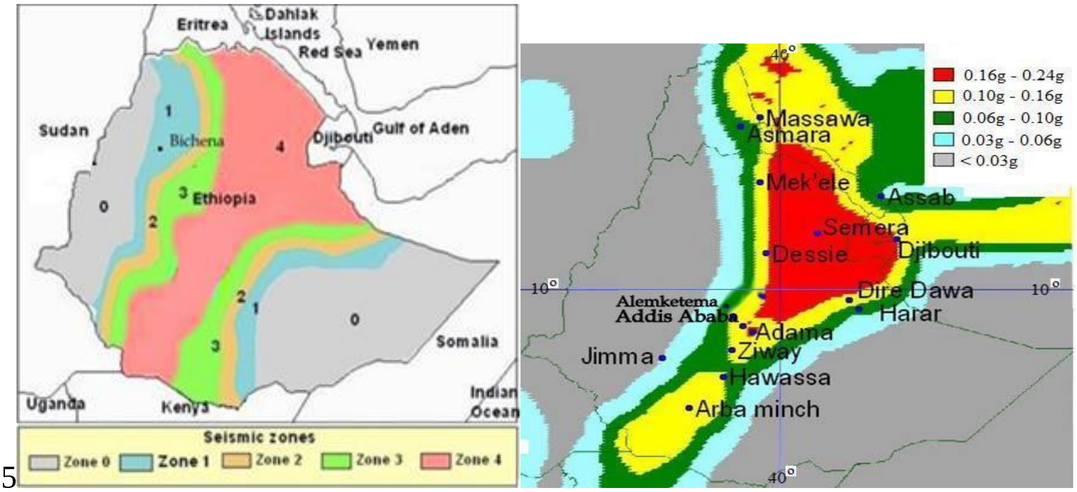

A) Seismic Hazard Map of Ethiopia as per EBC-8:1995

b) The seismic hazard map of Ethiopia based on the GSHAP data for a return period of 475 years

Figure 3.6: Seismicity Maps

3.2. Research Design

In order to evaluate landslide hazards and create mitigation plans along the Gore-Masha-Tepi Road in southwest Ethiopia, this project uses a mixed-method research strategy that combines field research, GIS analysis, and geotechnical modeling. A field survey, lab tests, and software analysis were all part of the study. In order to map recent and historical landslides, evaluate slope conditions, and gather soil and rock data for laboratory analysis, organized field investigations were carried out. GIS data to facilitate spatial analysis, high-resolution satellite imagery, digital elevation models (DEMs), rainfall data, and thematic maps (geology, land use, drainage) were obtained. Critical inputs for slope stability modeling came from laboratory testing of the data that was gathered, such as moisture content, shear strength, unit weight, and grain size distribution.

Key landslide occurrence factors, including lithology, elevation, rainfall, slope, slope aspect, land use/cover, distance to streams, distance to roads, and curvature, were arranged hierarchically, given relative weights, and integrated in a GIS environment using the Analytical Hierarchy Process (AHP). A landslide susceptibility map was created using ArcGIS's weighted overlay method, which divided the region into low, medium, and high-risk zones. Comprehensive geological and geotechnical analyses were carried out for the critical cut slopes. Slope behavior under current conditions and under several reinforcement scenarios was simulated using finite element modeling withPLAXIS2D software. These models assessed variables such safety factors, failure surfaces, and slope deformation.

Site-specific remedial methods were developed using the combined findings of slope stability analysis and susceptibility mapping. In order to ensure practical execution, the suggested steps sought to improve long-term stability and technological feasibility. The purpose of the recommendations was to advise road management officials and direct upcoming slope stabilization initiatives. During the course of this study different instruments such as hand-held GPS, geological hammers, measurement tapes, laptops and multiple software like Arc GIS, PLAXIS 2D Microsoft Office, Google Earth Pro, Global Mapper and Real Statistics in Excel were utilized. Similarly, various raster maps such as geological, geomorphological and topographic maps were also used as an input for this study.

3.2.1. Landslide Susceptibility Mapping using Analytical Hierarchy Process (AHP)

An area's likelihood of experiencing a landslide can be predicted using a landslide susceptibility map. The techniques used for the landslide susceptibility analysis often have advantages and disadvantages of their own. A great deal of professional subjectivity, for instance, goes into organizing the several causative factor data layers that contribute to landslide occurrences when using qualitative methodologies. When using a geotechnical approach, the method analyzes the slope that was impacted by the landslide using geotechnical factors; nevertheless, it is costly because it necessitates the mobilization of large teams and machinery, and it is unable to replicate the landslide's spatial distribution. (Azeze, 2019). A semi-quantitative method called the Analytical Hierarchy Process (AHP) was chosen for this study in order to create the landslide susceptibility map for the Gore-Masha-Tepi Road segment.

This approach characterizes the current state of the moving mass and the potential sliding area by integrating all intrinsic and extrinsic elements to study the spatial distribution of landslides. Thomas Saaty first developed the Analytical Hierarchy Process (AHP) as a method for making decisions (Saaty, 1987) It has previously been used to solve decision-making difficulties in multivariate cases, where different possibilities for achieving certain goals are compared based on a number of factors. By arranging primary goals, criteria, and sub-criteria in a hierarchical fashion, the AHP determines contributing weights for alternatives (Bemasconi, 2009). This approach is semi-quantitative and includes a tool that makes it the most dependable way to calculate the relative proportion of factors and the weight of each criterion using a pairwise comparison with expert judgment and experience (Mehmod, 2022). By highlighting the significance of a particular element and using statistical computing to correlate it with other factors, the AHP has a significant use in the field of landslide susceptibility analysis and mapping.

Building a spatial database for important landslide contributing elements is the first stage in the landslide susceptibility mapping process. Nine factors in all have been discovered for this investigation. These factors are slope, aspect, elevation, curvature, lithology, distance to drainage, distance to road, land use/ cover and rainfall. Using the AHP technique, these elements were examined, and weights were assigned to each variable according to their proportion of involvement in causing a landslide. To create a landslide susceptibility map of the road, the weights assigned to each causative element are combined into a single assessment index, known as the landslide susceptibility index.

Driving the weight for a collection of components according to their contribution is a key challenge of the landslide susceptibility study, despite the fact that intricate knowledge about movement in the area and the triggering causes is crucial when creating the susceptibility map (Saaty, 1987). With the help of Arc GIS's spatial analysis tool, the weight determined by the Analytic Hierarchy Process (AHP) was applied to each thematic map of the causative elements according to their relative relevance, producing a single landslide susceptibility score. The weighting of landslide contribution elements using the AHP technique involves a number of steps. The process entails breaking down the issue into a hierarchy that contains all of the problem's fundamental components.

The primary measurement element utilized in the AHP approach, the factor elements are then compared pairwise to the objective to organize the data (Dou J. , 2015). The priority vector is computed using the comparative judgment matrix. Furthermore, the number of contributing elements is given in relation to the Random Consistency Index Value (RI).The average value(a) and the Coherence Index (CI) are calculated to check the Coherence Ratio (CR).The model with CR value of greater than 0.1 were omitted immediately and CR less than 0.1 shows the reasonable level of consistency in the pair-wise comparison matrix and accepted, as presented in Table 3-1, the grading of contributing factors is conducted through assigning weight in range of 1to9. Where I represent the equivalent significance and 9 is the significant importance of one factor over the other.

Table 3.3: Scale of preference between two parameters in AHP ***(Saaty, T. L. Vargas, L. G., 2001)***

Scale	Degree of preference	Explanation
1	Equally	Two activities contribute equally to the objective
3	Moderately	Experience and judgment slightly to moderately
5	Strong	Experience and judgments trongly or essentially
7	Very strong	An activity is strongly favored over another and
9	Extremely	The evidence of favoring one activity over affirmation.
2,4,6,8	Intermediate values	Used to represent compromises between the preferences in weights

(Abay, 2019); T. L. (Saaty, 1987)) Summarizes the procedures that must be followed in order to use the Analytical Hierarchy Process (AHP) to make decisions and prioritize tasks in an orderly manner.

1. The goal of the choice should be at the top of the hierarchy, followed by the broad perception's aims, the intermediate levels (which serve as criteria for later aspects), and the lowest level (which is typically a collection of the alternatives). This makes it possible to organize the difficult choice in a hierarchy, starting with the general goal and working down to several criteria, sub-criteria, and so forth.
2. The next stage in applying the AHP approach is to construct a set of pairwise comparison matrices. Pairwise comparison matrices, which comprise aspects of one rank that help achieve the goal of the next level at the top, are included in the data for the subject problem in this stage. The quantitative values used for the pair wise comparison matrix is either of set: {1,2,3,4,5,6,7,8,9,1/2,1/3,1/4,1/5,1/6,1/7,1/8,1/9}. The qualitative measurement for each paired element is transformed into quantitative values using this scale, according to the idea that the criteria with a higher rating contributes more than the one with a lower rating.
3. Determine the consistency ratio and local weight. In this phase, the normalized Eigen vector of the rated elements in the pairwise matrix is used to calculate the local weight of the matrix. The following operations were part of the matrix's Eigen

vector procedure:

i. The reciprocal matrix's values in each column are added together.
ii. To calculate the normalized pairwise comparison matrix, each element in the matrix is divided by the sum of the columns, until the sum of all the columns equals 1.0.
iii. To determine the relative weight of each comparing criterion, the average of the values in each row of the normalized matrix 1s is calculated by dividing the sum of the values in each row of the normalized matrix by the total number of criteria, keeping in mind that the most significant criterion is the one with the highest weight.
iv. The consistency ratio was calculated to verify that the reciprocal matrix for pairwise comparisons was consistent (Abay, 2019). The Principal Eigen value is first calculated by adding the products of the reciprocal matrix's column and each element's normalized pairwise comparison matrix. After that, each matrix of order "n" has its Consistency Index (CI) calculated. lastly, the reciprocal matrix's Consistency Ratio (CR) value is calculated as follows: where RI is the Random Consistency Index obtained from a large number of trials and studies that varied according to the matrix's order. (Table3.3).

Table 3.4: Random Consistency Index (RI)

n	1	2	3	4	5	6	7	8	9	10	11	12	13	14	15
RI	0	0	0.58	0.9	1.12	1.24	1.32	1.41	1.45	1.49	1.51	1.53	1.56	1.57	1.59

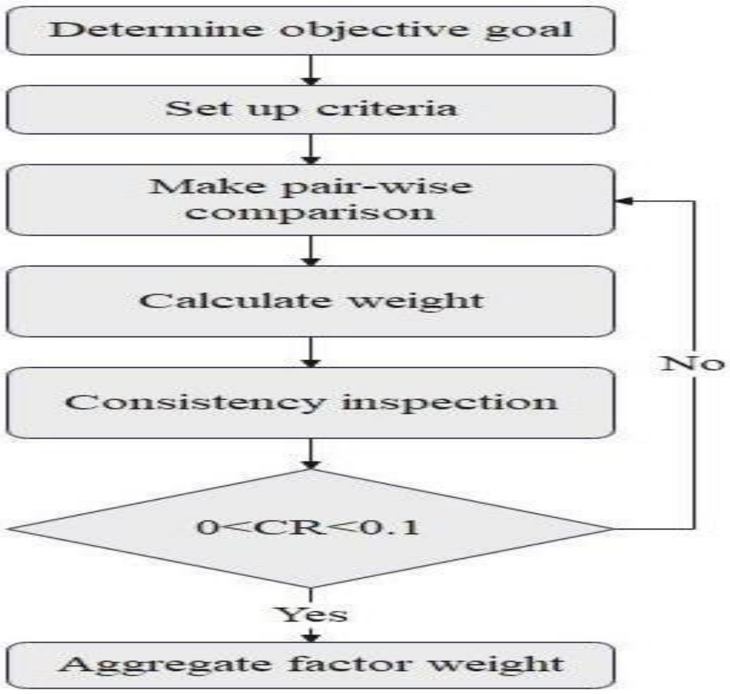

Figure3.7: Landslide contributing factors weighting using Analytical Hierarchy process

By combining the thematic raster map of nine pertinent features with their assigned weights, the Analytic Hierarchy Process (AHP) technique was used to construct the landslide susceptibility map for the study road section.

Recalling (4-3), the weighted overlay tool in spatial analysis is used to merge the weighted raster maps to construct the landslide susceptibility index (LSI) (3-1);

$$LSI = \sum_{i}^{n} W_j * R_{ij} \qquad \text{……………………………………….. (3-1)}$$

Where Wj: Weight for each of the landslide conditioning factor; R_{ij} rating value of class i in landslide contributing factor j; n: number of landslides contributing factors.

3.2.2. Slope Stability Analysis Using PLAXIS Software

Specifically utilized for stability and deformation analysis in geotechnical applications, it is a finite element program or simulation tool for numerous finite element-based issues.

Users may quickly create geometric models and finite element meshes with the package's helpful graphical user interface. The user can select several soil models according to the mechanical deformation behavior of the soil to be simulated because the PLAXIS 2D code and the associated soil models are designed to calculate any of the realistic physical problems. It has the capabilities to use reliable and theoretically sound computational approaches to handle many facets of intricate geotechnical constructions and construction processes. (Brinkgreve, 2002) An essential idea in the analysis that has a big impact on the software package's computation results is dimension. Therefore, depending on the physical limitations of the problems that need to be examined, PLAXIS software can be either 2D or 3D. Therefore, some changes between 2D and 3D analysis are predicted given the complexity of the model geometry and the variety of material properties. (Habibnezhad, 2014)

3.2.3. Constitutive Model

A collection of mathematical formulas known as the Constitutive/Material Model explains how stress and strain relate to one another in materials. Numerous academics have created a variety of constitutive models to explain different facets of soil behavior. These widely used constitutive models, which explain the soils' stress-strain relationship, include the Elastic Model, Soft soil-creep model (time-dependent behavior), Mohr-Coulomb model (MC), modified cam-clay model, and hardening soil model (isotropic hardening). The Mohr-Coulomb Model is used in this thesis among these models because

- It is relatively quick and simple
- Its procedure reduces error and
- It is appropriate for most soils

According to the elastic-completely-plastic Mohr-Coulomb model, soil behaves as linearly elastic up to a stress limit and then as perfectly plastic, with strain becoming irreversible as stress decreases. This model requires five input parameters for the soil; Young’s modulus (E), Poisson’s ratio (ν), Friction angle (Φ), Cohesion (C) and Dilatancy angle(Ψ). The value of the stiffness parameter (E) and cohesion (C) is in general chosen as a representative value that is consistent with the stress level in the soil. (Brinkgreve, 2002)

3.2.4. Geotechnical Parameters

According to the Mohr-Coulomb model, PLAXIS 2D software uses the following fundamental geotechnical parameters:

I. Stiffness Modulus (Es)

It is an elastic soil parameter that controls the outcomes of settlement-related issues and characterizes the load-settlement behavior of soils. In the region of elastic soil behavior, it is the ratio of the stress along an axis to the strain along that axis. It is strongly advised to utilize realistic and practical stiffness values that reflect the in-situ circumstances while simulating the actual soil condition using the finite element method. There are several methods available to estimate the soil stiffness modulus which includes;

- Test methods: unconfined compression tests, triaxial compression tests and in situ tests.
- Empirical relations and range values
- Using code provisions: German code

However, the German code provision is used for this study since it takes in to account soil types, confining pressure, and penetration resistance; as a result, equation 3.2 gives the code's provision. (DIN4094-3,2002).

$$E_s = \mu p_a \left(\frac{\sigma_z + 0.5\Delta\sigma_z}{p_a}\right)^w \qquad (3\text{-}2)$$

Where:

μ = stiffness coefficient depending on values of N-SPT

w = stiffness exponent, which has a value of 0.5 for non-cohesive soil & 0.6 for cohesive soils

σz = overburden pressure at a depth z below the foundation level

$\Delta\sigma z$ = additional vertical stress due to the loads from the superstructure at a depth z Pa=average atmospheric pressure, take nas101.4KN/m².

Additionally, equation 2.2 is frequently used to account for the effective modulus elasticity for PLAXIS analysis. (Brinkgreve, 2002)

$$E' = \frac{2(1+\nu')E_S}{3} \qquad (3\text{-}3)$$

II. Cohesion (c)

The force that holds molecules or similar particles together within a soil is known as soil cohesion. The direct shear test and the triaxial shear test are typically used in laboratories to determine it. The triaxial test or the unconfined compressive strength test can be used in a lab setting to measure unconfined compressive strength. Additionally, there are relationships between Such and shear strength as determined by field measurements utilizing vane shear tests. The triaxial shear test and SPT N-value have already been used to establish the soil's cohesiveness for this investigation.

III. Friction Angle(ϕ)

A unit of soil or rock's resistance to shear force is measured by its friction angle. The direct shear test or the triaxial shear test can be used to determine it in a lab setting. To measure the friction angle of granular soils, correlations are also available. The triaxial shear test and SPT N-value were used to calculate the soil's friction angle for this investigation.

IV. Unit Weight(γ)

The ratio of a soil mass's total weight to its total volume is known as its unit weight. The weight and volume of a generally undisturbed soil sample taken from the field are often measured in the lab to establish unit weight. A nuclear densitometer, rubber balloon, or sand cone test can all be used to measure the unit weight of soil in the field. The results of the laboratory tests were obtained for this investigation.

V. Poisson’s Ratio (ν)

A feature known as Poisson's ratio characterizes how much a material's volume changes perpendicular to the application of a load. It is the ratio of a soil's axial compression to its lateral expansion.

For most clay, a Poison's ratio range of 0.4 to 0.5 is advised, while for medium-to-dense cohesionless soil, 0.2 to 0.4 (Bowles J. E., 1996) However, because the PLAXIS 2D did not accept a number higher than this one, a typical value of 0.35 was chosen for the study's numerical analysis. In (Brinkgreve, 2002)

VI. Dilatancy Angle(Ψ)

Clay soil typically exhibits minimal dilatancy, with the exception of highly over-consolidated layers. Sandy soil dilatancy is influenced by both friction angle and density. Regarding quartz sands the formula Ψ=ä-30 provides the order of magnitude. However, dilatancy values are typically zero for X values below 30°. Only very loose sands can really have a modest negative value. (Brinkgreve, 2002)

3.2.5. Drainage Conditions

To properly determine whether total or effective stress analysis is appropriate during the analysis process, a differentiation between the drained and undrained states of the soil should be made based on the length of loading and permeability. (Getnet, 2016)

I. Drained and Undrained Condition

Whether or not changes in load result in changes in pore pressure is the key question here. Time makes a difference in these circumstances. The term "undrained condition" describes a situation in which drainage is hindered or where changes in loads happen more quickly than water can enter or exit the soil. When the loads change, the pore pressures either rise or fall. The term "drained condition" describes a situation in which load variations are sufficiently gradual or persistent to allow water to enter or exit the soil and allow the soil to achieve a state of equilibrium with regard to water flow. In a nutshell, the drained condition is the state in which drainage is permitted. The hydraulic boundary conditions regulate the pore pressures in the drained circumstances, and load variations have no effect on them. Water flow is limited whenever there is a change in volume because cohesive materials, such as clays, often have lower permeability than sand. Therefore, it takes years for clay soils to attain the effective equilibrium before the extra pore water pressure is dissipated. In short, an undrained situation is one in which drainage is restricted, whereas a drained condition indicates one in which drainage is permitted. In addition to cohesive soils' drained and undrained conditions, it should be mentioned that restructuring causes cohesive soils' strength to decrease from its peak to its residual strength. (Getnet, 2016)

II. Effective and Total Stress Analyses

Effective normal stresses, which are used to assess shear strengths, are calculated by subtracting the pore pressures along the shear surfaces from the total stresses in effective stress assessments.

Consequently, it is essential to predict the pore pressures at each location along the shear surface in order to conduct efficient stress studies. For drained circumstances, where the soil's reaction to external loads determines the values of these pore pressures, they can be assessed with a fair degree of accuracy (Getnet, 2016) Because shear strengths are correlated with total stresses, pore pressures are not deducted from total stresses in total stress calculations. Therefore, in order to do total stress studies, pore pressures do not need to be evaluated and subtracted. Only circumstances that are undrained are included by the total stress analysis. The fundamental idea behind total stress analysis is that the behavior of the soil dictates the pore pressure caused by undrained loading. A unique value of pore pressure and, consequently, a unique value of effective stress exist for a given value of total stress on the possible failure plane. Therefore, even if effective stress does regulate shear strength, the undrained state can be related to the undrained condition. This line of thinking does not hold true in drained situations, when hydraulic boundary conditions regulate pore pressures instead of the soil's reaction to outside stresses. (Duncan, J. P., & Wright, G, 2000)

III. Undrained and Drained Shear Strengths

Parameters of measured soil strength are not exclusive. When choosing strength parameters, the main aspects to take in to account are soil type, strain history, and loading conditions (duration). Here, the time element applies to both short-term, undrained situations and long-term, drained ones, while the strain history determines whether peak, ultimate, or residual strength will prevail.

Undrained Strength is the soil's shear strength under undrained conditions when it is loaded to failure. When loads are applied to a mass of soil more quickly than the soil can drain, the resulting circumstances in the field roughly resemble undrained conditions. Undrained circumstances are created in the lab by either sealing test specimens in impermeable membranes or loading them so quickly that they cannot drain. Here, drainage must be controlled using an impermeable membrane rather than extremely high loading rates in order to prevent the high strain rates that are not indicative of the field conditions. The soil's drained strength is its shear strength when loads are applied gradually enough to prevent the creation of excessive pore pressures. When loads are applied gradually to a bulk of soil or are sustained long enough for the soil to drain, drained conditions are created in the field. To create drained conditions in the lab, test specimens are loaded gradually to prevent the development of excess pore pressures as the soil is loaded. (Duncan, J. P., & Wright, G, 2000); (Getnet, 2016)

IV. Analyses of Drained and Undrained Conditions Short-Term Analyses:

Short-term analyses utilizing either drained or undrained strengths can be carried either during or after construction, depending on the soil's permeability. Because cohesive soils, such as clay, are much less permeable than sand, water flow is impeded for this brief period of time whenever the volume changes.

Effective shear strength parameters must be used in PLAXIS 2D, although undrained shear strength is used for these cohesive soils and is calculated using total unit weights and total shear strength parameters (Getnet, 2016) Although drained strengths are utilized for sand soils that may drain freely, pore pressures are established using either water table data or suitable seepage studies, and shear strengths are stated in terms of effective stresses. The same study can be performed using drained strengths for some soils and undrained strengths for others. (Getnet, 2016)

V. Long-Term Analyses:

Following construction, the soil in the slopes may either consolidate as the water content decreases or swell as the water content increases. Analysis of long-term stability is done to take in to account the circumstances after these changes.

Following construction, the soil in the slopes may either consolidate as the water content decreases or swell as the water content increases. Analysis of long-term stability is done to take in to account the circumstances after these changes. (Duncan, J. P., & Wright, G, 2000); (Getnet, 2016)

3.2.6. Factor of Safety

The available shear strength divided by the mobilized shear stress at emerging failure is the standard definition of the factor of safety in slope stability analysis.

It is a key indicator for figuring out how close or how distant the slope is from the failure state. The factor of safety, or FS, can be formulated in a number of ways, including

- Fr/Fd Resisting Force / Driving Force
- Mr /Md Resisting Moment / Driving Moment
- Hc / H Critical Height / Slope Height
- S/τ Available shear stress/shear stress at equilibrium

Among these the lst definition is widely used. (Meng, 2006). Various code sand guide lines recommended for the minimum factor of safety to be from1to 1.5 as showninTable3-5.

Table 3.5: Different recommended values of minimum FS for d/t conditions of the slope

No.	Condition of the slope	Factor of safety	Sources
1	For the first time slide	1.3to1.4	(BS6031.,2009)
	For a slide with a pre-existing slip surface	1.2	
2	For permanent loading condition	1.5	(NAVFAC DM 7.1, 1986)
	For transient load such as earthquake	1.15 to1.2	
3	For unreinforced slope and embankment on soft ground	1.2	(JKRRoadWork,2010)
	For reinforced slope	1.5	
4	For new slope depending on the risk	1.0to1.4	(Geoguide 1 1984)
	For existing slope depending on the risk	1.0to1.2	
	If no risk of danger to person/property for peak strength	1.25	
5	For static roadside slope stability	1.3	(Ethiopian Roads Authority)

The factor of safety in PLAXIS 2D is computed using the ϕ-c reduction concept. In this type of calculation, the load advancement procedure is followed. The incremental multiplier 'Msf' is used to specify the increment of the strength reduction of the previous calculation step. The strength parameters are reduced successively in each step until all the steps have been performed. The final step should result in a fully developed failure mechanism, if not the calculation must be repeated with a larger number of additional steps. Once the failure mechanism is reached, the factor of safety is given in equation 3.4.

$$FS=\frac{\qquad}{\qquad}=\Sigma Msf \tag{3.4}$$

This is a global factor of safety at failure. (Brinkgreve, 2002)

3.3. Site visitation and field data collection

In order to examine specific geotechnical aspects and assess slope stability after a landslide incident, the site was surveyed, and pictures, land use, and topography of the affected region were recorded. Using plastic bags and cylinder tubes, disturbed and undisturbed soil samples were taken from various test pit depths while GPS coordinates of the sampling pits were recorded. The samples were then analyzed in a soil laboratory to determine the soil's stability against failure in landslide-prone areas. Reading the coordinates of the landslide-prone area, measuring its length, width, and depth, determining whether gullies and springs were present at the slope's base, examining landslide indicators, performing, drilling test pit boreholes for subsurface soil investigations, collecting samples for laboratory analysis, and recording the total catastrophic damage caused by the landslide were all part of the fieldwork.

3.3.1. Laboratory Testing

Soil samples from boreholes, both disturbed and undisturbed, were chosen and examined for classification, strength parameter calculation, and sliding mass index property identification. Atterberg limits, grain size analyses, moisture content, unit weight, specific gravity, shear strength parameters utilizing the direct shear test, and other crucial tests are all part of the laboratory test program. Samples will be sieved in accordance with the standards stated in the AASHTO or ASTM standard laboratory manual.

The detailed investigation process includes borehole drilling and preparation of borehole logs, field tests, sampling and laboratory testing, surveying data collection and groundwater level measurement.

Table 3.6: Standard Test Method for Laboratory Test

Laboratory Test	Standard Reference
Preparation of soil samples for Test	AASHTO T-87 - Standard Test Method for Sample Preparation
Moisture content	ASTM D 2216(AASHTO T-265) standard test methods for laboratory determination of water (moisture) content of soil
Atterberg limits	ASTM D 4318 (AASHTO T-90) - Standard Test Method for Liquid Limit, Plastic Limit, and Plasticity Index of Soils.
Particle size distribution	ASTM D 546(AASHTO T-37) standard test methods for particle size distribution of soils
Bulk density	ASTM C 29 (AASHTO T-19) - Standard Test Method for unit weight
Specific gravity	ASTM D-854 or C 188 (AASHTO T-100 or 133) - Standard Test Method for Specific Gravity
Shear strength	ASTMD3080 Standard Test Method for the correlation between consolidation stress and Undrained shear strength

3.3.2 Drilling of Borehole

As Landslide section, drilling of boreholes is carried out by Gondwana Engineering PLC. All the required drilling accessories were deployed. Each of the boring positions located using a total station on the logging sheet of each borehole, the Total Core Recovery (TCR), Solid Core Recovery (SCR), Rock Quality Designation (RQD), Average Fracture Spacing (AFS) and degree of weathering of the rock are indicated. All recovered materials from boreholes are kept in core boxes, properly labeled and photographed according to their depth of recovery. The log sheets and core box photographs are attached to Appendix B

The soils encountered are classified according to the Unified Soil Classification System. Undisturbed and bulk samples of the subsurface materials were obtained at selected intervals to conduct laboratory tests.

3.3.3. Standard Penetration Test (SPT)

Standard Penetration Test (SPT) was conducted inside boreholes using a standard hammer through counting of Blows for a total penetration depth of 450mm from the bottom of a cleaned borehole were recorded. Counts for the first 150mm penetration were discarded since the ground is considered to be disturbed during drilling activity prior to the test. SPT N-values for the last 300mm penetration were taken. The N-values of the SPT are an indication of the relative density of cohesion less soils and the consistency of cohesive soil. General N-value ranges are correlated with relative density and consistency. It is emphasized that for gravels and clays the correlations to relative density and consistency should serve only as general estimates. In situ field testing was carried out starting from 1.50m depth below natural ground level. The tests on representative soil samples were carried out by Gonduwan Engineering plc. and the summarized results are presented in Appendix-B.

I. Corrections Applied for SPT N-Values

Variations in hammers, drill rigs, rod lengths, hammer blow rates, energy delivery systems, borehole fluids, and sampling tubes all affect the standard penetration test (SPT). Hammer efficiency, borehole diameter, sampling technique, and rod length are important variables that impact the SPT N-value. It is advised to standardize the N-value using correction factors that take into consideration soil energy input and dissipation in order to minimize variability. For consistency, SPT N-values per 300 mm should be converted to a standardized energy level. The SPT N-values are converted to the N60 standard energy ratio value for various factors before being used for analysis. (Bowles J. E., 1988) using

$$N_{60}= (E_H x\ C_B x C_S x\ C_R x\ N)/0.60$$

Where;

N60 = Corrected SPT N-value for field procedures EH = Hammer efficiency

CB = Borehole diameter correction CS = Sampler correction

CR = Rod length correction

N = Measured SPT N-value in field

II. Correlation with Un-drained Shear Strength

N-value results in geotechnical engineering can be used directly for design calculations like settlement, liquefaction potential, and allowable bearing capacity, or indirectly to estimate geotechnical parameters like volume compressibility, undrained shear strength, effective friction angle, and unconfined compressive strength. (Bowles J. E., 1996) states that the following equation can be used to empirically estimate the unconfined compressive strength:

$$qu = K*Ncor$$

Where

k=proportional factor, k=12.5hasbeenrecommendedbyBowles

This is a synopsis of your passage: The primary indicator of undrained shear strength (Cu), which is essential for figuring out foundation bearing capacity, is penetration resistance in fine-grained soils. Cu is equal to half the unconfined compressive strength (qu) at full saturation and φ = 0 (Hara, A., Ohta, T., Niwa, M., Tanaka, S., & Banno, T., 1974)

$$Cu = 0.5qu$$

III. Correlations of SPT Test with Soil Properties

Determination of Shear Strength Parameters from SPT N-values the most used in situ test for determining the in-situ characteristics of soil in geotechnical investigations is the SPT. Multiple soil parameters, including unit weight, relative density, compressive strength, and angle of internal friction, have been correlated using it. It has also been used to calculate the stress-strain modulus and determine the bearing capacity of foundations. Since the SPT test is particularly well-suited for cohesionless soils, numerous correlations have been developed between the SPT N-value and while there are only a few correlations between the SPT N-value and the soils' undrained strength parameters.

Nevertheless, the SPT N-value and cohesive or c-̄ soil strength indices no longer correlate. As a result, the strength characteristics are estimated based on the clay soil's consistency ranges, as suggested by Look (2007) and displayed in Table 3.6 below.

Table 3.7: Clay strength from SPT data (Look, 2007)

Material	**Description**	**SPT-N**	**Strength (cu) (kPa)**
Clay	V. Soft	≤ 2	0-12
	Soft	2-5	12-25
	Firm	5-10	25-50
	Stiff	10-20	50-100
	V. Stiff	20-40	100-200
	Hard	>40	>200

Look (2007) has further recommended ranges values of the effective ϕ and c for the corresponding consistency of clay soils as stated inTable3.8.

Table 3.8: Effective strength of soil (Look, 2007)

Material	**Description**	**c' (kPa)**	**ϕ' (°)**
Clay	Soft-Organic	5-10	10-20
	Soft-Inorganic	10-20	15-25
	Stiff	20-50	20-30
	Hard	50-100	25-30

3.3.4. Laboratory analysis

The shear strength parameters of the relevant boreholes are determined from the associated SPT N-values by taking in to account the relations in Tables 3.6 and 3.7. the estimations from the SPT N-values are also utilized to compare the parameters derived from the laboratory testing. It is deemed acceptable if the laboratory strength parameters lie between the minimum and maximum values as established by the SPT N-value; if not, the closest boundary (max. or min.) values are used for the laboratory values. Appendix-B (Borehole diagram) displays the uncorrected SPT N-values for each station that were recorded during drilling, while and displays the corrected SPT N-values for the subject stations together with their corresponding layers. The soil's stiffness and shear strength parameter values both rise with an increase in SPT blow counts. The following describes/presents the layer designation and shear strength parameters for each station.

3.3.5. Data Processing and Analysis

Data from laboratory results and a review of research papers' literature will be examined throughout processing and analysis. The correctness of the laboratory results will be verified, and the output will be compared to the existing standards. Lastly, structuring and presenting the analysis's findings in accordance with the study's goal.

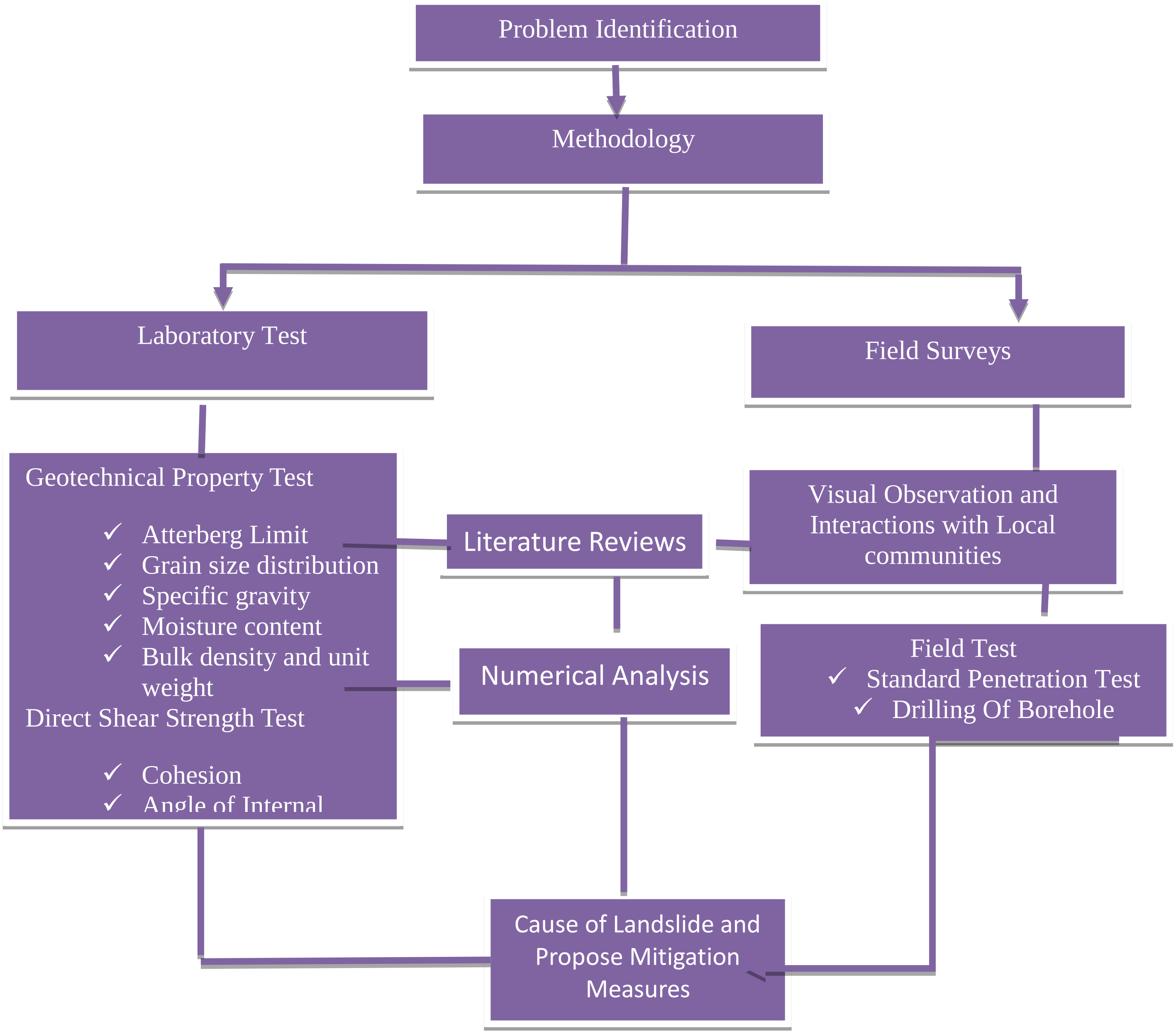

Figure 3.8: Methodology Flow Chart

CHAPTER FOUR

RESULTS AND DISCUSSIONS

4.1. Inventory of Landslide

Landslide assessment and inventory is a vital stage when investigating the landslide risk of a specific location. The specific site conditions of sections with slope stability problems and subsidence were assessed based on the information collected during the site visit accompanied Desk study was made by referring to different Google Earth imageries, Digital Elevation Model (DEM), geological map and previously conducted subsurface investigation & laboratory test results. The findings of the desktop study have been verified by landslide inventory work is conducted by site data collection along the route, measuring the actual landslide features during the field survey, interviewing the locals, The main purpose of Theses is to present the site condition sand remedial measures for then countered geotechnical problems such as subsurface water flow and cut slope failure. Analysis is made for instable sections by assigning proper input parameters taken from the subsurface investigation and laboratory testing. Based on the information collected during the site visit accompanied by desk study the following 8 sites with geotechnical problems were observed in the following stations.

- km 14+200 – km 14+540 RHS(LS-01)
- km45+300-km45+440RHS(LS-02)
- km 67+500 - km 67+570 RHS & LHS(LS-03)
- km 69+180 - km 69+220 LHS(LS-04)
- km 78+940-78+960 RHS((LS-05)
- km 79+980 – km 80+010(LS-06)
- km80+700 –km81+600(LS-07)
- km81+700 – km83+400(LS-8)

The assessment of the existing landslides is conducted based on the geographical location, general description of the landslide, geological formation of the affected area, drainage condition along the road corridor, distinct landslide features, and the possible causes of the existing landslides.

4.1.1. Detailed Description of the Existing Landslides

4.1.1.1. Landslide from km 14+200-14+540RHS/(SL-01)

Site Condition:

The material forming the cut slope is brownish yellow highly weathered and decomposed rock material overlain by reddish brown silty Clay soil; there are very big boulders within the underlining highly weathered and decomposed material. the excavation work of the slope was not completed and during excavation failure of the back slope was observed. With time, the big boulders which are found within thedecomposedrockmaterialstartedtomovedownwardduetogravityandaffectedthe toe and later lead to failure of the slope locally; The site photographs showing the slope stability problem is illustrated in the figure below.

Geology:

The geological formation of the area is described as Greyish brown crushed aggregate embedded with silty Clay (Gravel wearing course) Firm deep brown Silty Clay, Residual Soil Firm to hard yellowish-brown Silty Clay, Medium strong light brownish gray to light gray fine grained closely jointed moderately to slightly weathered Trachyte with becoming highly decomposed towards depth residual soil with relicts of rock fabric It is massive looking with widely spaced fractures.

Possible Cause of Landslide:

The big boulders which are found within the decomposed rock material started to move down ward due to gravity and affected the toe and later lead to failure of the slope locally.

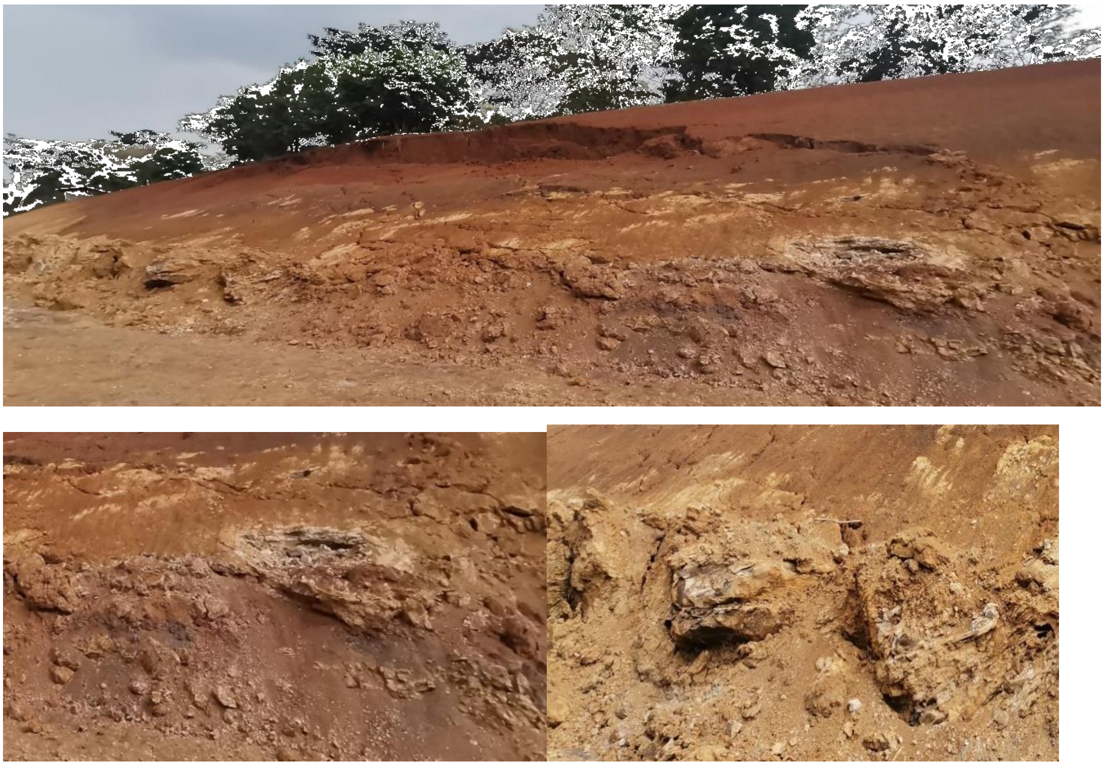

Figure 4.1: Landslide movement at station 14+200-540

A detailed description of the sampled soil

Based on the data obtained from laboratory tests on representative soil samples and the core box along the slide section, the subsurface materials are approximately subdivided into two layers. The detail of the test results, classification using USCS, and description of the borehole of the sampled soils at this station are shown in Table 4.1 below.

Table 4.1: Test result and description of the sampled soil at station 14+260

Layer	Test result (average values were taken for each layer with similar formation	Classification of soil as per USCS	Borehole log description
Layer-1 (0-3m)	Natural Moisture Content, NMC: 24% Liquid Limit, LL:99% Plastic Limit, PL: % Plasticity Index, PI: % Pass no. 200 (0.075mm) sieve: % Pass no. 4(4.75mm) sieve: %	The soil is dominantly gravely Lean Clay (CL)	Firm deep brown Silty clay, Residual Soil with relicts of rock fabric

Layer-2 (3- m)	Natural Moisture Content, NMC: (59% Liquid Limit, LL: 77% Plastic Limit, PL: 37% Plasticity Index, PI: 40% Pass no. 200 (0.075mm) sieve: 97% Pass no. 4(4.75mm) sieve: 99%	The soil is dominantly Silty clay (MH)	Firm to hard yellowish-brown Silty clay residual soil with relicts of rock fabric

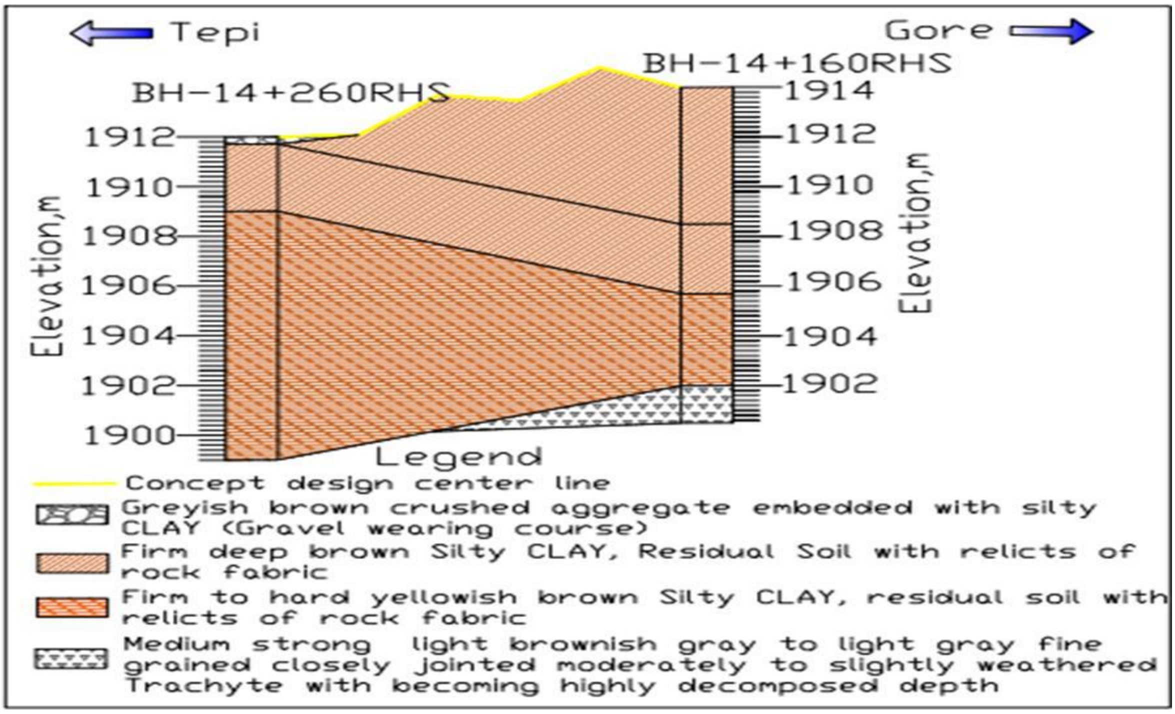

Figure 4.2: Cross section along Boreholes (BH-14+160 RHS and 14+260 RHS)

4.1.1.2. Landslide from km 45+300–km45+440/(LS-02)

Site Condition:

The main reason for failure is the action of rainfall which resulted in the saturated weight of soil and subsurface water draining between adjoining planes of the different soil types decreasing the friction between constituent particles. and collapse of soil layer that couldn't able to stand with the designed back slope ratio. The designed typical cross section for the cut slope material and the photographs showing the slope stability problem is illustrated in the Figure shown below.

Geology: The geological soil profile presented in Figure 4-3 reveals that the topmost layer is generally firm to stiff reddish brown or yellowish-brown silty clay which is a residual soil containing rock structure and fabric. The thickness varies from 9 to 14 meter but generally is about 10 meters. Below the silty clay layer, highly to moderately weathered basalt layer appears with different thicknesses. Then medium strong dark grey basalt follows.

Drainage Condition:

The presence of streams and spring waters greatly influences the stability by toe erosion or by saturating the slope material or both. It is clear that the water which flowed into the osmosis and the mountain streams of surface water by rain turned into groundwater, and has contributed to the rise of the groundwater level. In the area high drainage density is observed.

Possible Cause of Landslide:

The main reason for failure is the saturation of weak cut slope material by the action of rainfall which resulted in the saturation and collapse of soil layer that couldn’t able to stand with the existing back slope ratio.

Figure 4.3: Landslide movement at station 45+350-45+440

A detailed description of the sampled soil

In general, the subsurface condition of this cut section is composed of four geotechnical layers as per the information gained from field and laboratory investigation. The test results, classification and borehole log description of the sampled soils at this station are shown in

Table 4.2: Test result and description of the sampled soil at station 45+720

Layer	Test result (average values were taken for each layer with similar formation	Classification of soil as per USCS	Borehole log description
Layer-1 (0-8m)	Natural Moisture Content (NMC): 36% Liquid Limit, LL: 48% Plastic Limit, PL: 36% Plasticity Index, PI: 2% Passno.200(0.075mm) Sieve: 98%	The soil is dominantly elastic silt (MH) with sand the soil is dominantly Silty clay (MH)	Firm moist reddish-brown silty clay (residual soil with relict of rock structures and fabric)
Layer-2 (8-9m)			Firm dark grey silty clay (in situ weathered soil with some rock structures and fabric)
Layer-3 (9-9.6m)			Medium strong fine grained dark grey partially weathered very closely jointed aphanitic basalt.
Layer 4 (9.6-20m)			Strong fine grained dark grey fresh closely jointed aphanitic basalt with some thin crack joint has nearly horizontal orientation.

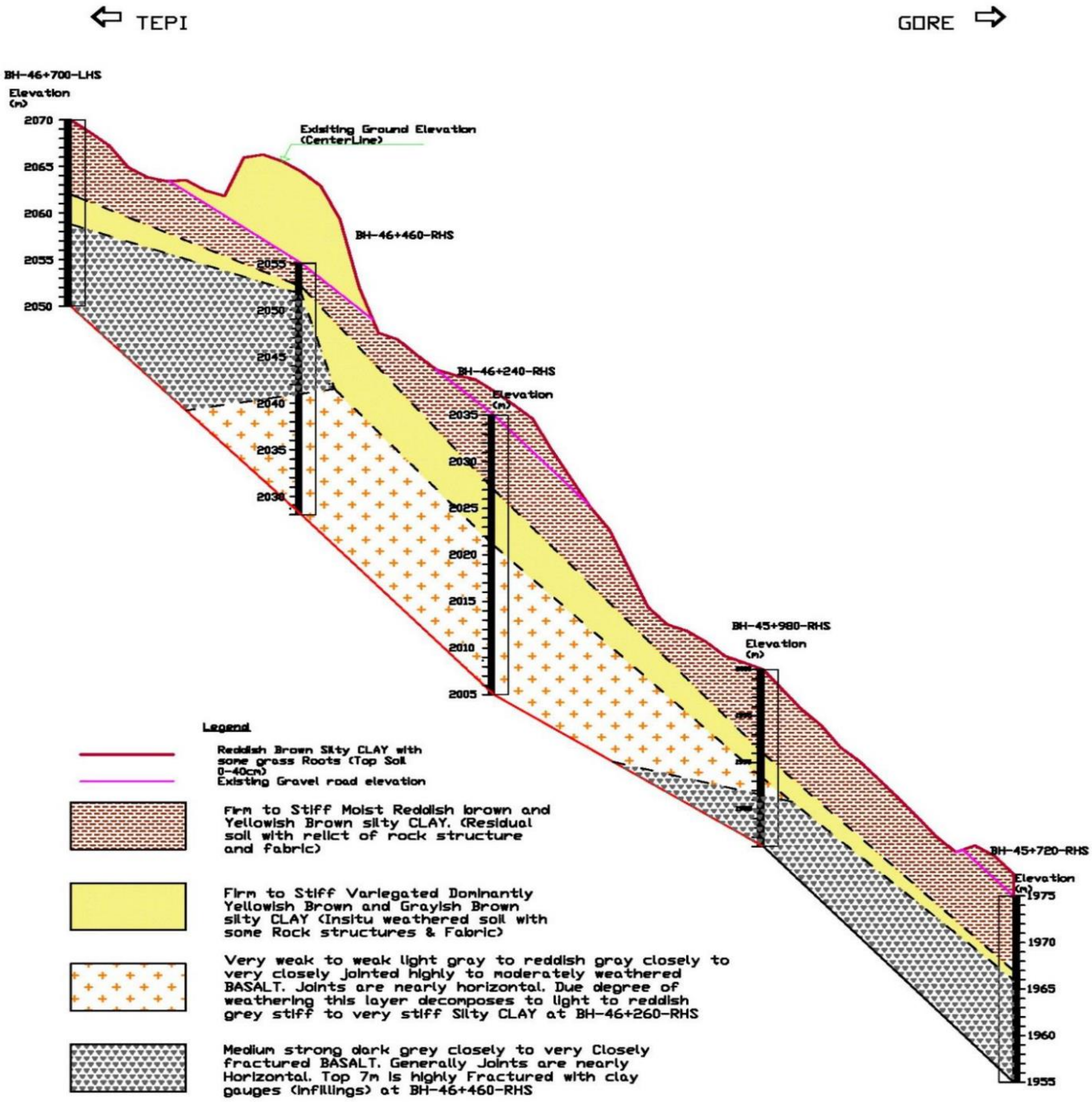

Figure 4.4: Cross section along Boreholes (BH-45+720 RHS and 46+700 RHS)

4.1.1.3. Landslide from 67+500–km67+570/(LS-03)

Site Condition:

The whole ground at this location is pre-existing moved mass with active sliding was observed at RHS. From the information obtained from local people, houses which were previously located were destroyed due to the land slide and the people were relocated. During the site visit, collapsed trees were observed indicating active sliding. The geometric cross sections at this location shows the construction of high fill section hence the natural ground will be used as working plat form for in the typical section below.

Geology:

The geological soil profile presented reveals that the topmost layer is generally deep yellow silty clay (residual weathered material). The thickness varies from 0 to 1.2 meter Below the that, yellowish gray silty clay.

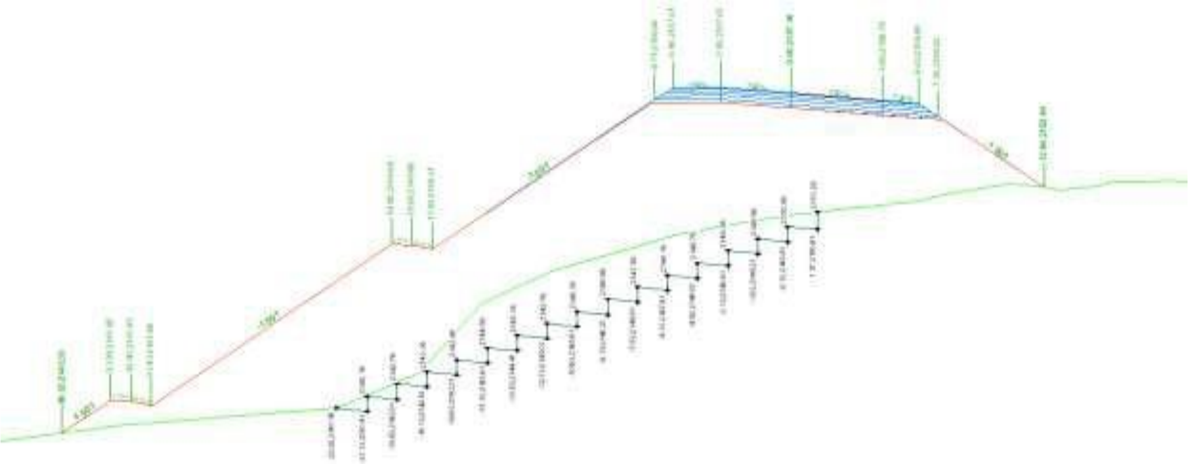

Figure 4.5: Landslide movement from station 67+500 – km 67+570

4.1.1.4. Landslide from km69+180–km69+220LHS/(LS-04)

Site Condition:

The observed section with anticipated sliding is found at the aforementioned stretch. The original ground has sudden drop on the LHS and the geometric cross section depicts large side fill on the LHS. The ground has sound rock outcrops in RHS direction where rock excavation for cut slope was under progress during the site visit whereas the section on the LHS with depressed ground will be fill section which need properly constructed. The designed typical cross section for the fill slope material and the photo graphs showing the slope stability problem is illustrated in the Figure shown below

Geology:

The geological soil profile presented reveals that the topmost layer is generally very dense brownish grey and dark grey gravelly silty sand. Below the silty sand layer, strong dark grey fine-grained basalt very closely to medium spaced fractured and slightly weathered fractures has nearly horizontal orientation and strong dark grey fine grained closely fractured and slightly weathered vesicular basalt joints and vesicles are mainly filled with quartz fractures has nearly horizontal orientation.

Drainage Condition:

The main triggering factor for the land slide at this section is related with the actives stream crossing this section of the road. The highly erosive stream crosses the road from the upstream ridge and cause severe toe erosion at the downstream side. Proper river bank protection work has not provided at the downstream side of the stream which leads to the occurrence of landside on the natural slope as well as on the embankment propagating towards the road.

Possible Cause of Landslide:

The toe erosion and undercutting of the natural slope material by the stream crossing the road is identified as the main cause of the active landslide. In addition, the saturation of the sides lope material by rainfall and surface runoff water contributes for the strength reduction of the slope material which contribute for the landslide.

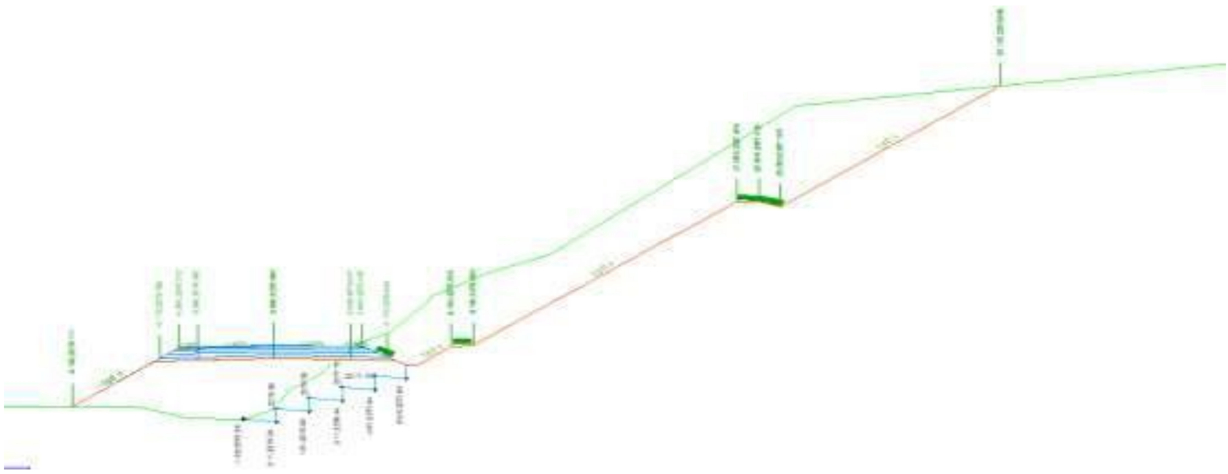

Figure 4.6: Landslide movement at station 69+180 – km 69+220 LHS

4.1.1.5. Landslide from km 78+940-78+960 RHS/(LS-05)

Site Condition:

The problem observed at this specific site is a failure of the old embankment material which is a brownish grey Sandy Clayey Silt with gravel (Fill material) found at a very steep slope for the type of material forming the slope the main cause of the failure around this section is its morphology of the slope/steep slope profile and the nature of the material forming the slope which is a fill material. Even though the failure is observed very far from the center of the current alignment, it will cause future damage on the road unless proper remedial measure is taken on time.

Geology:

The geological soil profile presented reveals that the topmost covered with light brown sandy silty clay with some crushed stone underlain by soft variegated dominantly yellowish brown sandy silty clay (residual soil with relict of rock structures and fabric), soft reddish brown sandy silty clay (residual in situ soil)

Possible Cause of Landslide:

The main cause of the failure around this section is its morphology of the slope/steep slope profile and the nature of the material forming the slope which is a fill material. Even though the failure is observed very far from the center of the current alignment, it will cause future damage on the road unless proper remedial measure is taken on time.

.

Figure 4.7: Landslide movement station from km 78+940-78+960 RHS

4.1.1.6. Settlement from km 79+980 – km 80+010/(LS-06)

Site Condition:

The area is characterized by the presence of thick fill and looks like an area where there was old stream/spring which comes/emanates from the hill side (LHS) and flows down the slope; besides, surface runoff has also affected the side slope by erosion (picture below). The geotechnical investigation result conducted has also revealed that the top 2.5m is a soft yellowish brown fill material underlain by a soft deep brown Sandy Silt SOIL.In this section, a general subsidence is observed and the most probable cause is compaction of the soft fill material with time due to the traffic load and underground erosion of the soft geological materials present below the fill which causes a piping effect and later subsidence due to the traffic load and load of the fill material dumped during the road maintenance. The property of the fill material there as per the nearest investigation result conducted is soft and the subsurface residual soil is soft also and are susceptible for subsidence and deformation too when load is applied; besides, water is observed coming from the bottom and flows down slope and plays a great role in eroding the soft subsurface soil and cause piping effect.

Geology:

The geological soil profile presented reveals that the topmost layer is generally deep brown sandy silty clay. Below the very soft dry light yellowish brown silty clay and soft moist deep brown sandy silty clay (residual soil with relict of rock structure) firm moist deep brown sandy silty clay (residual soil with relict of rock structure) soft moist deep brown sandy silty clay (residual soil with relict of rock structure)

Possible Cause of Landslide:

In this specific section, the main causes of the subsidence/settlement is the underground erosion due to subsurface water flow and compaction due to traffic load of the soft fill material and the soft residual soil present in the subsurface.

Figure 4.8: Landslide with settlement or movement station from 79+980 – km 80+010

4.1.1.7. Landslide from km 80+700 – km 81+600/(LS-07)

Site Condition:

It is noted that the weak highly plastic residual silty clay founds in the section and hence this material having high plasticity can be a potential for land slide for the section under investigation. More over the ground water can also found in the two bore holes that can saturate the soil and reduce the shear strength and can trigger the land slide

Geology:

The geological soil profile presented reveals that the topmost layer is silty clay material clayey silt and Colluviums material or highly to completely weathered rock is the potential zone

Possible Cause of Landslide:

As per this investigation the main factors for the instability problem in the Section are geological structure of fault observed Along 80+630- km81+740, highly weathered colluvms material along left hand side of box cut section (as the LHS and RHS back slope material completely different that means the RHS cut back slope material is highly weathered closely jointed basaltic rock and stable back slope), very weak saturated layer of dark gray silty clay soil interlayer between light brown silty clay soil, saturation of the slope material due to surface and subsurface water and intense rainfall during summer season.

A detailed description of the sampled soil

As per the information gained from field and laboratory investigation, the subsurface of this cut section is significantly composed of two lithological layers; however, to consider the effect of modulus of elasticity (its increasing nature) in the analysis part, it is divided into three layers. To efficiently describe this section, the nearby borehole located at station 81+060 and 81+700 needs detailed characterization and hence, this cut section is divided into three lithological layers for the sake of analysis. The details of the test results, classification and borehole description of the sampled soils at station 81+060 and 81+700 are shown in Table 4.3and4.4, respectively.

Table 4.3: Test result and description of the sampled soil at station 81+060

Layer	Test result (average values were taken for each layer with similar formation	Classification of soil as per USCS	Borehole log description
Layer-1 (0-6m)	Natural Moisture Content, NMC:44.3%-45.1% Liquid Limit, LL: 62%-66% Plastic Limit, PL: 34%-25% Plasticity Index, PI: 25%-29% Pass no. 200 (0.075mm) sieve: 96%	The soil is dominantly elastic silt (MH) with sand	Yellowish brown firm silty clay with some gravel
Layer-2 (6- 11m)	Natural Moisture Content, NMC: 51.2% Liquid Limit, LL: 63% Plastic Limit, PL: 42% Plasticity Index, PI: 21% Pass no. 200 (0.075mm) sieve: 98%	The soil is dominantly elastic silt (MH) with sand	Light brown silty clay soil with little gravel
Layer-3 (11- 20m)	Natural Moisture Content, NMC: 40.7% Liquid Limit, LL: 58% Plastic Limit, PL: 41% Plasticity Index, PI: 17% Pass no. 200 (0.075mm) sieve:95.9%	The soil is dominantly elastic silt (MH) with sand	Light brown silty clay soil with little gravel

Table 4.4: Test result and description of the sampled soil at station 81+700

Layer	Test result (average values were taken for each layer with similar formation	Classification of soil as per USCS	Borehole log description
Layer-1 (0-7m)	Natural Moisture (NMC): 54.2%-60.5% Liquid Limit, LL: 58%-80% Plastic Limit, PL: 43%-44% Plasticity Index, PI: 15%-36% Passno.200(0.075mm) sieve: 93.9%-96.9%	The soil is dominantly elastic silt (MH) with sand	Light brown soft to firm silty clay and yellowish brown soft silty clay
Layer-2 (7-13m)	Natural Moisture NMC: 65.6% Liquid Limit, LL: 65% Plastic Limit, PL: 39% Plasticity Index, PI: 26% Pass no. 200 (0.075mm) sieve: 89.8%	The soil is dominantly elastic silt (MH) with sand	Light brown firm to stiff silty clay with little gravel

Layer-3 (13-20m)	Natural Moisture NMC: 68.2% Liquid Limit, LL: 77% Plastic Limit, PL: 46% Plasticity Index, PI: 46% Pass no. 200 (0.075mm) sieve: 95.2%	The soil is dominantly elastic silt (MH) with sand	Light brown firm to stiff silty clay with little gravel

4.4.1.1.8. Landslide from 82+610-83+400/(LS-08)

Site Condition:

it is noted that the soft to firm silty claye soil is indentified and hence this material having low resistivity value due to the shallow groundwater.

Geology:

The geological soil profile presented reveals that the topmost covered a residual/silty clay soil and highly weathered basalt formation Colluviums and clay materials.

Possible Cause of Landslide:

Where slope failure could occur very weak saturated thin silty clay soil observed from borehole logging from 4.0– 4.20m depth and this layer is defiantly different from the upper and lower layer in its moisture content which is almost changed into mud material. Therefore, this layer is one of slipping surface for the top material landslide and generally this road section is unstable.

A detailed description of the sampled soil

As per the information gained from field and laboratory investigation, the subsurface of this cut section is significantly composed of two lithological layers; however, to consider the effect of modulus of elasticity (its increasing nature) in the analysis part, it is divided into three layers. To efficiently describe this section, the nearby borehole located at station 62+200 needs detailed characterization and hence, this cut section is divided into two lithological layers for the sake of analysis. The details of the test results, classification and borehole description of the sampled soils at station 82+200 are shown in Table 4.5.

Table 4.5: Test result and description of the sampled soil at station 82+200

Layer	Test result (average values were taken for each layer with similar formation	Classification of soil as per USCS	Borehole log description
Layer-1 (0-8m)	Natural Moisture Content, NMC: 42.3% Liquid Limit, LL: 62% Plastic Limit, PL: 37% Plasticity Index, PI:25% Pass no. 200 (0.075mm) sieve: 97.4%	The soil is dominantly elastic silt (MH) with sand	Light brown soft to firm silty clay.
Layer-2 (8-11.8m)	Natural Moisture Content, NMC: 23% Liquid Limit, LL: 47% Plastic Limit, PL: 35% Plasticity Index, PI: 12% Pass no. 200 (0.075mm) sieve: 98.6%	The soil is dominantly elastic silt (MH) with sand	yellowish brown silty CLAY with some gravels
Layer-3 (11.8-15m)			Medium strong to strong dark gray slightly weathered and fragmented basalt rock

4.1.2. Analysis of the Failed Slope

Even though several failed slopes were encountered at this road project, only the Three critical and more of representative locations (Km45+360, 81+060, and 83+200were selected for this analysis purpose.Almost all geotechnical constructions have 3D representations of their failure modes, and the analysis results obtained using these representations accurately depict the situation's actual behavior. The 3D analysis is used for situations such as short width geotechnical structures, soils that are subjected to concentrated loading, soil properties that vary significantly along the longitudinal direction of the slope, and complex geometry, even though it can be applied to any geotechnical structure.In contrast to 3D analysis,2D analysis works better on slopes with consistent soil development and similar failure types. Additionally, it provides a conservative FS value, which is advised for the majority of slope designs. As a result, 2D analysis is used for the particular issues this study experienced.

4.1.2.1. Effect of Mesh Density

At the bottom of the horizontal boundary, the model was completely fixed., (Ux=0 and Uy=0) and only horizontal fixity was used for the left and right vertical bounds. (Ux=0). Using conventional fixated, PLAXIS 2D provides automatic boundary fixities. In PLAXIS2D analysis, there are many mesh density options that can vary from extremely coarse mesh to extremely tiny mesh. Additionally, the meshes can be fine-tuned along the slope's cut face or in places of large load concentration (taking in to account the high concentration of load during cutting). For the first station, which is representative of the rest stations, a sensitivity analysis was conducted for the various global coarseness densities with respect to the number of elements and the factor of safety very fine mesh was used in this study. According to the outcome, the number of pieces rises and the factor of safety falls as the mesh density grows. Even though it requires a high-performance computer and takes time, the accuracy of the work grows as the number of pieces increases. The accuracy required for the task and this study often determines the mesh density; fine mesh with local refinement is utilized (Figure 4.9).

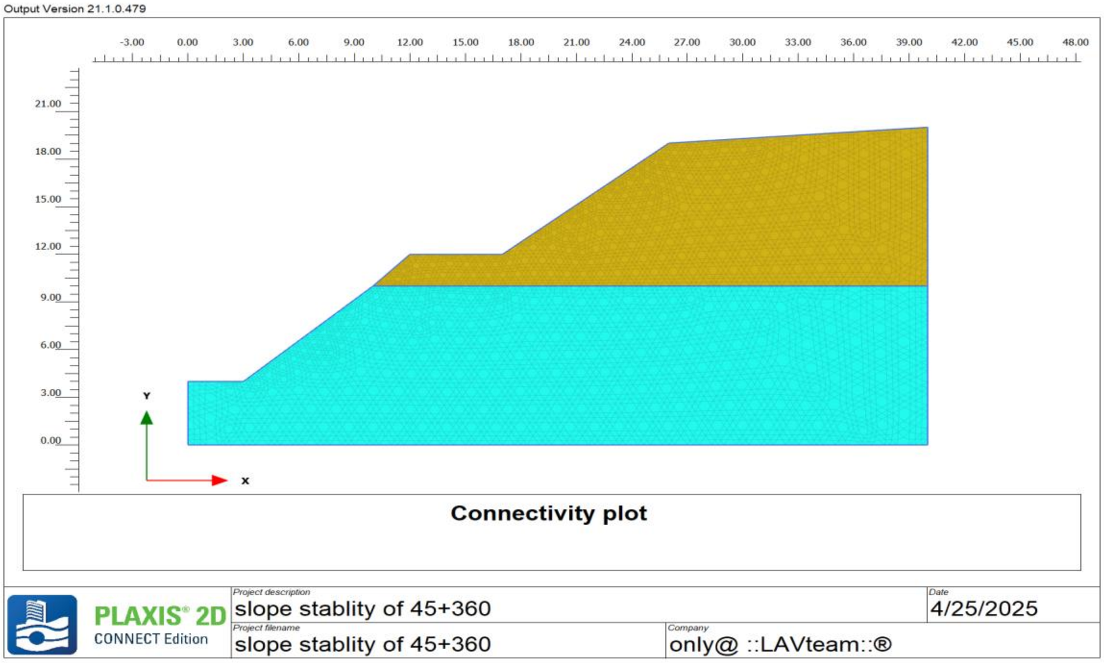

Output Version 21.1.0.479

Connectivity plot

Project description: slope stablity of 45+360

Date: 4/25/2025

Project filename: slope stablity of 45+360

Company: only@ ::LAVteam::®

Figure 4.9 : Finite element mesh at station 45+360

4.1.2.2. Cases Considered for the Analysis

In slope stability analysis, it is essential to take consideration for different situations of the slope in accordance with the site condition. Accordingly, the following were considered in this thesis:

Case-1: drained analysis to consider the long-term stability condition the cut slope. Slope stability analysis shall be conducted for drained conditions as per the slope's loading condition; soil type and geotechnical structures (whether cut or embankment fill slope).

4.1.2.3. Analysis Procedure of PLAXIS-2D

Input phase: Mohr-Columb model was applied to simulate soil behavior and material model. The K_0-procedure was not used rather gravity loading was used to account for the inclination of the ground.

Calculation phase: after mesh generation, the calculation phase started through building up of initial stresses within the deposit soils. For phase 0, the total multiplier was used and for the other cases /steps, plastic calculation type was used except the last step which is phi-c reduction.

Output phase: in the last phase, phase 2, the calculation type is applied as a safety factor to determine collapse loads and calculate stability. The program uses ΣMsf to specify the increment of strength reduction.

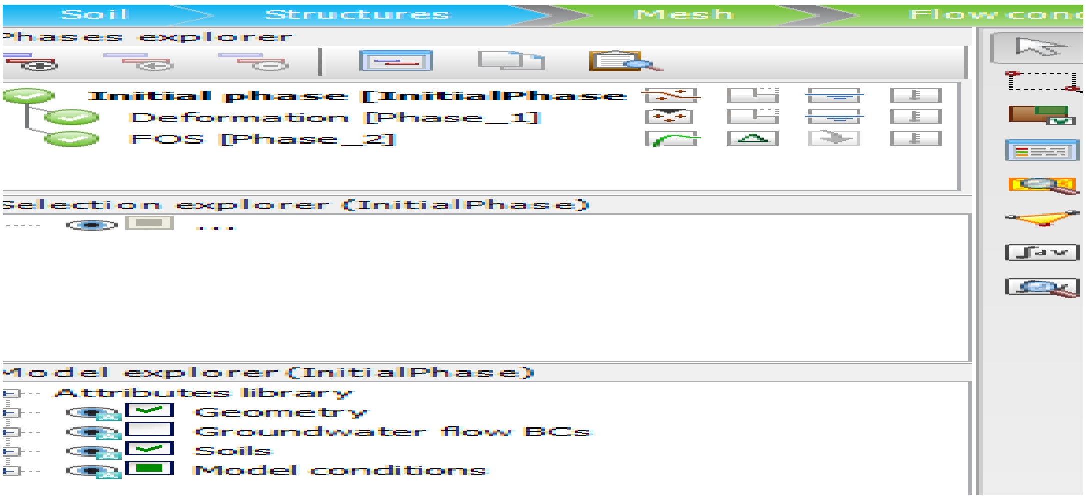

Figure 4.10: Stages of construction

4.1.2.4. Output of the Analysis

The stability of the cut is analyzed on the notion of Factor of Safety (FS) against sliding to indicate the potential slide. Most parameters are determined from laboratory and site investigation results except the Poison's ratio, which was taken from presumptive values based on the soil types.

I. Station45+360 RHS

The material forming the cut slope is highly weathered rock overlain by reddish brown silty Clay soil. The weak highly decomposed and reddish-brown overburden soil in the second bench is slipped over the weathered rock. The main reason for failure is the saturation of weak cut slope material by the action of rainfall which resulted in the. The designation of the soil layers with a number is shown in Figure 4.34 to simply understand the layers with their properties during analysis saturation and collapse of soil layer that couldn’t be able to stand with the designed back slope ratio of 1.5 H: 1V. The designed typical cross section for the cut slope material is shown below.

Figure 4.11: Layer designation for the cross-section at station 45+360

Table 4.6: Input parameters for PLAXIS software at station 45+360

Layers No.	**Description of layers**	γ_b **[kN/m^3]**	**c' [kN/m^2]**	**ϕ' [°]**	**E' [kPa]**	**ν' [-]**
1	Stiff Silty Clay	15.34	10	20	5,400	0.3
2	Hard Silty Clay	15.34	92	30	20,00	0.3

*** Note that the value of modulus of elasticity was evaluated from the soil consistency based on SPT-N value.

For the two stations, the analyses were done for the different cases that are mentioned in section 4.1.2.2 Drained condition was used as the investigated cut slope soils are mainly a clay soil then considering the long-term effect is necessary. The analysis results of this conditions are shown in figure 4.12 for station 45+360.

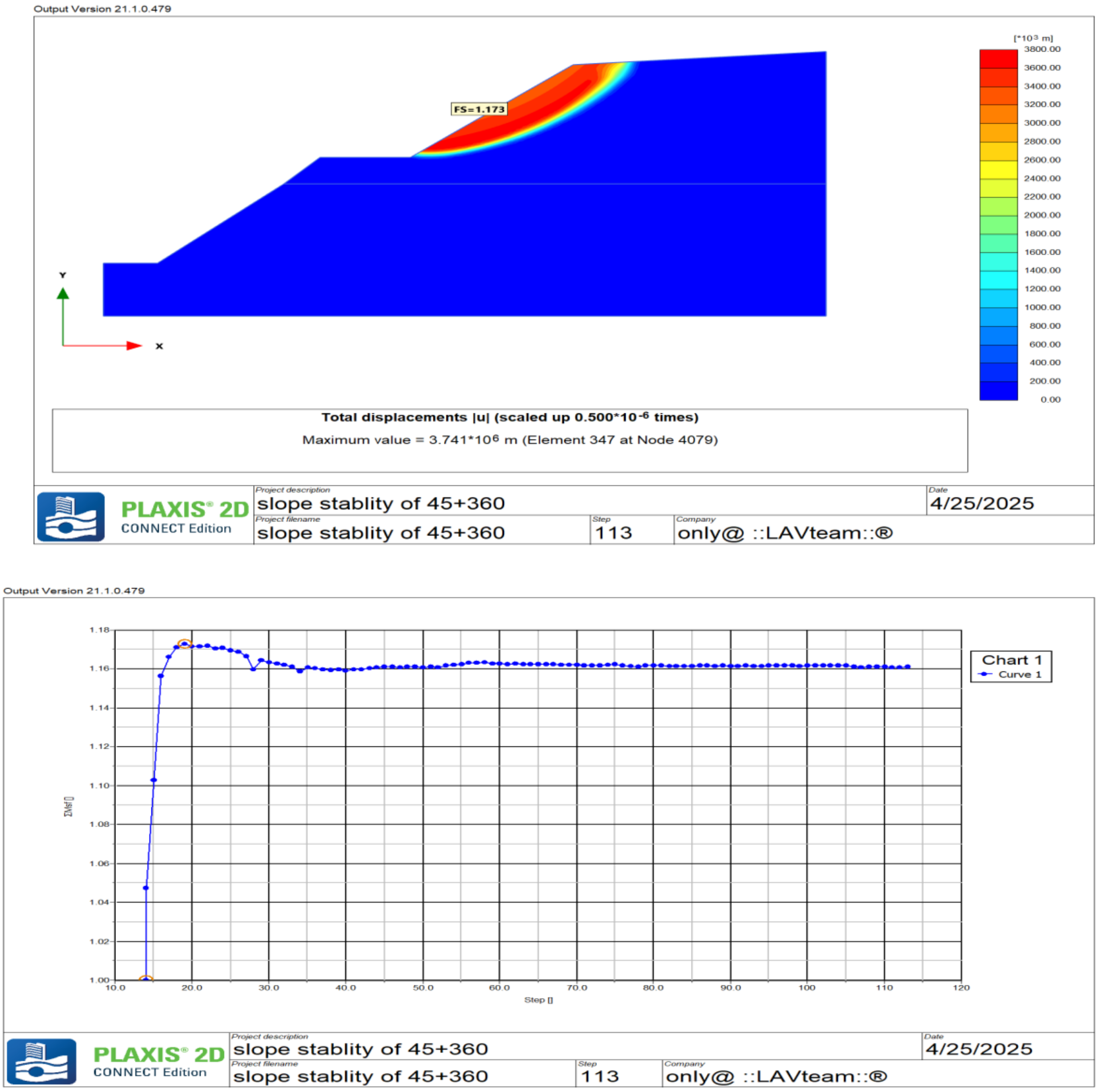

Total displacements |u| (scaled up 0.500*10⁻⁶ times)

Maximum value = 3.741*10⁶ m (Element 347 at Node 4079)

Project description: slope stablity of 45+360
Date: 4/25/2025
Project filename: slope stablity of 45+360
Step: 113
Company: only@ ::LAVteam::®

Project description: slope stablity of 45+360
Date: 4/25/2025
Project filename: slope stablity of 45+360
Step: 113
Company: only@ ::LAVteam::®

Figure 4.12 : Analysis result at station 45+360

The actual cut slope analysis showed that the slope is not safely stable (FS=1.173).It can be observed that the cut slope is not satisfactorily stable. It is found that the slope is more critical for this cut slope 1. 5H:1V (FS=1.173> F). Remedial solutions should be proposed based on condition since it is critical among the three cases.

For station 45+360:in this station, the slip surface on the ground and obtained after analysis are almost coincided with each other except at the toe of the excavated road, the actual slip surface is overestimated and is shown in Figure 4.14 below.

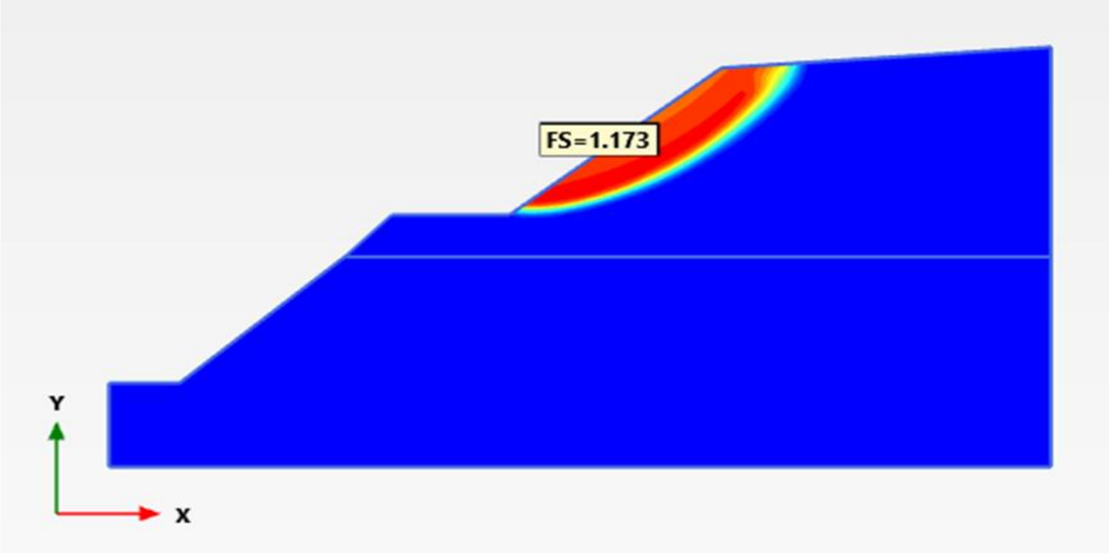

Figure 4.13*:* Analyzed slip surfaces at station 45+360

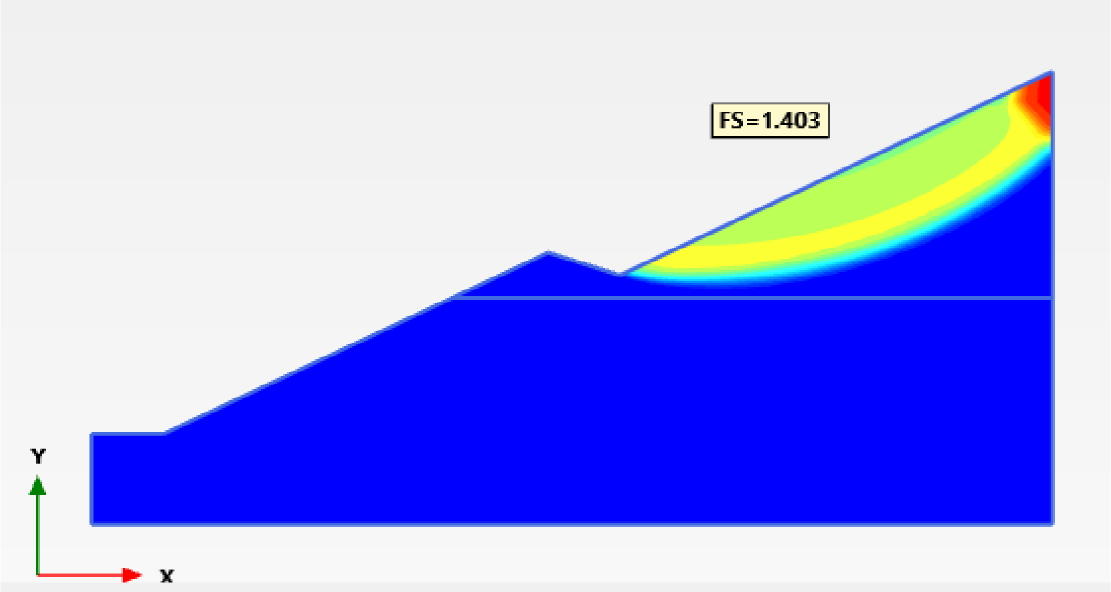

Figure 4.14 : Analyzed slip surfaces at station 45+360

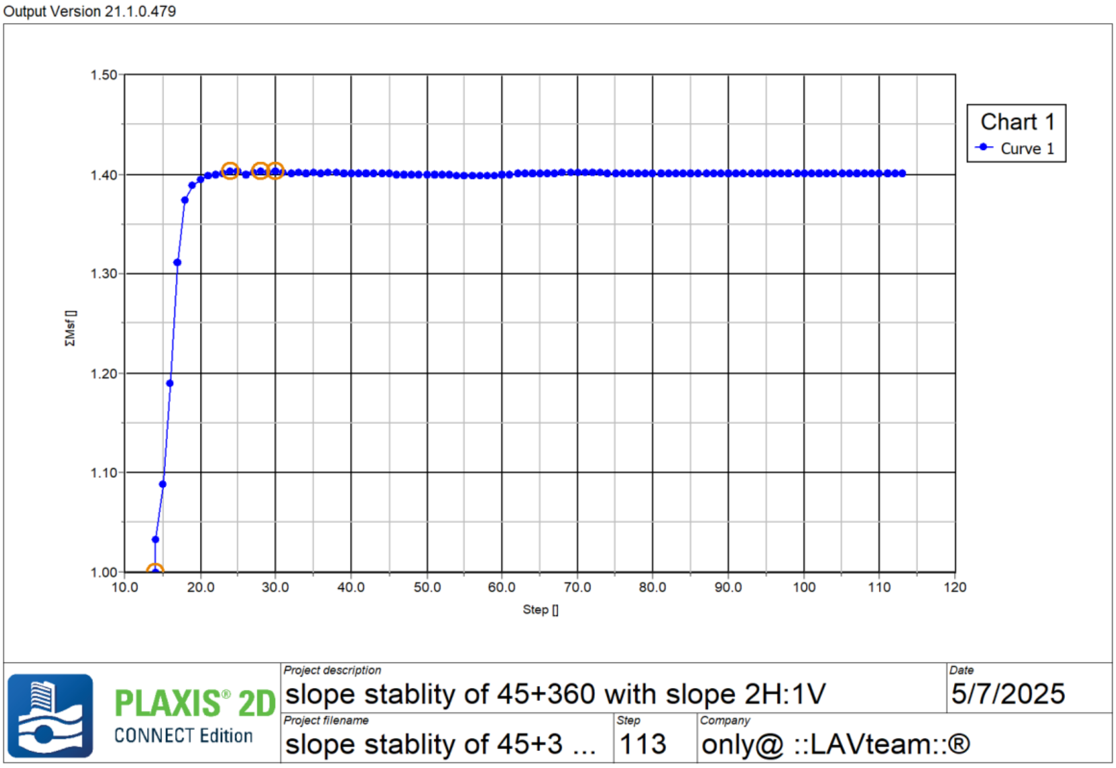

Project description: slope stablity of 45+360 with slope 2H:1V

Date: 5/7/2025

Project filename: slope stablity of 45+3 ...

Step: 113

Company: only@ ::LAVteam::®

Figure 4.15: Analysis result at station45+360 with slope of 2H:1V

It can be noted that the slope with the original slope is on the verge of failure (FS=1.173) and with the slope ratio of 2:1, it is somewhat satisfactory with FS=1.43. In this regard, providing a retaining is more important structure. This is due to:

- The slope flattening is not more sufficient to stabilize the cut slope in the safest way
- As the failure is associated with the destabilization of the slope in the time of cutting coupled with the increase of shear stress due to rainfall, spring and surface streams and steepness of the slope. As a result, a rigid structure can accommodate such failures than any other flexible structure like gabions.
- The vicinity of the cut slope is agricultural land which is not allowed to flatten the cut slopes in excess due to right of way constraints. Hence, the provision of retaining structure is more appropriate.

Table 4.7: Parameters in the analysis of masonry/retaining wall ***(Bowles J. E., 1996)***

Masonry wall parameter	Units	Value
Unit weight	kN/m^3	25
Elasticity modulus	kN/m^2	2.5E+07
Poisson's ratio	-	0.15
Material model	Linear elastic	
Material type	Non-porous	
Granular material		
Unit weight	kN/m^3	18
Elasticity modulus	kN/m^2	8.0E+04
Poisson's ratio	-	0.3
Cohesion	kN/m^2	1
Angle of internal friction	°	40
Material type	Drained	

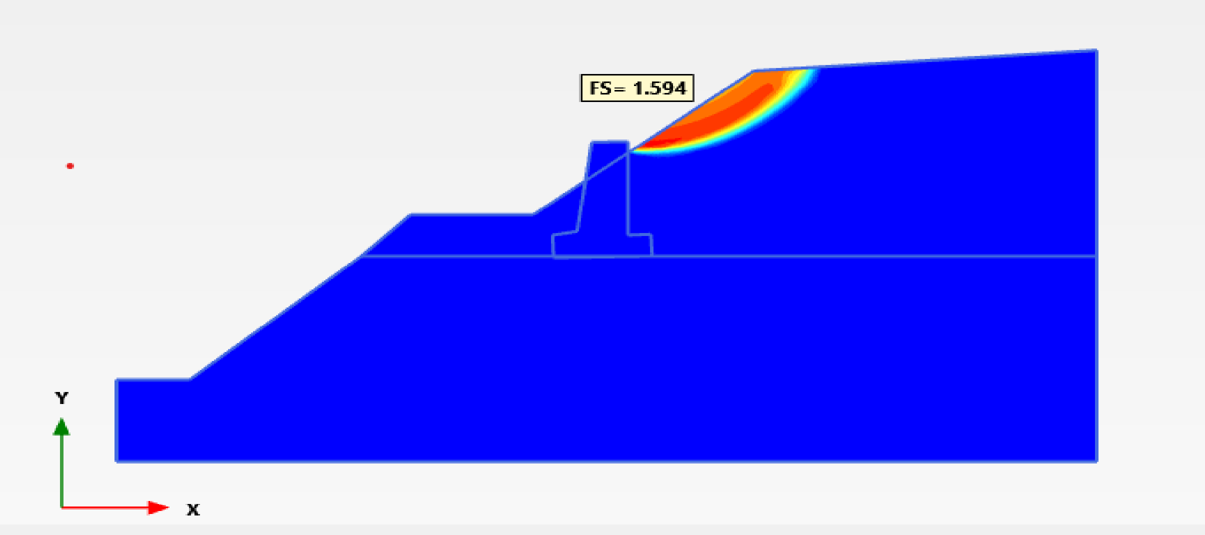

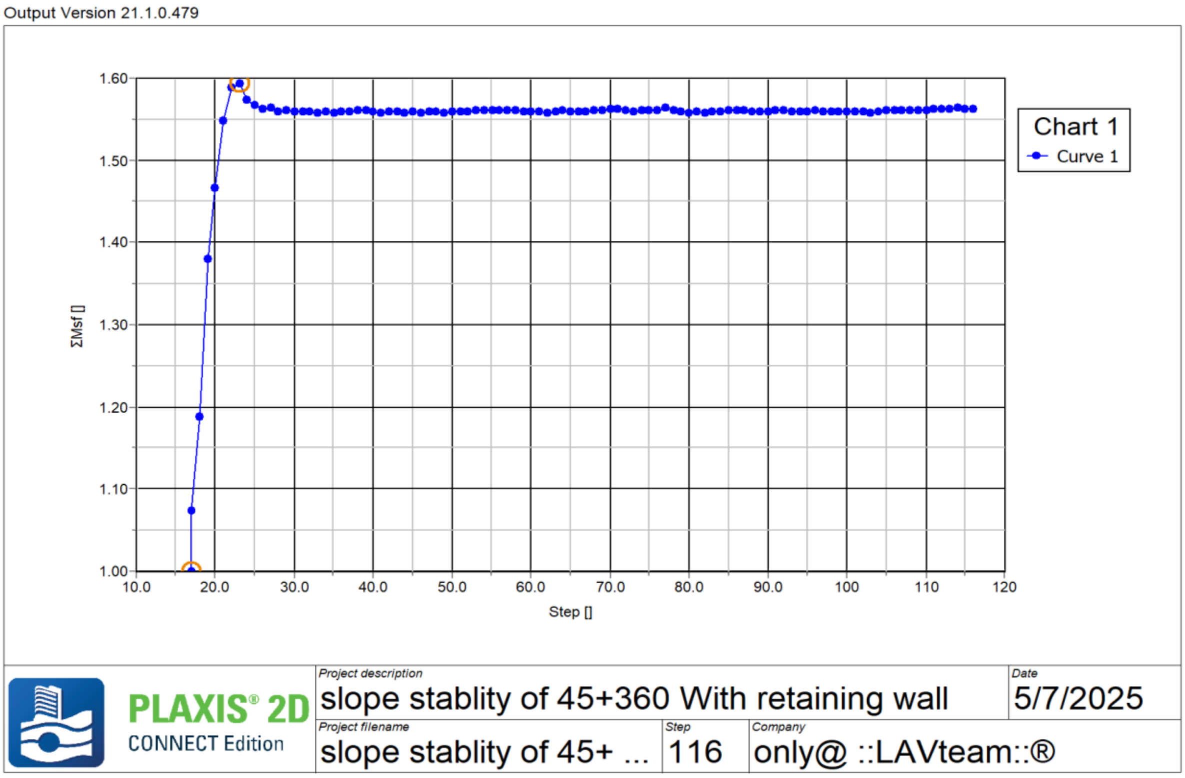

Project description: slope stablity of 45+360 With retaining wall

Date: 5/7/2025

Project filename: slope stablity of 45+ ...

Step: 116

Company: only@ ::LAVteam::®

Figure 4.16: Analysis result at station 45+360 with retaining wall

II. Station 81+060

The material forming the cut slope the topmost layer is silty clay material clayey silt and Colluviums material or highly to completely weathered rock as per this investigation the main factors for the instability problem in the Section are geological structure of fault. The designation of the soil layers with a number is shown in Figure 4.17 to simply understand the layers with their properties during analysis saturation and collapse of soil layer that couldn’t be able to stand.

Table 4.8: Input parameters for PLAXIS software for station 81+060

Layer No.	**Description of layers**	**Depth (m)**	**γ_b [kN/m^3]**	**c’ [kN/m^2]**	**ϕ’ [°]**	**E’ [kPa]**	**ν’ [-]**
1	Soft to firm silt clay	0-5	14.89	10	15	6000	0.3
2	Firm silty clay with gravel	5-20	16.14	20	25	10,000	0.3

*** Note that the value of modulus of elasticity was evaluated from the soil consistency based on SPT-N value.

the analyses were done for the cases that are mentioned in section 4.1.2.2 Drained condition was used as the investigated cut slope soils are mainly a clay soil then considering the long-term effect is necessary. The analysis results of this conditions are shown in figure 4.17 for station 81+060.

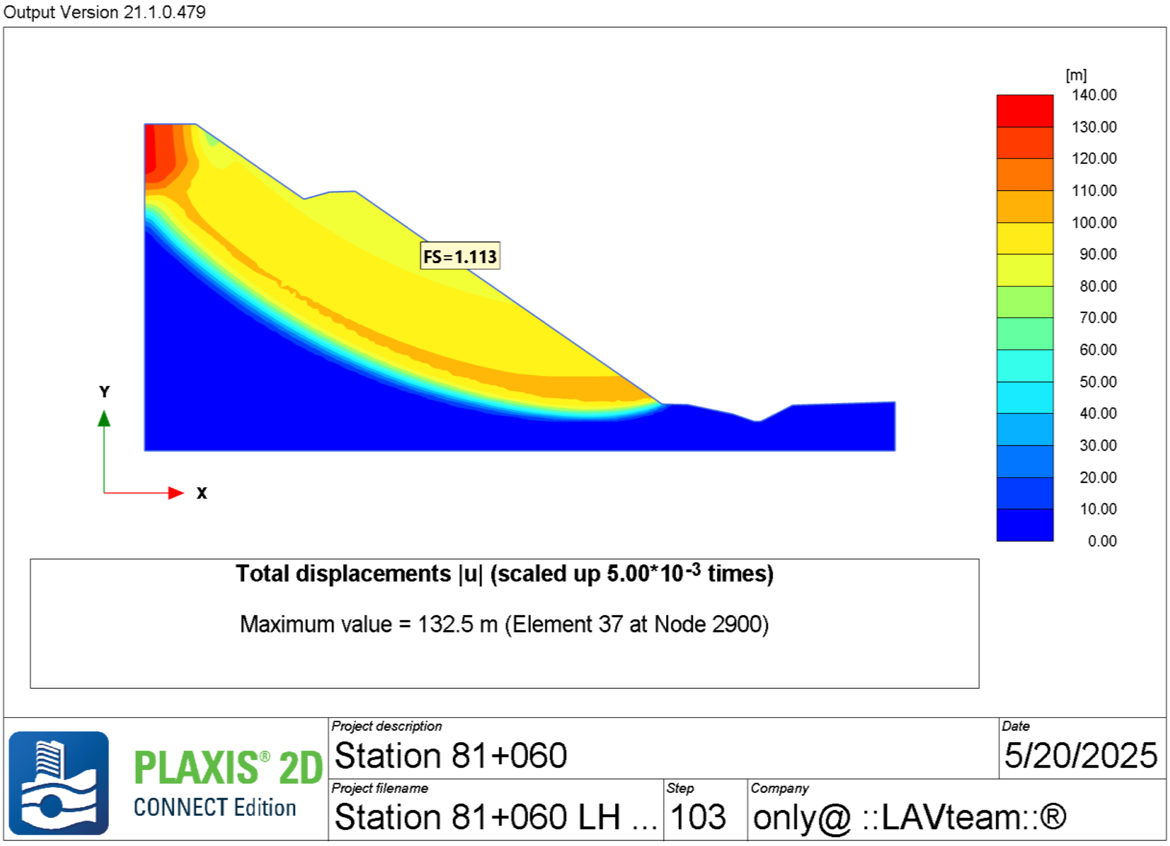

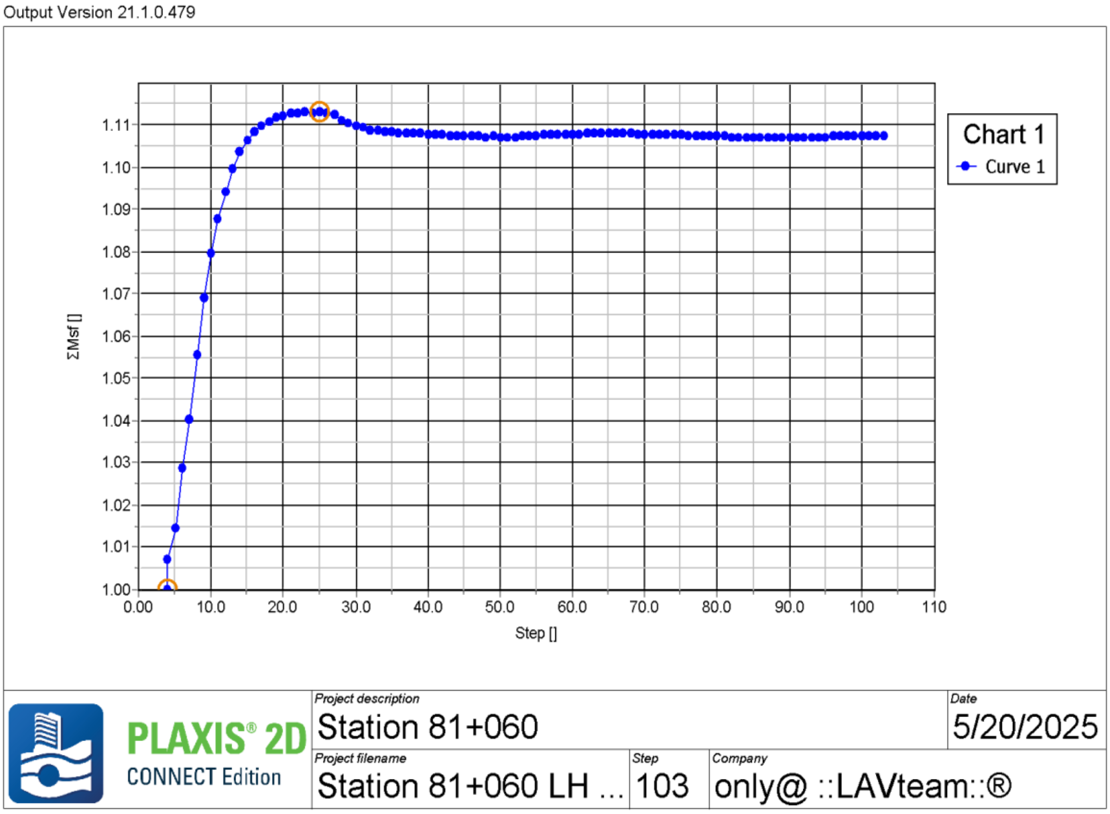

Project description: Station 81+060

Date: 5/20/2025

Project filename: Station 81+060 LH ...

Step: 103

Company: only@ ::LAVteam::®

Figure 4.17: Analysis result at station 81+060

The actual cut slope analysis showed that the slope is not safely stable (FS=1.173). It can be observed that the cut slope is not satisfactorily stable. It is found that the slope is more critical for this cut slope 1. 5H:1V (FS=1.113> F). Remedial solutions should be proposed based on condition since it is critical among the three cases.

For station 81+060: in this station, the construction technique adopted, which left the back slope unfinished and sharp at the toe, is what caused the landslide at this point. According to the ERA Geometric Design Manual (2013), flattening the slope to a 2:1 (H: V) will stabilize it because of the existing failing is shown in Figure 4 - 18 below.

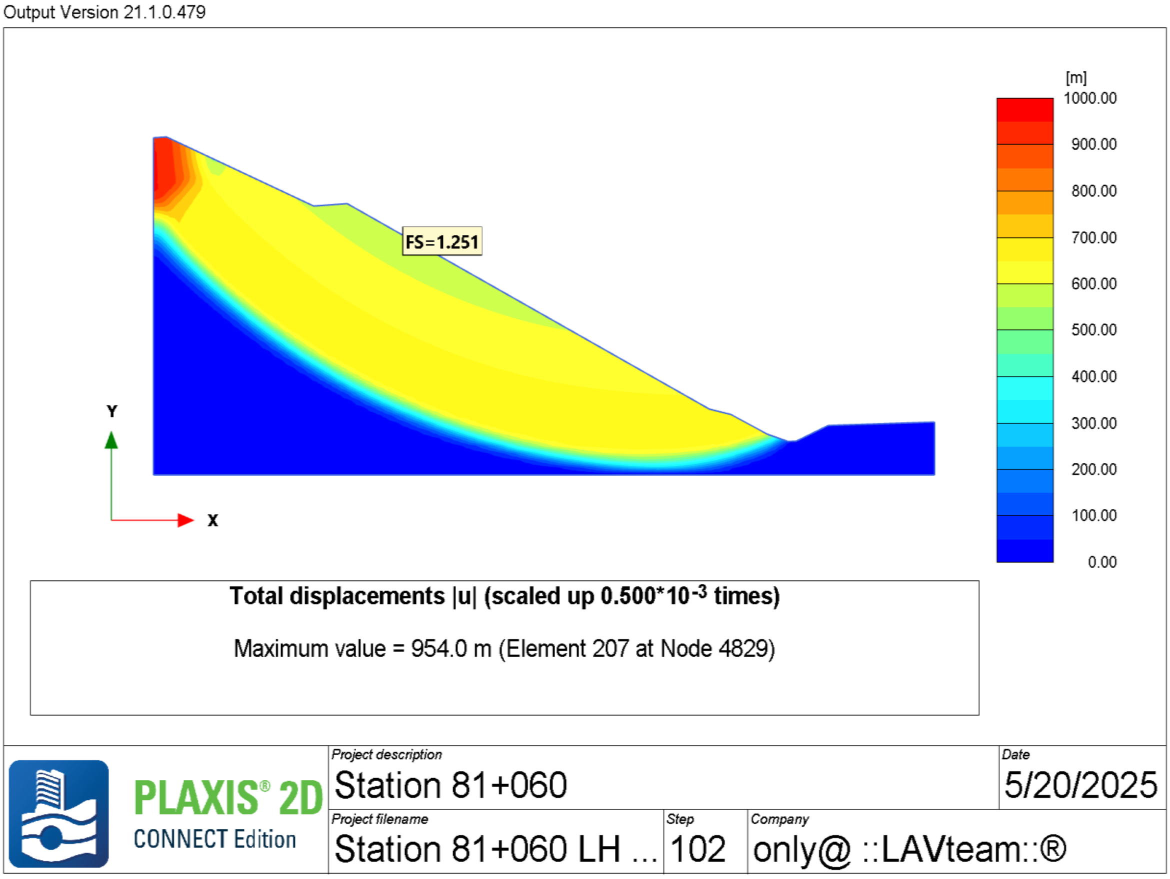

Output Version 21.1.0.479

Total displacements |u| (scaled up 0.500*10^{-3} times)

Maximum value = 954.0 m (Element 207 at Node 4829)

Project description Station 81+060

Date 5/20/2025

Project filename Station 81+060 LH ...

Step 102

Company only@ ::LAVteam::®

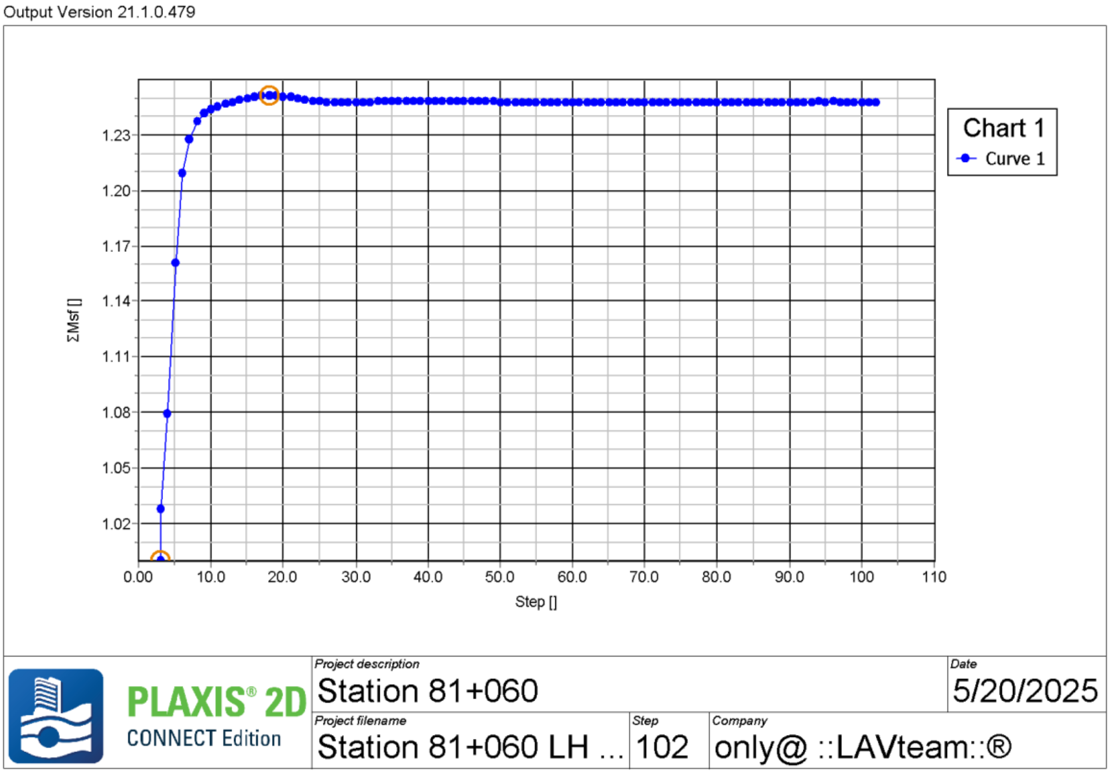

Output Version 21.1.0.479

Project description Station 81+060

Date 5/20/2025

Project filename Station 81+060 LH ...

Step 102

Company only@ ::LAVteam::®

Figure 4.18: Analysis result at station 81+060 with slope of 2H:1V

It can be noted that the slope with the original slope is on the verge of failure (FS=1.113) and with the slope ratio of 2:1, it is not satisfactory with FS=1.251. In this regard, to have a more stable slope providing retaining walls and gabion is more important.

III. Station 83+200

The material forming the cut slope the topmost covered a residual/silty clay soil and highly weathered basalt formation Colluviums and clay materials and hence this material having low resistivity value due to the shallow groundwater. The designation of the soil layers with a number is shown in Figure 4.19 to simply understand the layers with their properties during analysis saturation and collapse of soil layer that couldn't be able to stand.

Table 4.9: Input parameters for PLAXIS software for station 83+200

Layer No.	**Description of layers**	**Depth (m)**	**γ_b [kN/m^3]**	**c' [kN/m^2]**	**ϕ' [°]**	**E' [kPa]**	**ν' [-]**
1	Soft to firm silt clay	0-8	15.13	10	15	6000	0.3
2	Firm silty clay with gravel	8-12	16.59	20	20	10,000	0.3

***Note that the value of modulus of elasticity was evaluated from the soil consistency based on SPT-N value.

the analyses were done for the cases that are mentioned in section 4.1.2.2 Drained condition was used as the investigated cut slope soils are mainly a clay soil then considering the long-term effect is necessary. The analysis results of this conditions are shown in figure 4 - 19 for station 83+200.

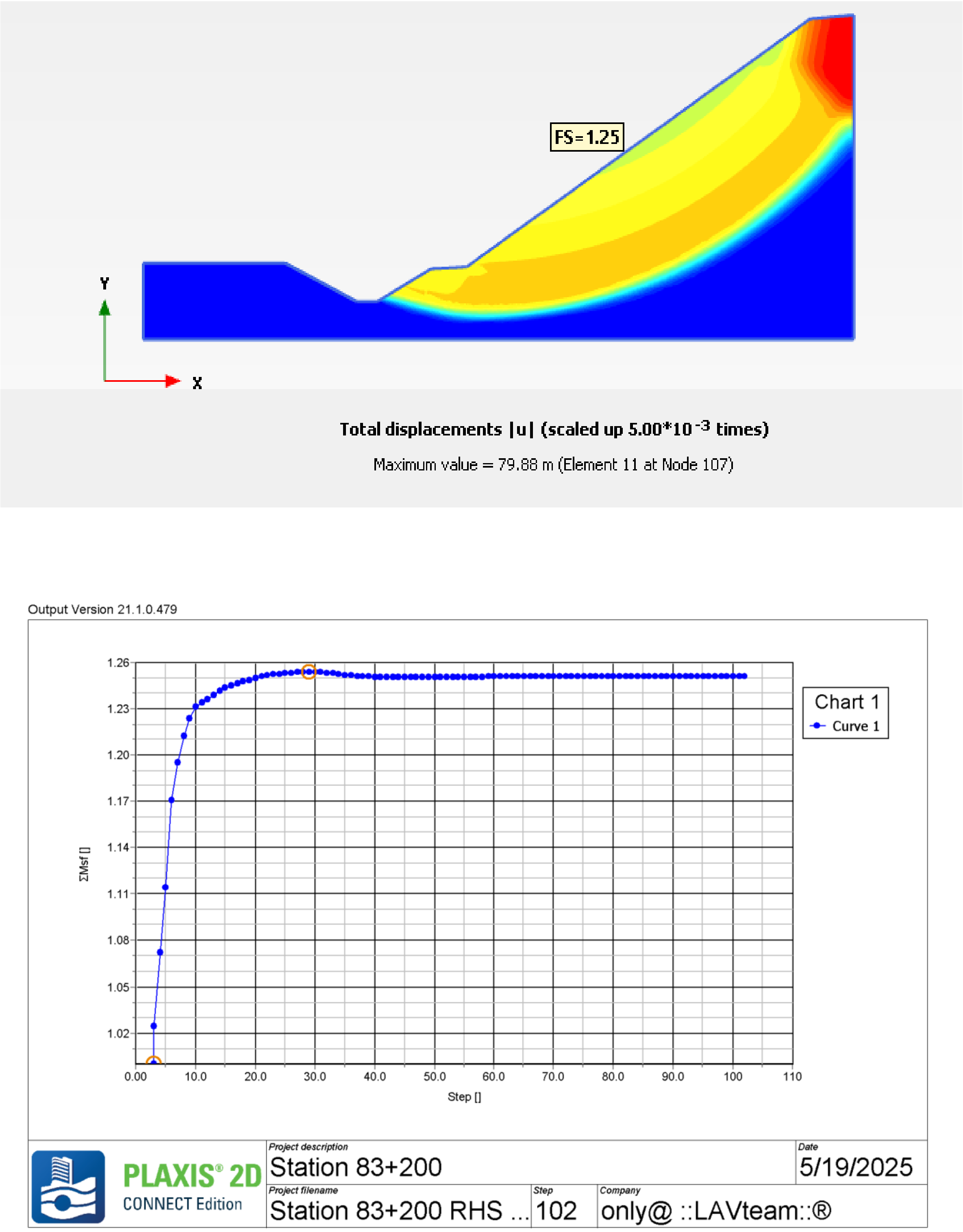

Project description: Station 83+200

Date: 5/19/2025

Project filename: Station 83+200 RHS ...

Step: 102

Company: only@ ::LAVteam::®

Figure 4.19: Analysis result at station 83+200 RHS

The actual cut slope analysis showed that the slope is not safely stable (FS=1.25). It can be observed that the cut slope is not satisfactorily stable. It is found that the slope is more critical for this cut slope 1. 5H:1V (FS=1.25> F). Remedial solutions should be proposed based on condition since it is critical among the three cases.

For station 83+200: in this station, the construction technique adopted, which left the back slope unfinished and sharp at the toe, is what caused the landslide at this point. According to the ERA Geometric Design Manual (2013), flattening the slope to a 2:1 (H: V) will stabilize it because of the existing failing is shown in Figure 4.20 below.

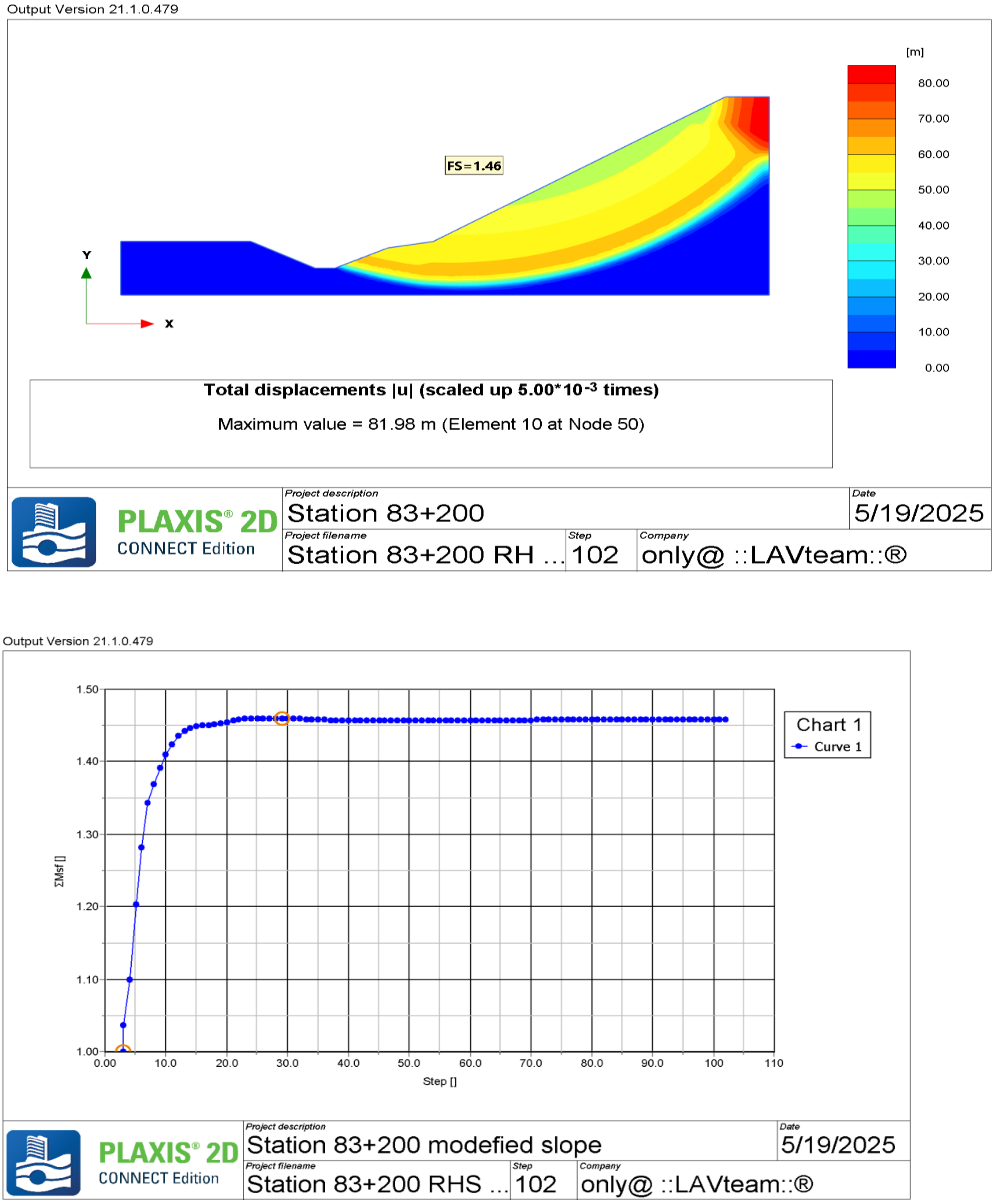

Output Version 21.1.0.479

Total displacements |u| (scaled up 5.00*10⁻³ times)

Maximum value = 81.98 m (Element 10 at Node 50)

Project description: Station 83+200

Date: 5/19/2025

Project filename: Station 83+200 RH ...

Step: 102

Company: only@ ::LAVteam::®

Output Version 21.1.0.479

Project description: Station 83+200 modefied slope

Date: 5/19/2025

Project filename: Station 83+200 RHS ...

Step: 102

Company: only@ ::LAVteam::®

Figure 4.20: Analysis result at station 83+200 with slope of 2H:1V

It can be noted that the slope with the original slope is on the verge of failure (FS=1.113) and with the slope ratio of 2:1, it is not satisfactory with FS=1.251. In this regard, to have a more stable slope providing retaining walls and gabion is more important.

4.2. Landslide Contributing Factors

The final landslide susceptibility map (LSM)'s accuracy depends critically on the identification, selection, and assessment of the landslide contributing and triggering elements. Different landslide factors have been utilized by different researchers to create landslide susceptibility maps (LSM). According to T. Raghuvanshi et al. (2014), there are no set selection criteria for landslide triggering variables or parameters. The primary drivers for the selection of elements are the study area's geomorphological, geological, hydrological, and human/man-made conditions, as well as the data's accessibility. Through site inspection, field reconnaissance, literature review, and resident interviews, the triggering elements that contribute to the occurrence of landslides in the study region have been examined. For landslide susceptibility mapping, the chosen factor must be quantifiable, distinct, comprehensive, and useful (Melese et al., 2022). Eight (8) landslide causal factors/parameters are chosen for this study based on the aforementioned prerequisites. Geomorphological elements include slope angle, height, slope aspect, and curvature; geological considerations include lithology; hydrological factors include rainfall and distance to the stream; and human influences include land use and land cover.

4.2.1. Slope Angle

One of the most important elements influencing the occurrence of landslides is slope angle; the steeper the slope, the more likely it is that a landslide will occur. According to ((Mehmod, 2022), the slope angle is a metric that expresses how steep and inclined something is in relation to the horizontal plane.

According to various researchers, including (Ayenew, T., & Giulio, G, 2005) (Guzzetti F. , 1999) (Wendim A. , 2023) and (Woldearegay K. , 2019), a substantial number of earlier studies indicated that the majority of landslide phenomena occurred in areas with slope angles between 15^0 and 45^0.

The area's slope shape influences the driving stress within the slope as well as the depth of the weathering layer and runoff water (Guzzetti f. , 2005)

The main notion here is that a water table at a shallower depth will be necessary to cause failure, and that the low likelihood of landslides in flat and gentle slopes may be due to the corresponding increase in the slope's safety factor (Woldearegay K. , 2019)

The opposing viewpoint holds that because most steep slopes are made up of new to highly weathered rock formations, the lack of significant landslide phenomena on topography with steep slope gradients is related to the very thin or nonexistent unconsolidated deposits on such terrains. As was already established, the area's stability is greatly influenced by the slope angle. A number of natural and man-made processes change the area's natural slope angle, which in turn affects the likelihood of landslides occurring. Using an Arc GIS spatial tool, the slope map of the Gore-Masha-Tepi section was created from DEM data and divided into nine (9) classes: $<5^0,5^0-9^0,9^0-14^0,14^0-20^0,20^0-27^0,27^0-32^0,32^0-39^0$, 39^0-48^0 and 48^0-75^0 (Figure 4-21).The project road is primary traversing rolling and mountains terrain following the classes of the ERA geometric design manual the terrain along the project road can be described as follows

- Flat terrain for a total of 2km (1.4% of the project road length)
- Rolling terrain for a total of 103.6km (73.7% of the project road length)
- Mountainous terrain for a total of 30.9km (22% of the project road length)
- Escarpment terrain for a total of 4.2km (3% of the project road length)

The above shown lengths of terrain classes result from an analysis of the different ranges of ground slopes along the project route extracted from available topo graphic survey data and based on the definitions of the ERA geometric Design manual where a Minimum length of 1 km of terrain class has been considered.

- Gatira ridge, chainage Km 45 to Km 47.2 (length 2.2km)

- Toti ridge, chainage Km 78.7 to Km 85.3 (length 6.6km)
- Tugiri ridge, chainage Km 97.9 to Km 99.6 (length 2.2km)

From figure 4.22itisindicated that majority of the existing landslides are occurred in a slope class 0-5^0 5^0-$9^0$$9^0$-$14^0$and 14^0-20^0which composed 17.7%, 24.5%,20.5% and 15.8% of the total landslides along the section of the road respectively, the slope classes,20^0-27^0,27^0-32^0,32^0-39^0and39^0-48^0 are composed 9.8%,6%,3.4%,1.7% and 0.6% of the total recorded landslides respectively, along the studied road section.

The majority of landslides that currently occur on rolling and rolling to mountainous terrain, according to this discussion. This suggests that the slope angle alone does not play a significant role in the occurrence of landslides along the study road section.

Slope angle has a cumulative effect with the other components, even if it is not the primary factor that causes landslides along the road. Based on the in-situ assessment of the current active landslides, it is observed that the rolling and rolling to mountainous areas are primarily affected by the relative roughness of the local topography, the lithology and geological formation of the area, or their proximity to streams and distance from the engineered road (primarily on the high fill and deeper cut sections).

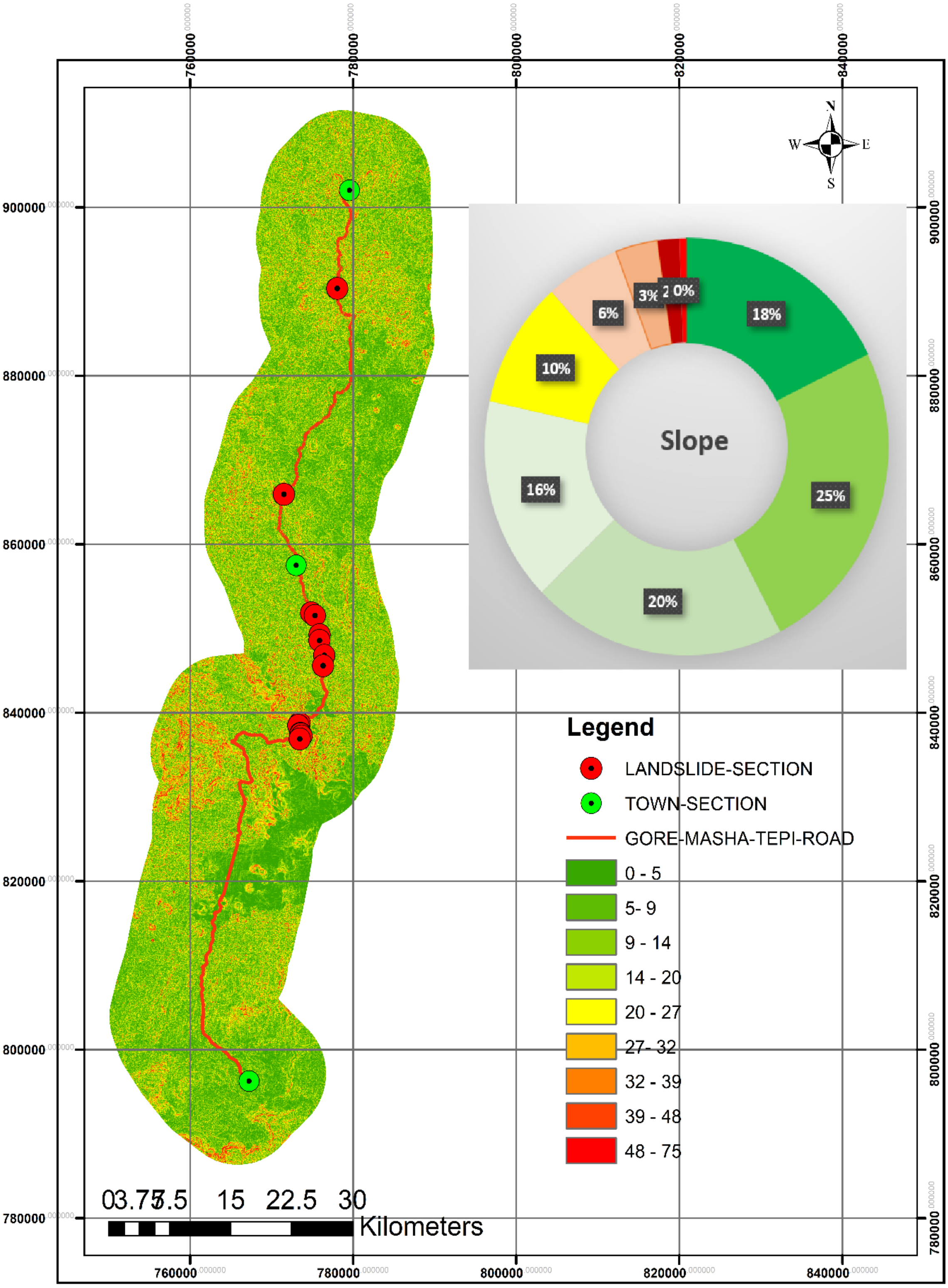

Figure 4.21: Slope map

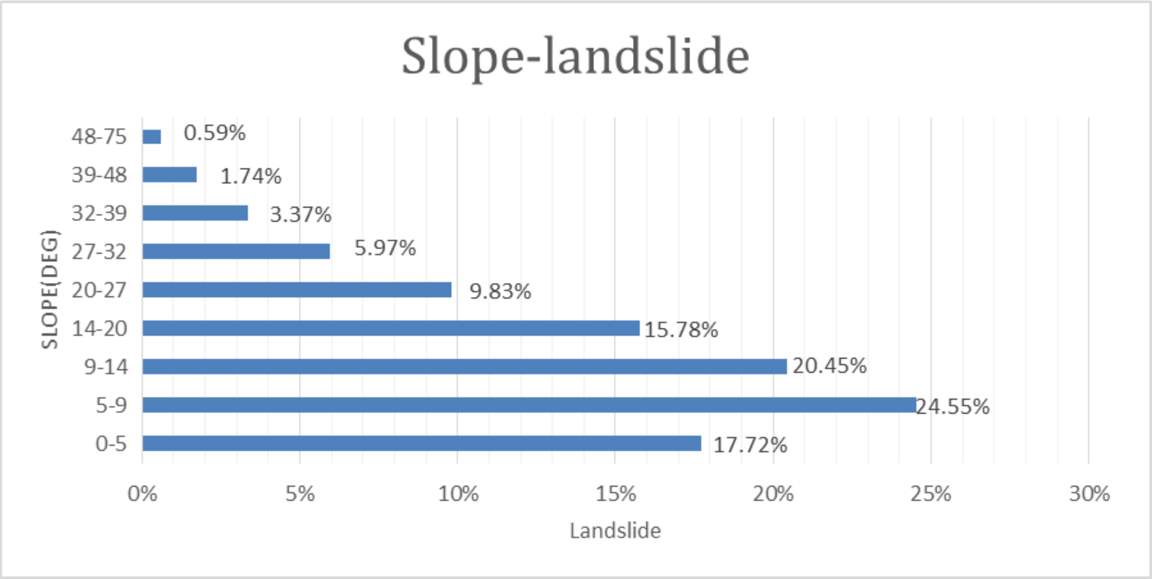

Figure 4.22: Distribution of the slope angle factor classes for the existing landslides

4.2.2. Slope Aspect

The direction that the slope faces is known as the slope aspect (Tesfa, 2022). based on interactions with local geological, climatic, and human factors in southwest Ethiopia. Heavy monsoon rains (*Kermet* season), volcanic soil characteristics, deforestation, and changes in land use are some of the main causes. This matrix evaluates the relative landslide susceptibility of slope aspects (flat, north, northeast, east, southeast, south, southwest, west, northwest) in southwest Ethiopia Flat vs. All Slopes: Flat terrain (slope <5°) has minimal landslide risk due to low runoff and gravity-driven instability. Exceptions occur if human activities (e.g., road construction) destabilize flat areas. Southwest, West, Northwest: These aspects are most susceptible due to Exposure to prevailing monsoon winds, leading to heavy rainfall saturation, Higher erosion rates from wind-driven rain and deforestation for agriculture. In South vs. North: South-facing slopes: Moderate risk. While solar radiation dries soil, deforestation and farming on these slopes reduce vegetation stability, and North-facing slopes: Higher moisture retention (shaded) increases pore pressure, but denser vegetation in some regions mitigates risk. Southeast/East: Moderate susceptibility. These aspects receive morning sun, reducing soil moisture, but are less exposed to monsoon rains compared to southwest/west.

The amount of soil moisture can be linked to the slope aspect's role to landslide incidence. The association between slope aspect facing and landslides is represented in this study by using the slope aspect as one of the triggering factors.

The slope aspect map is created using the ArcGIS software's aspect tool on the 30.0 m x 30.0 m DEM data, as shown in Figure 4.23. The slope aspect map that was created for the study area in question is divided into nine different classes: flat, northwest (NW), west (W), southwest (SW), south (S), southeast (SE), east (E), northeast (NE), and north (N). The of landslides occurred in the West(W),East(E),South(S) North (N), Southwest (SW), Northwest (NW), Northeast (NE), Southeast (SE) and Flat (F) slope aspect classes, which accounted for 13.6%, 13.0%, 12.8% 12.5%,12.3%,12.2%,11.8%,11.7 and 0.2% of all landslides, respectively, according to the analysis between the slope aspect map (Figure 4-24) and the existing landslide sections.

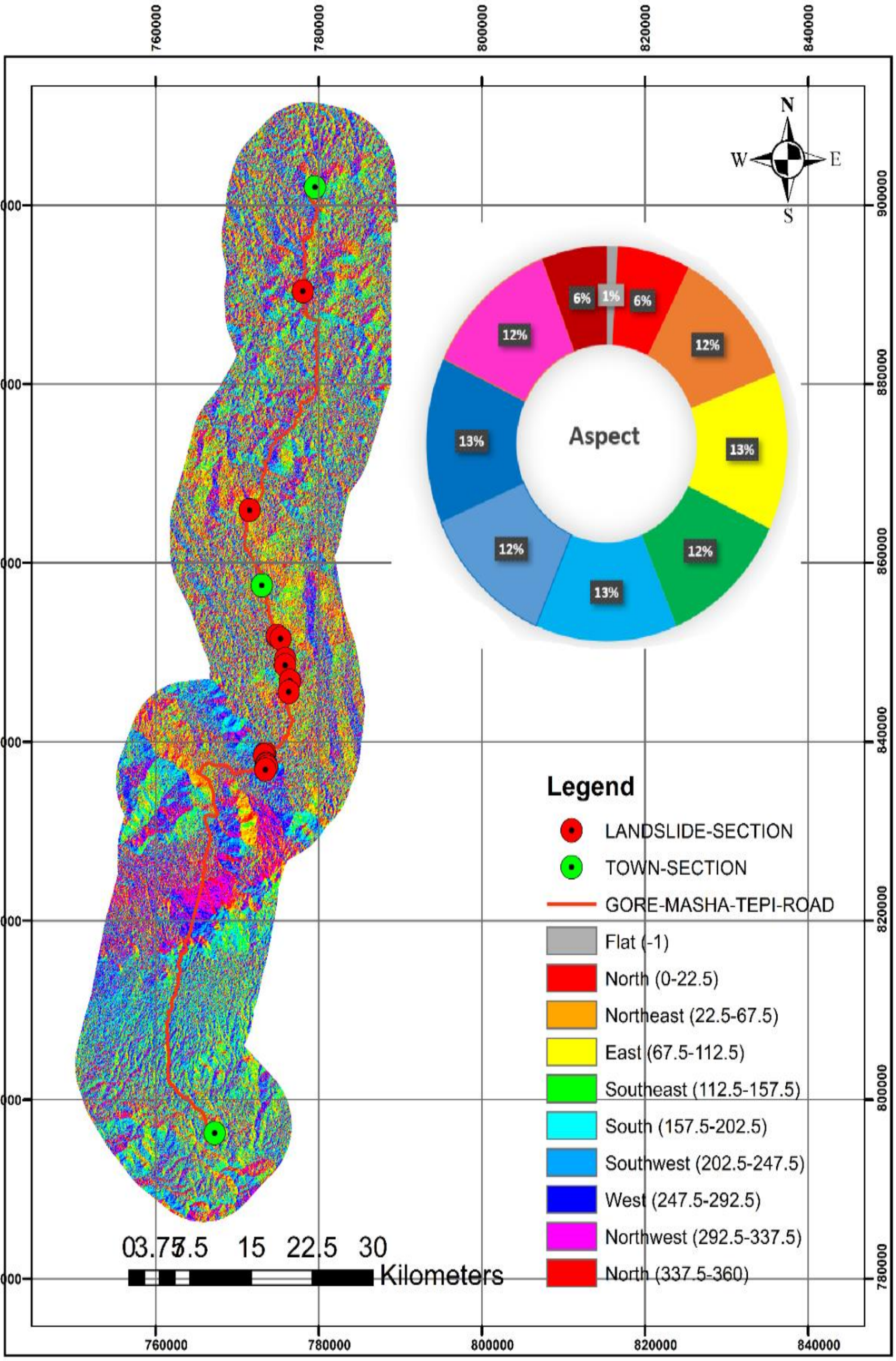

Figure 4.23: Slope aspect map

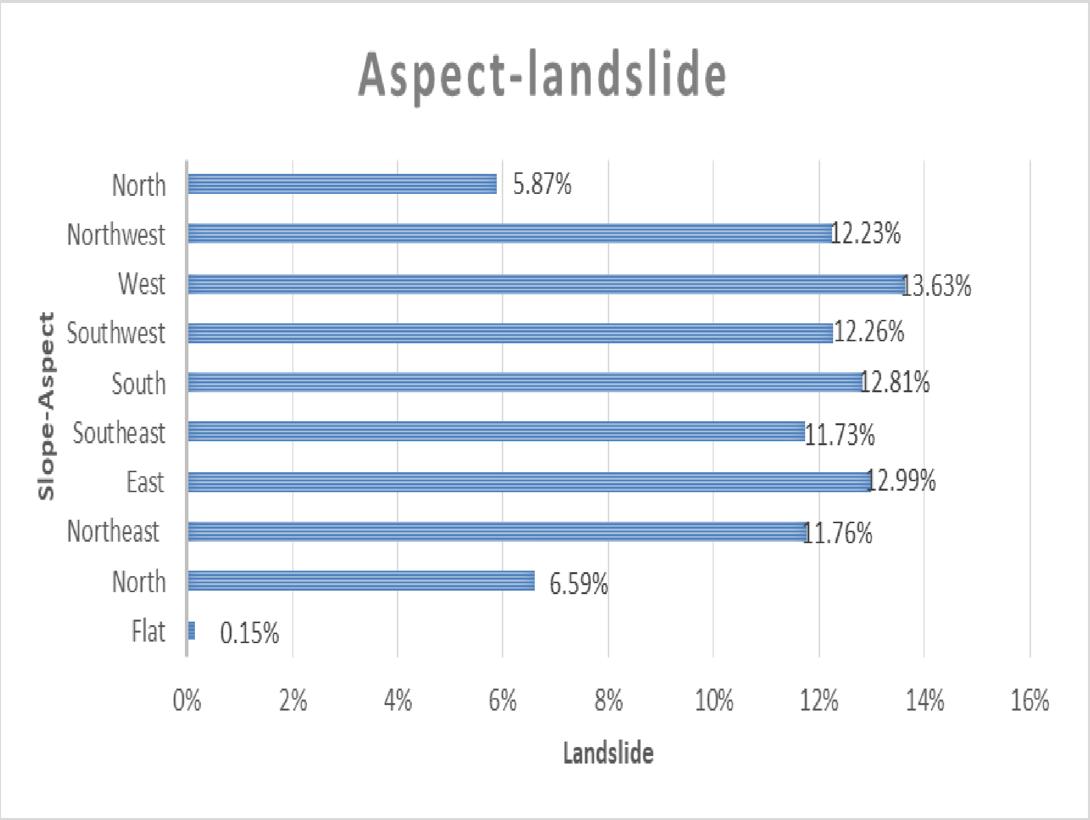

Figure 4.24: Distribution of the slope aspect factor classes for the existing landslides

4.2.2. Elevation

Many studies utilize elevation, which is defined as the area's height in relation to sea level, as a contributing factor when assessing the area's susceptibility to landslides. In theory, landslides are more likely to occur in places with greater elevations. Elevation is primarily associated with several environmental factors, including the kind of vegetation, density of the area, and the intensity of rainfall received (Catani, 2013)Using the ArcGIS software program, the elevation of the research region was created and derived from a digital elevation model with a resolution of 30.0 m. The region was categorized into seven classes based on elevation, which varied from 807 m to 2783 m (Figure 4.25). Higher elevation areas experience more precipitation, which suggests that landslides are more likely to occur there and that they have a history of happening frequently. Referring to Figure 4.26,

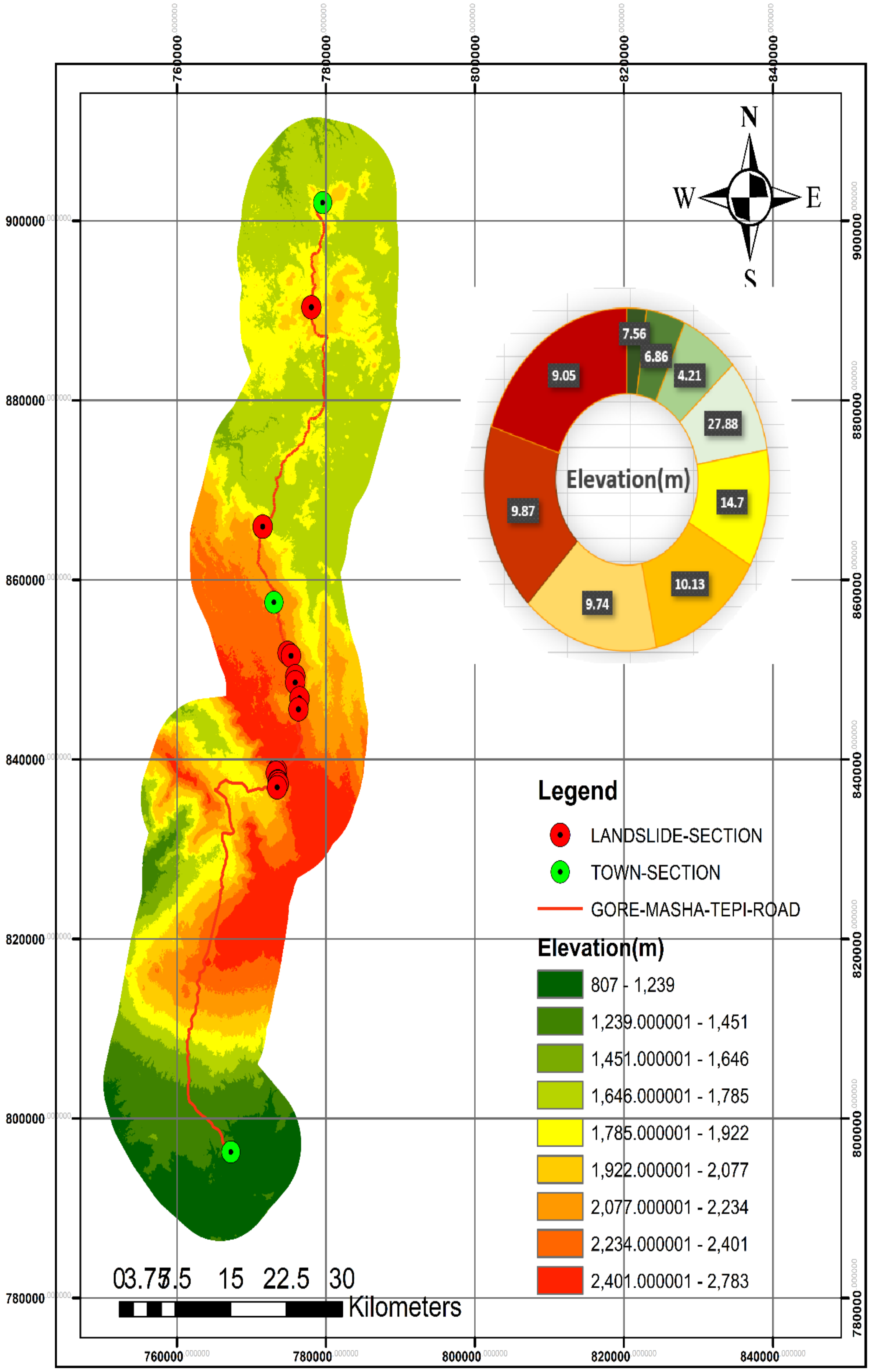

Figure 4.25: *Elevation map*

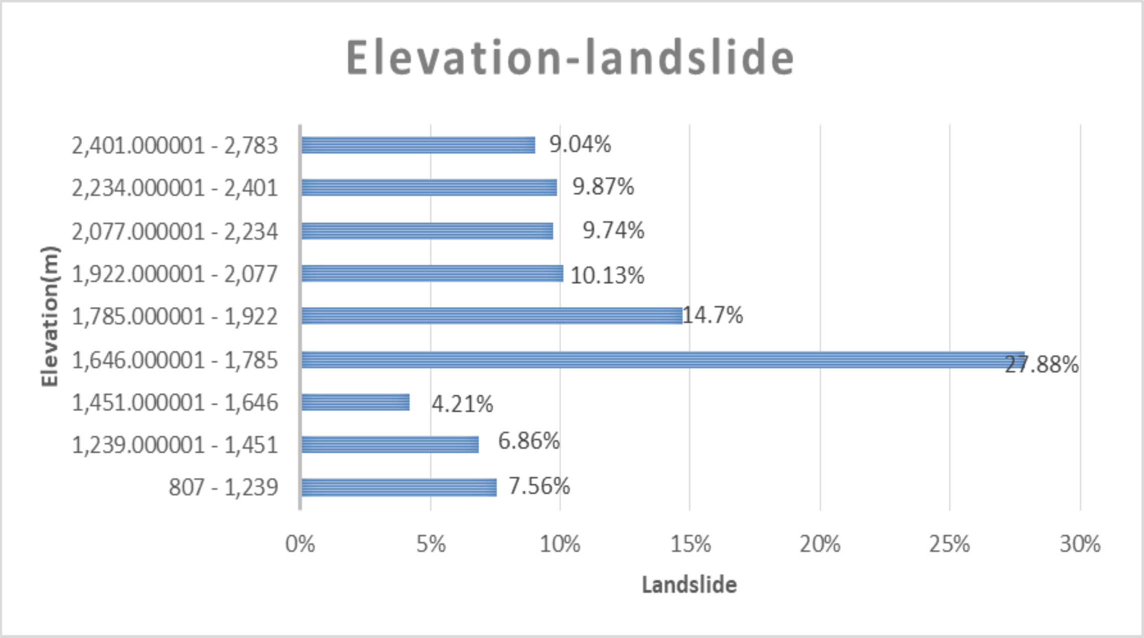

Figure 4.26: Distribution of the elevation factor classes for the existing landslides

4.2.3. Curvature

The curvature of the slopes is a key geomorphological indicator of topographic features for the study area ((Melese, T., Belay, T., & Andemo, A., 2022), (Foumelis, 2019)). In addition to influencing surface runoff, which in turn influences surface erosion, curvature also contributes to the occurrence of landslides. For example, concave slopes were more likely to experience landslides than convex ones. The explanation for this is that concave slopes are more likely to retain rainfall water, which gives the water more time to seep into the slope and increase the likelihood of a landslide (Farhan, 2020)

Furthermore, curvature has a major impact on the shear and resistance stresses of landslides, according to (Ohlmacher, 2007)

Similarly, the study area's curvature map was divided into three primary classifications. Figure 4-27 shows that positive curvature is convex (> 0), zero curvature is flat (0), and negative curvature is concave (< 0). The surface is convex upward at that cell if the curvature is positive, and concave upward at that cell if it is negative. In a similar vein, a surface with zero curvature is flat (Solaimani & Mousavi, 2012). Figure 4.28 shows that the current landslide along the Gore-Masha-

Tepi Road segment has a flat curvature with a composition of 54.8%, followed by concave and convex curvatures with contributions of 25.6% and 19.6%, respectively.

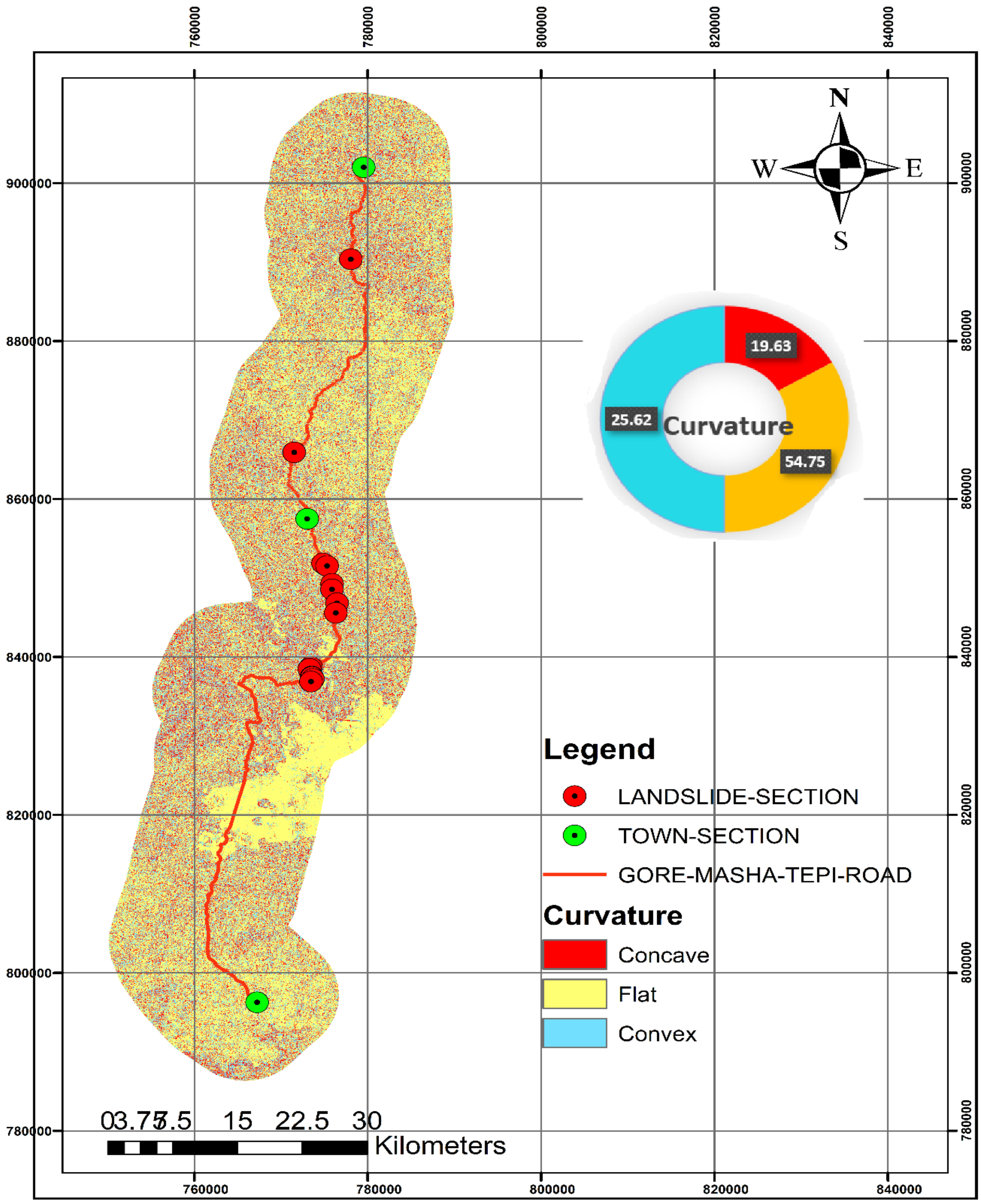

Figure4.17: Curvaturemap

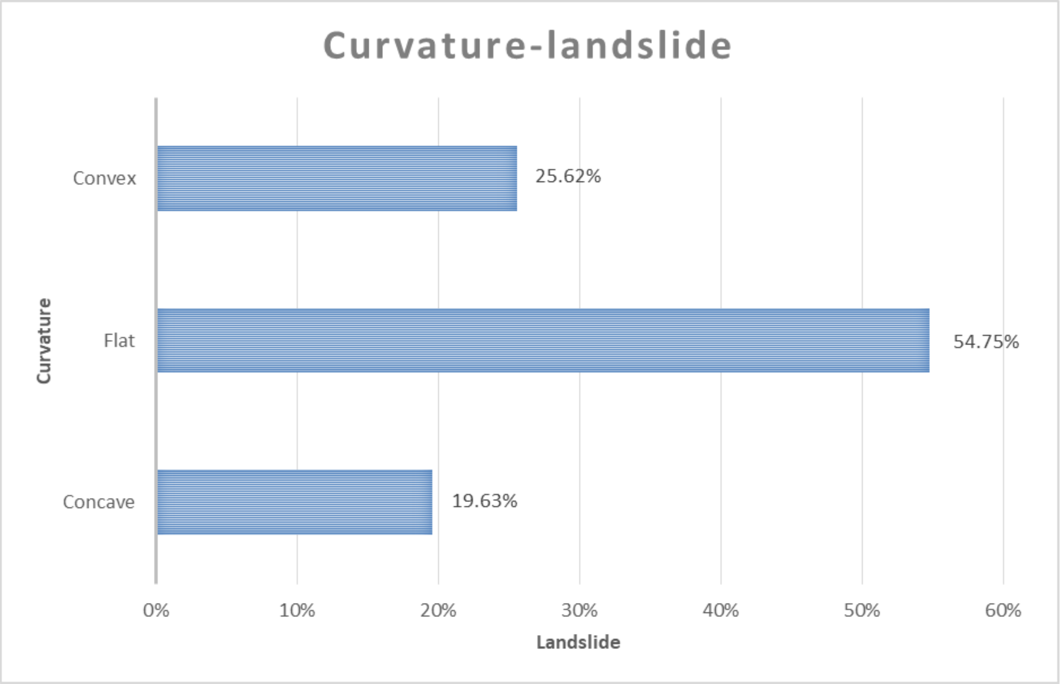

Figure 4.28: Distribution of the curvature factor classes for the existing landslides

4.2.4. Lithology

According to Figure 4.30, which shows the composition of the lithological formation of the current landslides, the Dystric nitisols up 40% of the landslide section, followed by the Dystric Fluvisols which is exhibit moderate to highly land slide susceptibility, depending on environmental and human factors. Calcicic Fluvisols, calcicic Cambisols, and Orthic Acrisols, which have respective compositions of 10%, 9.9%, and 7.3%.

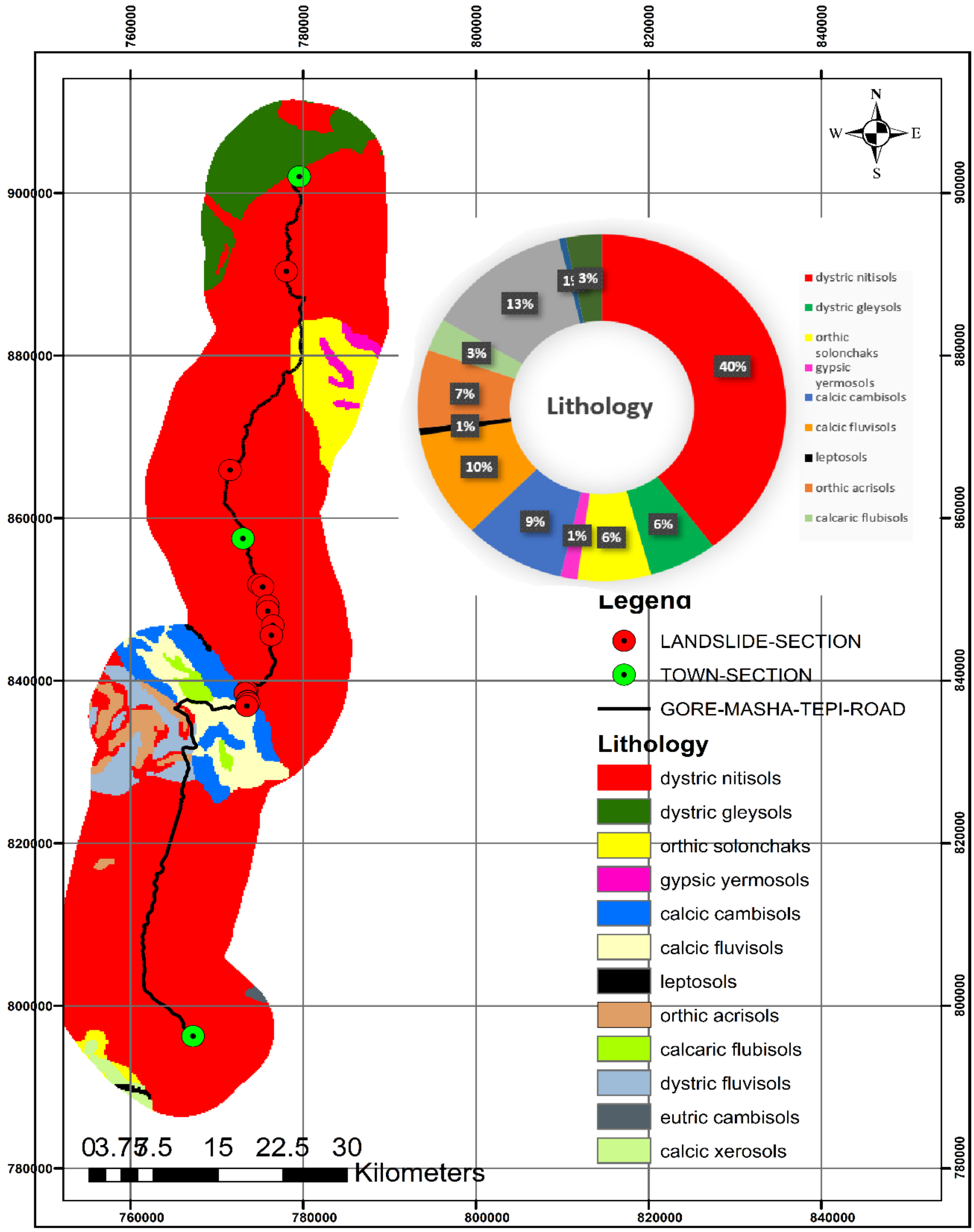

Figure 4.18: Lithology map

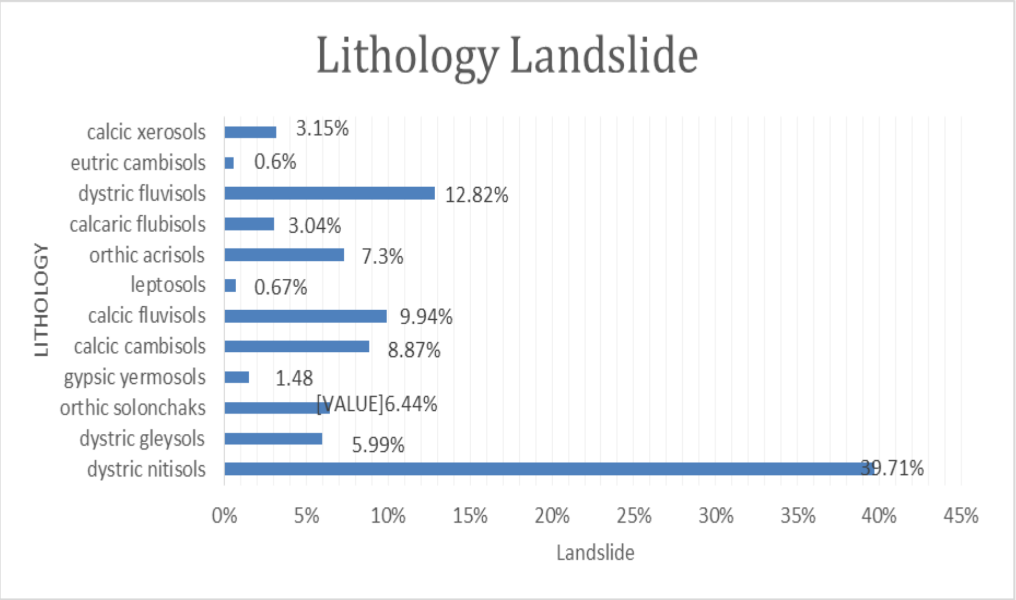

Figure 4.30: Distribution of the lithological factor classes for the existing landslides

4.2.5. Distance to Stream

Streams have a significant impact on how landslides form. Banks and slope faces may fail as a result of the stream's ability to alter groundwater levels and erode the slope's toe ((Dai, F. C., & Lee, C. F., 2001).Conversely, the drainage pattern is strongly dependent on the degree of surface material characteristic of the stream channel. This is demonstrated by the fact that a denser stream network means that the area's slope material is more erodible and looser. The majority of landslides on the Gore-Masha-Tepi Road route have happened near streams and when cross drainage structures are built. Using Arc-Hydro tools in a GIS environment, the drainage network for this project was created using a 30.0 m x 30.0 m Aster DEM. To describe the drainage's role in the road section's instability, four distinct proximity zones were created, primarily tracing the slopes of river banks (Figure 4.31).

The 50 m, 100 m, 300 m, 1000 m, and >1000 m stream zones along the road corridor were created in order to assess their role in the occurrence of landslides. The distribution of existing landslides at 50, 100, 300, 1000, and >1000 m distances to the stream is 1.36%, 1.34%, 5.21%, 17.4%, and 74.7%, respectively, as shown in (Figure 4.32).

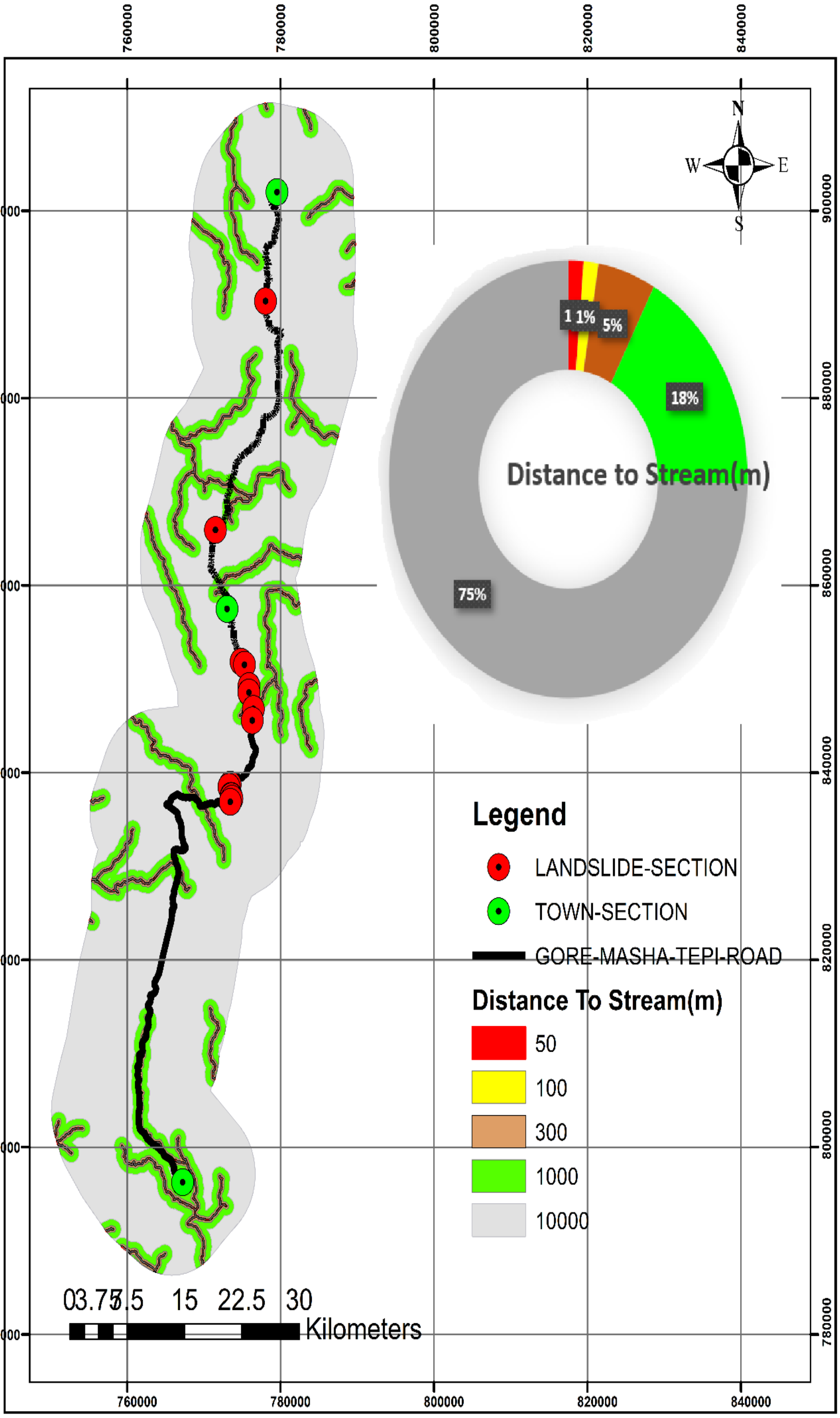

Figure 4.31: Distance to stream Map

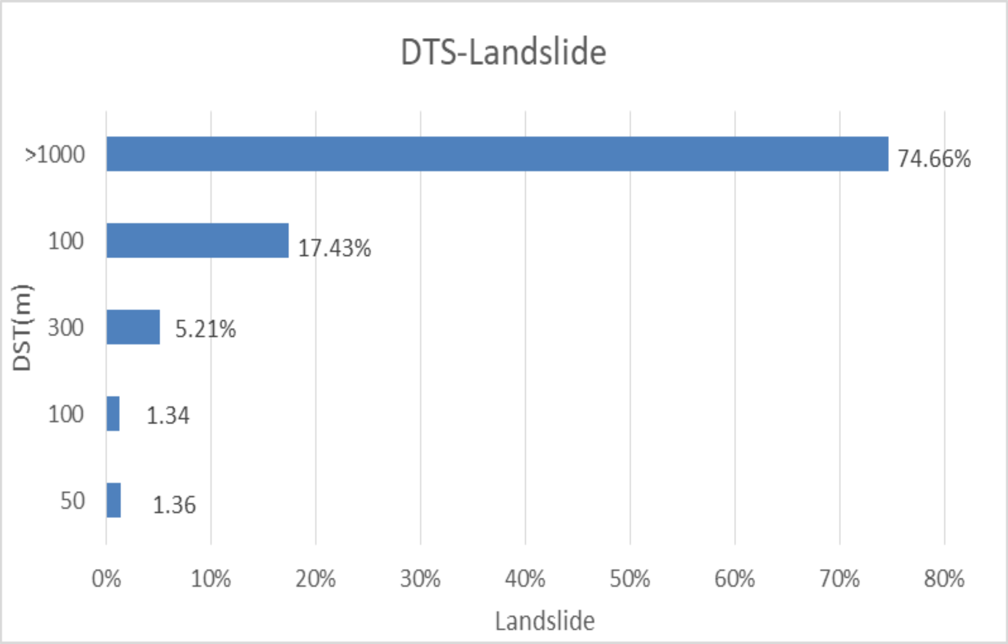

Figure 4.32: Distribution of the distance to stream factor classes for the existing landslides

4.2.6. Distance to Road

One of the primary anthropogenic variables influencing the presence of landslides in the region is the location's relative distance from the road (Jazouli, A. E., & Barakat, A., 2019)). By upsetting the natural slope, excavation works on the mountainous and rolling section of the Gore-Masha-Tepi Road section significantly contribute to the area's instability. Following excavation, this results in a loss of support at the slope's toe, which lowers the resisting force and causes the mass to slide downslope. Road construction close to the hillside greatly increases the likelihood of a landslide. On the remaining soil slope material, this is primarily seen. Five different buffer zones were created and categorized for the Gore-Masha-Tepi Road section: 50, 50-150, 150-500, 500-1000, and > 1000 m (Figure 4.33). The likelihood of a landslide occurring is higher in places close to the road corridor than in locations farther away. As indicated on Figure 4.34, most of landslides are occurred within 50,150,500,1,000 and 10,000 m distance from the road with their composition of 4%,7% ,24%,33% and 33%, respectively.

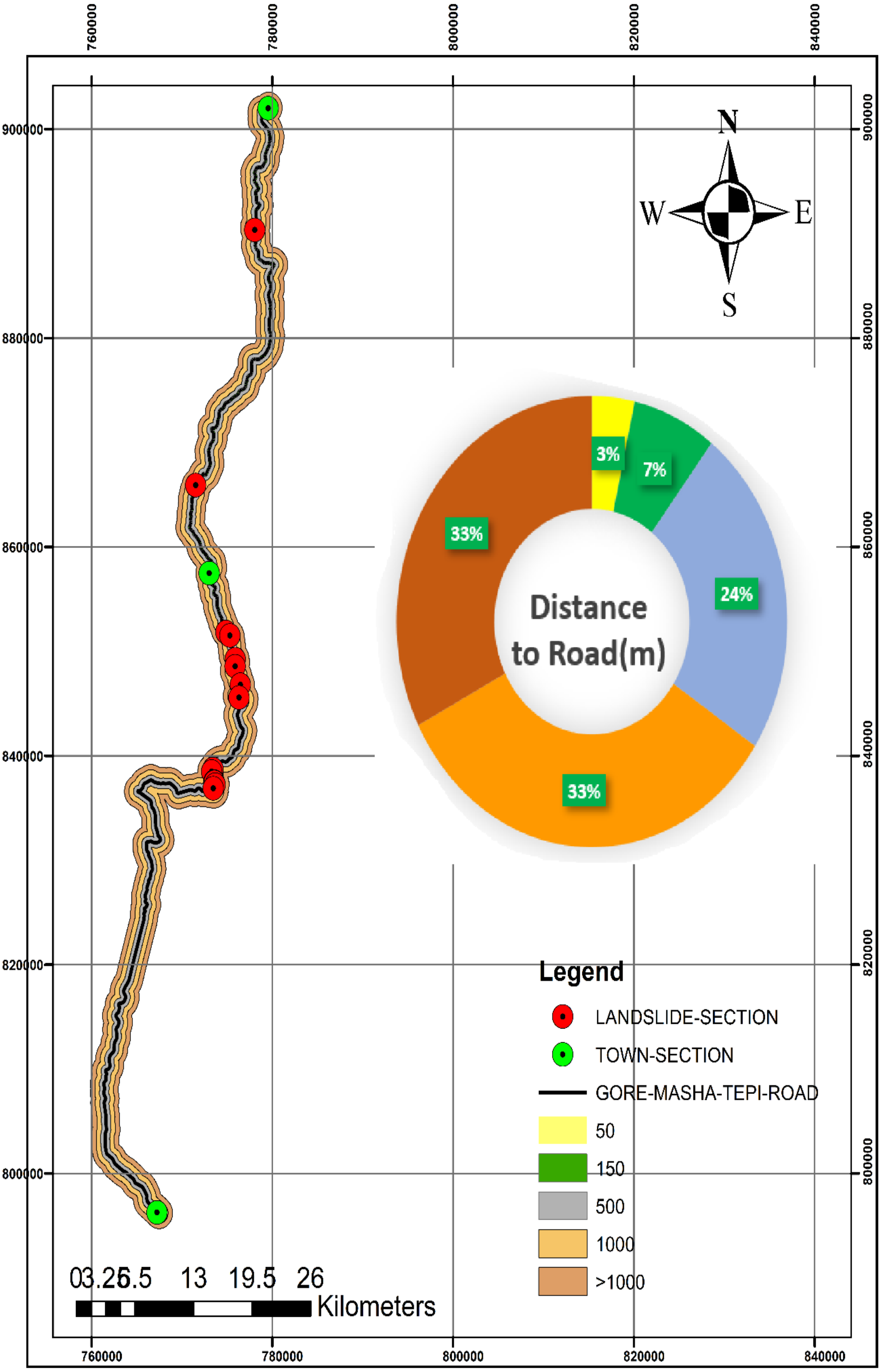

Figure 4.33: Distance to road map

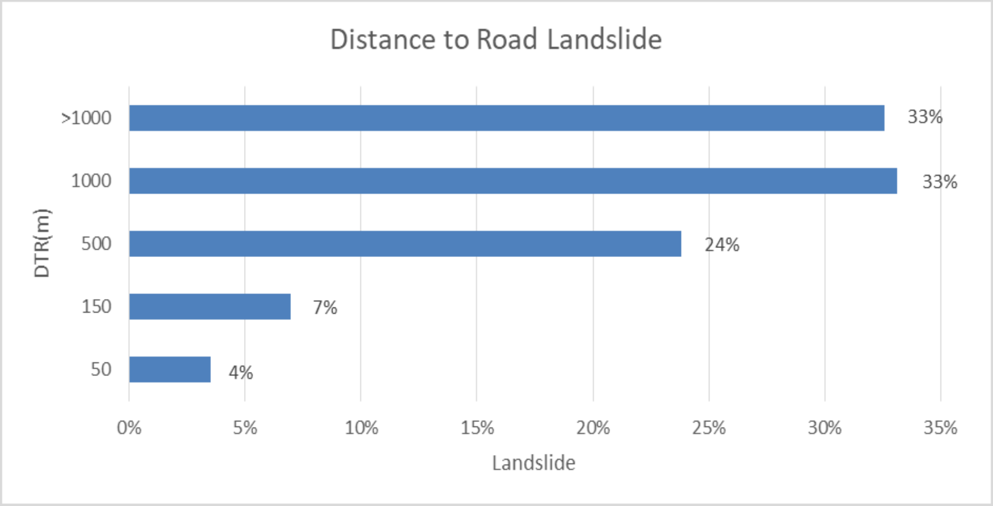

Figure 4.34: Distribution of the distance to road factor classes for the existing landslides

4.2.7. Land use/ cover

The other significant factor that contributes to the occurrence of landslides is land cover and use. Landslides are more common in locations with rugged terrain, bare land, or sparse vegetation cover, whereas they are less common in areas with dense forests than in areas with less forest cover. The needs of the local inhabitants are closely linked to the land's use and cover. For instance, shifting dense forest land to an urban area, turning forest with a distinct ecological composition into farmland because of increased demand and inadequate farmland management, and changing the area's natural slope for infrastructure development are all examples of human intervention in land use (Jazouli, A. E., & Barakat, A., 2019)

Water bodies, trees, flooded vegetation, crops, constructed places, barren ground, and range lands are the primary land cover/uses seen along the road segment (Figure 4.35). A considerable portion of the landslides on the Gore-Masha-Tepi Road segment have been caused by the severe erosion of the riverbanks and slope faces, which are devoid of vegetation. Along the road segment, there are also ongoing agricultural practices that involve chopping trees on a rolling to mountainous ground slope. This causes the slope material to erode, which greatly increases the likelihood of landslides. According to Figure 4.36, the areas covered by Vegetation, Bare lands, Settlement, crops, and water bodies contribute to the current landslides in the following proportions: 28%, 1%, 20%, 30%, and 21%, respectively.

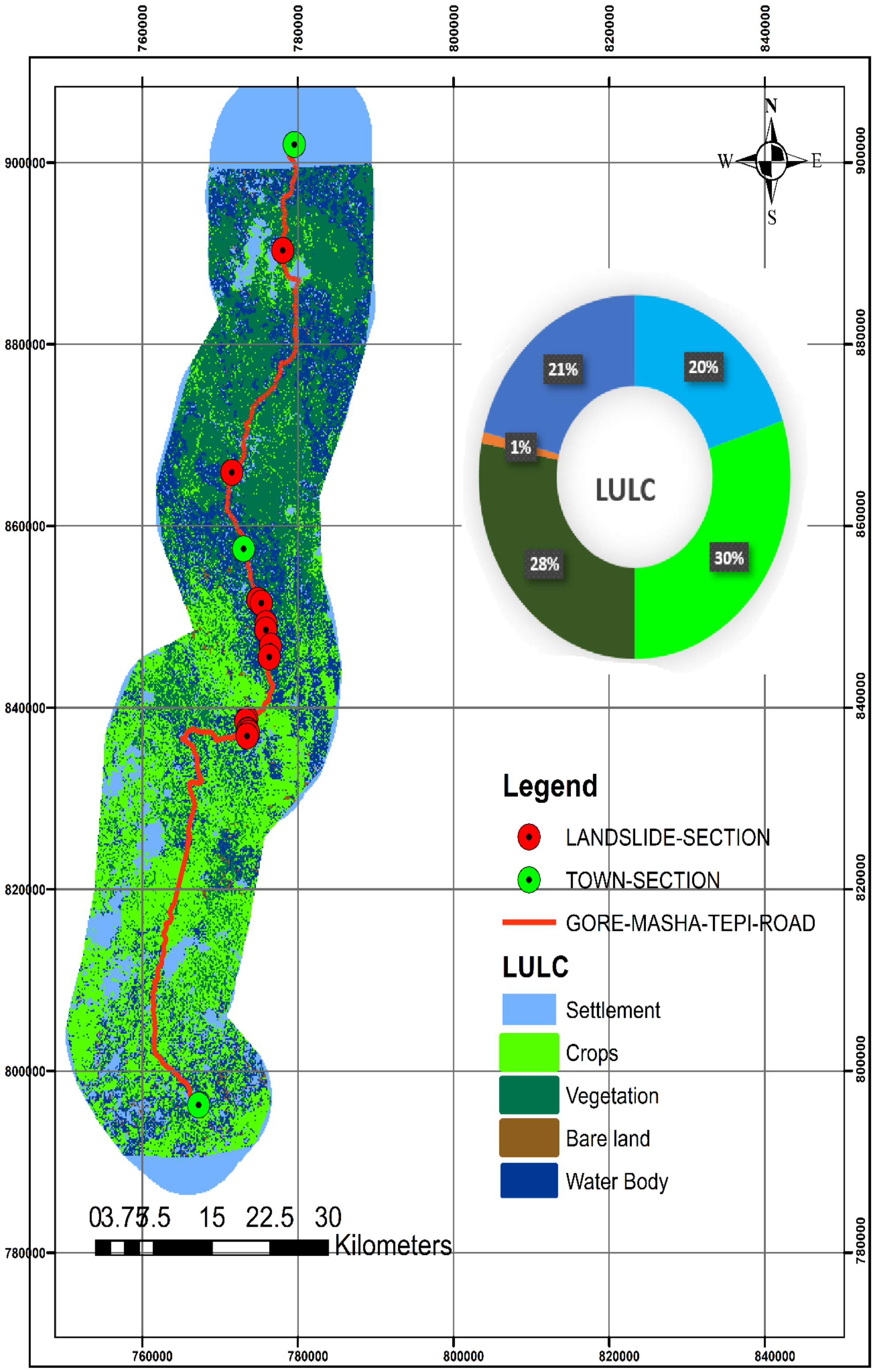

Figure 4.35: Land use/ cover map

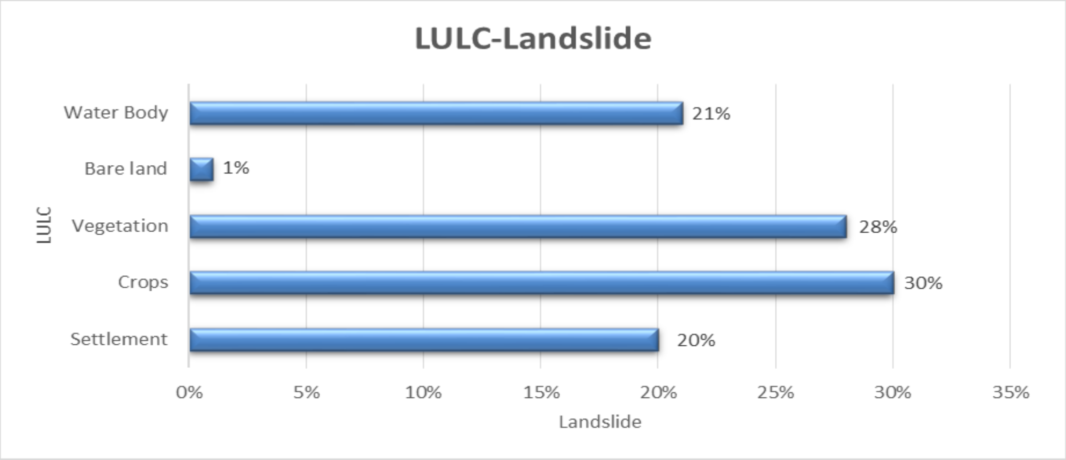

Figure 4.36: Distribution of the land use/cover factor classes for the existing landslides

4.2.8. Rainfall

The relationship between climatic factors such as rainfall and landslides has been observed by (Ayalew, 1999) Climate can have a dramatic influence on mass wasting events. Heavy precipitation can initiate certain types of mass wasting by creating hydrostatic pressure and serve to lubricate slides once they are in motion. when combined with all other factors, it greatly increases the area's instability and destabilizes the slope ((Tešić, 2021). This is corroborated by the fact that the majority of landslides occur during and after the rainy season, when the region experiences high levels of rainfall. As a result, the slope surface becomes heavy and wet due to increased water infiltration, which significantly reduces shear strength and soil cohesiveness and causes instability Landslide problem has been little researched on in Ethiopia, especially in southern part. There is lack of information on rainfall threshold, nature of occurrence and characteristics which are vital information for GIS data base creation for easy landslide monitoring (Charlotte, 2010).

According to Ethiopia's National Meteorological Agency's historical rainfall statistics, the project area is one of the areas receiving very high rainfall in the country. The average annual rainfall ranges from about 1,600-2,200 mm. The highest is around Masha (2,200 mm) and the lowest around Tepi (1,600 mm) while it is about 1,900 mm around Gore. Despite variation in the amount of rainfall, there is rain almost throughout the year with record highs in May to October. Rainfall's impact on the majority of slope failures have occurred in the Gore-Masha-Tepi Road segment. however, is examined in conjunction with other contributing factors such slope gradient, slope aspect, slope material type, and soil erosion potential. Using a spatial analysis tool in a GIS context, the rainfall data acquired for the Gore-Masha-Tepi Road segment was interpolated into four classes (Figure 4-26). Landslides currently occur in the rainfall regions of 1395-1689 mm and 1689-1983 mm, with distributions of 36.5% and 38.5%, respectively, as shown in Figure 4.38.

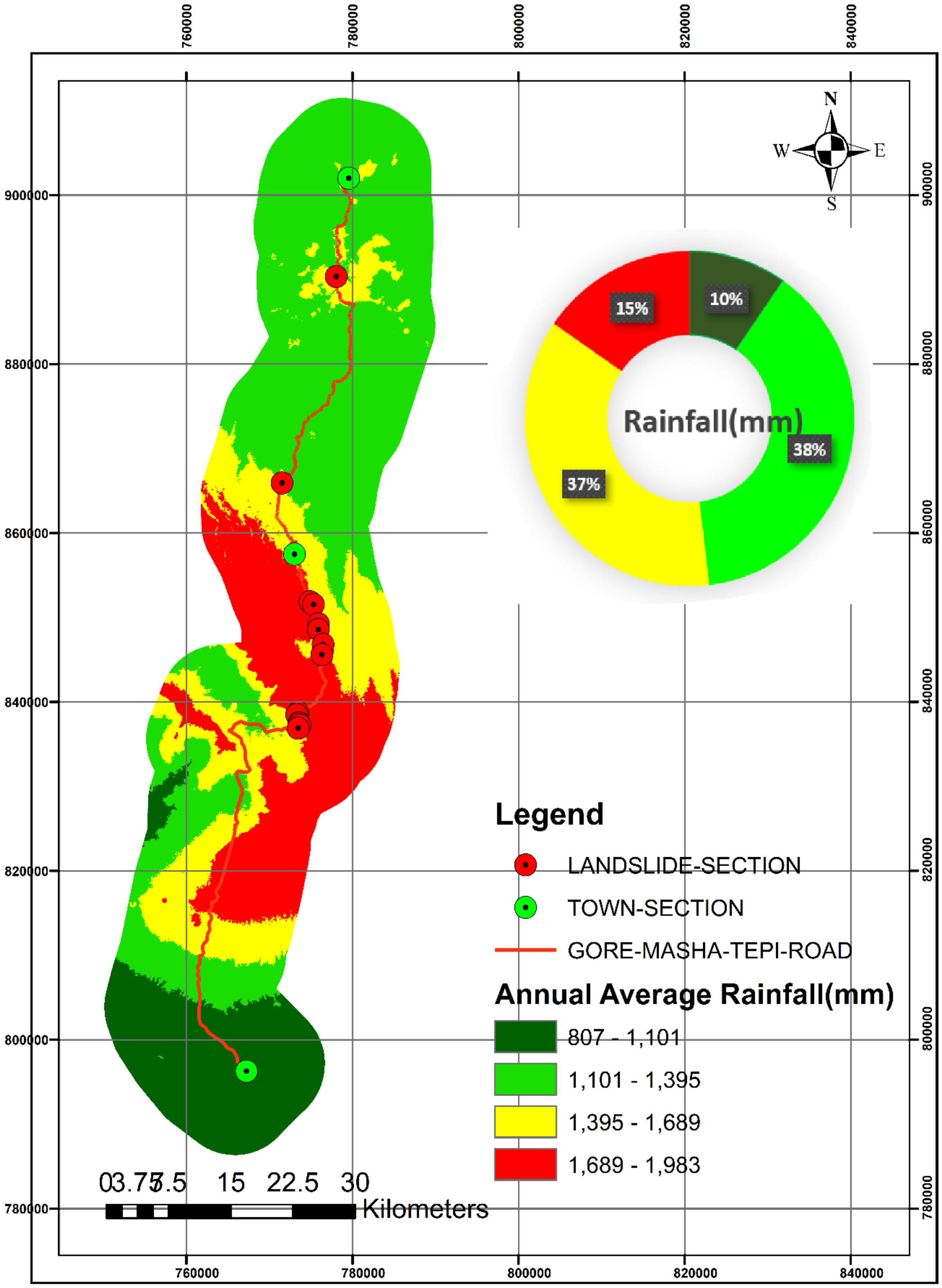

Figure 4.37: Rainfall map

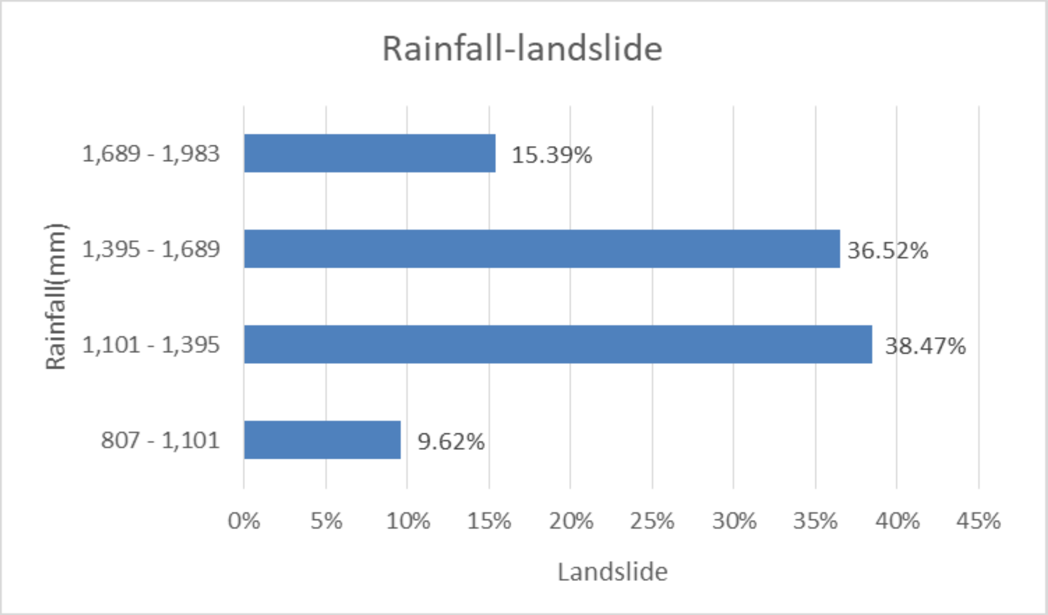

Figure 4.38: Distribution of the rainfall factor classes for the existing landslides.

4.3. Landslide Susceptibility Analyses

The Analytic Hierarchy Process (AHP) method is used to calculate the relative susceptibility of landslide occurrence along the Gore-Masha-Tepi Road segment by calculating the weight of the associated causal variables of the landslide. To perform landslide susceptibility analysis, nine landslide triggering parameters were used: slope degree, aspect, curvature, elevation, lithology, land use/land cover, distance to road, distance to stream, and rainfall.

4.3.1. Landslide Contributing Factor Score using Analytic Hierarchy Process (AHP)

Analyzing the AHP model requires an understanding of the spatial relationship between the site of the landslide and the contributing component. In order to make a logical decision, site observation and the spatial analysis of all relevant metrics and contributing elements were considered. The components and sub-factors' respective weights are determined by analyzing their pairwise comparison matrix, as shown in table below.

The pair-wise comparison matrix, factor weights, class weights (rating) and consistency ratio represented bellow as fallows

Table 4.10: AHP Table for curvature

Pair-wise Comparison Matrix				
Curvature	**Flat**	**Concave**	**Convex**	**Criteria Weights**
Flat	1	1/5	1/3	**0.106**
Concave	5	1	3	**0.633**
Convex	3	1/3	1	**0.260**
Sum	**9.00**	**1.53**	**4.33**	**1.000**

Table 4.11: AHP Table for Distance to Road

Pair-wise Comparison Matrix						
Distance to Stream(m)	**50**	**100**	**300**	**1000**	**10000**	**Criteria Weights**
50	1	3	5	9	9	**0.517**
100	1/3	1	3	5	7	**0.254**
300	1/5	1/3	1	3	5	**0.131**
1000	1/9	1/5	1/3	1	3	**0.063**
10000	1/9	1/7	1/5	1/3	1	**0.035**
Sum	**1.76**	**4.68**	**9.53**	**18.33**	**25.00**	

Table 4.12: AHP Table for Distance to Stream

Pair-wise Comparison Matrix						
Distance to Stream(m)	**50**	**100**	**300**	**1000**	**10000**	**Criteria Weights**
50	1	3	5	9	9	**0.517**
100	1/3	1	3	5	7	**0.254**
300	1/5	1/3	1	3	5	**0.131**
1000	1/9	1/5	1/3	1	3	**0.063**
10000	1/9	1/7	1/5	1/3	1	**0.035**
Sum	**1.76**	**4.68**	**9.53**	**18.33**	**25.00**	**1.00**

Table 4.13: AHP Table for Elevation

Pair-wise Comparison Matrix										
Elevation (m)	**2401-2783**	**2234-2401**	**2077-2234**	**1922-2077**	**1785-19922**	**1646-1785**	**1451-1646**	**1239-1451**	**807-1239**	**Criteria Weights**
2401-2783	1	2	3	4	5	6	7	8	9	**0.284**
2234-2401	1/2	1	2	3	4	5	6	7	8	**0.238**
2077-2234	1/3	1	1	2	3	4	5	6	7	**0.155**
1922-2077	1/4	1/3	1/2	1	2	3	4	5	6	**0.108**
1785-19922	1/5	1/4	1/3	1/2	1	2	3	4	5	**0.075**
1646-1785	1/6	1/5	1/4	1/3	1/2	1	2	3	4	**0.052**
1451-1646	1/7	1/6	1/5	1/4	1/3	1/2	1	2	3	**0.035**
1239-1451	1/8	1/7	1/6	1/5	1/4	1/3	1/2	1	2	**0.035**
807-1239	1/9	1/8	1/7	1/6	1/5	1/4	1/3	1/2	1	**0.019**
Sum	**2.83**	**4.72**	**7.59**	**11.45**	**16.28**	**22.08**	**28.83**	**36.50**	**45.00**	**1.000**

Table 4.14: AHP Table for Land Use Land Cover

Pair-wise Comparison Matrix						
Distance to Stream(m)	**50**	**100**	**300**	**1000**	**10000**	**Criteria Weights**
50	1	3	5	9	9	**0.517**
100	1/3	1	3	5	7	**0.254**
300	1/5	1/3	1	3	5	**0.131**
1000	1/9	1/5	1/3	1	3	**0.063**
10000	1/9	1/7	1/5	1/3	1	**0.035**
Sum	**1.76**	**4.68**	**9.53**	**18.33**	**25.00**	**1.00**

Table 4.8: AHP Table for Slope Aspect

Pair-wise Comparison Matrix										
Factors	**NW**	**W**	**SW**	**N**	**S**	**SE**	**E**	**NE**	**F**	**CW**
NW	1	1	3	4	5	6	7	7	9	**0.284**
W	1	1	2	3	4	5	6	6	8	**0.238**
SE	1/3	1/2	1	2	3	4	5	5	7	**0.155**
N	1/4	1/3	1/2	1	2	3	4	4	6	**0.108**
S	1/5	1/4	1/3	1/2	1	2	3	3	5	**0.075**
SE	1/6	1/5	1/4	1/3	1/2	1	2	2	4	**0.052**

E	1/7	1/6	1/5	1/4	1/3	1/2	1	1	3	**0.035**
NE	1/7	1/6	1/5	1/4	1/3	1/2	1	1	3	**0.035**
F	1/9	1/8	1/7	1/6	1/5	1/4	1/3	1/3	1	**0.019**
Sum	**3.35**	**3.74**	**7.63**	**11.50**	**16.37**	**22.25**	**29.33**	**29.33**	**46.00**	**1.000**

Key

North West (NW), West (W), South West (SW), North (N), South (S), Southeast (SE), East(E), North East (NE), Flat (F) and Criteria Weights (CW).

Table 4.16: AHP Table for Slope

Pair-wise Comparison Matrix										
Slope Angle	**48-75**	**39-48**	**32-39**	**27-32**	**20-27**	**14-20**	**9-14**	**5-9**	**0-5**	**Criteria Weights**
48-75	1	2	3	4	5	6	7	8	9	**0.31**
39-48	1/2	1	2	3	4	5	6	7	8	**0.22**
32-39	1/3	1/2	1	2	3	4	5	6	7	**0.15**
27-32	1/4	1/3	1/2	1	2	3	4	5	6	**0.11**
20-27	1/5	1/4	1/3	1/2	1	2	3	4	5	**0.08**
14-20	1/6	1/5	1/4	1/3	1/2	1	2	3	4	**0.05**
9-14	1/7	1/6	1/5	1/4	1/3	1/2	1	2	3	**0.04**
5-9	1/8	1/7	1/6	1/5	1/4	1/3	1/2	1	2	**0.03**
0-5	1/9	1/8	1/7	1/6	1/5	1/4	1/3	1/2	1	**0.02**
Sum	**2.83**	**4.72**	**7.59**	**11.45**	**16.28**	**22.08**	**28.83**	**36.50**	**45.00**	**1.00**

Table 4.17: AHP Table for Lithology

Pair-wise Comparison Matrix						
Lithology	**OA**	**DF**	**CF**	**CC**	**DN**	**C W**
OA	1	3	5	9	7	**0.503**
DF	1/3	1	3	7	5	**0.260**
CF	1/5	1/3	1	5	3	**0.134**
CC	1/9	1/7	1/5	1	1/3	**0.035**

DN	1/7	1/5	1/3	3	1	**0.068**
Sum	**1.79**	**4.68**	**9.53**	**25.00**	**16.33**	**1.00**

Key

Orthic Acrisols (OA), Dystric Fluvisols (DF), Calcic Fluvisols (CF), Calciic Cambisols: (CC), Dystric Nitisols: (DN), Distance to Road (DR), Curvature (Cu), Distance to and Criteria Weights (CW).

Table 4.18: AHP Table for Rainfall

Pair-wise Comparison Matrix					
Annual Average Rainfall(mm)	**1689-1983**	**1395-1689**	**1101-1395**	**807-1101**	**Criteria Weights**
1689-1983	1	3	5	7	**0.558**
1395-1689	1/3	1	3	5	**0.263**
1101-1395	1/5	1/3	1	3	**0.122**
807-1101	1/7	1/5	1/3	1	**0.057**
Sum	1 2/3	4 1/2	9 1/3	16	**1.00**

Table 4.19: AHP Table for

Pair-wise Comparison Matrix									
Factors	**SA**	**RF**	**Li**	**LC**	**El**	**DR**	**Cu**	**DS**	**Sas**	**Criteria Weights**
SA	1	3	5	5	7	7	9	7	9	**0.356**
RF	1/3	1	3	3	5	5	7	5	7	**0.207**
Li	1/5	0	1	3	3	3	5	3	5	**0.125**
LC	1/5	1/3	1/3	1	3	3	5	3	5	**0.101**
El	1/7	1/5	1/3	1/3	1	3	3	1	3	**0.058**
DR	1/7	1/5	1/3	1/3	1/3	1	3	1/3	3	**0.042**
Cu	1/9	1/7	1/5	1/5	1/3	1/3	1	1/5	1/3	**0.02**
DS	1/7	0	1/3	1/3	1	3	5	1	3	**0.063**

SAs	1/9	1/7	1/5	1/5	1/3	1/3	3	1/3	1	**0.028**
Sum	**2.38**	**5.55**	**10.73**	**13.4**	**21**	**25.67**	**41**	**20.87**	**36.33**	**1.00**

Key

Slope Angle (SA), Rain fall (RF), Lithology (Li), Land Cover (LC), Elevation (El), Distance to Road (DR), Curvature (Cu), Distance to Stream (DS), Slope Aspect (SAs) and Criteria Weights (CW).

4.4. Landslide Susceptibility Mapping (LSM)

By combining the thematic raster map of nine pertinent features with their assigned weights, the Analytic Hierarchy Process (AHP) technique was used to construct the landslide susceptibility map for the study road section. The weighted overlay tool in spatial analysis is used to merge the weighted raster maps to construct the landslide susceptibility index (LSI) (4-1);

$$LSI = \sum_{i}^{n} W_j * R_{ij} \qquad \ldots\ldots\ldots\ldots\ldots\ldots\ldots\ldots\ldots\ldots\ldots\ldots\ldots.... \text{(4-1)}$$

Where Wj: Weight for each of the landslide conditioning factor; R_{ij} rating value of class i in landslide contributing factor j; n: number of landslides contributing factors.

LSI=0.356*Slope+0.207*Rainfall+0.125*Lithology+0.101*Land use/cover 0.058*Elevation+ 0.042*Distance to road +0.020*Curvature+0.063*Distance to stream + 0.028*Aspect

Figure 4-30 shows the five landslide susceptibility classes that were created by reclassifying the landslide susceptibility index: very low (VLS), low (LS), moderate (MS), high (HS), and very high (VHS). According to the final landslide susceptibility map, 74.2% (1956.1 km2), of the road section passes through regions that are is categorized as being in the moderate, highly, very highly susceptibility landslides, which should be taken into account while designing and building new roads.

Slope aspect and curvature have the least effect on the chance of landslides, although the formation, height, distance to streams, and distance to the road all have a moderate effect. Rainfall, lithology, land use/cover, and slope aspect are the main contributing elements.

It is crucial to remember that in some cases, the landslide could be caused by the previously mentioned less major contributing factors ((He, Y., & Beighley, R. E, 2008)).

For instance, even though the study area's land use and land cover have a very little role in the Any human or natural activity that alters the land cover after landslides have begun could cause further landslides. The landslides that were observed close to the road corridor in the Gore-Masha-Tepi Road section were also caused by the road construction activity, which required a large amount of earthwork, streams that were collected from their natural channel and channelized by drainage structures across the road, and the growth of settlement along the road corridor, which resulted in deforestation.

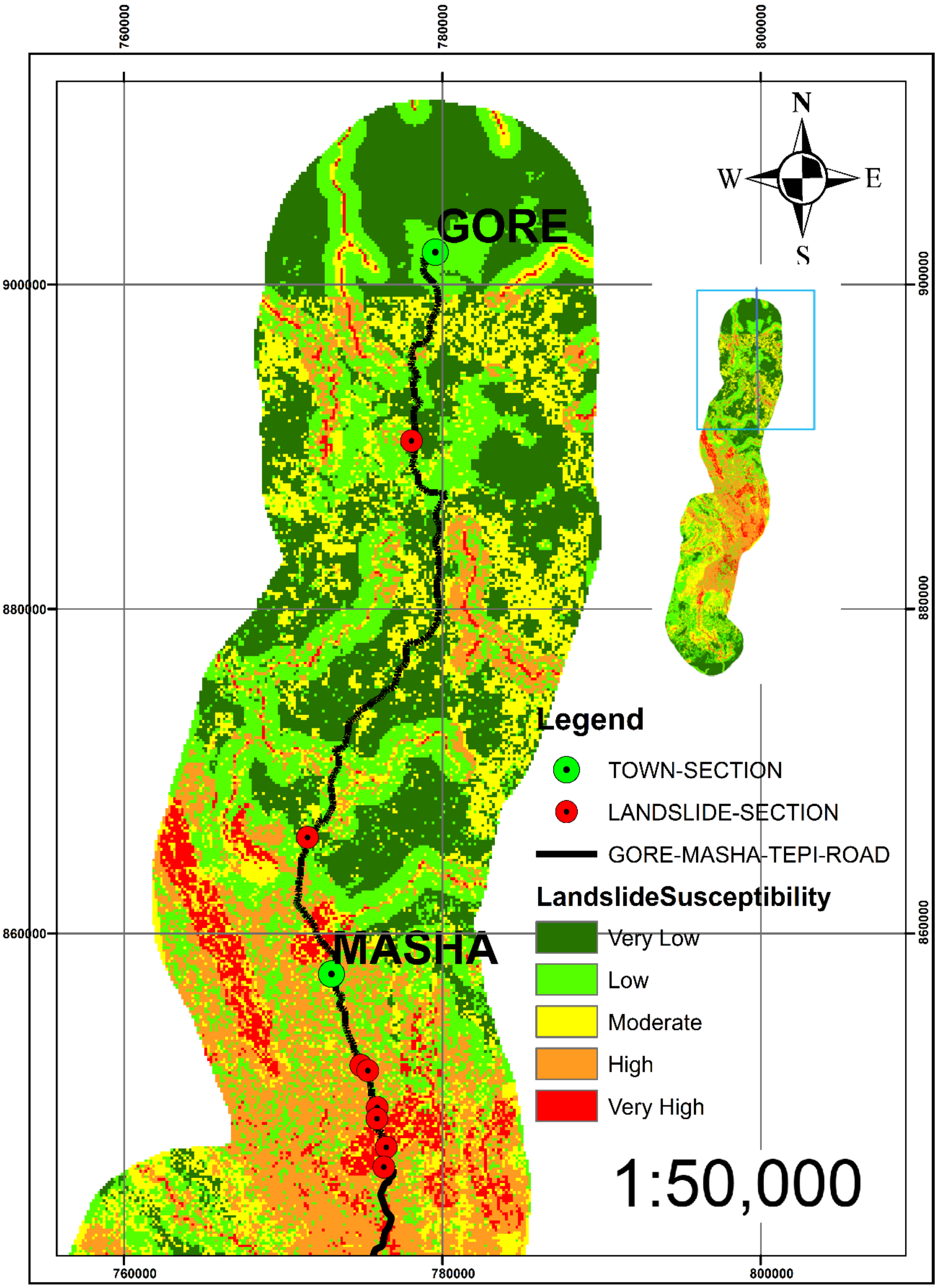
760000
780000
800000
N
W
E
S
GORE
900000
880000
860000
MASHA
Legend
TOWN-SECTION
LANDSLIDE-SECTION
GORE-MASHA-TEPI-ROAD
LandslideSusceptibility
Very Low
Low
Moderate
High
Very High
1:50,000
760000
780000
800000

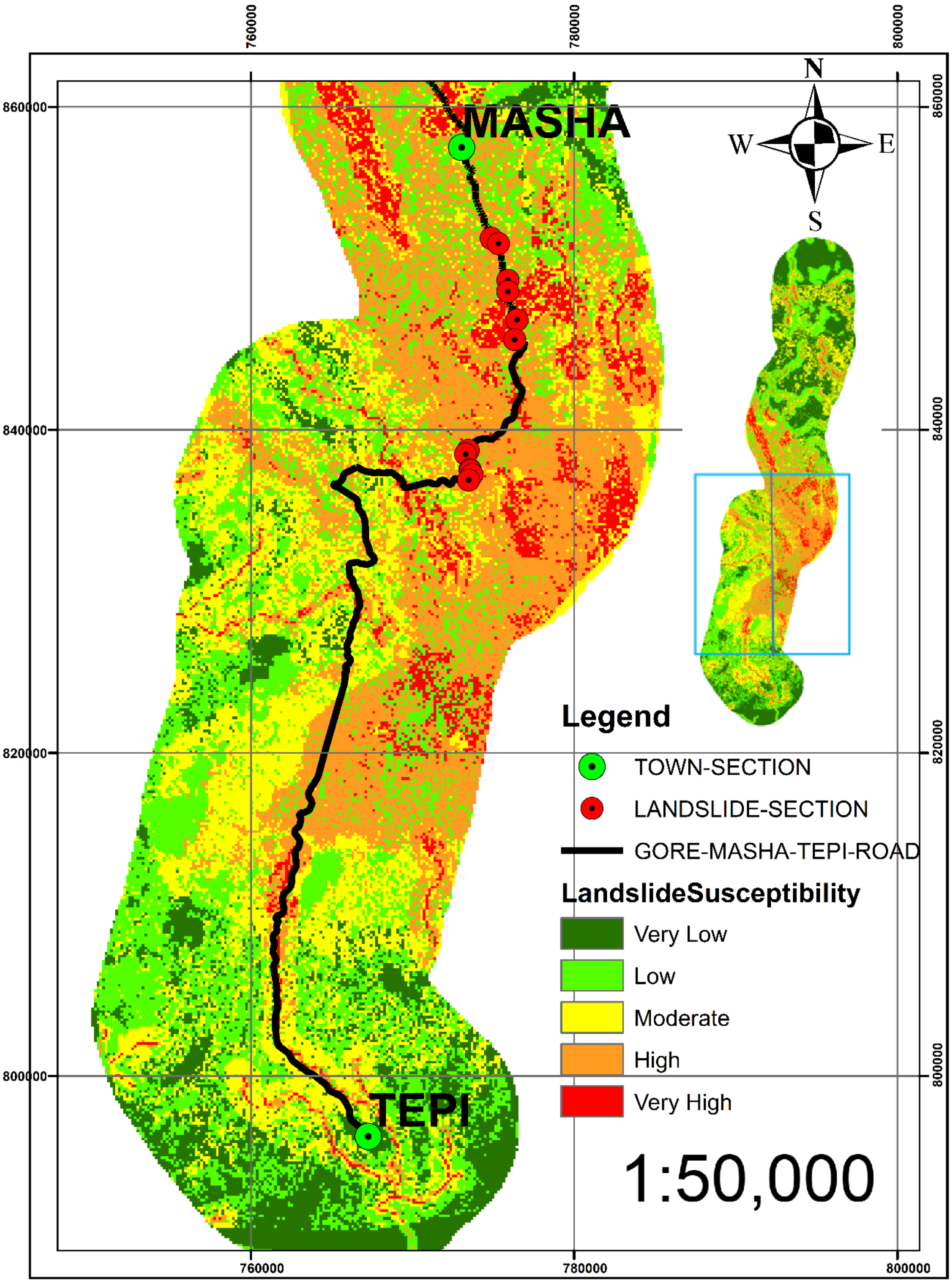

Figure 4.39: Landslide susceptibility map of Gore-Masha-Tepi Road Section

Five (5) landslide susceptibility classes—very low susceptibility (VLS), low susceptibility (LS), moderate susceptibility (MS), high susceptibility (HS), and very highly susceptibility (VHS)—have been identified for the road corridor along the Gore-Masha-Tepi stretch. The majority of the road corridor, 74.2% (1956.1 km2), is categorized as being in the moderate, highly, very highly susceptibility class according to the results of the landslide susceptibility map created using the Analytic Hierarchy Process (AHP), which are shown in Table 4-18. The remaining 4.8% (127.4km2), and 21.0% (553.3 km2) of the road section are classified as being in the low, and very low, susceptibility classes, respectively.

Table 4.20: Landslide susceptibility classes, landslide area and percent

S. No	LSP	%LSM	LSM Area(km^2)	Description
1	24186	4.83	127.4324	VLS
2	26742	20.99	553.3102	LS
3	22126	22.52	593.7708	MS
4	20126	24.71	651.5681	HS
5	4771	26.95	710.5804	VHS

Key

In this case, very low, low, moderate, high, and very high landslide susceptibility are denoted by VLS LS, MS, HS, and VHS, respectively. And landslide susceptibility pixel denoted by LSP, (landslide susceptibility map area denoted by LSMA

Road sections designated as highly susceptible for landslides are primarily found between km 45+000 and km 85+000 in the watershed along valleys near drainages with steep slope topography, which greatly contributes to the occurrence of erosion and landslides, according to the landslide susceptibility map that is comparable to the current situation on site. Because of the residual soil deposit beneath a parent low strength rock mass that is traversed by several streams and crosses the rolling terrain, the road segment on the outskirts of Masha town up to the km 84+000 is likewise classified as a highly sensitive location. Likewise, as the landslide susceptibility map makes evident, landslides are more common on a residual/silty clay soil and highly weathered basalt formation. Colluviums and clay materials. particularly on steep slopes. For the purpose of growing crops, the local farmers clear the clay-covered areas, making them more susceptible to landslides.

4.5. Discussion

The relationship between the landside contributing variables and the current landslide was taken into consideration when creating the landslide susceptibility map for the Gore-Masha-Tepi Road Section. The primary idea taken in to account when creating the landslide susceptibility map is that various points within the designated area that have comparable internal and external environmental conditions and landslide histories are also likely to experience landslides in the future (Tsege, 2017).

The Analytical Hierarchy Process (AHP) model is used for this study in order to examine the relationship between contributing elements and landslide occurrence. In light of the current active landslides and the data available, a total of nine contributing factors—slope aspect, slope angle, curvature, elevation, lithology, distance to stream, distance to road, land use/land cover, and rainfall—were used as potential landslide triggering factors. The following is a presentation of the role of influencing elements for the occurrence of predicted landslides based on the landslide susceptibility map developed.

Slope is one of the primary contributing factors to the occurrence of landslides, as was covered in section 4.2.1. The AHP model assigns a weight of 0.073 to the slope angle contribution for the road stretch under examination. The bulk of very susceptible landslides (24.5%) are expected to occur on the slope class between 5^0 and 9^0, and around 20.5% of all highly sensitive areas are situated in the slope angle range between 9^0 and 14^0, according to the landslide susceptibility map. The majority of landslides (24.5%) are expected to occur in the slope angle range of 5^0 to 9^0, followed by the slope angle range of 9^0 to 14^0, much like in the highly vulnerable areas for the moderately sensitive road sections (Figure 4-40 (a)). As mentioned in section 4.2.1, landslides are much less likely to occur in places with gentle slopes and flat terrain than in areas with high slope topography. By showing that around 75% of the areas are classified as very low and low susceptible, the susceptibility map's findings support the earlier assertion.

According to the landslide susceptibility map, there have been some instances where landslides have occurred on topography with a mild slope, despite the fact that the majority of landslides have occurred on terrain with a steep slope angle. The development of gullies on streams that primarily run at the slope's toe, rainfall-induced slope saturation, excavation-induced alteration of the natural slope, and deforestation of the natural slope, which causes slope erosion and landslide formation, could all contribute to this.

One of the key elements influencing landslides is slope aspect. The landslide susceptibility map has a weight of 0.023 applied to the slope aspect.

The road segment under examination is more susceptible to landslides in the southwest, west, and northwest slope aspect directions. Figure 4.40(b) shows that approximately 11.7%, 13.7%, and 12.2% of the area classified as extremely sensitive has a slope aspect direction that is East, west, and northwest, respectively.

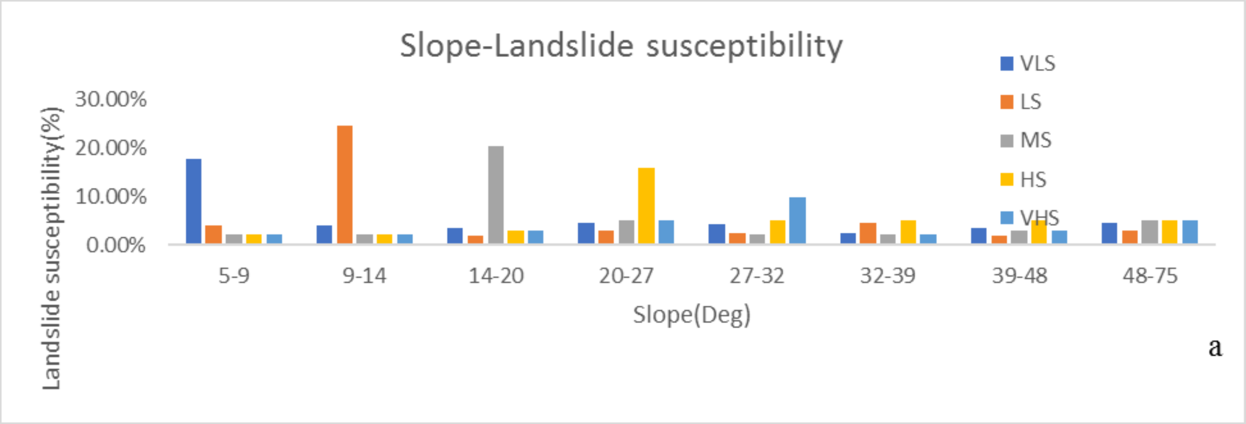

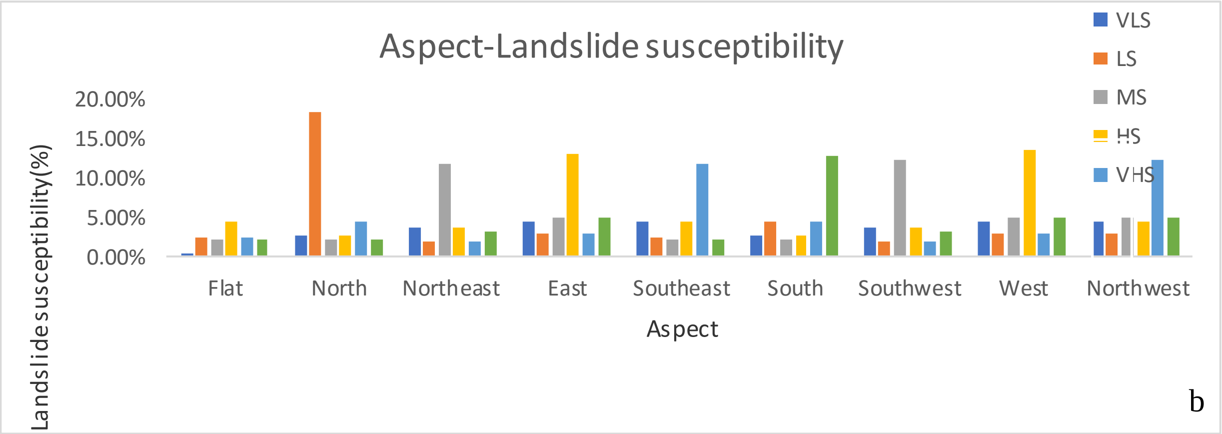

Figure 4.190: a) Slope-Landslide susceptibility b) Aspect-Landslide susceptibility

Regarding elevation, Figure 4.41a) shows that the elevation range of 1646 m to 1785 m significantly affects the likelihood of landslides, with approximately 27.9% of the area being highly susceptible. This supports the general notion that areas at higher elevations are more likely to experience landslides. The majority of the road corridor under study is covered by elevations between 1646 and 1785 meters, which together make up about 27.9% of the highly susceptible road segment. Similarly, with compositions of 14.70% and 10.1%, respectively, the elevation ranges of 1785–1922 m and 1922–2077 m significantly impact the moderately vulnerable area. The mechanism and characteristics of surface runoff are mostly controlled by the slope's curvature, which also affects the likelihood of landslides. Concave, convex, and flat curvatures are the three types of curvature seen throughout the Gora-Masha-Tepi Road segment; flat curvature accounts for around 54.8% of the total (Figure 4.41(b)).

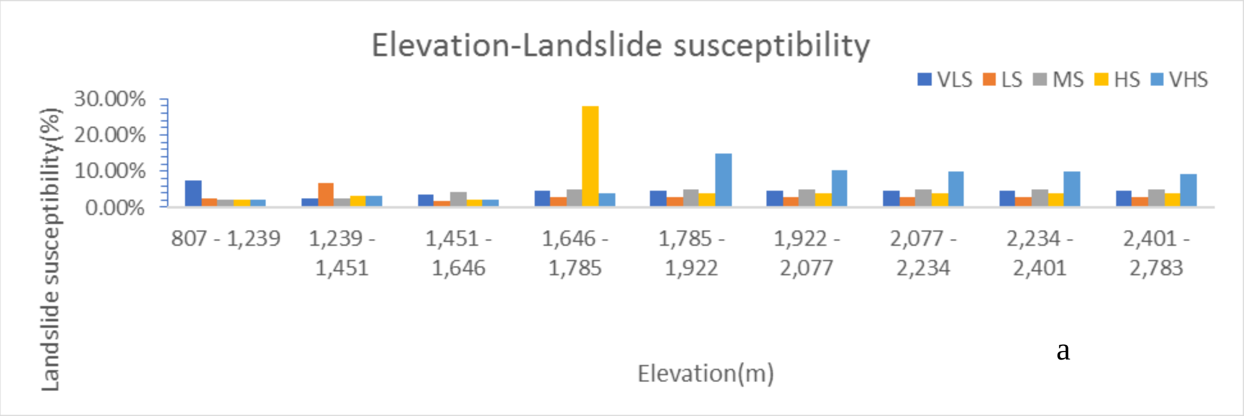

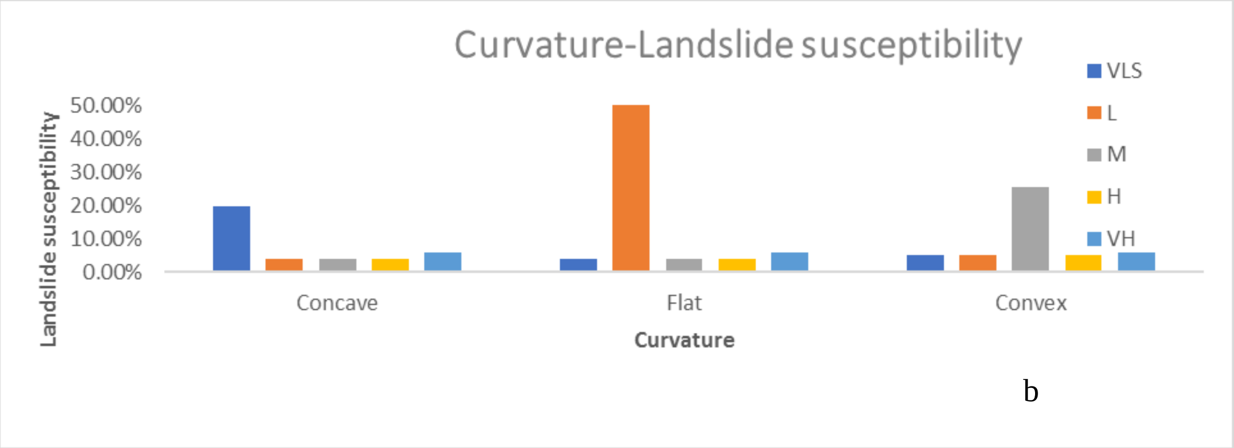

Figure 4.41: a) Elevation-Landslide susceptibility b) Curvature-Landslide susceptibility

One cannot overstate the importance of the site lithology in causing a landslide to occur; it is dependent on both the surface condition and the intrinsic factors (mineralogy, formation process, and engineering qualities). The study road section's lithological map (Figure 4.29) shows that Dystric Nitrosols cover the majority of the road segment, accounting for 40% of the total road segment. Around 12.8% of the study road section is made up of Dystric Fluvisols, another notable lithological formation that is mostly defined by residual soil beneath a low strength rock mass unit. This is also where the majority of active landslides occurred.

The Orthic Aerisols formation, which was identified on site with varying depths of residual soil underlain by highly weathered to decomposed, low strength rock mass, accounted for the landslide susceptibility maps predicted highly susceptible area with a percentage of 50.3%. After the Orthic Aerisols, with a proportion of 26.0% and 12.8%, respectively, middle basaltic and Dystric Fluvisols are contributing to the calcic Fluvisols zones. The least lithological formations that contribute to the high susceptibility of the anticipated landslide are Orthic Aerisols and the Dystric Fluvisols. Similar to this, the Calcic Fluvisols,Leptosols, Dystric Fluvisols around of the moderately susceptibility landslide prone areas. It is followed by the Dystric Nitrosols, and Calciic Cambisols lowsusceptibility which have respective compositions of 6.8% and 3.5%, respectively.

Based on field observations and desk research on the geological formation, soil extension, borehole, and geophysical investigation data of the road section under study, the highly weathered to decomposed, low strength upper basaltic flow rock formation beneath the residual soil with variable thickness is what causes multiple landslides along with other triggers.

One important and crucial feature that is connected to the majority of landslides that occur in the research region is the road section's proximity to the notable streams that cross and run beside the route. By either eroding the slopes and river banks or soaking the slope material, particularly the material at the slope's toe, streams play a significant role in the onset of landslides. The majority of landslides on the study road segment occur near streams and are connected to the gully cut created by erosion. The road section's stream and erosion gullies are followed by weak, extremely saturated, and shear zones along the landslide-affected areas, according to the site survey. The highly erodible, mostly silty clay residual soil was increasingly eroded by the prominent streams and their tributaries adding to the prolonged and intense rainfall on the area. The distance to stream of the area were considered as the most influential factor for In order to create the landslide susceptibility map, the occurrence of landslides was weighted with 0.203. Based on the site survey observations, 45.5% of the area classified as very susceptible for landslides is situated within 50 meters of the stream. In a similar vein, 25.94%, 13.52%, 3.55%, and 1.20% of the very vulnerable regions are situated 100, 300, 1000, and more than 1000 meters from the streams. The majority of the areas designated as moderately susceptible (36.05%) are situated within 50 meters of the stream, while the remaining portions, which made up 29.39%, 18.40%, 9.56%, and 6.59% of the total, are situated within 100, 300, 1000, and more than 1000 meters of the stream, respectively (Figure 4.42(b)).

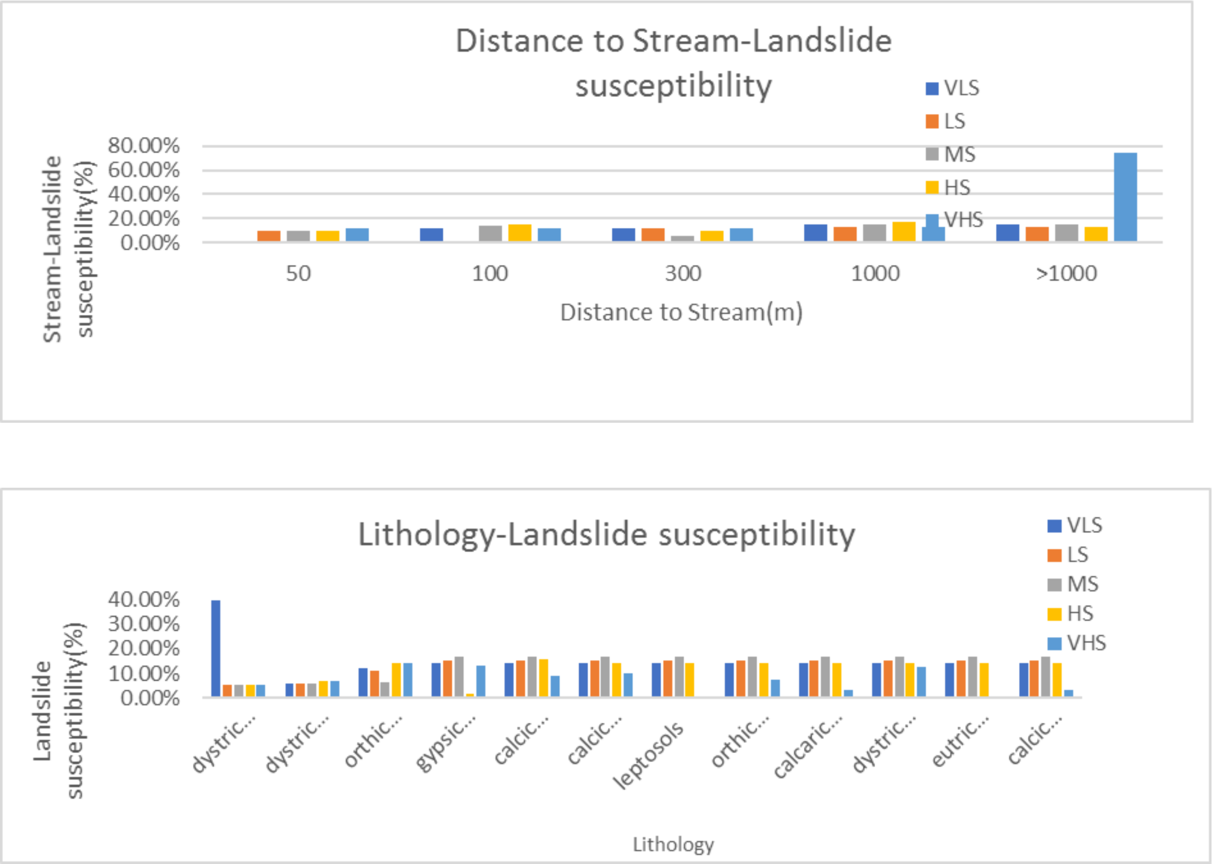

Figure 4.42: a) Lithology-Landslide susceptibility b) Distance to Stream-Landslide susceptibility

Whether or not a region has a history of landslides, road development is a human intervention that increases the likelihood of landslides occurring there. In particular, highways on rugged mountainous and escarpment terrains require a lot of earthworks because of their geometric demands. Such excavation projects often result in slope instability, which can have disastrous consequences for the road, its users, and the neighborhood.

Given this, the road's closeness is regarded as a causal factor and, following AHP analysis, is assigned a weight of 0.042. Therefore, according to the landslide susceptibility map, the majority of the predicted landslides occur in areas 10,00 meters off the road, while areas 10,000 meters from the road account for 4.2% of high susceptibility areas. The incidence of landslides within the 50–10,000m range on both sides of the road, primarily between the road and the end of the slope, and the combined effect of other elements are the main causes of this. In a similar vein, the entire regions designated as extremely low and extremely high landslide susceptibility are situated more than 10,000 meters and less than 50 meters away from the road prism, respectively (Figure 4.43(a)). The appearance of slope stability issues is significantly influenced by the land use and cover of the area across the study road section, in addition to the significant infrastructure development projects now underway on the road corridor. Because root reinforcement strengthens the soil, the likelihood of a landslide occurring is reduced in places with dense forest and vegetation. When creating a landslide susceptibility map, the contribution of land use and cover is taken in to account and assigned a weight of 0.101. According to the site survey and land use/cover map of the road corridor, residents who live next to the road corridor—who make up 30% of the area—widely farm a variety of crops, including tea plantation, sorghum, coffee, enset, and chat. In a similar vein, several trees, including eucalyptus, juniperous (Tid), pinus, zigba (podocarpus), wanza (Cordia), kosso (Hagenia), and others, cover thirty percent of the road corridor. The majority of the trees listed are deeply rooted and beneficial for stabilizing the slope mass from the perspective of slope stability.

According to the landslide susceptibility map, 30% of the zones classified as low susceptible for landslides are covered by agricultural fields. Deforestation is mostly the result of local settlers' activity, which involves chopping down trees for farming and settlement growth. Similarly, vegetative lands make up 28.0% of the class and comprise the majority of the region designated as having a moderate vulnerability to landslides (Figure 4.43(b)).

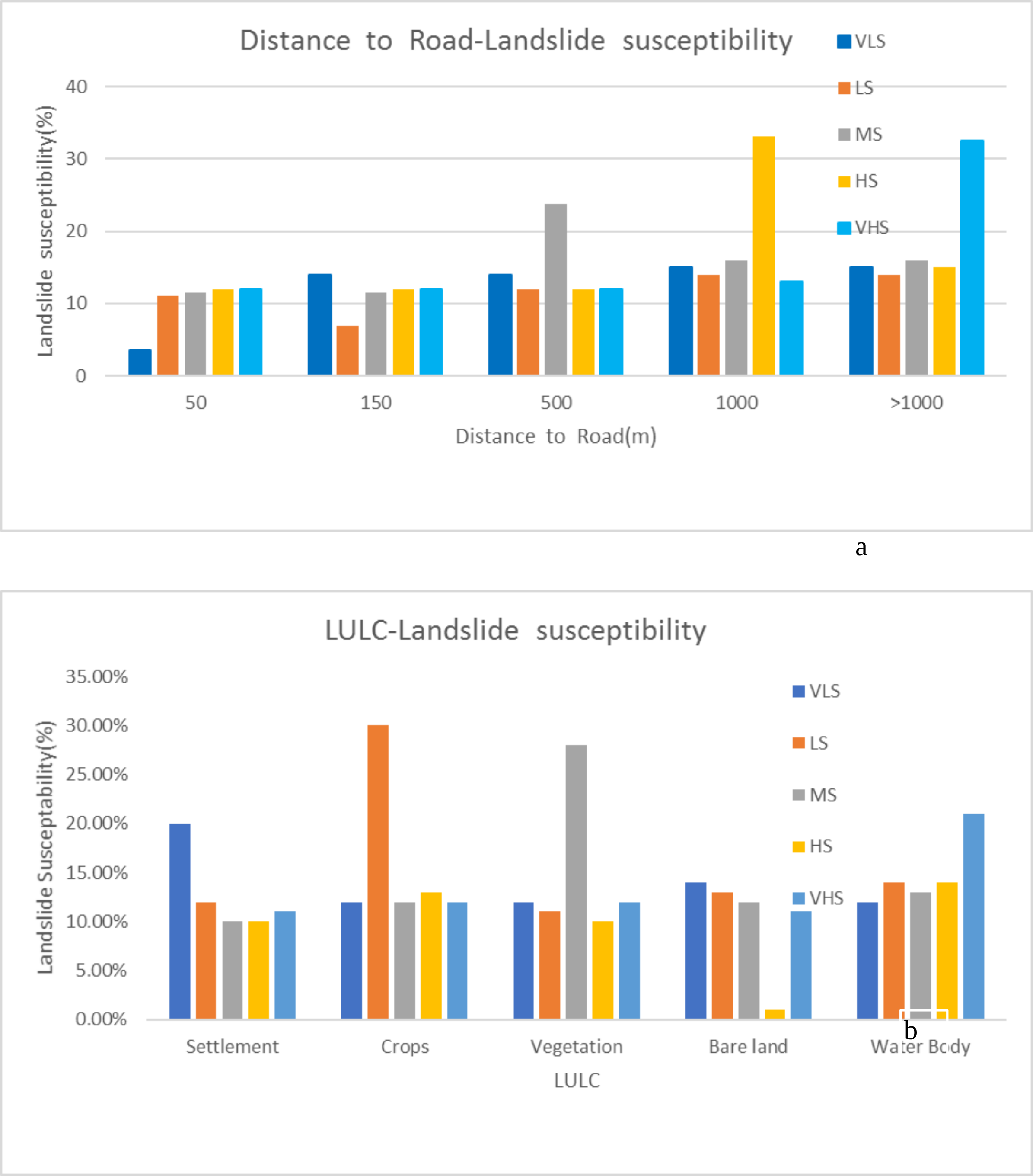

Figure 4.43: a) Distance to Road-Landslide susceptibility b) LULC-Landslide susceptibility

One of the most important and significant triggering factors for practically all types of landslides is rainfall. Rainfall is a major contributing factor to landslides, and all analyses and corrective actions must take this into account, particularly in locations that get heavy rainfall on a regular basis and over extended periods of time.

The Ethiopian Metrological Agency (EMA) provided the average annual rainfall data for the Gora-Masha-Tepi Road stretch over the previous ten years, from 2010 to 2022. The rainfall map was created using the ArcGIS environment's interpolation tool. Following examination utilizing a semi-quantitative, multi-criteria evaluation technique using the AHP model, the rainfall contribution is given a weight of 0.199. after analysis using a semi-quantitative, multi-criteria evaluation technique using the AHP model.51.7% of the places that are most vulnerable to landslides are situated in zones with average annual rainfall records between 1395 and 1983 mm. This confirms that, in comparison to a location with the highest maximum rainfall, one with less rainfall has a lower chance of experiencing a landslide.

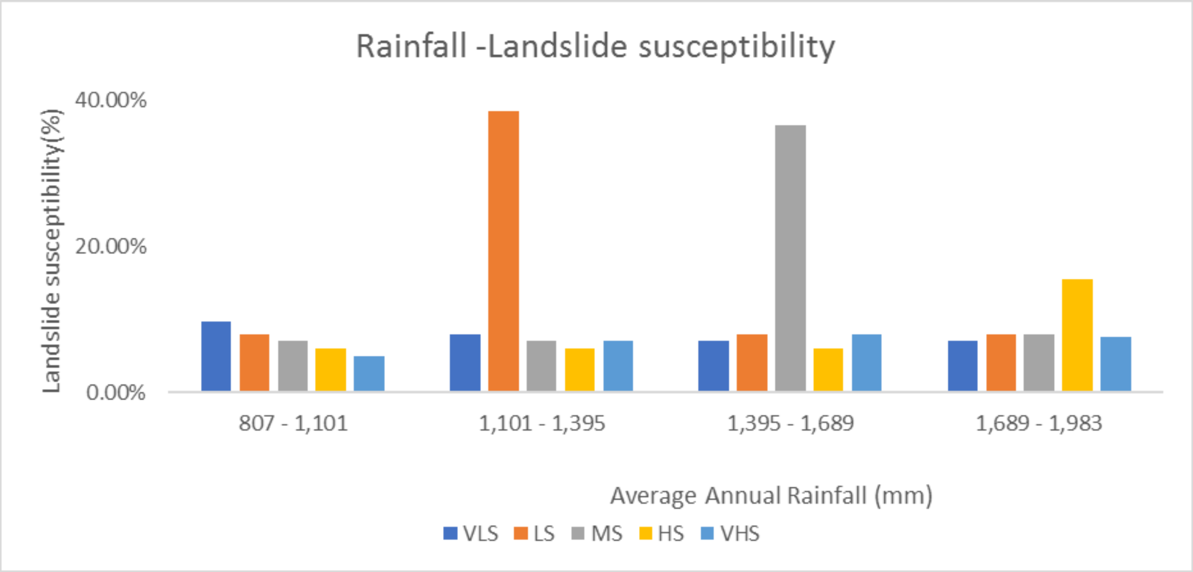

Figure 4.44: Rainfall -Landslide susceptibility

According to the investigation, the components' contributions vary depending on the study road section's internal and exterior environmental conditions. In a given factor, certain of the factors and factor classes have a greater contribution to the occurrence of landslides than others. However, the total contribution of all involved components determines the ultimate susceptibility class of the specified area. This is addressed in detail by the fact that landslides have happened in places with gentle slope topography that are far from streams and were caused by the combined action of several additional triggering events.

4.6. Remedial Measures for Landslides along Gore-Masha-Tepi Road Section

The results of the investigation and site visit for the corresponding geotechnical sensitive sites require that appropriate corrective actions be put in place. It is evident from the thorough observations that the majorities of stability issues are simple and result from inadequate construction; in most cases, corrective action may be carried out without much trouble.

Alternative recommendations for slides and subsidence are created after taking in to account the actual characteristics of each site, as well as the causes and triggering mechanisms. These recommendations can be implemented after being assessed for cost and convenience of installation. Below is a summary of the corrective actions taken for each section.

4.6.1. Landslide Section @ km 14+200-14+540(SL-01)

To remove mobilized cutting mass and reduce the load and hence pushing force at the head of a landslide area, cutting (mass removal) and flattening work are employed. When adopting this technique for a specific landslide area, there are important factors to consider.

I. Only at the head of a landslide that has a driving influence on the slope's downslope side may the cutting (mass removal) work be carried out. At the slope's toe, no excavation or cutting work is required;

II. If the landslide is continuous, cutting on the destabilized material is not possible.

III. Extreme caution must be used to prevent the neighboring slope behind the removed slope mass from becoming unstable due to a lack of support;

IV. Integrated slope protection work that uses vegetation to cover the slope face and provides surface drainage should be taken into consideration at the same time as the removal of the moving (unstable) material.

The construction technique adopted, which left the back slope unfinished and sharp at the toe, is what caused the landslide at this point. According to the ERA Geometric Design Manual (2013), flattening the slope to a 2:1 (H: V) will stabilize it because of the existing failing. Since the slope is not executed in accordance with the ERA Geometric Design Manual, as can be seen from the prior design, the cut height has been reduced. This results in failure likelihood. And for heavy fill/deep cut areas of the project, bio-engineering techniques such planting deep-rooted grasses should be used in good time to improve slope material anchorage and prevent soil erosion, ensuring slope stabilization.

4.6.2. Landslide Section @ km 45+350-45+440 (SL-02)

To remove mobilized cutting mass and reduce the load and hence pushing force at the head of a landslide area, cutting (mass removal) and flattening work are employed. When adopting this technique for a specific landslide area, there are important factors to consider.

I. Only at the head of a landslide that has a driving influence on the slope's downslope side may the cutting (mass removal) work be carried out. At the slope's toe, no excavation or cutting work is required;
II. If the landslide is continuous, cutting on the destabilized material is not possible.
III. Extreme caution must be used to prevent the neighboring slope behind the removed slope mass from becoming unstable due to a lack of support;
IV. Integrated slope protection work that uses vegetation to cover the slope face and provides surface drainage should be taken into consideration at the same time as the removal of the moving (unstable) material.

Analysis result from slope flattening

It can be noted that the slope with the original slope is on the verge of failure (FS=1.173) and with the slope ratio of 2:1, it is somewhat satisfactory with FS=1.43. In this regard, providing a retaining is more important structure. This is due to:

- The slope flattening is not more sufficient to stabilize the cut slope in the safest way
- As the failure is associated with the destabilization of the slope in the time of cutting coupled with the increase of shear stress due to rainfall, spring and surface streams and steepness of the slope. As a result, a rigid structure can accommodate such failures than any other flexible structure like gabions.
- The vicinity of the cut slope is agricultural land which is not allowed to flatten the cut slopes in excess due to right of way constraints. Hence, the provision of retaining structure is more appropriate.

Table 4.21: Analysis result from slope flattening

	Design cut slope flattening (1.5:1)	Design Cut Slope Flattening (2:1)	With Retaining Wall
FS	1.173	1.403	1.594

4.6.3. Landslide Section @ km 67+500-67+570 (SL-03)

The complete ground at this location is pre-existing moving mass with active sliding was seen at RHS. From the information gathered from local people, houses which were previously located were demolished owing to the land slide and the occupants were relocated. Trees that had collapsed during the site inspection were evidence of active sliding. The geometric cross sections at this point reveals the construction of high fill section consequently the natural ground will be employed as working platform for the embankment as shown the typical section.

Because of the ongoing and pre-existing landslides that were seen during the site visit, geotechnical investigations using borehole drilling and geophysical surveys are required in order to understand the subsurface conditions before embankment fill is constructed.

To get enough information, a geophysical survey must be conducted along and across the borehole and at least one must be dug. Remedial actions will be recommended in accordance with the results of the subsurface investigations.

4.6.4. Landslide Section from km 69+180-69+220 (SL-04)

The river bank is particularly susceptible for erosion unless suitable protective activities are done. Among the often-utilized erosion protection measures for river banks are sheet piling, gabion walls, masonry or concrete retaining walls, stone pitching, block pitching, and concrete pitching.

Streams and rivers with varying volumes and velocities primarily intersect the road segment under investigation. The area's geography, soil characteristics, and stream hydrology all have a major impact on how severe river bank erosion is. In order to minimize the current landslide and avoid future ones, coordinated river bank erosion prevention works are needed throughout the Gore-Mash-Tepi Road segment.

The geometric cross section shows a substantial side fills on the LHS, and the landslide at this section is the original ground with a rapid drop on the LHS.

While the section on the LHS with the depressed ground will be a fill section that needs to be properly constructed, the ground contains sound rock outcrops in the RHS direction where rock excavation for the cut slope was underway during the site visit. Section 4.1.1.4 provides illustrations of the geometric cross section and the site picture.

Following a sharp drop, the original ground will level off, suggesting that the embankment should be built on easy terrain. However, in order to ensure stability, check dams must be built in order to construct the headwall and protection for the drainage structure at km 69+209. These dams should ideally be built on rock or a carefully treated foundation. The figure below depicts the suggested position for the pipe culvert.

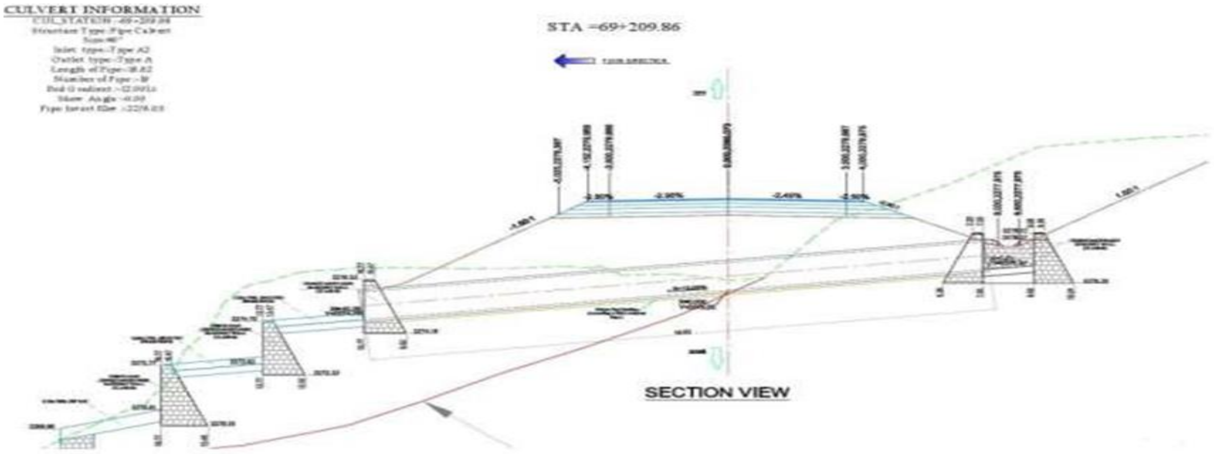

Figure 4.45: Proposed Remedial Measure at km 69+209

4.6.5. Landslide Section @ km 79+940-78+960 (SL-05)

One of the corrective actions could be to build fill near the slope's toe to provide support for the advancing mass. The following factors should be taken in to account when thinking about fill construction as a landslide remediation measure:

I. Only at the toe of the landslide area should fill be constructed as the resistant mass; otherwise, it may worsen the issue by creating more driving force;

II. The material at the landslide's toe is frequently weak and disordered as a result of the large volume of mass being mobilized from the accumulation and depletion zones. Therefore, a thorough investigation into the foundation material's bearing capacity is necessary for fill building;

III. Great care must be taken to prevent the fill material from creating a driving force that could result in another landslide on the slope next to the current one;

IV. Positive pore water pressure may arise as a result of filling work, particularly when fine, cohesive material is used to prevent the flow of subsurface water. Therefore, a suitable drainage system to release the fill's underground water must be taken in to account.

V. The fill slope itself may fail and create more instability if it is not correctly planned and built. The fill's stability must be examined, and a suitable fill slope must be suggested.

The morphology of the steep slope profile and the type of material that forms the slope—fills material—are the primary causes of the failure surrounding this segment. Future road damage will result from the failure, despite the fact that it is visible far from the center of the current alignment. For the kind of material that makes up the slope, the existing slope is excessively steep. According to the 2013 ERA Geometric Design Manual, it is therefore advised to level the slope to a 3:2 (H: V) slope ratio for this kind of material.

4.6.6. Settlement Section @ km 79+980 – km 80+010 (SL-06)

Subsurface drainage is now necessary to decrease the growth of a driving positive pore water pressure in the subsoil, which increases the soil mass's effective stresses and shear strength. (Popescu, M. E., & Sasahara, K. , 2005) In order to reduce the development of a driving positive pore water pressure in the subsoil, which raises the effective stresses and shear strength of the soil mass, subsurface drainage is now required.

Recharging the ground water by infiltration from the extended rains is the primary supply of ground water for the region along the Gore-Masha-Tepi Road stretch.A considerable amount of water evaporates and is lost through the transpiration of green plants when an area experiences high rainfall volumes for an extended length of time.Surface runoff is the residual water from the rainfall that seeps below the surface to replenish the earth system.

Subsurface erosion from subsurface water flow and compaction from the traffic load of the soft fill material and the soft residual soil in the subsurface are the primary causes of subsidence and settlement in this particular segment. In order to facilitate water flow without creating stress or subsurface erosion, it is advised to assess the area's true in situ condition during the extensive excavation period, improve the soft ground with appropriate material or rock fill, and/or build subsurface drainage. Additionally, a suitable drainage system must be installed to collect surface water from the hill.

4.6.7. Landslide Section @ km 80+700-81+600 (SL-07) & Landslide Section @ km 81+700-83+400 (SL-08)

(Terzaghi, 1950) stated that "the means for stopping movement must be adapted to the processes which started the slide if a slope has started to move." If subsurface water is the primary cause of landslides, for instance, a good remedial technique must offer a practical way to remove the subsurface water.

The project area is known to receive more than eight months of rainfall, and the natural ground below 2.0 meters is primarily saturated by groundwater. If we excavate a road about 10 meters deep with a cutback slope ratio of 1. 5H:1V, the lower portion of the soil cutback slope will first bulge out, and the upper layer will then fail. This is because the water in the soil adds load to the bottom cutback slope section, and the presence of water also reduces the soil's shear strength. Because of the aforementioned facts, the region is exposed to:

1. Seepage water causes an increase in pore water pressure.
2. The reduction of effective stress
3. Surface runoff-induced erosion
4. As the soil becomes saturated, the activity force to collapse the slope increases, decreasing resistance to slope collapse and severely impairing slope stability.

On the basis of site observation and prior research, the combined geophysical and geotechnical data is interpreted. Rainfall is the primary cause of slope instability in the project area, which is characterized by a weak moist layer of dark gray silty clay soil, saturated silty clay soil within light brown silty clay residual soil, and highly weathered and decomposed colluvium material. These materials are relatively susceptible to instability during the rainy season because surface and groundwater increase their moisture content, decrease their shear strength, or increase stress due to water content.

Underneath the heavily worn and cracked rock are the majority of the thick top remnant silty clay soil and extremely weathered and decomposed colluviums. As a result, gully formations in these places have an impact on the stability of hydraulic structures like culverts as well as the cutback slope. As a result, a suitable mitigation strategy must be provided.

I. Installation of Stone lined waterways

Regular rainfall raises the soil's pore water pressure, which speeds up sliding. Rainwater will thus be successfully avoided by constructing stone-lined rivers in the sliding part.

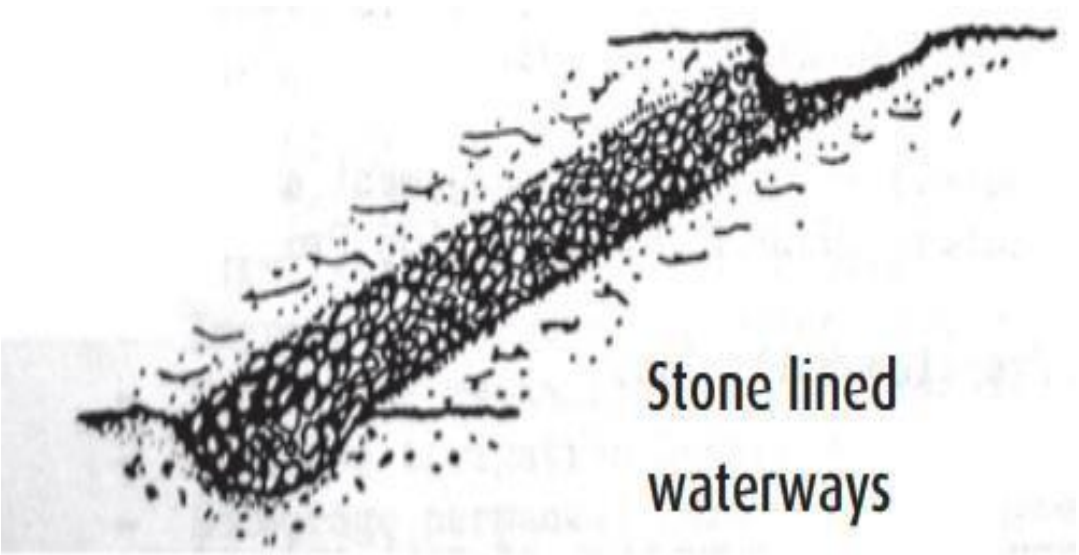

Figure 4.46: Stone lined waterways

Vegetation

planting plants and leveling the area where the sliding happened. provides ground cover to shield the soil surface from precipitation, lowers runoff velocity by blocking it, and improves land quality by reducing erosion.

II. Installation of Retaining wall or Gabion wall with drainage

- To stop further sliding, install a retaining wall or gabion wall at the bottom of the sliding.
- Install a ditch in front of the retaining wall and a subsurface drain at the bottom to quickly drain water, which is crucial for sliding

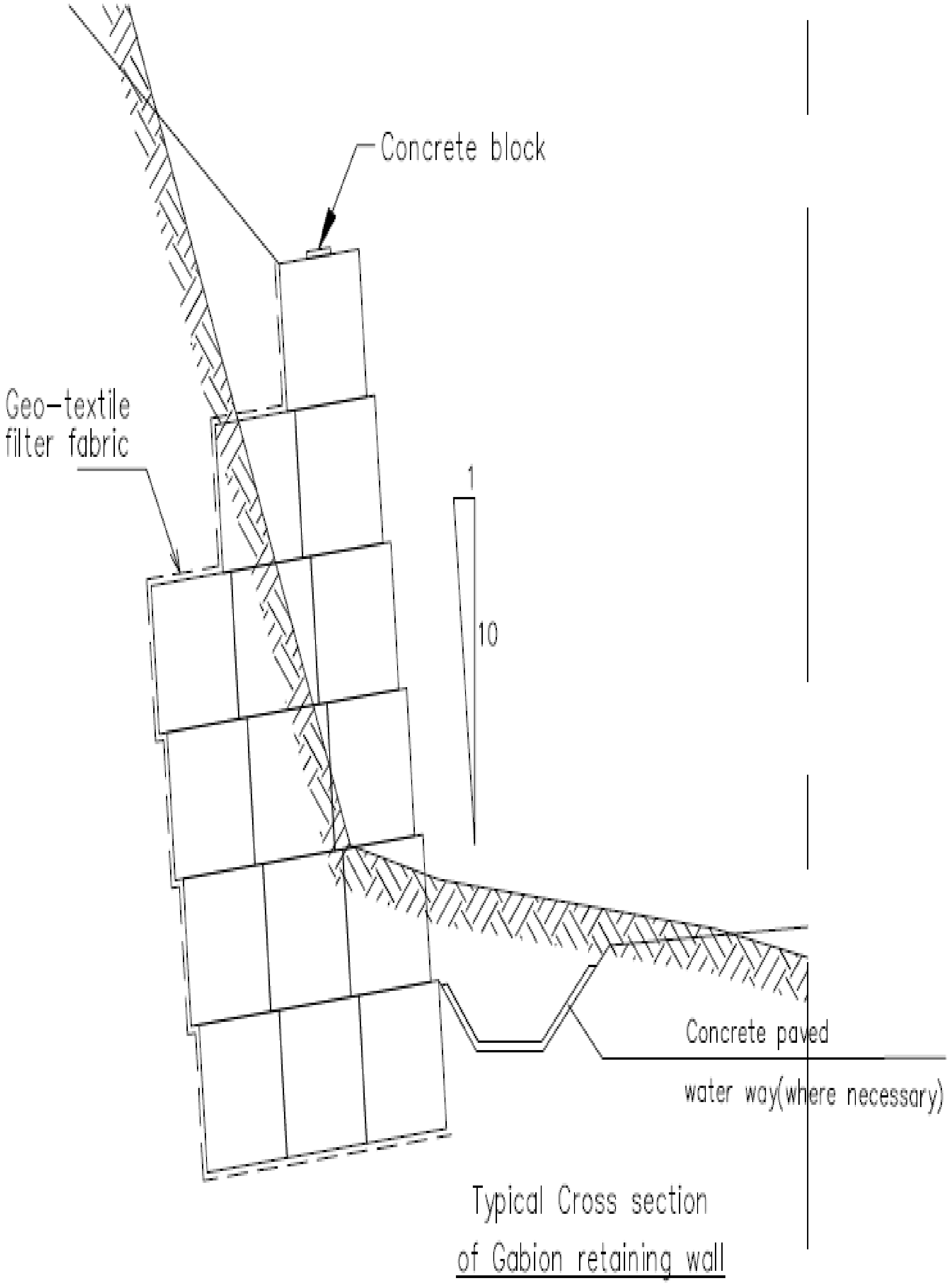

Typical Cross section of Gabion retaining wall

GABION RETAINING WALL

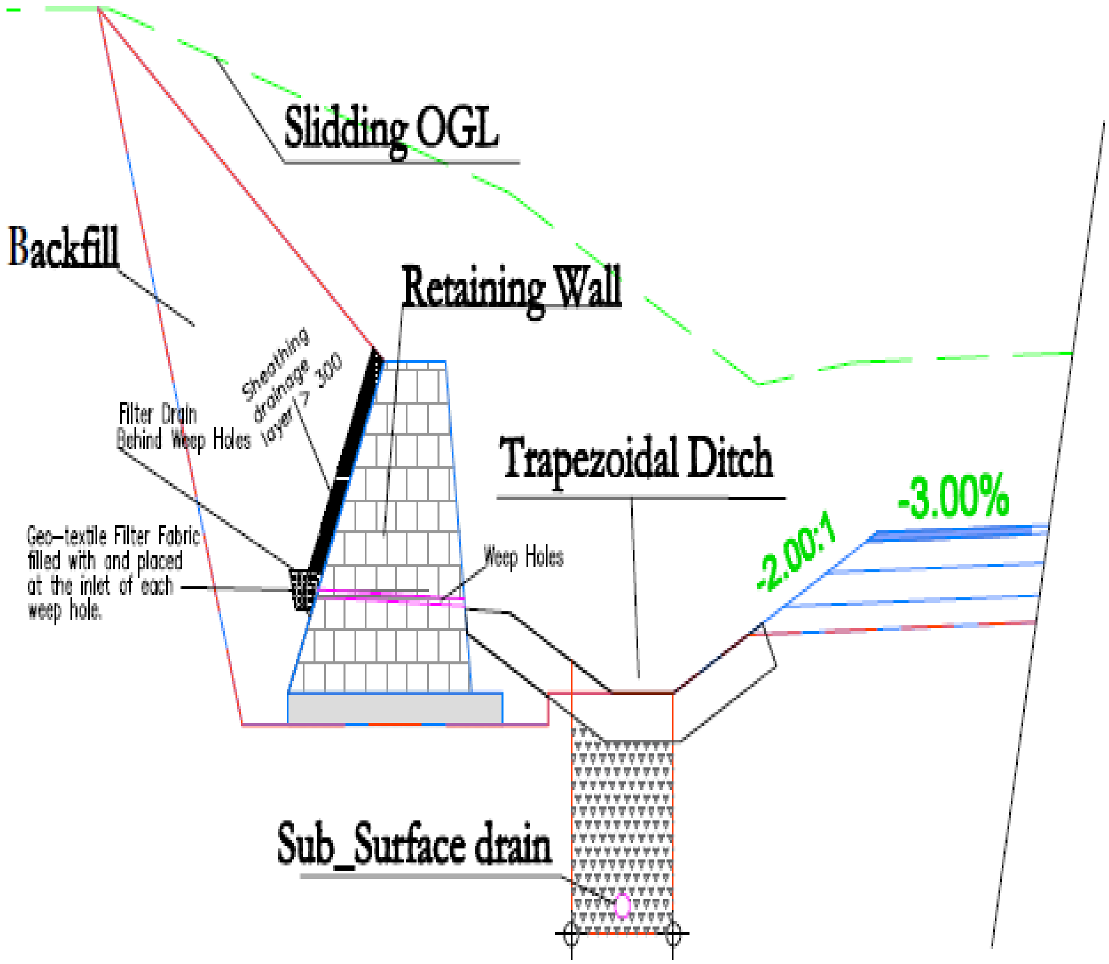

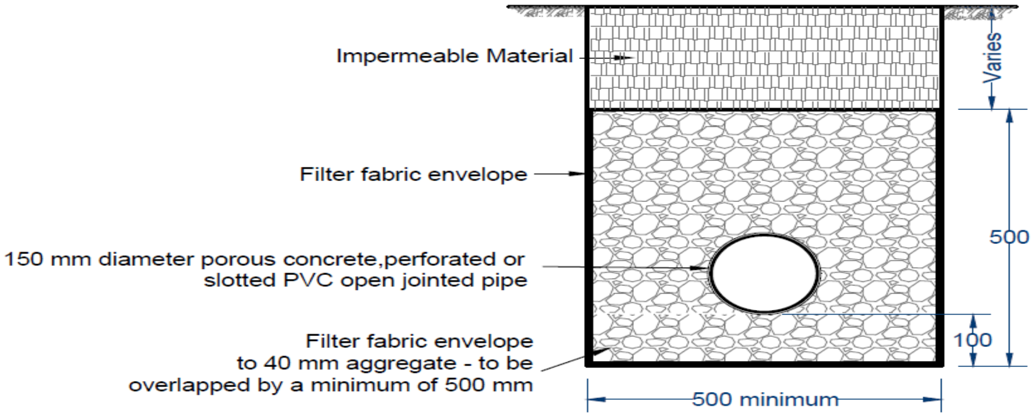

FRENCH DRAIN TYPE B

Figure 4.47: Retaining Wall Subsurface Drane & Gabion Wall with km 80+700- 83+400

Table 4.22: Recommendations for sections with geotechnical problems

S.No	Slide Section	Triggering factor	Proposed Remedial Measure
1	SL/01 (Km14+200– 14+540 RHS)	The big boulders which are found within thedecomposedrockmaterialstartedtomoved ownwardduetogravityandaffectedthe toe and later lead to failure of the slope.	• As per ERAGDM Re-Grading the profile as per the condition of the ground and re design the road Geometry with slope flattening • Removing the heap of spoil at the hill's head and leveling the slope; • providing drainage systems, both subsurface and surface; • Planting deep rooted grasses like vetiver grass for slope protection
2	SL/02/Km45+300-45+440 RHS	The main reason for failure is the action of rainfall which resulted in the saturated weight of soil and subsurface water draining between adjoining planes of the different soil types decreasing the friction between constituent particles. and collapse of soil layer that couldn't able to stand with the designed back slope ratio.	• Provide retaining wall at the bottom of the sliding to prevent additional sliding. • Removing the heap of spoil at the hill's head and leveling the slope; • providing drainage systems, both subsurface and surface; • Planting deep rooted grasses like vetiver grass for slope protection

4	(LS03)/ Km67+500-67+570	Due to the high fill section's development, the natural ground will function as a working platform because there is pre-existing movable mass with active sliding over the entire ground at RHS.	• Further investigation by geotechnical and geophysical investigation to suggest appropriate remedial measure
5	(SL04/Km 69+180-69+220	The toe erosion and undercutting of the natural slope material by the stream crossing the road is identified as the main cause of the active landslide. In addition, the saturation of the sides lope material by rainfall and surface runoff water contributes for the strength reduction of the slope material which contribute for the landslide.	• Construct masonry retaining walls to properly safeguard the riverbank and monitor the Construction of series of check dams at the pipe outlet • To handle the subsurface water, which is the primary cause of landslides in this area, deep drainage tubes must be provided • Planting deep rooted grasses for fill slope protection
6	(LS-05)/km 78+940-78+960 RHS	The main cause of the failure is its morphology of the slope/steep slope profile and the nature of the material forming the slope which is a fill material. it will cause future damage	• As per ERAGDM re-grading the profile as per the condition of the ground and re design the road Geometry with slope flattening • Construction of furrow ditch upslope to intercept surface runoff from the catchment dissipated by chutes to the side drain. • Planting deep rooted grasses like vetiver grass for slope

			protection
	(LS-06)/ Km 79+980 – 80+010	The main causes of the subsidence/settlement is the underground erosion due to subsurface water flow and compaction due to traffic load of the soft fill material and the soft residual soil present in the subsurface	• Check the actual in-situ condition of the area during wide excavation period along the longitudinal and check the water point (Eye point) and improve the soft ground by filling suitable material especially by rock fill across the road. If the eye point is located in one place better to leave to drain out by crossing the cross section at the required place and if the eye point of water shows many location • treat the subsurface drainage longitudinally and lead the water to the rock fill to drain out the water. The surface drainage will also be guided to the next pipe culvert structure through the open drainage system.
	(LS-07)/km 80+700 – 81+600	The main factors for the instability problem are geological structure of fault and highly weathered colluvms material along left-hand side of box cut section	• Provide retaining wall or gabion wall at the bottom of the sliding to prevent additional sliding. • installing stone lined waterways in the sliding section, rainwater will be effectively prevented • Install subsoil drain at the bottom and ditch in front of retaining wall for draining water immediately, which is the most important factor in sliding

	(LS-08) Km 82+610-83+400	Where slope failure could occur very weak saturated thin silty clay soil observed from borehole logging from 4.0– 4.20m depth and this layer is defiantly different from the upper and lower layer in its moisture content which is almost changed into mud material.	• Provide retaining wall or gabion wall at the bottom of the sliding to prevent additional sliding. • installing stone lined waterways in the sliding section, rainwater will be effectively prevented • Install subsoil drain at the bottom and ditch in front of retaining wall for draining water immediately, which is the most important factor in sliding

CHAPTER FIVE

CONCLUSIONSAND RECOMMENDATIONS

5.1. Conclusions

The topography of the Gore-Mash-Tepi Road has a significant impact on its vulnerability to landslides. Compared to smoother terrain, the route's steep slopes greatly increase the risk of landslides. In order to create a landslide inventory and assessment for the route, this study used satellite imaging, field surveys, community feedback, and historical data. Nine (9) historical landslides that were caused by various factors were found. Important findings include:

- Topographic Vulnerability: The route passes undulating terrain (5–25° gradients) and transitions into hilly/mountainous sections. These steeper areas connect with previous landslide events, leading to traffic obstructions and fatalities

- Rainfall as a Catalyst: The southwestern region of Ethiopia experiences prolonged annual rainfall, amplifying landslide frequency. This climatic factor was integrated into the area’s landslide susceptibility mapping.

- Hydrological Factors: Poorly managed surface and subsurface water exacerbates landslide risks. Drainage maps and field surveys highlight extensive stream networks and groundwater seepage, necessitating prioritized water management strategies. Erosion of stream banks and beds further destabilizes slopes.

- Soil and Geological Conditions: Slope materials in the study area—primarily loose, saturated, erodible residual soils with low strength—heighten landslide susceptibility. Variations in soil composition correlate with landslide severity.

- Landslide Geometry: Effective mitigation requires analyzing landslide structure. Most landslides along the road occur at flexural zones (toe of rupture), with detachment zones uphill and displaced debris accumulating downhill.

These results highlight how soil characteristics, rainfall, slope gradient, and hydrological dynamics interact to create landslides. For sustainable road infrastructure in areas vulnerable to landslides, it is imperative to address these problems comprehensively.

The Analytical Hierarchy Process (AHP) method which is a semi-quantitative multi-criterial decision-making approach is used to prepare the landslide susceptibility map of Gore-Mash-Tepi Road section. A total of nine landslide causative factors were selected and analyzed to produce the landslide susceptibility map of the road section.

The selected factors are slope angle, slope aspect, elevation, curvature, lithology, distance to stream, distance to road, land use/cover and rainfall of the road section under study. Thecomparativeimportanceofthementionedfactorsandfactorsclassesfortheactivation oflandslideandtopredictthelandslidesusceptibilityoftheareaisanalysisbasedonthepair-wise comparison matrix to generate the weight and check the consistency of the decision. The following are the observations from the landslide susceptibility analysis:

Based on the analysis conducted, Slope angle, rainfall and lithology are the most in fluencing factors to initiate the landslide and their weight is 0.356,0.207 and 0.125, respectively. The other influential contributing factor is land cover which composed a weight of 0.101, followed by distance to stream, elevation, distance to road, slope aspect, and curvature with the weight of 0.063, 0.058, 0.0, 0.042, 0.28 and 0.020, respectively.

- Theareashighlysusceptibleforthelandslidealong Gore-Masha-TipeRoadsectionare areas characterized by **(A)**Slope angle 48^{0}-75^{0}(30.70%) and 39^{0}-48^{0}(21.8%) **(b)**Rainfall 1689-1983mm (55.8%) and 1395-1689mm (26.3%) **(C)** LithologyofOrthic Acrisols(50.3%)andDystric Flurisols(26.0%)curvature flat (41.18%) and concave (40.55%) (**D**) Land Use/Cover of Bare Land (50.3%) and Settlement (26.0%) **(E)**DistancetoStreamof50m(51.7%)and100 m (25.4%) **(F)** Elevation 2401-22783 (30.7%) and 2234-2401(21.8%) (g) Distance to road of 50 m (51.7%)and150m(24.4%)(h)Slope Aspect ofNorthwest (28.4%)andWest (23.8%) (I) curvature Concave (63%) and convex (26%).

- The landslide susceptibility map generated using the AHP method has classified into five classes very high susceptibility (26.95%), Highly Susceptible (24.71%)

moderate Susceptible (62.87%), Low Susceptible (20.99%), and the very low Susceptible (4.83%).

5.2. Recommendation

The following suggestions are put forth to improve future research and mitigation initiatives in light of the study's findings:

1) **Expanded Research Scope**: Although the Gore-Masha-Tepi Road Project was the focus of this study's landslide assessment, susceptibility mapping, and initial mitigation strategies, more research should take into account other contributing factors (such as soil water content, erosion, and variations in groundwater levels) to increase the accuracy of landslide risk mapping.

2) **Rainfall Impact Analysis**; -In depth studies of rainfall patterns, especially their relationship to the frequency and severity of landslides, are essential given the region's protracted rainy season. For reliable hazard forecasting, sophisticated susceptibility models that incorporate hydrological data are advised.
3) **Planning for Landslide-Resilient Infrastructure: -** Before beginning any long-term infrastructure projects, landslide risk assessment must be given top priority in future road infrastructure planning and development. This is especially important in areas with difficult terrain and long rainy seasons. To guide project design, in-depth research on landslide characteristics, failure causes, and practical mitigation strategies should be carried out.
4) **Analysis Methodology**: -Future research should use 3D modeling to more accurately replicate real-world slope failure conditions, even though 2D finite element analysis was used to estimate conservative safety factor (FS) values for slope design.
5) **Soil Sampling and Testing Challenges: -**Detailed lithological cross-sectional characterization was hampered by the lack of borehole data along the failed slopes. In order to overcome this, outcrop observations from nearby boreholes and excavated areas were used to infer idealized borehole profiles. For accurate

subsurface profiling, however, extensive longitudinal and transverse drilling across failure zones is advised.

These Thesis can be divided into two groups: preventive (which indirectly reduces risks by addressing contributing factors) and corrective (which directly improves slope stability by increasing resistance). This strategy adheres to sustainable infrastructure practices while guaranteeing proactive hazard reduction.

References

Irshad, T. Harikrishnan, Bose, M. Kurniati, T. (2024). AHP-basedgeospatial analysis for landslide susceptibility zonation in Wayanad District. *EDP Sciences* , 04, 01004.

Abay, A. (2019). *GIS-based landslide risk assessment in Ethiopian highlands.* Addis Ababa University.

Abbate, E., Bruni, P., & Sagri, M. (2015). *Geology of Ethiopia: A Review and*. Retrieved from https://doi.org/10.1007/978-94-017-.

Anbalagan, Azeze, A., & Fell. (2019,2019,2008). Landslide hazard evaluation and zonation mapping in mountainous terrain Landslide hazard evaluation and zonation mapping in mountainous terrain.

Anbalagan, R. (1992). Landslide hazard Evaluation and Zonation mapping in Mountainous terrain. *Engineering Geology* , 32(4) 269-277.

Anbalagan, R., Azeze, A., & Fell. (2019).). Landslide hazard evaluation and zonation mapping in mountainous terrain Landslide hazard evaluation and zonation mapping in mountainous terrain.

Arbanas & Arbanas. (2015). a modle of mudflow propagation dwonstream from the grohove landslide near the city of Rijeka (Croatia). *Natural Hazards and Earth System Sciences* , 15(2), 293-304.

Asmelash, A. (2012). Slope stability analysis in the Tigray Highlands, Ethiopia: A GIS-based approach. *Journal of Mountain Science* , 9(4), 523–535.

Asmelash, A. (2012). GIS-based landslide susceptibility mapping in the Abay Gorge, Central Ethiopia. *Central Ethiopia. Journal of the Geological Society of Ethiopia* , 36(2), 1-14.

Authority, E. R. (2013). *Road Design Manual* . Ethiopan Road Authority .

Ayalew, L. (1999). Landslide hazards in the Ethiopian highlands. *AAU Press.* , 58(1), 9–19.

Ayele, A. (2009). Landslide hazard zonation in the Blue Nile Gorge, Central Ethiopia. *Ethiopian Journal of Science,* , 32(1), 1-10.

Ayenew, T., & Giulio, G. (2005). Hydrogeology of volcanic terrains: Case studies from East Africa.

Azeze, A. (2019). Landslide Susceptibility Assessment and Mapping Using Statistical And Deterministic Methods In Goncha Siso Eneses Area, Northwestern Ethiopia.

Bekele, A. (2010). *Managing watersheds for resilient livelihoods in Ethiopia.* IFPRI and EDR.

Bell, R. (2007). Landslide susceptability mapping for the Swabian AIB (Germany) Logistic regression Approach. *Geomorphology* .

Bemasconi, M. (2009). *Slope stability analysis: Methods and applications. Springer.* Geotechnical Engineering.

Bowles, J. E. (1988). *Foundation analysis and design* . McGraw-Hil.

Bowles, J. E. (1996). *Foundation Analysis and Design,*. Prentice Hall .

Brabb, E. (1985). *Innovative approaches to landslide hazard and risk mapping.* Toroto: Canada Geotechinical Society.

Brenner, R. P. (2003). *Evaluation of ground improvement methods.* Geotechnical Research Institute.

Brinkgreve, R. (2002). *Plaxis 2D 2002 full manual: Finite Element code for soil and rock analyses.* The Netherlands: A.A. Balkema.

Caine, N. (1980). The rainfall intensity-duration control of shallow landslides and debris flows. *Physical Geography* , 1(1), 1-27.

Casagli, N. (2004). *An inventory-based approach to landslide susceptibility assessment and its application to the Virginia River Basin, Italy. Environmental and Engineering Geoscience*. Retrieved from https://doi.org/10.2113/10.3.203.

Catani, F. (2013). Landslide susceptibility estimation by random forests technique:. *Natural Hazards and Earth System Sciences* , 13(11), 2815-2831.

Charlotte, N. (2010). Urban planning challenges in developing nations. *Sustainable Development* , *12*(3), 45-60.

Command, N. F. (1986). *NAVFAC DM 7.1 Soil Mechanics* . US Department of the Navy.

Crozier, M. J. (1986). Landslide activity and geomorphic significance in the Southern Alps. *New Zealand. Earth Surface Processes and Landforms* , 11(1), 69-78.

Cruden, D. (1996). Landslide Types and Processes ,Special Report , Transportation Research Board .

Dai, F. C., & Lee, C. F. (2001). Frequency–volume relation and prediction of rainfall-induced landslides. *Engineering Geology* , *59*(3–4) 253–266.

Dai,F & Lee,C.F. (2002). Landslide Charateristics and Slope Instability Modeling Using GIS, Lantau Island HOng Kong. *Geomorhology* , 42,213-238.

David,M. Cruden & David J.varnes. (1996). *Landslide Investigation and Mitigation.* National Academy Press.

Dou, J. (2015). *Optimization of Causative Factors for Landslide Susceptibility Evaluation Using Remote Sensing and GIS Data in Parts*. Retrieved from https://doi.org/10.1371/journal.pone.0133262.

Dou, J. (2015). *Statistical approaches for landslide assessment.* 89-112).

Duncan, J. M. (1996). State of the art: Limit equilibrium and finite-element analysis of slopes. Journal of Geotechnical Engineering,. *Geotechnical Engineering* , 122(7), 577–596.

Duncan, J. P., & Wright, G. (2000). Risk assessment in property markets. *Real Estate Economics* , 28(3), 345-370.

Farhan, A. (2020). Urbanization impacts on groundwater resources in arid regions. *Environmental Science & Technology,* , 54(8), 4567–4578.

Fell, R. (2008). *Guidelines for landslide susceptibility, hazard and risk zoning for land-use planning. Engineering Geology.*

Foumelis, M. (2019). Monitoring land deformation using InSAR techniques. Remote Sensing. *11*(14), 1672.

Getnet, K. (2016). *Impact of microfinance on poverty reduction in rural Ethiopia.* East Africa: Addis Ababa University.

Glade, T. (2000). Modelling landslide-triggering rainfalls in different regions of New Zealand - the soil water status model. *Zeitschrift für Geomorphologie* , 44(3) 299-325.

Guzzetti, f. (2005). Analysis of landslide triggers in Central Italy. *Italian National Research Council* , Report No. 2005-123.

Guzzetti, F. (1999, 1-4 31). Landslide hazard evaluation : a review of current techniques and their application in a multi-scale study, Central Italy. *Geomophology* , pp. 181-216.

Habibnezhad. (2014). *Stability Analysis of Embankments Founded on Clay - a comparison between LEM & 2D/3D FEM.* Royal Institute of Technology, Stockholm.

Haile, A. T. (2022). GIS-based landslide early warning systems for the Ethiopian

Highlands. *Addis Ababa Universit* .
Hara, A., Ohta, T., Niwa, M., Tanaka, S., & Banno, T. (1974). Shear modulus and shear strength of cohesive soils. *,. *Soils and Foundations* , 14*(3), 1–12.
He, Y., & Beighley, R. E. (2008). GIS-based stream network modeling for hydrologic applications. *Journal of Hydrologic Engineering* , 13(4), 395–405.
Highland, L. & Bobrowsky, P. (2008). *The Landslide Handbook -A guide to Understanding Landslides (US Geological Survey Circular 1325pp.).* US Department of the interior US Geological Survey.
Highland, L. M. & Bobrowsky, P. (2008). The landslide handbook—A guide to understanding landslides. *U.S. Geological Survey* , U.S. Geological Survey Circular 1325.
Hoek.E & Bray,J.W. (1981). *Rock Slope Engineering (Revised 3rd ed).* London: Institution of Mining and Metallurgy.
Institution, B. s. (2009). *Code of Practice For Earth Works.* BSI Standards .
Jazouli, A. E., & Barakat, A. (2019). Landslide risk assessment in mountainous regions. *In Advances in Geospatial Technologies* , 123–145.
kanungo, D.P., Arora, M.K., sarkar, s. & Gupta, R.P. (2009). Landslide Susceptibility Zonation (LSZ) Mapping . *south Asia Disaster Studies* , 2(1),81-105.
Kissi, N. (2012). Spatial patterns Causes and Consequences Of landslides in the Gilgel Gibe Catchment. *Catena* , 127-136.
Lemenew, M. (2024). Landslide Assessment, Susceptibility Analysis and Recommendation of Remedial Measures for Jimma-Chida Road Segment. *Adiss Abeba Univeristy* .
Lu, C.-Y., & Chih-Wei, L. (2011). Rainfall-induced landslide risk assessment in Taiwan using historical rainfall data. *Natural Hazards and Earth System Sciences* , 1623-1634.
Malaysia, P. W. (2010). *Standard Specification for Road Work.* Work Department Malaysia.
Mehmod, K. (2022). *Machine learning for landslide prediction.* In AI in Geosciences.
Melese, T., Belay, T., & Andemo, A. (2022). Application of analytical hierarchal process, frequency ratio, and Shannon entropy approaches for landslide susceptibility mapping using geospatial technology. *Environmental Earth Sciences,* , *81*(15), 1–18.
Meng. (2006). *Slope Stability Analysis. SSP Geotechnics.*
Mewa, G; Megistu, F. (2022). *Assessment of Landslide Risk in Ethiopia: Distributions, Causes, and Impacts*. Retrieved from https://doi.org/10.5772/intechopen.101023.
Mikos, M., Cetina, M., & Brilly, M. (2004). Hydrologic conditions responsible for triggering the Stože landslide,. *Slovenia. Engineering Geology* , 73(3–4), 193–213.
Ngecu, W. M., & Mathu, E. M. (1999). The El-Nino-triggered landslides and their economic impact on Kenya. *Environmental Geology* , *38*(4).277–284.
Nugroho, e. (2012). Analying and estimating the impact of landslide to road in samigaluh district,kulon progo regency. *Forum Geografi* , 26(2), 132-145. https//dio.org/10.23917/forgeo.v26i2.5068.
Office, G. C. (1984). *Guide to site Investigation* . Hong Kong: Hong Kong Government.
Ohlmacher, G. C. (2007). Mechanisms of landslide frequency in the Kansas River valley. *Environmental Geology* , 52(5), 985-995.
Panchal , S; Shrivastave, A.K. (2022). Landslide hazard assessment using analytic hierarchy process (AHP): A case study of National Highway. *Ain Shams Engineering*

Journal .

Petchko, H. (2014). Assessing the quality of landslide susceptibility maps-case study Lower Austria. *Natural Hazards and Earth System Sciences* , (14)(1), 95-118.

Popescu, M. E., & Sasahara, K. . (2005). *Landslide hazard assessment: Methods and case studies.*

R.B., B. (2002). *Plaxis 2D 2002 full manual: Finite Element code for soil and rock analyses.* Netherlands: A.A: T. Balkema Publishers, a member of Swets & Zeitlinger.

R.B., B. (2002). *Plaxis 2D 2002 full manual: Finite Element code for soil and rock analyses.* The Netherlands: A.A. Balkema.

Reghuvanshi, T. (2014). *Landslide Disaster Management and Reduction AnApproach Through Remote Sensing and GIS.* Springer Japan.

Saaty, T. L. Vargas, L. G. (2001). *Models, Methods, Concepts & Applications of.*

Saaty, T. L. (1987). The analytic hierarchy process: Planning, priority setting. *Mathematical Psychology* , 15(3), 234-281.

Serdarevic, A., & Babic, F. (2019).

Serdavic, A; Babic, F. (2019). *Landslide Causes and Corrective Measures-Case Study of the Sarajevo Canton*. Retrieved from https://doi.org/10.5923/j.jce.20190902.02.

Shakoor, A., & Smithmyer, A. J. (2005). An analysis of landslide susceptibility in Ohio based on geologic and geomorphic factors . *Environmental & Engineering Geoscience* , *11*(2) 109–128.

SOOSUNG Engineering Co., Ltd. in JV with Korea Consultants International Co., Ltd. And DOSAN Consultants Co., Ltd. In Sub-Consultancy, with Net Consult Consulting Engineers and Architects Plc. . (2021). *Geotechnical Investigation Report Landslide section Along Gore-Mash-Tepi Road Project.*

Suryanarayana, T., Gezahegn, D., Assefa, E., Seid, A., & Belachew, E. B. (2021). Assessment of landslide hazard in Dessie town. *International Journal of Applied Research,* , 7(3), 70–75.

Temesgen, B. (1999). Landslide hazard on the slope of Dabicho Ridge, Wondo Genet Area The case of june 18 1996 Event. *Ethiopian Journal of Science* , 22(1)127-140.

Temple, P. H. (1972). Landslides in the Mgeta area, western Uluguru Mountains, Tanzania. *Geografiska Annaler: Series A, Physical Geography* , 54(3-4), 157-193.

Tešić, D. (2021). Environmental risk assessment in mountainous regions. *Environmental Science & Policy* , 124, 45–58.

Tsege, A. (2017). Geotechnical Conditions and Stability Analysis of Landslide Prone Area: A Case Study in Bonga Town, South-Western Ethiopia. Journals.

Turrini, A., & Visintainer, P. (1998). Soil erosion dynamics in alpine ecosystems: A case study from northern Italy. *22*(3), 456–470.

Tyagi, A Tiwari,R & James, N. (2022). Temporal and Magnitude prediction of Landslide Hazard X A review on spatial, temporal and magnitude prediction of landslide hazard. Journal of Asian Earth Sciences:. *Journal of Asian Earth Sciences :* , X,7,100099.

Vařilová, Z., Kropáček, J., Šťastný, M., & Vilímek, V. (2014). Reactivation of mass movements in Dessie graben: The example of an active landslide area in the Ethiopian Highlands. Landslides. 12(5), 991–1001.

Varnes. (1984). *Landslide Hazard Zonation A Review of Principles and Practical Natural Hazards.* UNESCO.

Varnes. (1978). Slope Movement Types and Processes. Transportation Research.

Wachal D. , Hudak P.F. (2000). Mapping Landslide Susceptibility in Travis County, Taxas, USA. *Geojournal* , 51(3),245-253 hhtps//org/10.1023/A:1017524604463.

Wachal, R., & Hudak, P. (n.d.). Groundwater contamination in urban watersheds. *A GIS-based analysis. Environmental Geology* , *38*(4), 345–356 https://doi.org/xxxx.

Waltham, T. (2009). *Foundations of engineering geology*. Chicago: CRC Press.

Wendim, A. (2023). The impact of urbanization on biodiversity. *World Wildlife Fund* .

Wendim, S. (2023). Causes, failure mechanisms, and susceptibility zonation of landslides along Gedo-Dilb road corridor, Northern Ethiopia. *Research Square* .

Wieczorek, G. F. (2000). *Landslides: Proceedings of the 8th International Symposium on Landslides.* A.A. Balkema: 76-90.

Woldearegay, K. (2019). Groundwater potential assessment using GIS and remote sensing. *Journal of Hydrology,* , 12(4), 45-60.

Woldearegay, K. (2017). Landslide hazard assessment in Ethiopia. *Landslides in Developing Countries* .

Woldearegay, K. (2005). Review of the occurrences and influencing factors of landslides in the Horn of Africa: With emphasis on Ethiopia. *Addis Ababa University.*

Woldearegay, K. (2013). Slope stability analysis under unsaturated conditions. *DOI or URL* , *45*(3), 123-135. https://doi.org/xxxx.

Woldeargay, K. (2013). Review of the Occurrences and Influencing Factors of Landslides in the Highlands of Ethiopia with implications for infrastructural Development. *Momona Ethiopan Journal of Science* , 5(1),3-31.

Woldesenbet, T. ((2023)). Landslide susceptibility mapping in the Blue Nile Basin using machine learning techniques. *Geoenvironmental Disasters* , *10*(1), 15.

APPENDIX A

Analytic Hierarchy Process (AHP) Analysis for Landslide Contributing Factors and Classes

AHP Table for curvature

Pair-wise Comparison Matrix

Curvature	**Flat**	**Concave**	**Convex**
Flat	1	1/5	1/3
Concave	5	1	3
Convex	3	1/3	1
Sum	9.00	1.53	4.33

Calculating Consistency

C.W	0.1062	0.6333	0.2605	**Weighted sum value**	**Criteria Weight**	**WSV/CW**
Factors	**Flat**	**Concave**	**Convex**			
Flat	0.1062	0.1267	0.0868	0.3197	0.1062	3.01
Concave	0.5308	0.6333	0.7815	1.9456	0.6333	3.07
Convex	0.3185	0.2111	0.2605	0.7901	0.2605	3.03
					λmax=	**3.04**

Normalized Pair-wise Comparison Matrix

Factors	**Flat**	**Concave**	**Convex**	**Sum**	**Criteria Weights**
Flat	0.111	0.130	0.077	0.3185	0.106
Concave	0.556	0.652	0.692	1.9000	0.633
Convex	0.333	0.217	0.231	0.7815	0.260
				Sum	**1.00**

λmax = 3.039
λmax-n 0.039
n-1 = 2
RI=0.58
CI = 0.019
CR = 0.033

OK!!!

AHP Table for Distance to Road

APPENDIX

Pair-wise Comparison Matrix

Distance to road(m)	**50**	**150**	**500**	**1000**	**>1000**
50	1	3	5	9	9
150	1/3	1	3	5	7
500	1/5	0	1	3	5
1000	1/9	1/5	1/3	1	3
>1000	1/9	1/7	1/5	1/3	1
Sum	**1.76**	**4.68**	**9.53**	**18.33**	**25.00**

Calculating Consistency

C.W	**0.5173**	**0.2542**	**0.1307**	**0.0631**	**0.0346**	**Weighted sum value**	**Criteria Weight**	**WSV/CW**
Factors	**50**	**150**	**500**	**1000**	**>1000**			
50	0.5173	0.7627	0.6537	0.5680	0.3114	**2.8132**	0.517	**5.44**
150	0.1724	0.2542	0.3922	0.3156	0.2422	**1.3767**	0.254	**5.42**
500	0.1035	0.0847	0.1307	0.1893	0.1730	**0.6813**	0.131	**5.21**
1000	0.0575	0.0508	0.0436	0.0631	0.1038	**0.3188**	0.063	**5.05**
>1000	0.0575	0.0363	0.0261	0.0210	0.0346	**0.1756**	0.035	**5.07**
							λmax=	**5.24**

Normalized Pair-wise Comparison Matrix

Factors	**50**	**150**	**500**	**1000**	**>1000**	**Sum**	**Criteria Weights**
50	0.570	0.642	0.524	0.491	0.360	2.5866	0.517
150	0.190	0.214	0.315	0.273	0.280	1.2711	0.254
500	0.114	0.071	0.105	0.164	0.200	0.6537	0.131
1000	0.063	0.043	0.035	0.055	0.120	0.3156	0.063
>1000	0.063	0.031	0.021	0.018	0.040	0.1730	0.035
Sum	**1.00**	**1.00**	**1.00**	**1.00**	**1.00**	**5.00**	**1.00**

λmax = 5.238

λmax-n = 0.238

n-1 = 4

RI = 1.12
CI = 0.060

CR = 0.039

OK!!!

AHP Table for Distance to Stream

APPENDIX

Pair-wise Comparison Matrix

Distance to Stream(m)	**50**	**100**	**300**	**1000**	**10000**
50	1	3	5	9	9
100	1/3	1	3	5	7
300	1/5	0	1	3	5
1000	1/9	1/5	1/3	1	3
10000	1/9	1/7	1/5	1/3	1
Sum	**1.76**	**4.68**	**9.53**	**18.33**	**25.00**

Calculating Consistency

C.W	**0.5173**	**0.2542**	**0.1307**	**0.0631**	**0.0346**	**Weighted sum value**	**Criteria Weight**	**WSV/CW**
Factors	**50**	**100**	**300**	**1000**	**10000**			
50	0.5173	0.7627	0.6537	0.5680	0.3114	2.8132	0.517	5.44
100	0.1724	0.2542	0.3922	0.3156	0.2422	1.3767	0.254	5.42
300	0.1035	0.0847	0.1307	0.1893	0.1730	0.6813	0.131	5.21
1000	0.0575	0.0508	0.0436	0.0631	0.1038	0.3188	0.063	5.05
10000	0.0575	0.0363	0.0261	0.0210	0.0346	0.1756	0.035	5.07
							L.max=	**5.24**

Normalized Pair-wise Comparison Matrix

Factors	**50**	**100**	**300**	**1000**	**10000**	**Sum**	**Criteria Weights**
50	0.570	0.642	0.524	0.491	0.360	2.5866	0.517
100	0.190	0.214	0.315	0.273	0.280	1.2711	0.254
300	0.114	0.071	0.105	0.164	0.200	0.6537	0.131
1000	0.063	0.043	0.035	0.055	0.120	0.3156	0.063
10000	0.063	0.031	0.021	0.018	0.040	0.1730	0.035
Sum	**1.00**	**1.00**	**1.00**	**1.00**	**1.00**	**5.00**	**1.00**

λmax = 5.238

λmax-n = 0.238

n-1 = 4

RI = 1.12

CI = 0.060

CR = 0.039

Ok!!!

AHP Table for Elevation

APPENDIX

Pair-wise Comparison Matrix

Elevation (m)	**2401-2783**	**2234-2401**	**2077-2234**	**1922-2077**	**1785-19922**	**1646-1785**	**1451-1646**	**1239-1451**	**807-1239**
2401-2783	1	2	3	4	5	6	7	8	9
2234-2401	1/2	1	2	3	4	5	6	7	8
2077-2234	1/3	1	1	2	3	4	5	6	7
1922-2077	1/4	1/3	1/2	1	2	3	4	5	6
1785-19922	1/5	1/4	1/3	1/2	1	2	3	4	5
1646-1785	1/6	1/5	1/4	1/3	1/2	1	2	3	4
1451-1646	1/7	1/6	1/5	1/4	1/3	1/2	1	2	3
1239-1451	1/8	1/7	1/6	1/5	1/4	1/3	1/2	1	2
807-1239	1/9	1/8	1/7	1/6	1/5	1/4	1/3	1/2	1
Sum	**2.83**	**4.72**	**7.59**	**11.45**	**16.28**	**22.08**	**28.83**	**36.50**	**45.00**

Calculating Consistency

C.W	**0.3070**	**0.2182**	**0.1543**	**0.1089**	**0.0764**	**0.0533**	**0.0370**	**0.0259**	**0.0189**	**Weighted sum value**	**Criteria Weight**	**WSV/CW**
Factors	**2401-2783**	**2234-2401**	**2077-2234**	**1922-2077**	**1785-19922**	**1646-1785**	**1451-1646**	**1239-1451**	**807-1239**			
2401-2783	0.3070	0.4364	0.4630	0.4355	0.3822	0.3199	0.2592	0.2076	0.1702	2.9809	0.307	9.71
2234-2401	0.1535	0.2182	0.3086	0.3266	0.3058	0.2665	0.2222	0.1816	0.1513	2.1344	0.218	9.78
2077-2234	0.1023	0.1091	0.1543	0.2178	0.2293	0.2132	0.1851	0.1557	0.1324	1.4993	0.154	9.72
1922-2077	0.0767	0.0727	0.0772	0.1089	0.1529	0.1599	0.1481	0.1297	0.1135	1.0397	0.109	9.55
1785-19922	0.0614	0.0546	0.0514	0.0544	0.0764	0.1066	0.1111	0.1038	0.0946	0.7143	0.076	9.34
1646-1785	0.0512	0.0436	0.0386	0.0363	0.0382	0.0533	0.0741	0.0778	0.0757	0.4888	0.053	9.17
1451-1646	0.0439	0.0364	0.0309	0.0272	0.0255	0.0267	0.0370	0.0519	0.0567	0.3361	0.037	9.08
1239-1451	0.0384	0.0312	0.0257	0.0218	0.0191	0.0178	0.0185	0.0259	0.0378	0.2362	0.026	9.10
807-1239	0.0341	0.0273	0.0220	0.0181	0.0153	0.0133	0.0123	0.0130	0.0189	0.1744	0.019	9.22
											λmax=	**9.41**

APPENDIX

Normalized Pair-wise Comparison Matrix

Factors	2401-2783	2234-2401	2077-2234	1922-2077	1785-19922	1646-1785	1451-1646	1239-1451	807-1239	Sum	Criteria Weights
2401-2783	0.353	0.424	0.395	0.349	0.307	0.272	0.243	0.219	0.200	**2.7626**	**0.307**
2234-2401	0.177	0.212	0.263	0.262	0.246	0.226	0.208	0.192	0.178	**1.9638**	**0.218**
2077-2234	0.118	0.106	0.132	0.175	0.184	0.181	0.173	0.164	0.156	**1.3889**	**0.154**
1922-2077	0.088	0.071	0.066	0.087	0.123	0.136	0.139	0.137	0.133	**0.9799**	**0.109**
1785-19922	0.071	0.053	0.044	0.044	0.061	0.091	0.104	0.110	0.111	**0.6880**	**0.076**
1646-1785	0.059	0.042	0.033	0.029	0.031	0.045	0.069	0.082	0.089	**0.4798**	**0.053**
1451-1646	0.050	0.035	0.026	0.022	0.020	0.023	0.035	0.055	0.067	**0.3333**	**0.037**
1239-1451	0.044	0.030	0.022	0.017	0.015	0.015	0.017	0.027	0.044	**0.2335**	**0.026**
807-1239	0.039	0.026	0.019	0.015	0.012	0.011	0.012	0.014	0.022	**0.1702**	**0.019**
Sum	**1.00**	**1.00**	**1.00**	**1.00**	**1.00**	**1.00**	**1.00**	**1.00**	**1.00**	**9.00**	**1.00**

λmax = 9.408

λmax-n = 0.408

n-1 = 8

RI =1.45

CI = 0.051

CR = 0.034

OK!!!

AHP Table for Land Use Land Cover

Pair-wise Comparison Matrix

Land Use cover	Bare land	Settlement	Crops	Vegetation	Water Body
Bare land	1	3	5	7	9
Settlement	1/3	1	3	5	7
Crops	1/5	1/3	1	3	5
Vegetation	1/7	1/5	1/3	1	3
Water Body	1/9	1/7	1/5	1/3	1
Sum	**1.79**	**4.68**	**9.53**	**16.33**	**25.00**

Calculating Consistency

C.W	0.5028	0.2602	0.1344	0.0678	0.0348	Weighted sum value	Criteria Weight	WSV/CW
Bare land	**Bare land**	**Settlement**	**Crops**	**Vegetation**	**Water Body**			
Settlement	0.5028	0.7807	0.6718	0.4744	0.3134	2.7431	0.503	5.46
Crops	0.1676	0.2602	0.4031	0.3389	0.2437	1.4135	0.260	5.43
Vegetation	0.1006	0.0867	0.1344	0.2033	0.1741	0.6991	0.134	5.20
Water Body	0.0718	0.0520	0.0448	0.0678	0.1045	0.3409	0.068	5.03
Bare land	0.0559	0.0372	0.0269	0.0226	0.0348	0.1773	0.035	5.09
							λmax=	**5.24**

Normalized Pair-wise Comparison Matrix

Factors	Bare land	Settlement	Crops	Vegetation	Water Body	Sum	Criteria Weights
Bare land	0.560	0.642	0.524	0.429	0.360	2.5141	0.503
Settlement	0.187	0.214	0.315	0.306	0.280	1.3012	0.260
Crops	0.112	0.071	0.105	0.184	0.200	0.6718	0.134
Vegetation	0.080	0.043	0.035	0.061	0.120	0.3389	0.068
Water Body	0.062	0.031	0.021	0.020	0.040	0.1741	0.035
Sum	**1.00**	**1.00**	**1.00**	**1.00**	**1.00**	**5.00**	**1.00**

λmax = 5.243 λmax-n = 0.243 n-1 = 4 RI = 1.12 CI = 0.061 CR = 0.040	**OK!!!**

APPENDIX

AHP Table for Slope Aspect

Pair-wise Comparison Matrix

Factors	**Northwest**	**West**	**Southwest**	**North**	**South**	**Southeast**	**East**	**Northeast**	**Flat**
Northwest	1	1	3	4	5	6	7	7	9
West	1	1	2	3	4	5	6	6	8
Southwest	1/3	1	1	2	3	4	5	5	7
North	1/4	1/3	1/2	1	2	3	4	4	6
South	1/5	1/4	1/3	1/2	1	2	3	3	5
Southeast	1/6	1/5	1/4	1/3	1/2	1	2	2	4
East	1/7	1/6	1/5	1/4	1/3	1/2	1	1	3
Northeast	1/7	1/6	1/5	1/4	1/3	1/2	1	1	3
Flat	1/9	1/8	1/7	1/6	1/5	1/4	1/3	1/3	1
Sum	**3.35**	**3.74**	**7.63**	**11.50**	**16.37**	**22.25**	**29.33**	**29.33**	**46.00**

Calculating Consistency

C.W	**0.2839**	**0.2379**	**0.1549**	**0.1085**	**0.0753**	**0.0515**	**0.0346**	**0.0346**	**0.0186**	**Weighted sum value**	**Criteria Weight**	**WSV / CW**
Factors	**Northwest**	**West**	**Southwest**	**North**	**South**	**Southeast**	**East**	**Northeast**	**Flat**			
Northwest	0.2839	0.2379	0.4648	0.4340	0.3767	0.3092	0.2422	0.2422	0.1678	2.7587	0.2839	9.72
West	0.2839	0.2379	0.3099	0.3255	0.3013	0.2577	0.2076	0.2076	0.1491	2.2806	0.2379	9.59
Southwest	0.0946	0.1190	0.1549	0.2170	0.2260	0.2061	0.1730	0.1730	0.1305	1.4942	0.1549	9.64
North	0.0710	0.0793	0.0775	0.1085	0.1507	0.1546	0.1384	0.1384	0.1118	1.0302	0.1085	9.49
South	0.0568	0.0595	0.0516	0.0542	0.0753	0.1031	0.1038	0.1038	0.0932	0.7014	0.0753	9.31
Southeast	0.0473	0.0476	0.0387	0.0362	0.0377	0.0515	0.0692	0.0692	0.0746	0.4720	0.0515	9.16
East	0.0406	0.0397	0.0310	0.0271	0.0251	0.0258	0.0346	0.0346	0.0559	0.3143	0.0346	9.08

APPENDIX

Northeast	0.0406	0.0397	0.0310	0.0271	0.0251	0.0258	0.0346	0.0346	0.0559	0.3143	0.0346	9.08
Flat	0.0315	0.0297	0.0221	0.0181	0.0151	0.0129	0.0115	0.0115	0.0186	0.1712	0.0186	9.18
										λmax=	**9.36**

Normalized Pair-wise Comparison Matrix

Factors	**Northwest**	**West**	**Southwest**	**North**	**South**	**Southeast**	**East**	**Northeast**	**Flat**	**Sum**	**Criteria Weights**
Northwest	0.299	0.267	0.393	0.348	0.305	0.270	0.239	0.239	0.196	2.5553	0.284
West	0.299	0.267	0.262	0.261	0.244	0.225	0.205	0.205	0.174	2.1413	0.238
Southwest	0.100	0.134	0.131	0.174	0.183	0.180	0.170	0.170	0.152	1.3944	0.155
North	0.075	0.089	0.066	0.087	0.122	0.135	0.136	0.136	0.130	0.9765	0.108
South	0.060	0.067	0.044	0.043	0.061	0.090	0.102	0.102	0.109	0.6780	0.075
Southeast	0.050	0.053	0.033	0.029	0.031	0.045	0.068	0.068	0.087	0.4638	0.052
East	0.043	0.045	0.026	0.022	0.020	0.022	0.034	0.034	0.065	0.3114	0.035
Northeast	0.043	0.045	0.026	0.022	0.020	0.022	0.034	0.034	0.065	0.3114	0.035
Flat	0.033	0.033	0.019	0.014	0.012	0.011	0.011	0.011	0.022	0.1678	0.019
Sum	**1.00**	**1.00**	**1.00**	**1.00**	**1.00**	**1.00**	**1.00**	**1.00**	**1.00**	**9.00**	**1.00**

λmax = 9.362
λmax-n = 0.362
n-1 = 8
RI = 1.45
CI = 0.045

OK!!!

APPENDIX

CR = 0.030

AHP Table for Slope

Pair-wise Comparison Matrix

Slope Angle	48-75	39-48	32-39	27-32	20-27	14-20	9-14	5-9	0-5
48-75	1	2	3	4	5	6	7	8	9
39-48	1/2	1	2	3	4	5	6	7	8
32-39	1/3	1	1	2	3	4	5	6	7
27-32	1/4	1/3	1/2	1	2	3	4	5	6
20-27	1/5	1/4	1/3	1/2	1	2	3	4	5
14-20	1/6	1/5	1/4	1/3	1/2	1	2	3	4
9-14	1/7	1/6	1/5	1/4	1/3	1/2	1	2	3
5-9	1/8	0	1/6	1/5	1/4	1/3	1	1	2
0-5	1/9	1/8	1/7	1/6	1/5	1/4	1/3	1/2	1
Sum	**2.83**	**4.72**	**7.59**	**11.45**	**16.28**	**22.08**	**28.83**	**36.50**	**45.00**

Calculating Consistency

C.W	0.31	0.22	0.15	0.11	0.08	0.05	0.04	0.03	0.02	Weighted sum value	Criteria Weight	WSV/CW
Factors	**48-75**	**39-48**	**32-39**	**27-32**	**20-27**	**14-20**	**9-14**	**5-9**	**0-5**			
48-75	0.31	0.44	0.46	0.44	0.38	0.32	0.26	0.21	0.17	2.98	0.31	9.71
39-48	0.15	0.22	0.31	0.33	0.31	0.27	0.22	0.18	0.15	2.13	0.22	9.78
32-39	0.10	0.11	0.15	0.22	0.23	0.21	0.19	0.16	0.13	1.50	0.15	9.72
27-32	0.08	0.07	0.08	0.11	0.15	0.16	0.15	0.13	0.11	1.04	0.11	9.55
20-27	0.06	0.05	0.05	0.05	0.08	0.11	0.11	0.10	0.09	0.71	0.08	9.34

APPENDIX

14-20	0.05	0.04	0.04	0.04	0.04	0.05	0.07	0.08	0.08	0.49	0.05	9.17
9-14	0.04	0.04	0.03	0.03	0.03	0.03	0.04	0.05	0.06	0.34	0.04	9.08
5-9	0.04	0.03	0.03	0.02	0.02	0.02	0.02	0.03	0.04	0.24	0.03	9.10
0-5	0.03	0.03	0.02	0.02	0.02	0.01	0.01	0.01	0.02	0.17	0.02	9.22
											λmax=	**9.41**

Normalized Pair-wise Comparison Matrix

Factors	**48-75**	**39-48**	**32-39**	**27-32**	**20-27**	**14-20**	**9-14**	**5-9**	**0-5**	**Sum**	**Criteria Weights**
48-75	0.35	0.42	0.40	0.35	0.31	0.27	0.24	0.22	0.20	2.76	0.31
39-48	0.18	0.21	0.26	0.26	0.25	0.23	0.21	0.19	0.18	1.96	0.22
32-39	0.12	0.11	0.13	0.17	0.18	0.18	0.17	0.16	0.16	1.39	0.15
27-32	0.09	0.07	0.07	0.09	0.12	0.14	0.14	0.14	0.13	0.98	0.11
20-27	0.07	0.05	0.04	0.04	0.06	0.09	0.10	0.11	0.11	0.69	0.08
14-20	0.06	0.04	0.03	0.03	0.03	0.05	0.07	0.08	0.09	0.48	0.05
9-14	0.05	0.04	0.03	0.02	0.02	0.02	0.03	0.05	0.07	0.33	0.04
5-9	0.04	0.03	0.02	0.02	0.02	0.02	0.02	0.03	0.04	0.23	0.03
0-5	0.04	0.03	0.02	0.01	0.01	0.01	0.01	0.01	0.02	0.17	0.02
Sum	**1.00**	**1.00**	**1.00**	**1.00**	**1.00**	**1.00**	**1.00**	**1.00**	**1.00**	**9.00**	**1.00**

λmax = 9.41
λmax-n = 0.41
n-1 = 8.00
RI = 1.45
CI = 0.05

OK!!!

APPENDIX

CR = 0.03	

AHP Table for Lithology

Pair-wise Comparison Matrix					
Lithology	**Orthic Acrisols**	**Dystric Fluvisols**	**Calcic Fluvisols**	**Calciic Cambisols**	**Dystric Nitisols**
Orthic Acrisols	1	3	5	9	7
Dystric Fluvisols	1/3	1	3	7	5
Calcic Fluvisols	1/5	0	1	5	3
Calciic Cambisols	1/9	1/7	1/5	1	1/3
Dystric Nitisols	1/7	1/5	1/3	3	1
Sum	**1.79**	**4.68**	**9.53**	**25.00**	**16.33**

Calculating Consistency								
C.W	**0.5028**	**0.2602**	**0.1344**	**0.0348**	**0.0678**	**Weighted sum value**	**Criteria Weight**	**WSV/CW**
Factors	**Orthic Acrisols**	**Dystric Fluvisols**	**Calcic Fluvisols**	**Calciic Cambisols**	**Dystric Nitisols**			
Orthic Acrisols	0.5028	0.7807	0.6718	0.3134	0.4744	2.7431	0.503	5.46
Dystric Fluvisols	0.1676	0.2602	0.4031	0.2437	0.3389	1.4135	0.260	5.43
Calcic Fluvisols	0.1006	0.0867	0.1344	0.1741	0.2033	0.6991	0.134	5.20
Calciic Cambisols	0.0559	0.0372	0.0269	0.0348	0.0226	0.1773	0.035	5.09
Dystric Nitisols	0.0718	0.0520	0.0448	0.1045	0.0678	0.3409	0.068	5.03
							λmax=	**5.24**

APPENDIX

Normalized Pair-wise Comparison Matrix							
Factors	**Orthic Acrisols**	**Dystric Fluvisols**	**Calcic Fluvisols**	**Calciic Cambisols**	**Dystric Nitisols**	**Sum**	**Criteria Weights**
Orthic Acrisols	0.560	0.642	0.524	0.360	0.429	**2.5141**	**0.503**
Dystric Fluvisols	0.187	0.214	0.315	0.280	0.306	**1.3012**	**0.260**
Calcic Fluvisols	0.112	0.071	0.105	0.200	0.184	**0.6718**	**0.134**
Calciic Cambisols:	0.062	0.031	0.021	0.040	0.020	**0.1741**	**0.035**
Dystric Nitisols:	0.080	0.043	0.035	0.120	0.061	**0.3389**	**0.068**
Sum	**1.00**	**1.00**	**1.00**	**1.00**	**1.00**	**5.00**	**1.00**

λmax = 5.243 λmax-n = 0.243 n-1 = 4 RI = 1.12 CI = 0.061 CR = 0.040	**OK!!!**

APPENDIX

AHP Table for Rainfall

Pair-wise Comparison Matrix				
Annual Averge Rainfall(mm)	**1689-1983**	**1395-1689**	**1101-1395**	**807-1101**
1689-1983	1	3	5	7
1395-1689	1/3	1	3	5
1101-1395	1/5	0	1	3
807-1101	1/7	1/5	1/3	1
Sum	**1.68**	**4.53**	**9.33**	**16.00**

Calculating Consistency							
C.W	**0.5579**	**0.2633**	**0.1219**	**0.0569**	**Weighted sum value**	**Criteria Weight**	**WSV/CW**
Factors	**1689-1983**	**1395-1689**	**1101-1395**	**807-1101**			
1689-1983	0.5579	0.7900	0.6094	0.3982	2.3555	0.558	4.22
1395-1689	0.1860	0.2633	0.3656	0.2844	1.0994	0.263	4.17
1101-1395	0.1116	0.0878	0.1219	0.1707	0.4919	0.122	4.04
807-1101	0.0797	0.0527	0.0406	0.0569	0.2299	0.057	4.04
						λmax=	**4.12**

Normalized Pair-wise Comparison Matrix						
Factors	**1689-1983**	**1395-1689**	**1101-1395**	**807-1101**	**Sum**	**Criteria Weights**
1689-1983	0.597	0.662	0.536	0.438	2.2316	0.558
1395-1689	0.199	0.221	0.321	0.313	1.0534	0.263
1101-1395	0.119	0.074	0.107	0.188	0.4875	0.122
807-1101	0.085	0.044	0.036	0.063	0.2276	0.057
Sum	**1.00**	**1.00**	**1.00**	**1.00**	**4.00**	**1.00**

λmax = 4.118 λmax-n = 0.118 n-1 = 2 RI = 1.12 CI = 0.059 CR = 0.039	**OK!!!**

APPENDIX

APPENDIX

APPENDIX B

ጎንድዋና ኢንጂነሪንግ ኃ.የተ.የግል ማኅበር Gondwana Engineering PLC.	**Title**	**Borehole Log Sheet**	
	Document No.: GT-F-006	**Revision No.** 0	**Effective Date:** 10/01/2013

Project: Gore-Masha-Tepi Road Project
Location: BH-14+260 RHS
Coordinates: UTM 36N, 777979E,890191N
Ground Elevation:
Drilling method: Rotary
Type of Rig: APA 550

BH No: BH-14+260 RHS
BH Inclination: 90°
Bit type: Carbide/Diamond
Borehole diameter (mm): 89mm
Core diameter (mm): 75mm
Date Started: May,15/2019

Total Depth: 13.00 m
Water Level: Nill
Sheet 1 of 1
Date Completed: May,16/2019

Core run (m)	Casing depth (m)	Core Recovery TCR (%)	Core Recovery RQD (%)	Core Recovery AFS (cm) (No.of Frac.)	Sampling	SPT (No of blows)
1.00		100				
2.00		100			▨	3,6,8
3.00		100			🟦	
4.50		100			▨	1,2,3
5.50		100			▨	6,12,13
6.25		100			🟦 ▨	10,15,19
7.50		100				
8.50		100			▨	10,33,50/13cm
10.00		100			UDR ▨	26/9cm
11.00		100			▨	30,50/14cm
12.00		100				
13.00		100			▨	42,50/10cm

Field Description of Soil/Rock

(0.0 - 0.3m)
grayish brown Silty CLAY, Fill Material

(0.3 - 3.0m)
Firm to stiff varigated Silty CLAY residual soil relicts of rock fabric

(3.0 - 13.0m)
Stiff to hard yellowish brwon Clayey SILT resdual soil with relicts of rock fabric

Core photographs
5.00
10.00
13.00

Client: Ethiopian Roads Authority (ERA)
Consultant:
Contractor: HDC Korea
Sub Contractor: Gondwana Engineering Plc.
Logged by: Birhanu W.
Approved by: Zerihun Nuru

▨ (D)Disturbed Sample
🟦 (UD)Undisturbed Sample
🟧 (RC) Rock Core Sample

Site Photograph

APPENDIX

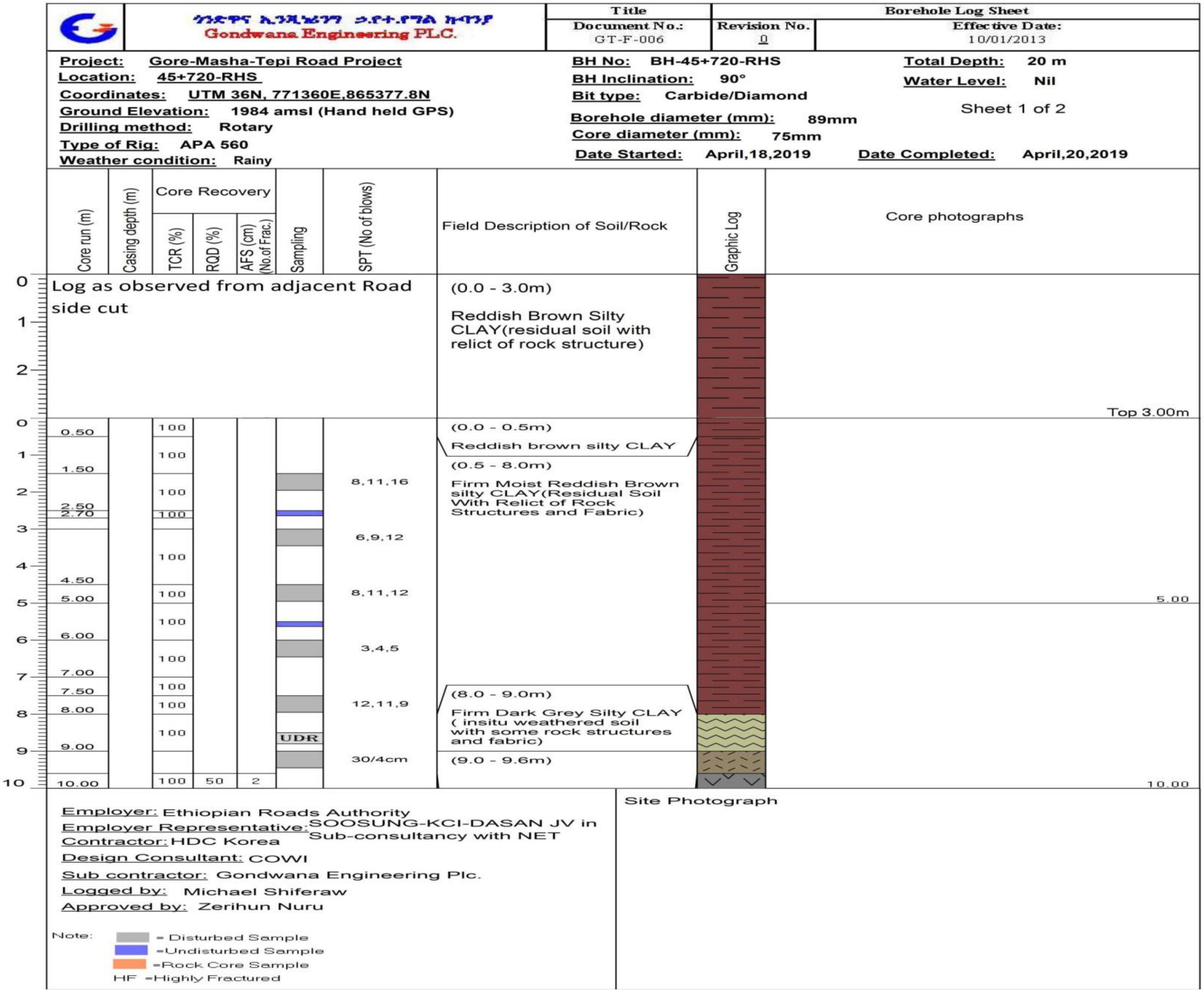

ጎንድዋና ኢንጂነሪንግ ኃ.የተ.የግል ኩባንያ
Gondwana Engineering PLC.

Title	Borehole Log Sheet	
Document No.: GT-F-006	Revision No. 0	Effective Date: 10/01/2013

Project: Gore-Masha-Tepi Road Project
Location: 45+720-RHS
Coordinates: UTM 36N, 771360E,865377.8N
Ground Elevation: 1984 amsl (Hand held GPS)
Drilling method: Rotary
Type of Rig: APA 560
Weather condition: Rainy

BH No: BH-45+720-RHS
BH Inclination: 90°
Bit type: Carbide/Diamond
Borehole diameter (mm): 89mm
Core diameter (mm): 75mm
Date Started: April,18,2019

Total Depth: 20 m
Water Level: Nil
Sheet 1 of 2
Date Completed: April,20,2019

Log as observed from adjacent Road side cut

(0.0 - 3.0m)
Reddish Brown Silty CLAY(residual soil with relict of rock structure)

Core run (m)	Casing depth (m)	Core Recovery TCR (%)	RQD (%)	AFS (cm) (No.of Frac.)	Sampling	SPT (No of blows)	Field Description of Soil/Rock
0.50		100					(0.0 - 0.5m) Reddish brown silty CLAY
1.50		100					(0.5 - 8.0m) Firm Moist Reddish Brown silty CLAY(Residual Soil With Relict of Rock Structures and Fabric)
2.50		100			▨	8,11,16	
2.70		100			🟦		
4.50		100			▨	6,9,12	
5.00		100			▨	8,11,12	
6.00		100			🟦		
7.00		100			▨	3,4,5	
7.50		100					
8.00		100			▨	12,11,9	
9.00		100			UDR		(8.0 - 9.0m) Firm Dark Grey Silty CLAY (insitu weathered soil with some rock structures and fabric)
					▨	30/4cm	(9.0 - 9.6m)
10.00		100	50	2			

Core photographs
Top 3.00m
5.00
10.00

Employer: Ethiopian Roads Authority
Employer Representative: SOOSUNG-KCI-DASAN JV in Sub-consultancy with NET
Contractor: HDC Korea
Design Consultant: COWI
Sub contractor: Gondwana Engineering Plc.
Logged by: Michael Shiferaw
Approved by: Zerihun Nuru

Note: ▨ = Disturbed Sample
🟦 =Undisturbed Sample
🟧 =Rock Core Sample
HF =Highly Fractured

Site Photograph

APPENDIX

ጎንድዋና ኢንጂነሪንግ ኃ.የተ.የግል ኩባንያ
Gondwana Engineering PLC.

Title	Borehole Log Sheet	
Document No.: GT-F-006	Revision No. 0	Effective Date: 10/01/2013

Project: Gore-Masha-Tepi Road Project
Location: 45+720-RHS
Coordinates: UTM 36N, 771360E,865377.8N
Ground Elevation: 1984 amsl (Hand held GPS)
Drilling method: Rotary
Type of Rig: APA 560
Weather condition: Rainy

BH No: BH-45+720-RHS
BH Inclination: 90°
Bit type: Carbide/Diamond
Borehole diameter (mm): 89mm
Core diameter (mm): 75mm
Date Started: April,18,2019
Date Completed: April,20,2019

Total Depth: 20 m
Water Level: Nil
Sheet 2 of 2

Depth	Core run (m)	Casing depth (m)	Core Recovery TCR (%)	Core Recovery RQD (%)	Core Recovery AFS (cm) (No.of Frac.)	Sampling	SPT (No of blows)	Core photographs
10								
11	11.00		100	58	14	🟧		
12	12.00		100	22	8			
13	13.00		100	30	10			
14	14.00		100	62	17	🟧		
15	15.00		100	43	20			15.00
16	16.00		100	38	13			
17	17.00		100	47	7			
18	18.00		100	95	50	🟧		
19	19.00		100	78	17			
20	20.00		100	86	25			20.00

Field Description of Soil/Rock

(9.0-9.6m)

Medium Strong fine Grained Dark Grey partially weathered very closely jointed Aphanitic BASALT

(9.6 - 20.0m)

Strong fine Grained Dark Grey Fresh closely jointed Aphanitic BASALT with some thin cracks. joints has nearly horizontal orientation

Graphic Log

Employer: Ethiopian Roads Authority
Employer Representative: SOOSUNG-KCI-DASAN JV in Sub-consultancy with NET
Contractor: HDC Korea
Design Consultant: COWI
Sub contractor: Gondwana Engineering Plc.
Logged by: Michael Shiferaw
Approved by: Zerihun Nuru

Site Photograph

Note:
▨ = Disturbed Sample
🟦 =Undisturbed Sample
🟧 =Rock Core Sample
HF =Highly Fractured

APPENDIX

Table B- 1 Broad Summary of sub surface material BH-45+720-RHS to BH-46+700-LHS

Layer No	Description	Depth occurrence(m)					SPT N 30	Lab Result				
		BH-45+720-RHS	BH-45+980-RHS	BH-46+260-RHS	BH-46+460-RHS	BH-46+700-LHS		LL%	PI%	%pass 0.075 mm	USCS	UCS (Rock) Mpa
1	Firm to stiff moist reddish brown and variegated silty CLAY. (Residual soil with relict of rock structure and fabric)	0.00 - 9.00	0.00 - 12.30	0.00 - 14.00	0.00 - 3.50	0.00 - 11.50	7-56	39-88	6-38	53-100	MH,ML	
2	Very weak to weak light grey to reddish grey closely to very closely jointed highly to moderately weathered BASALT. Joints are nearly horizontal. due degree of weathering this layer decomposes to light to reddish grey stiff to very stiff silty CLAY at BH-46+260-RHS	9.00 - 9.60	12.30 - 13.30	14.00 - 30.00	15.50 - 25.50	18.30 - 20.00	30->50	60-97	26-48	55-97	MH	
3	Medium strong dark grey closely to very closely fractured BASALT. Generally joints are nearly horizontal. Top 7m is highly fractured with CLAY gauges (infillings) at BH-46+460-RHS	9.60 - 20.00	13.30 - 18.60	-	3.50 - 5.50 & 25.50 -27.00	11.50 - 18.30	-	-	-	-	-	26-136

Figure B-22 summary of field SPT Value BH-46+700-BH-45+720

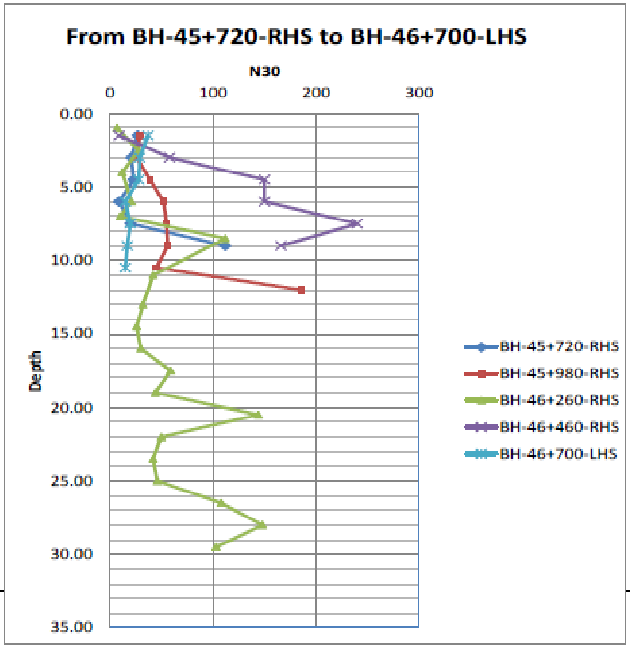

APPENDIX

Figure B- 2 Geotechnical Diagram Show

Project	Gore-Masha Tepi Road Project		
BH #	BH-45+720-RHS		
Easting	771360.2	Ground water level	
Northing	865377.8	Nil	
Elevation (m)	1984(Hand GPS)		

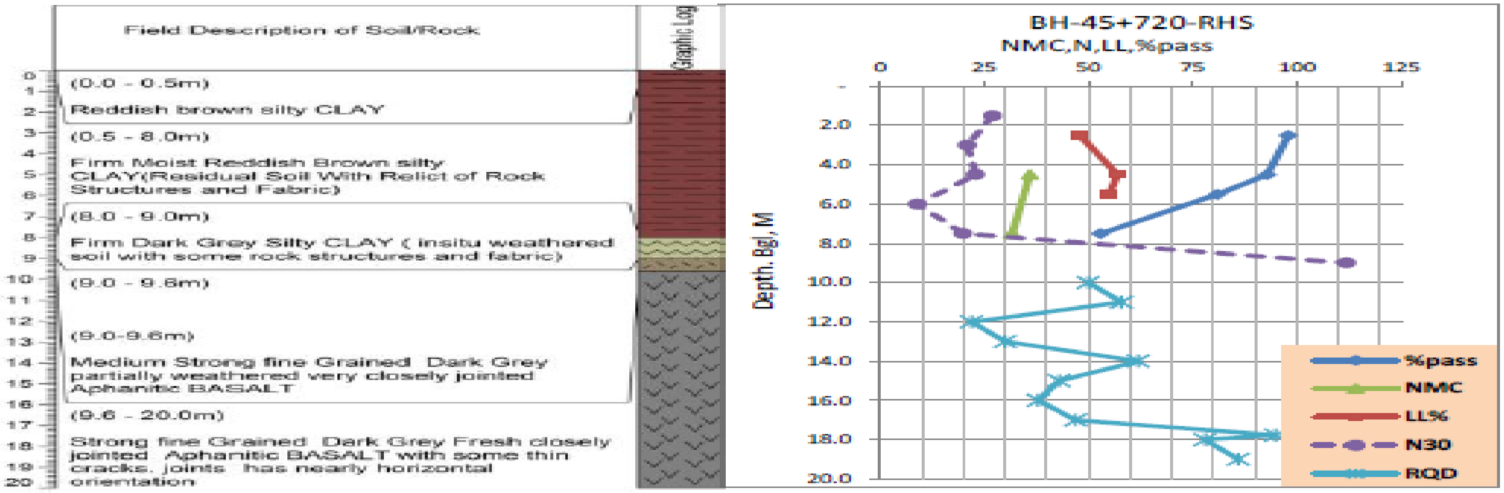

(0.0 - 0.5m)
Reddish brown silty CLAY

(0.5 - 8.0m)
Firm Moist Reddish Brown silty CLAY(Residual Soil With Relict of Rock Structures and Fabric)

(8.0 - 9.0m)
Firm Dark Grey Silty CLAY (insitu weathered soil with some rock structures and fabric)

(9.0 - 9.6m)

(9.0-9.6m)
Medium Strong fine Grained Dark Grey partially weathered very closely jointed Aphanitic BASALT

(9.6 - 20.0m)
Strong fine Grained Dark Grey Fresh closely jointed Aphanitic BASALT with some thin cracks. joints has nearly horizontal orientation

BH# 45+720-RHS Summary of Geotechnical Properties of site formations

Depth, M		N 30	NMC %	%Pass, 0.075mm	LL	PL	PI	LI	USCS	Direct shear		Rock Quality Indicator		
										C (Kpa)	ø Degree	RQD	AFS	UCS Mpa
1.50	1.95	27												
2.50	2.64			98	48	36	12		ML					
3.00	3.45	21												
4.50	4.95	23	36	93	57	42	15	-0.4	MH					
5.50	5.63			81	55	41	14		MH	8	5			
6.00	6.45	9												
7.50	7.95	20	32	53	NP				SC					
9.00	9.15	112												
9.60	10.00													136
10.00	11.00											50	2	
10.30	10.48													10
11.00	12.00											58	14	
12.00	13.00											22	8	
13.00	13.19													
13.00	14.00											30	10	
14.00	15.00											62	17	
15.00	16.00											43	20	
16.00	17.00											38	13	
17.00	18.00											47	7	
17.77	18.00											95	50	
18.00	19.00											78	17	
19.00	20.00											86	25	

APPENDIX

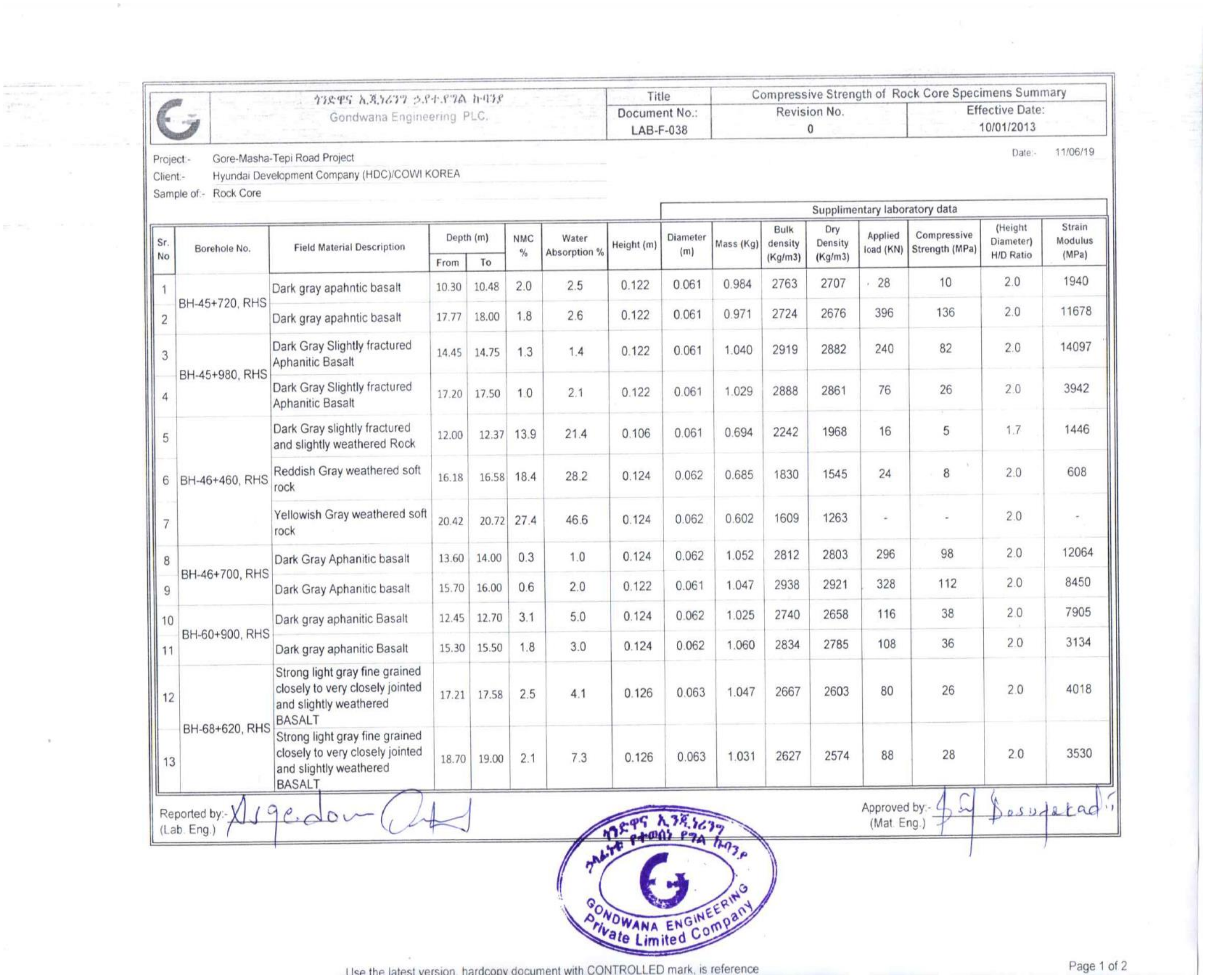

ጎንድዋና ኢ.ጂ.ነሪንግ ኃ.የተ.የግል ኩባንያ Gondwana Engineering PLC.	Title	Compressive Strength of Rock Core Specimens Summary	
	Document No.: LAB-F-038	Revision No. 0	Effective Date: 10/01/2013

Date:- 11/06/19

Project:- Gore-Masha-Tepi Road Project
Client:- Hyundai Development Company (HDC)/COWI KOREA
Sample of:- Rock Core

Supplimentary laboratory data

Sr. No	Borehole No.	Field Material Description	Depth (m)		NMC %	Water Absorption %	Height (m)	Diameter (m)	Mass (Kg)	Bulk density (Kg/m3)	Dry Density (Kg/m3)	Applied load (KN)	Compressive Strength (MPa)	(Height Diameter) H/D Ratio	Strain Modulus (MPa)
			From	To											
1	BH-45+720, RHS	Dark gray apahntic basalt	10.30	10.48	2.0	2.5	0.122	0.061	0.984	2763	2707	28	10	2.0	1940
2		Dark gray apahntic basalt	17.77	18.00	1.8	2.6	0.122	0.061	0.971	2724	2676	396	136	2.0	11678
3	BH-45+980, RHS	Dark Gray Slightly fractured Aphanitic Basalt	14.45	14.75	1.3	1.4	0.122	0.061	1.040	2919	2882	240	82	2.0	14097
4		Dark Gray Slightly fractured Aphanitic Basalt	17.20	17.50	1.0	2.1	0.122	0.061	1.029	2888	2861	76	26	2.0	3942
5	BH-46+460, RHS	Dark Gray slightly fractured and slightly weathered Rock	12.00	12.37	13.9	21.4	0.106	0.061	0.694	2242	1968	16	5	1.7	1446
6		Reddish Gray weathered soft rock	16.18	16.58	18.4	28.2	0.124	0.062	0.685	1830	1545	24	8	2.0	608
7		Yellowish Gray weathered soft rock	20.42	20.72	27.4	46.6	0.124	0.062	0.602	1609	1263	-	-	2.0	-
8	BH-46+700, RHS	Dark Gray Aphanitic basalt	13.60	14.00	0.3	1.0	0.124	0.062	1.052	2812	2803	296	98	2.0	12064
9		Dark Gray Aphanitic basalt	15.70	16.00	0.6	2.0	0.122	0.061	1.047	2938	2921	328	112	2.0	8450
10	BH-60+900, RHS	Dark gray aphanitic Basalt	12.45	12.70	3.1	5.0	0.124	0.062	1.025	2740	2658	116	38	2.0	7905
11		Dark gray aphanitic Basalt	15.30	15.50	1.8	3.0	0.124	0.062	1.060	2834	2785	108	36	2.0	3134
12	BH-68+620, RHS	Strong light gray fine grained closely to very closely jointed and slightly weathered BASALT	17.21	17.58	2.5	4.1	0.126	0.063	1.047	2667	2603	80	26	2.0	4018
13		Strong light gray fine grained closely to very closely jointed and slightly weathered BASALT	18.70	19.00	2.1	7.3	0.126	0.063	1.031	2627	2574	88	28	2.0	3530

Reported by:-
(Lab. Eng.)

Approved by:-
(Mat. Eng.)

Use the latest version, hardcopy document with CONTROLLED mark, is reference

Page 1 of 2

APPENDIX

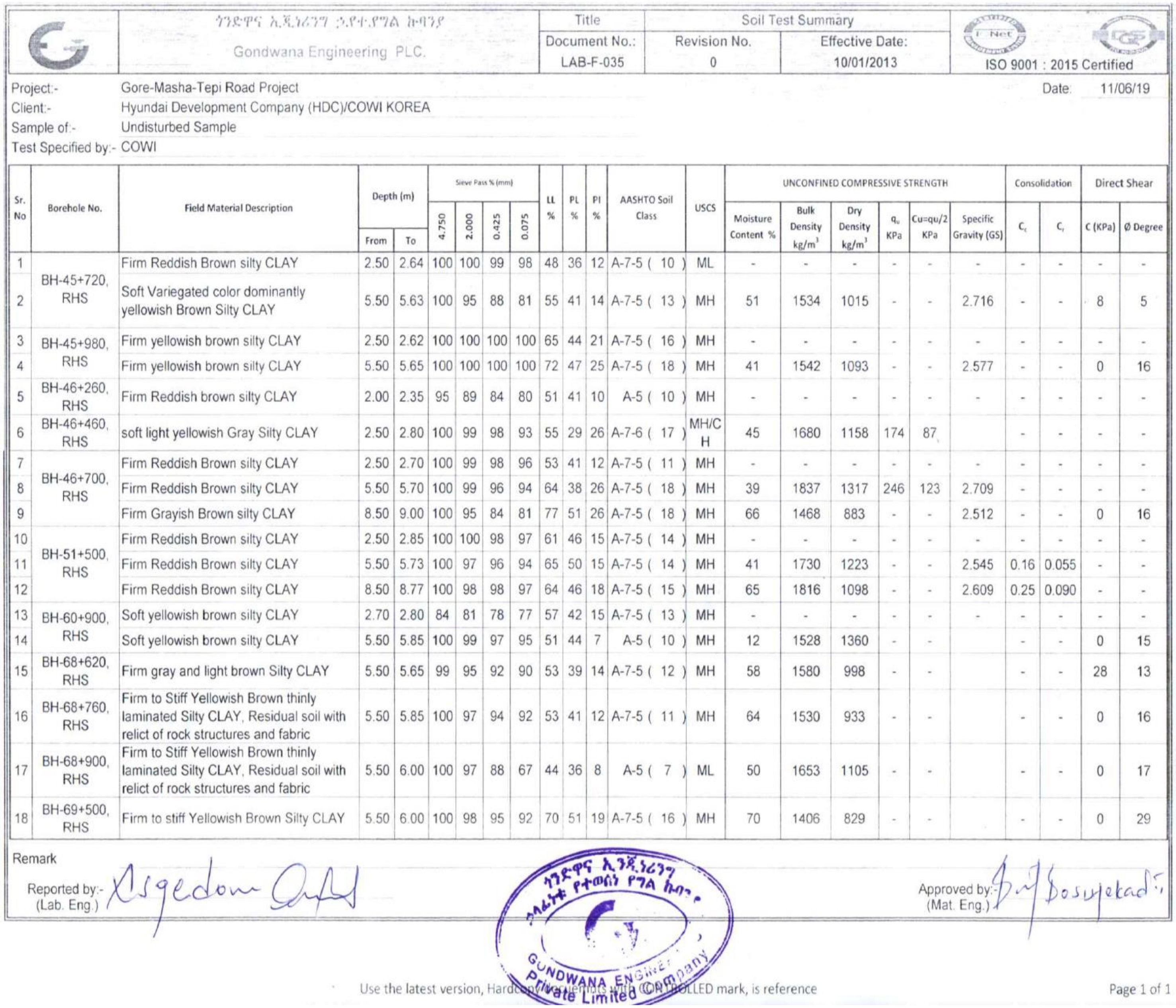

ጎንድዋና ኢንጂነሪንግ ኃ.የተ.የግል ኩባንያ
Gondwana Engineering PLC.

Title	Soil Test Summary	
Document No.: LAB-F-035	Revision No. 0	Effective Date: 10/01/2013

ISO 9001 : 2015 Certified

Project:- Gore-Masha-Tepi Road Project
Date: 11/06/19
Client:- Hyundai Development Company (HDC)/COWI KOREA
Sample of:- Undisturbed Sample
Test Specified by:- COWI

Sr. No	Borehole No.	Field Material Description	Depth (m)		Sieve Pass % (mm)				LL %	PL %	PI %	AASHTO Soil Class	USCS	UNCONFINED COMPRESSIVE STRENGTH						Consolidation		Direct Shear	
			From	To	4.750	2.000	0.425	0.075						Moisture Content %	Bulk Density kg/m³	Dry Density kg/m³	q_u KPa	Cu=qu/2 KPa	Specific Gravity (GS)	C_c	C_r	C (KPa)	Ø Degree
1	BH-45+720, RHS	Firm Reddish Brown silty CLAY	2.50	2.64	100	100	99	98	48	36	12	A-7-5 (10)	ML	-	-	-	-	-	-	-	-	-	-
2		Soft Variegated color dominantly yellowish Brown Silty CLAY	5.50	5.63	100	95	88	81	55	41	14	A-7-5 (13)	MH	51	1534	1015	-	-	2.716	-	-	8	5
3	BH-45+980, RHS	Firm yellowish brown silty CLAY	2.50	2.62	100	100	100	100	65	44	21	A-7-5 (16)	MH	-	-	-	-	-	-	-	-	-	-
4		Firm yellowish brown silty CLAY	5.50	5.65	100	100	100	100	72	47	25	A-7-5 (18)	MH	41	1542	1093	-	-	2.577	-	-	0	16
5	BH-46+260, RHS	Firm Reddish brown silty CLAY	2.00	2.35	95	89	84	80	51	41	10	A-5 (10)	MH	-	-	-	-	-	-	-	-	-	-
6	BH-46+460, RHS	soft light yellowish Gray Silty CLAY	2.50	2.80	100	99	98	93	55	29	26	A-7-6 (17)	MH/CH	45	1680	1158	174	87		-	-	-	-
7	BH-46+700, RHS	Firm Reddish Brown silty CLAY	2.50	2.70	100	99	98	96	53	41	12	A-7-5 (11)	MH	-	-	-	-	-	-	-	-	-	-
8		Firm Reddish Brown silty CLAY	5.50	5.70	100	99	96	94	64	38	26	A-7-5 (18)	MH	39	1837	1317	246	123	2.709	-	-	-	-
9		Firm Grayish Brown silty CLAY	8.50	9.00	100	95	84	81	77	51	26	A-7-5 (18)	MH	66	1468	883	-	-	2.512	-	-	0	16
10	BH-51+500, RHS	Firm Reddish Brown silty CLAY	2.50	2.85	100	100	98	97	61	46	15	A-7-5 (14)	MH	-	-	-	-	-	-	-	-	-	-
11		Firm Reddish Brown silty CLAY	5.50	5.73	100	97	96	94	65	50	15	A-7-5 (14)	MH	41	1730	1223	-	-	2.545	0.16	0.055	-	-
12		Firm Reddish Brown silty CLAY	8.50	8.77	100	98	98	97	64	46	18	A-7-5 (15)	MH	65	1816	1098	-	-	2.609	0.25	0.090	-	-
13	BH-60+900, RHS	Soft yellowish brown silty CLAY	2.70	2.80	84	81	78	77	57	42	15	A-7-5 (13)	MH	-	-	-	-	-	-	-	-	-	-
14		Soft yellowish brown silty CLAY	5.50	5.85	100	99	97	95	51	44	7	A-5 (10)	MH	12	1528	1360	-	-		-	-	0	15
15	BH-68+620, RHS	Firm gray and light brown Silty CLAY	5.50	5.65	99	95	92	90	53	39	14	A-7-5 (12)	MH	58	1580	998	-	-		-	-	28	13
16	BH-68+760, RHS	Firm to Stiff Yellowish Brown thinly laminated Silty CLAY, Residual soil with relict of rock structures and fabric	5.50	5.85	100	97	94	92	53	41	12	A-7-5 (11)	MH	64	1530	933	-	-		-	-	0	16
17	BH-68+900, RHS	Firm to Stiff Yellowish Brown thinly laminated Silty CLAY, Residual soil with relict of rock structures and fabric	5.50	6.00	100	97	88	67	44	36	8	A-5 (7)	ML	50	1653	1105	-	-		-	-	0	17
18	BH-69+500, RHS	Firm to stiff Yellowish Brown Silty CLAY	5.50	6.00	100	98	95	92	70	51	19	A-7-5 (16)	MH	70	1406	829	-	-		-	-	0	29

Remark

Reported by:- Asgedom
(Lab. Eng.)

Approved by:-
(Mat. Eng.)

Use the latest version, Hardcopy documents with CONTROLLED mark, is reference

APPENDIX

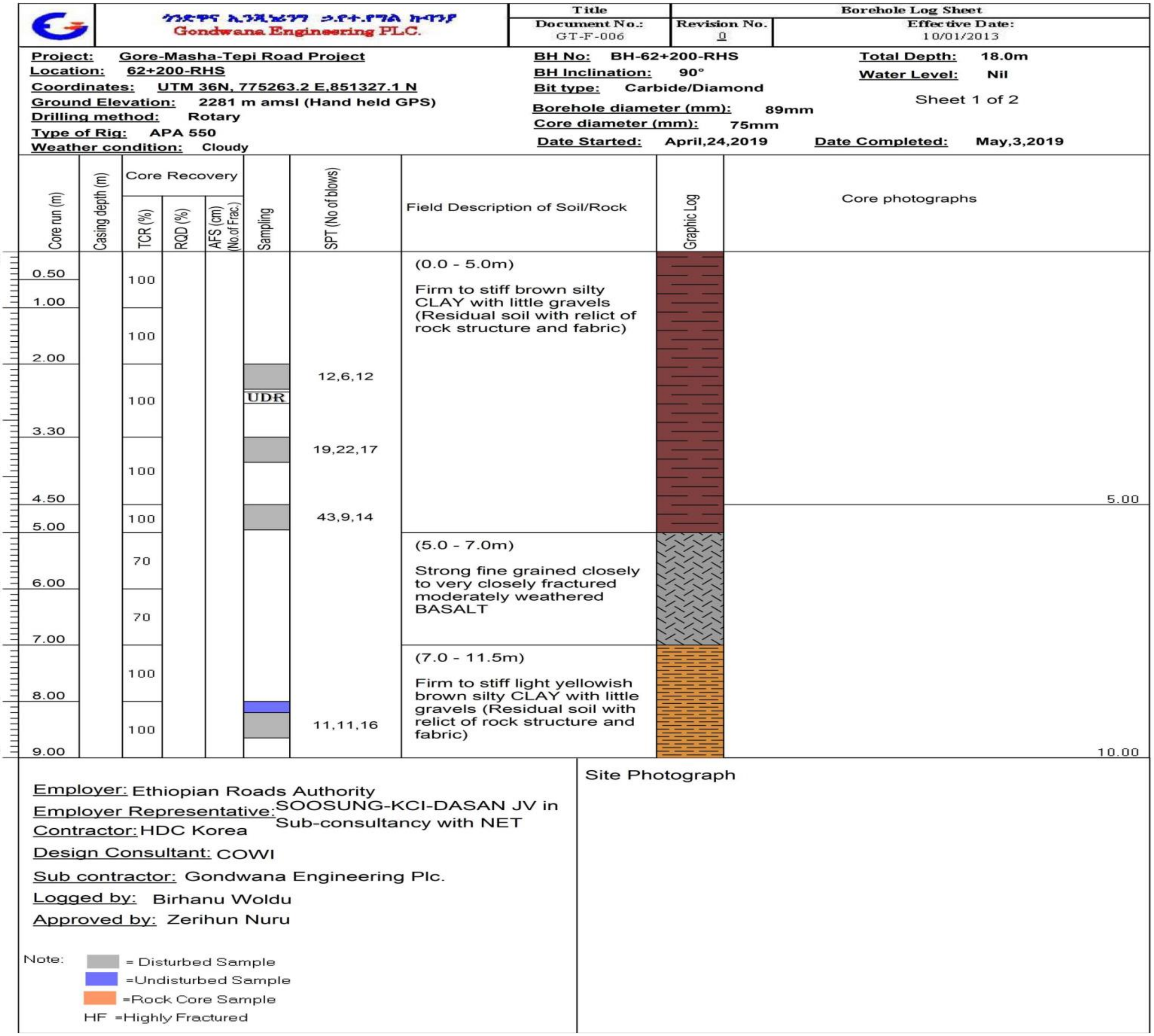

ጎንድዋና ኢንጂነሪንግ ኃ.የተ.የግል ኩባንያ
Gondwana Engineering PLC.

Title	Borehole Log Sheet	
Document No.: GT-F-006	Revision No. 0	Effective Date: 10/01/2013

Project: Gore-Masha-Tepi Road Project
Location: 62+200-RHS
Coordinates: UTM 36N, 775263.2 E,851327.1 N
Ground Elevation: 2281 m amsl (Hand held GPS)
Drilling method: Rotary
Type of Rig: APA 550
Weather condition: Cloudy

BH No: BH-62+200-RHS
BH Inclination: 90°
Bit type: Carbide/Diamond
Borehole diameter (mm): 89mm
Core diameter (mm): 75mm
Date Started: April,24,2019
Date Completed: May,3,2019

Total Depth: 18.0m
Water Level: Nil
Sheet 1 of 2

Core run (m)	Casing depth (m)	Core Recovery TCR (%)	Core Recovery RQD (%)	Core Recovery AFS (cm) (No.of Frac.)	Sampling	SPT (No of blows)
0.50						
1.00		100				
2.00		100				
3.30		100			▨ UDR	12,6,12
4.50		100			▨	19,22,17
5.00		100			▨	43,9,14
6.00		70				
7.00		70				
8.00		100				
9.00		100			■ ▨	11,11,16

Field Description of Soil/Rock

(0.0 - 5.0m)

Firm to stiff brown silty CLAY with little gravels (Residual soil with relict of rock structure and fabric)

(5.0 - 7.0m)

Strong fine grained closely to very closely fractured moderately weathered BASALT

(7.0 - 11.5m)

Firm to stiff light yellowish brown silty CLAY with little gravels (Residual soil with relict of rock structure and fabric)

Site Photograph

Employer: Ethiopian Roads Authority
Employer Representative: SOOSUNG-KCI-DASAN JV in Sub-consultancy with NET
Contractor: HDC Korea
Design Consultant: COWI
Sub contractor: Gondwana Engineering Plc.
Logged by: Birhanu Woldu
Approved by: Zerihun Nuru

Note:
▨ = Disturbed Sample
■ =Undisturbed Sample
▧ =Rock Core Sample
HF =Highly Fractured

APPENDIX

Project	Contractor	Sub Contractor	Consultant
GORE-MASHA-TEPI DEISIGN AND BUILD ROAD PROJECT GORE-MASHA-TEPI DEISIGN AND BUILD ROAD PROJECT	CCEGC	ELITE ENGINEERING WORKS CONSULTANT	

Location/Chainage: 81+0.60 (122M OFFSETRHS)	Drilling Method: Rotary	
Coordinates (E/N): 773533.56 837396.69	Core diameter (mm): 90 mm (0-20m)	Sheet: 1 of 1
Ground Elevation (masl.):	Casing type & depth: 110/90	BH Inclination: 90°
Borehole No.: BH-3	Date Started:	Bit type: Carbide/Diamond
Total Depth (m): 20	Date Completed:	Type of Rig: Conventional

Depth (m)	Core run	TCR (%)	SCR (%)	RQD (%)	AFS (cm)	Sample depth	Sample type	SPT	N	SPT graph N-value 30 40 50 60	Soil/Rock symbole	Soil/Rock description	Ground water level (m)
0	1.00	100									0.50	Fill material	
1	2.00	100				1.50 1.95	D	2,2,4	6			Yelowish brown, firm,silty Clay with some gravel	
2	3.00	100											2.00
3	4.00	100				3.00 3.45	D	3,4,5	9		4.00		
4	5.00	100				4.00 4.40	UD				5.00	Dark gray, soft to very, Clay soil	
5	6.00	100				5.00 5.30	UD					Light brown, firm to stiff, silty Clay soil with Little gravel	
6	7.00	100				6.00 6.45	D	4,4,6	10				
7	8.00	100											
8	9.00	100											
9	10.00	100											
10	11.00	100											
11	12.00	100				11.50 11.95	D	6,8,8	16				
12	13.00	100											
13	14.00	100				13.00 13.45	D	9,10,10	20				
14	15.00	100											
15	16.00	100				15.00 15.45	D	9,12,13	25				
16	17.00	100											
17	18.00	100				17.00 17.45	D	11,13,13	26				
18	19.00	100											
19 20	20	100									20.00		

Driller: Ayalewu

Logged by: Selamawit Tadesse

Checked by: Tinsae Ayele

Note:

D=Disturbed Sample (Split spoon)
UD=Undisturbed Sample
RC=Rock Core Sample
SPT=Standard Penetration Test

SCR=Solid Core Recovery
RQD=Rock Quality Designation
AFS=Average Fracture Spacing

APPENDIX

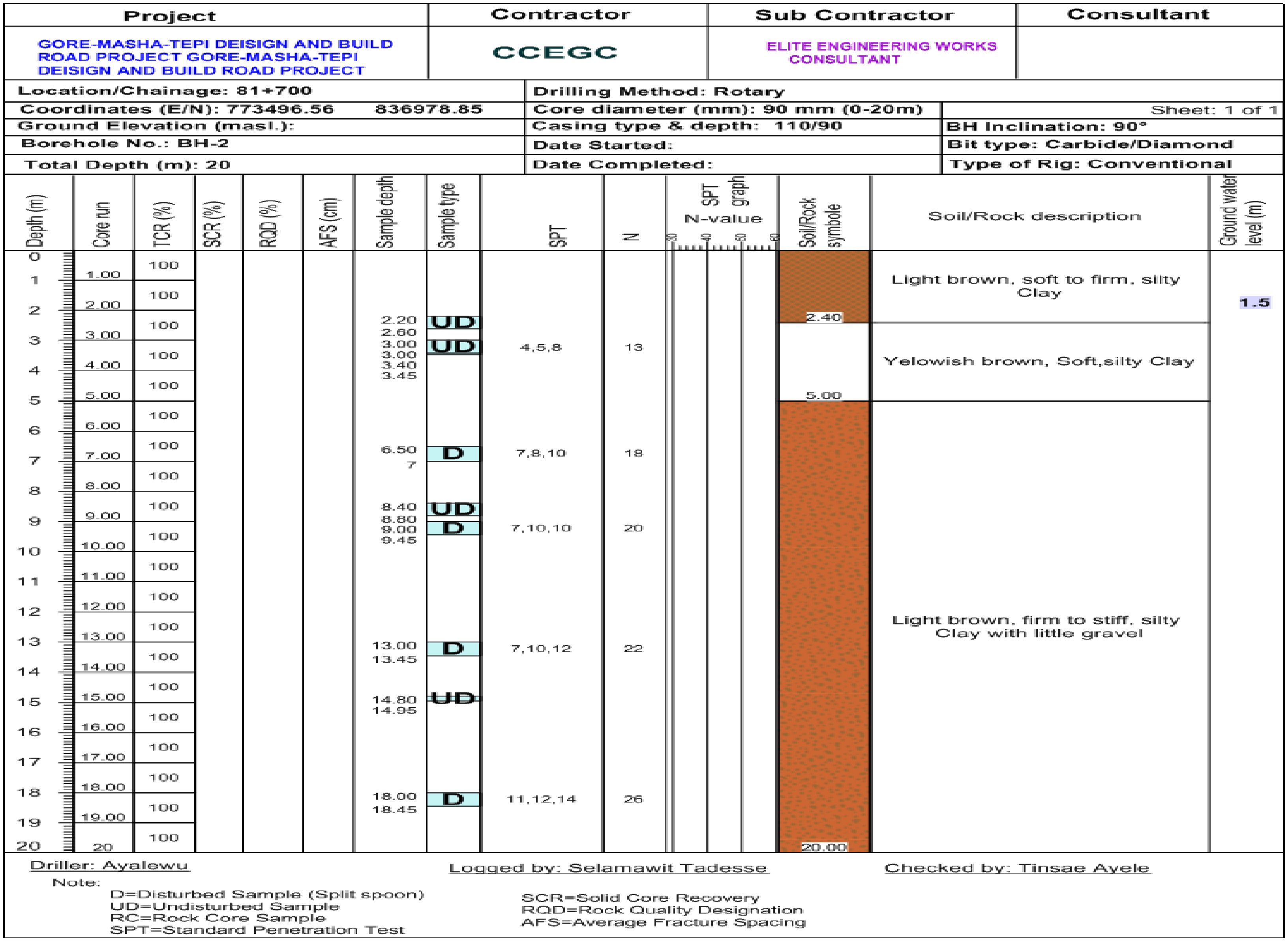

Project	Contractor	Sub Contractor	Consultant
GORE-MASHA-TEPI DEISIGN AND BUILD ROAD PROJECT GORE-MASHA-TEPI DEISIGN AND BUILD ROAD PROJECT	CCEGC	ELITE ENGINEERING WORKS CONSULTANT	

Location/Chainage: 81+700	**Drilling Method: Rotary**	
Coordinates (E/N): 773496.56 836978.85	**Core diameter (mm): 90 mm (0-20m)**	Sheet: 1 of 1
Ground Elevation (masl.):	**Casing type & depth: 110/90**	**BH Inclination: 90°**
Borehole No.: BH-2	**Date Started:**	**Bit type: Carbide/Diamond**
Total Depth (m): 20	**Date Completed:**	**Type of Rig: Conventional**

Depth (m)	Core run	TCR (%)	SCR (%)	RQD (%)	AFS (cm)	Sample depth	Sample type	SPT	N	SPT graph N-value 30 40 50 60	Soil/Rock symbole	Soil/Rock description	Ground water level (m)
0		100										Light brown, soft to firm, silty Clay	
1	1.00	100											1.5
2	2.00	100				2.20 2.60	UD				2.40		
3	3.00	100				3.00 3.00 3.40 3.45	UD	4,5,8	13			Yelowish brown, Soft,silty Clay	
4	4.00	100											
5	5.00	100									5.00		
6	6.00	100				6.50 7	D	7,8,10	18				
7	7.00	100											
8	8.00	100				8.40 8.80	UD						
9	9.00	100				9.00 9.45	D	7,10,10	20				
10	10.00	100											
11	11.00	100											
12	12.00	100										Light brown, firm to stiff, silty Clay with little gravel	
13	13.00	100				13.00 13.45	D	7,10,12	22				
14	14.00	100				14.80 14.95	UD						
15	15.00	100											
16	16.00	100											
17	17.00	100											
18	18.00	100				18.00 18.45	D	11,12,14	26				
19	19.00	100											
20	20										20.00		

Driller: Ayalewu   Logged by: Selamawit Tadesse   Checked by: Tinsae Ayele

Note:

D=Disturbed Sample (Split spoon)
UD=Undisturbed Sample
RC=Rock Core Sample
SPT=Standard Penetration Test

SCR=Solid Core Recovery
RQD=Rock Quality Designation
AFS=Average Fracture Spacing

APPENDIX

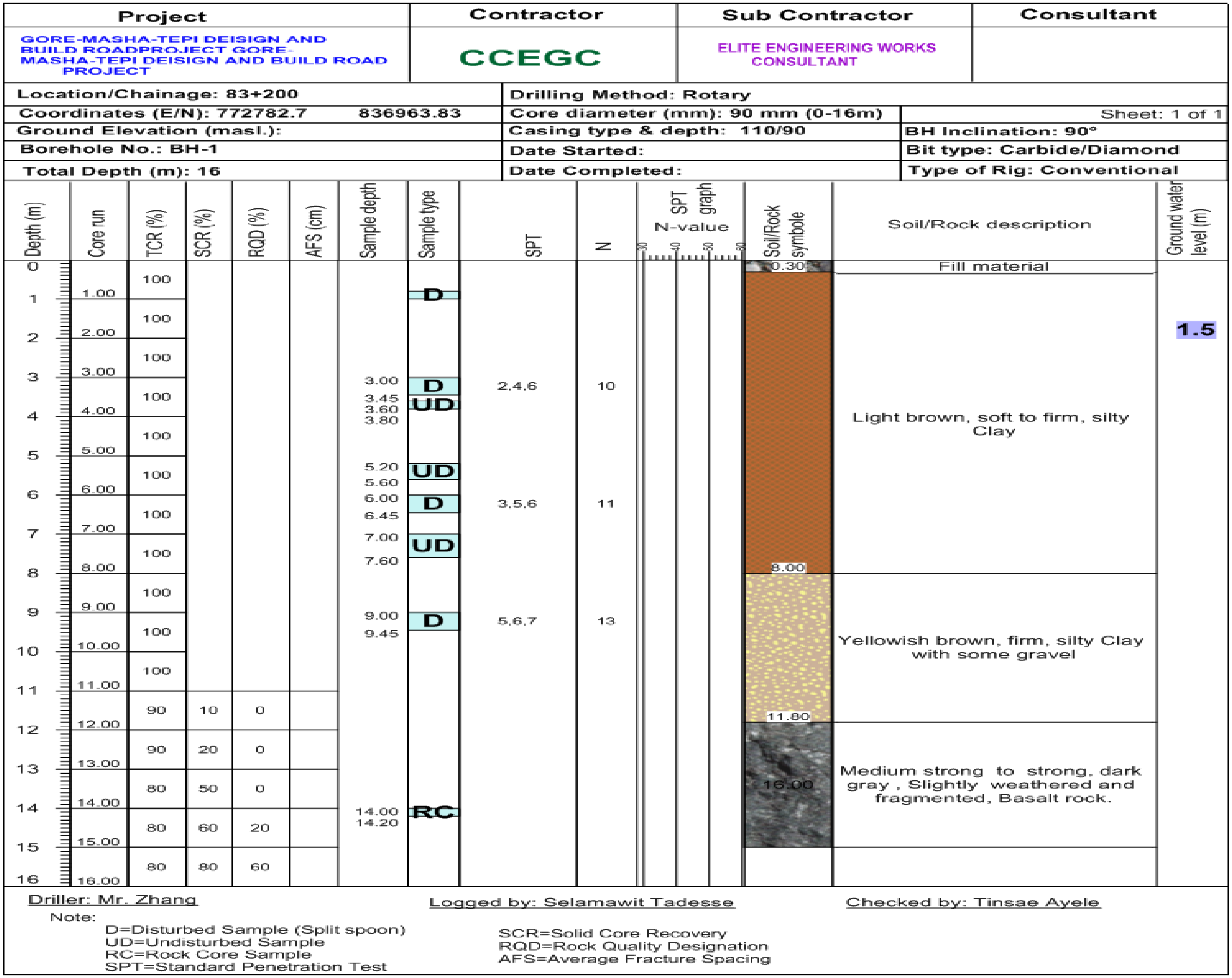

Project	Contractor	Sub Contractor	Consultant
GORE-MASHA-TEPI DEISIGN AND BUILD ROADPROJECT GORE-MASHA-TEPI DEISIGN AND BUILD ROAD PROJECT	CCEGC	ELITE ENGINEERING WORKS CONSULTANT	

Location/Chainage: 83+200	Drilling Method: Rotary	
Coordinates (E/N): 772782.7 836963.83	Core diameter (mm): 90 mm (0-16m)	Sheet: 1 of 1
Ground Elevation (masl.):	Casing type & depth: 110/90	BH Inclination: 90°
Borehole No.: BH-1	Date Started:	Bit type: Carbide/Diamond
Total Depth (m): 16	Date Completed:	Type of Rig: Conventional

Depth (m)	Core run	TCR (%)	SCR (%)	RQD (%)	AFS (cm)	Sample depth	Sample type	SPT	N	SPT graph N-value	Soil/Rock symbole	Soil/Rock description	Ground water level (m)
0	1.00	100					D				0.30	Fill material	
1	2.00	100											1.5
2	3.00	100											
3	4.00	100				3.00 3.45 3.60 3.80	D UD	2,4,6	10			Light brown, soft to firm, silty Clay	
4	5.00	100											
5	6.00	100				5.20 5.60	UD						
6	7.00	100				6.00 6.45	D	3,5,6	11				
7	8.00	100				7.00 7.60	UD				8.00		
8	9.00	100										Yellowish brown, firm, silty Clay with some gravel	
9	10.00	100				9.00 9.45	D	5,6,7	13				
10	11.00	100											
11	12.00	90	10	0							11.80		
12	13.00	90	20	0								Medium strong to strong, dark gray , Slightly weathered and fragmented, Basalt rock.	
13	14.00	80	50	0							16.00		
14	15.00	80	60	20		14.00 14.20	RC						
15 16	16.00	80	80	60									

Driller: Mr. Zhang

Logged by: Selamawit Tadesse

Checked by: Tinsae Ayele

Note:

D=Disturbed Sample (Split spoon)
UD=Undisturbed Sample
RC=Rock Core Sample
SPT=Standard Penetration Test

SCR=Solid Core Recovery
RQD=Rock Quality Designation
AFS=Average Fracture Spacing

APPENDIX

Appendix-GSummary of Laboratory Test Results

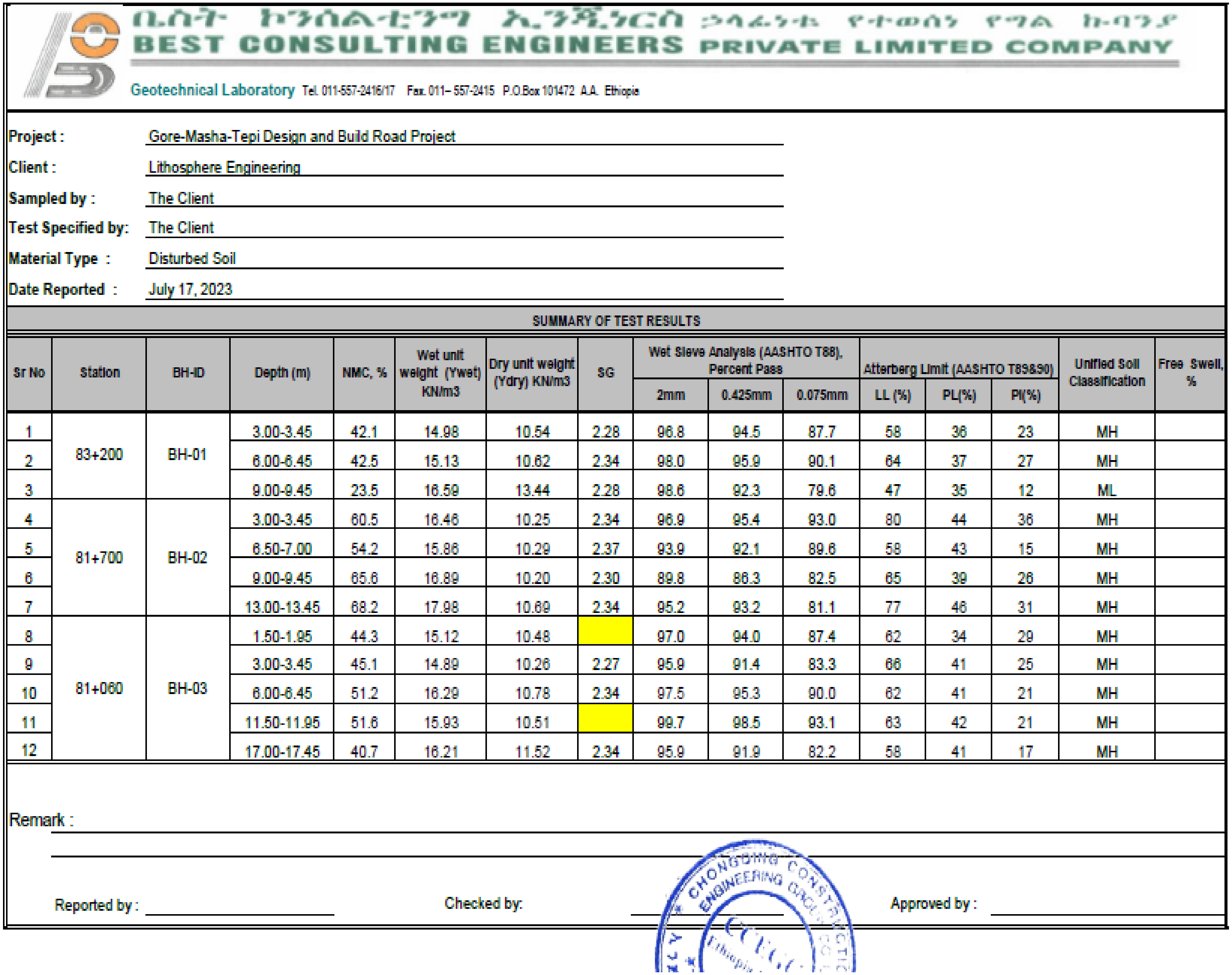

ቤስት ኮንሰልቲንግ ኢንጂነርስ ኃላፊነቱ የተወሰነ የግል ኩባንያ

BEST CONSULTING ENGINEERS PRIVATE LIMITED COMPANY

Geotechnical Laboratory Tel. 011-557-2416/17 Fax. 011– 557-2415 P.O.Box 101472 A.A. Ethiopia

Project : Gore-Masha-Tepi Design and Build Road Project

Client : Lithosphere Engineering

Sampled by : The Client

Test Specified by: The Client

Material Type : Disturbed Soil

Date Reported : July 17, 2023

SUMMARY OF TEST RESULTS

Sr No	Station	BH-ID	Depth (m)	NMC, %	Wet unit weight (Ywet) KN/m3	Dry unit weight (Ydry) KN/m3	SG	Wet Sieve Analysis (AASHTO T88), Percent Pass			Atterberg Limit (AASHTO T89&90)			Unified Soil Classification	Free Swell, %
								2mm	0.425mm	0.075mm	LL (%)	PL(%)	PI(%)		
1	83+200	BH-01	3.00-3.45	42.1	14.98	10.54	2.28	96.8	94.5	87.7	58	36	23	MH	
2			6.00-6.45	42.5	15.13	10.62	2.34	98.0	95.9	90.1	64	37	27	MH	
3			9.00-9.45	23.5	16.59	13.44	2.28	98.6	92.3	79.6	47	35	12	ML	
4	81+700	BH-02	3.00-3.45	60.5	16.46	10.25	2.34	96.9	95.4	93.0	80	44	36	MH	
5			6.50-7.00	54.2	15.86	10.29	2.37	93.9	92.1	89.6	58	43	15	MH	
6			9.00-9.45	65.6	16.89	10.20	2.30	89.8	86.3	82.5	65	39	26	MH	
7			13.00-13.45	68.2	17.98	10.69	2.34	95.2	93.2	81.1	77	46	31	MH	
8	81+060	BH-03	1.50-1.95	44.3	15.12	10.48	🟨	97.0	94.0	87.4	62	34	29	MH	
9			3.00-3.45	45.1	14.89	10.26	2.27	95.9	91.4	83.3	66	41	25	MH	
10			6.00-6.45	51.2	16.29	10.78	2.34	97.5	95.3	90.0	62	41	21	MH	
11			11.50-11.95	51.6	15.93	10.51	🟨	99.7	98.5	93.1	63	42	21	MH	
12			17.00-17.45	40.7	16.21	11.52	2.34	95.9	91.9	82.2	58	41	17	MH	

Remark :

Reported by : ______________

Checked by: ______________

Approved by : ______________

APPENDIX